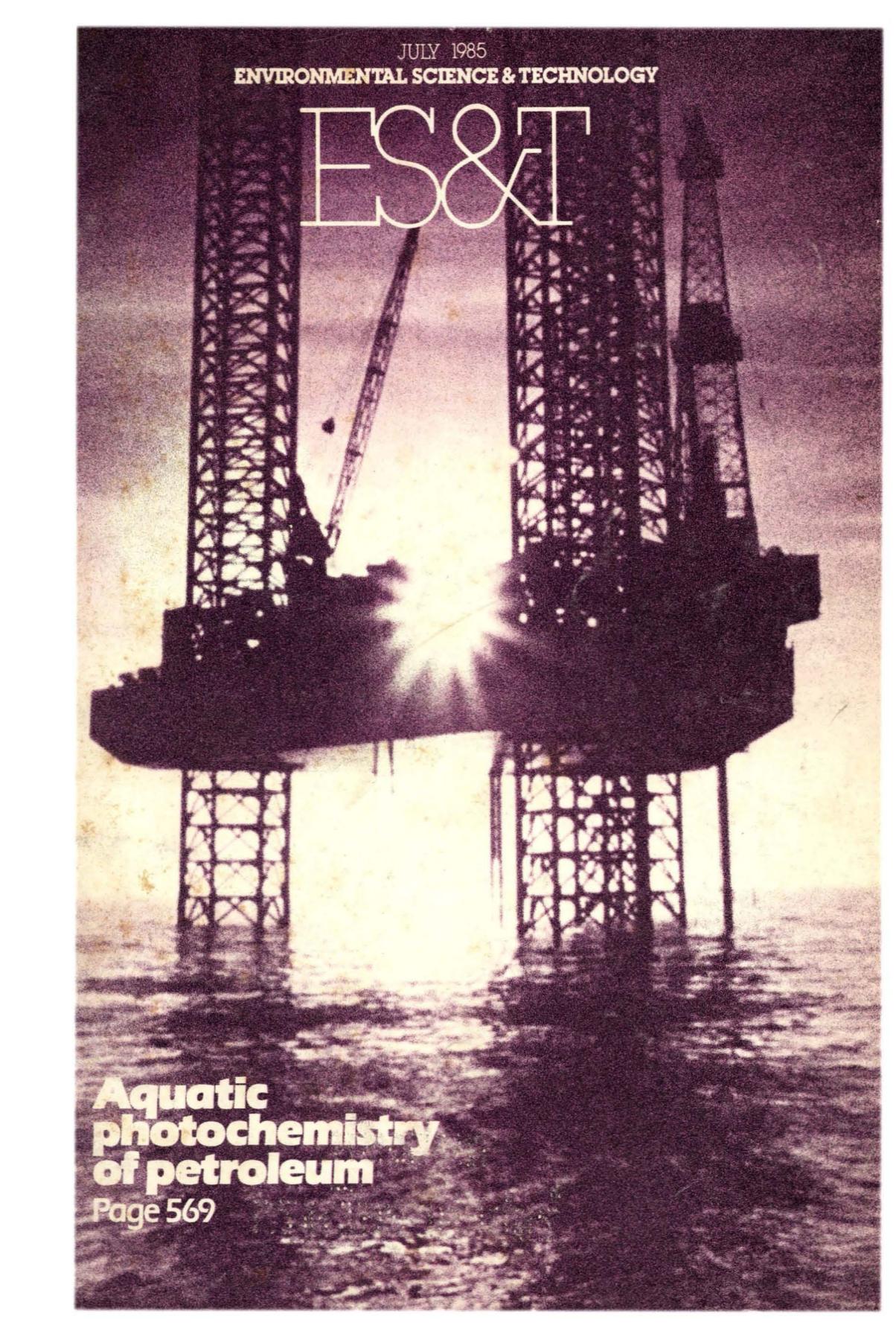


JULY 1985
ENVIRONMENTAL SCIENCE & TECHNOLOGY

ES&T

A photograph of an offshore oil platform at sunset. The platform's complex lattice structure is silhouetted against a bright, glowing sky where the sun is setting. The sun's light creates a strong lens flare effect, illuminating the platform and reflecting on the dark, choppy water below. The overall tone is dramatic and industrial.

**Aquatic
photochemistry
of petroleum**

Page 569

Vari-Clean™ 40 ml Vials: Pre-cleaned, Ready-to-Use For EPA* Water Sampling

Ready for immediate use, Vari-Clean 40 ml vials eliminate the time, inconvenience and expense involved in detergent washing, rinsing, oven drying and fully assembling 40 ml vials, caps and Teflon®/silicone discs prior to their use for discrete water sampling. Vari-Clean vials meet all EPA requirements and use the exact vials, caps and septa stated in the Nov. 29 and Dec. 3, 1979 Federal Register.

13510 Vari-Clean Water Sampling Vials
40 ml, pre-cleaned,
pkg. of 6 dz.

*Pre-cleaned for discrete water sampling according to EPA 40 CFR 136, *Guidelines for Establishing Test Procedures for the Analysis of Pollutants* and EPA 40 CFR 141 *National Interim Primary Drinking Water Regulations; Control of Trihalomethanes in Drinking Water*.

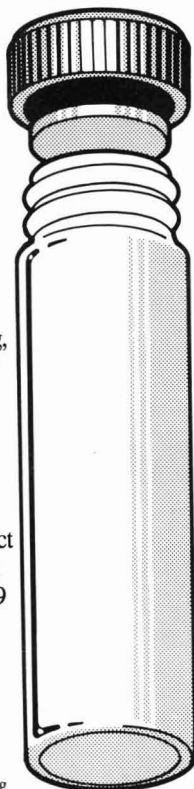
For further information call or write us:

800-435-2960

Or in Illinois call 800-874-3723

PIERCE CHEMICAL COMPANY
P.O. Box 117, Rockford, IL U.S.A. 61105

 **PIERCE**



INTRODUCING

NEW STATE-OF-THE-ART INSTRUMENTATION:

The SEASTAR IN SITU WATER SAMPLER

Uses microprocessor control and extraction columns to make the most significant advance in water sampling technology since the Nansen bottle.



FEATURES:

- Capable of large volume ultra-trace water sampling
- Equally useful for organic and inorganic applications
- Utilizes a variety of types of extraction columns, each with guaranteed blank levels

- Microprocessor-controlled for unprecedented flexibility of sampling, and precise control of flow rate and sample volume
- Can be moored (for days or weeks) or triggered with a messenger from a hydrowire
- Totally self-contained, powered by D-cell batteries

BUILT WITH PRIDE BY



SEASTAR INSTRUMENTS LTD

2045 MILLS ROAD, SIDNEY, B.C. CANADA V8L 3S1 (604) 656-0891 TELEX 049-7526

Geochemical Behavior of Disposed Radioactive Waste

G.S. Barney and W.W. Schulz,
Editors
Rockwell Hanford Operations
J.D. Navratil, Editor
Rockwell International Rocky Flats Plant

Examines the complex issue of radioactive waste disposal and the health hazards at underground waste sites. Assesses the chemical and physical behavior of wastes from the nuclear fuel cycle, from nuclear weapons testing, and from medical and research activities.

CONTENTS

Sorption and Desorption Reactions with Interbedded Materials • Reactions Between Tc and Fe-Containing Minerals • Radionuclide Sorption Mechanisms and Rates on Granitic Rock • Actinide and Technetium Sorption on Fe-Silicate and Dispersed Clay Colloids • Adsorption of Nuclides on Hydrous Oxides • High-Level Waste Components on Solubility and Sorption of Co, Sr, Np, Pu, Am • Hydrolysis of Am(III) and Pu(IV) • Aging Effect on Solubility and Crystallinity of Np(IV) Hydrous Oxide • Geochemical Controls on Radionuclide Releases from Waste Repository in Basalt • Radionuclide-Humic Acid Interactions • Oxygen Consumption and Redox Conditions in Basalt • Monitoring and Control of Eh-pH Conditions in Hydrothermal Experiments • Cs - Feldspars Interaction • Interaction of Groundwater and Basalt Fissure Surfaces and Effect on Actinide Migration • Organics and Radionuclides Subsurfaces Migration • Uranium Mining Releases • Uranium Mobility and Roll-Front Deposits • Crystal Chemistry of ABO₄ Compounds • Transformation Characteristics of LaV₂Nb_{1-x}O₄ Compounds • Stability of Tetravalent Actinides in Perovskites • α and β Decay in the Solid State • Effects of Water Flow Rates on Leaching • Borosilicate Glass-Containing Waste • Leach Resistance of Iodine Compounds • Nuclear Waste - View from Washington, D.C.



New!

Order from:
American Chemical Society
Distribution Office Dept. 70
1155 Sixteenth St., N.W.
Washington, DC 20036
or CALL TOLL FREE
800-224-6747 and use your
VISA, MasterCard, or
American Express credit
card.

ACS Symposium Series No. 246
424 pages (1984) Clothbound
LC 84-3106
US & Canada \$79.95

ISBN 0-8412-0827-1
Export \$95.95

Editor: Russell F. Christman
Associate Editor: John H. Seinfeld
Associate Editor: Philip C. Singer

ADVISORY BOARD

Julian B. Andelman, Marcia C. Dodge, Steven Eisenreich, William H. Glaze, Michael R. Hoffmann, Lawrence H. Keith, Donald Mackay, Jarvis Moyers, Kathleen C. Taylor, Eugene B. Welch

WASHINGTON EDITORIAL STAFF

Managing Editor: Stanton S. Miller
Associate Editor: Julian Josephson

MANUSCRIPT REVIEWING

Manager: Janice L. Fleming
Associate Editor: Monica Creamer
Assistant Editor: Yvonne D. Curry
Editorial Assistant: Diane Scott

MANUSCRIPT EDITING

Assistant Manager: Mary E. Scanlan
Assistant Editor: Ruth A. Linville

GRAPHICS AND PRODUCTION

Production Manager: Leroy L. Corcoran
Art Director: Alan Kahan
Staff Artist: Julie Katz
Production Editor: Kate Kelly

BOOKS AND JOURNALS DIVISION

Director: D. H. Michael Bowen
Head, Journals Department: Charles R. Bertsch
Head, Production Department: Elmer M. Pusey
Head, Research and Development Department: Lorrin R. Garson

ADVERTISING MANAGEMENT

Centcom, Ltd.
For officers and advertisers, see page 584.

Please send research manuscripts to Manuscript Reviewing, feature manuscripts to Managing Editor. For editorial policy and author's guide, see the January 1985 issue, page 22, or write Janice L. Fleming, Manuscript Reviewing Office, *ES&T*. A sample copyright transfer form, which may be copied, appears on the inside back cover of the January 1985 issue.

Environmental Science & Technology, *ES&T* (ISSN 0013-936X), is published monthly by the American Chemical Society at 1155 16th Street, N.W., Washington, D.C. 20036. Second-class postage paid at Washington, D.C., and at additional mailing offices. POSTMASTER: Send address changes to *Environmental Science & Technology*, Membership & Subscription Services, P.O. Box 3337, Columbus, Ohio 43210.

SUBSCRIPTION PRICES 1985: Members, \$26 per year; nonmembers (for personal use), \$35 per year; institutions, \$149 per year. Foreign postage, \$8 additional for Canada and Mexico, \$14 additional for Europe including air service, and \$23 additional for all other countries including air service. Single issues, \$13 for current year; \$13.75 for prior years. Back volumes, \$161 each. For foreign rates add \$1.50 for single issues and \$10.00 for back volumes. Rates above do not apply to nonmember subscribers in Japan, who must enter subscription orders with Maruzen Company Ltd., 3-10 Nihon bashi 2 chome, Chuo-ku, Tokyo 103, Japan. Tel: (03) 272-7211.

COPYRIGHT PERMISSION: An individual may make a single reprographic copy of an article in this publication for personal use. Reprographic copying beyond that permitted by Section 107 or 108 of the U.S. Copyright Law is allowed, provided that the appropriate per-copy fee is paid through the Copyright Clearance Center, Inc., 21 Congress St., Salem, Mass. 01970. For reprint permission, write Copyright Administrator, Books & Journals Division, ACS, 1155 16th St., N.W., Washington, D.C. 20036.

REGISTERED NAMES AND TRADEMARKS, etc., used in this publication, even without specific indication thereof, are not to be considered unprotected by law.

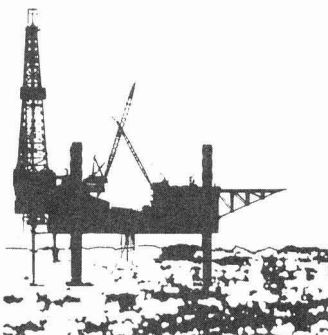
SUBSCRIPTION SERVICE: Orders for new subscriptions, single issues, back volumes, and microfiche and microform editions should be sent with payment to Office of the Treasurer, Financial Operations, ACS, 1155 16th St., N.W., Washington, D.C. 20036. Phone orders may be placed, using Visa, Master Card, or American Express, by calling toll free (800) 424-6747 from anywhere in the continental U.S. Changes of address, subscription renewals, claims for missing issues, and inquiries concerning records and accounts should be directed to Manager, Membership and Subscription Services, ACS, P.O. Box 3337, Columbus, Ohio 43210. Changes of address should allow six weeks and be accompanied by old and new addresses and a recent mailing label. Claims for missing issues will not be allowed if loss was due to insufficient notice of change of address, if claim is dated more than 90 days after the issue date for North American subscribers or more than one year for foreign subscribers, or if the reason given is "missing from files."

The American Chemical Society assumes no responsibility for statements and opinions advanced by contributors to the publication. Views expressed in editorials are those of the author and do not necessarily represent an official position of the society.

ES&T CONTENTS

Volume 19, Number 7, July 1985

CRITICAL REVIEW



569

Photochemistry of petroleum in water. A discussion of the effects of light on oil and petroleum products in aquatic systems. James R. Payne, Charles R. Phillips, Science Applications International, La Jolla, Calif.

REGULATORY FOCUS

580

Proposed air toxics legislation. Richard Dowd discusses the Toxic Release Control Act, which is aimed at controlling 85 specific contaminants.

VIEWS



581

Blind technology transfer. Guy R. Lanza of the University of Texas explains the pitfalls of introducing technology into regions with little or no previous technological experience.

DEPARTMENTS

- 563 Editorial
- 565 Currents
- 583 Consulting services

UPCOMING

Scientific uncertainties in risk assessment

Mortality and air pollution—is there a relationship?

RESEARCH

585

Occurrence of chlorinated polynuclear aromatic hydrocarbons in tap water. Hiroaki Shiraishi,* Norman H. Pilkington, Akira Otsuki, and Keiichiyo Fuwa

Chlorinated polynuclear aromatic hydrocarbons are detected at 10^{-1} to 10^{-2} ng/L levels by GC/MS using a fused-silica capillary column.

■ 590

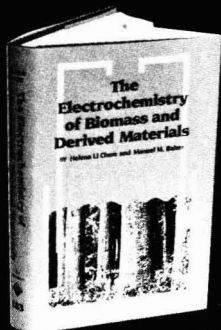
Henry's law constants for the polychlorinated biphenyls. Lawrence P. Burkhard, David E. Armstrong,* and Anders W. Andren

The reported constants, predicted from vapor pressure and solubility data, are in fair agreement with experimental constants, and their average error is estimated to be a factor of 5.

ESTHAG 19(7) 561-648 (1985)
ISSN 0013 936X

Credits: p. 566, Jim Page, North Carolina Department of Natural Resources and Community Development; p. 569, AMOCO Corp., courtesy American Petroleum Institute; p. 572, courtesy American Petroleum Institute; p. 578, Chevron, courtesy American Petroleum Institute; p. 581, Will Lepkowski, *Chemical & Engineering News*
Cover: B. J. Nixon, Tenneco, Inc., courtesy American Petroleum Institute

The Electrochemistry of Biomass and Derived Materials



NEW!

by Helena Li Chum and Manuel M. Baizer

Promotes the successful coupling of two major technologies — biomass conversion and electrochemistry — in making feedstocks for the chemical and fuel industries. Defines and describes various reactions occurring during the electrochemical breakdown of biomass into fuels, fuel components, and valuable chemicals. Covers the basics of electrochemistry, the available forms of renewable resources, and the electrochemical reactions involving carbon dioxide, lignins, hydrocarbons, polysaccharides, and more. Records all the relevant work being done in this ecologically and economically important field and suggests necessary areas of future research and development.

CONTENTS

From Biomass, Broadly Defined, to Electrochemical Feedstocks • Introduction to Organic Electrochemistry of Biomass and Derived Materials • The Electrochemistry of Carbon Dioxide • Electrochemistry Involving Nonsaccharidic Alcohols • Electrochemistry of Other Functional Groups • Some Aspects of the Electrochemistry of Monosaccharides • The Electrochemistry of Biopolymers Derived from Biomass • Synthetic Photoelectrochemistry and Other Techniques • Perspectives and Suggestions for Further Work

ACS Monograph No. 183
328 pages (1985) Clothbound
LC 85-1377 ISBN 0-8412-0868-9
US & Canada \$89.95 Export \$107.95

Order from:
American Chemical Society
Distribution Office Dept. 32
1155 Sixteenth St., N.W.
Washington, DC 20036
or CALL TOLL FREE 800-424-6747
and use your VISA, MasterCard,
or American Express credit card.

597

Carbonized coal products as a source of aromatic hydrocarbons to sediments from a highly industrialized estuary. Elizabeth G. Merrill and Terry L. Wade*

Chemical fingerprinting provides information on the relative contributions of carbonized coal and petroleum to hydrocarbon contamination in a highly industrialized estuary.

603

High molecular weight hydrocarbons including polycyclic aromatic hydrocarbons in natural gas from consumer distribution pipelines and in pipeline residue. G. A. Eiceman,* B. Davani, M. E. Wilcox, J. L. Gardea, and J. A. Dodson

Detailed analyses are used to identify and quantify C_9 to C_{20} alkanes and aromatic hydrocarbons in natural gas and pipeline condensate.

609

X-ray photoelectron spectroscopy studies of coal fly ashes with emphasis on depth profiling of submicrometer particle size fractions. Nurit Kaufherr, Mohsen Shenasa, and David Lichtman*

The composition of the outer layers of submicrometer fly ash particles originating from the Mojave Power Generating Station is studied by means of XPS in conjunction with Ar ion bombardment.

615

Variability of elemental concentrations in power plant ash. Larry J. Holcombe,* Barry P. Enyon, and Paul Switzer

Sampling and analysis are conducted at a U.S. power plant to determine the time variability of coal ash composition.

620

The mutagenic activity of the products of propylene photooxidation. Tadeusz E. Kleindienst,* Paul B. Shepson, Edward O. Edney, Larry T. Cupitt, and Larry D. Claxton

Gas-phase products from the photooxidation of propylene are found to be mutagenic by the Ames test.

628

Aqueous solubility and octan-1-ol to water partition coefficients of aliphatic hydrocarbons. Michael Coates, Des W. Connell,* and Diane M. Barron

Solubility and partition coefficient values for several homologous series of aliphatic hydrocarbons are obtained by extrapolation of known results, direct measurements, and HPLC.

632

Influence of aggregation on the uptake kinetics of phosphate by goethite. Marc A. Anderson,* M. Isabel Tejedor-Tejedor, and Robert R. Stanforth

A coagulation model is presented in which phosphate bridges to primary goethite particles and causes increased aggregate order, phosphate burial, and oscillatory uptake kinetics.

638

Determination of equilibrium and rate constants for binding of a polychlorinated biphenyl congener by dissolved humic substances. John P. Hassett* and Edwina Milicic

Gas purging is used to distinguish between free and bound hydrophobic organic solutes in water and to obtain equilibrium and rate constants simultaneously.

NOTES

643

Toluene-humic acid association equilibria: Isopiestic measurements. Charles N. Haas* and Brian M. Kaplan

The association equilibrium is described by a linear partition coefficient model in which the equilibrium constant is a function of the humic-acid concentration.

CORRESPONDENCE

645

Comment on "Comparison of the carcinogenic risks from fish vs. groundwater contamination by organic compounds." Christopher J. Schmitt* and J. Larry Ludke

Michael Stewart Connor

646

Comment on "Red herrings in acid rain research." W. B. Innes

Magda Havas,* Thomas C. Hutchinson, and Gene E. Likens

* To whom correspondence should be addressed.

■ This article contains supplementary material in microform. See ordering instructions at end of paper.

ES&T
EDITORIAL

New features in *ES&T*

It is with great pleasure that I announce that a number of editorial pages will be returned to the front section of *ES&T*. The cost-saving actions described in the October 1984 editorial (p. 297A) have been effective in stabilizing the journal's financial condition, although everyone who knows and admires *ES&T* has deplored the need to contract the front section even temporarily. About 100 pages will be returned by the end of this year, and another 100 pages will be added in 1986. These actions will essentially restore the size and balance the journal has enjoyed over the past several years.

We also will be doing some new things with our additional pages. The contributed features have been very popular with our readers, and many have suggested that we increase the pages allotted to them. The *ES&T* Advisory Board agreed with this idea at its April 1985 meeting and suggested that at least some of the new feature space be given to publication of integrated series of features on selected topics.

Current areas of interest containing elements of scientific controversy might be chosen. For example, a series might address the cause-and-effect relationship between acid precipitation and water quality or forest productivity. Potential topics for a three-article series include conflicting hypotheses of lake acidification, lake acidification process

models, and causes of forest decline. Other series might be devoted to topics that are less controversial but that are still under active investigation because of their acknowledged importance, for example, various important intermedia transport processes.

Serialized publication is one of the most difficult editorial tasks a journal publishing voluntary contributions can undertake. In addition to subject selection, problems include locating appropriate and willing authors, timing manuscript preparation and revision, and maintaining uniform quality within the series. We will endeavor to produce these feature series with the special assistance of board members Steven Eisenreich, Marcia Dodge, and Donald Mackay, who will serve as chairman.

You can help by sending your suggestions for topics and authors to Donald Mackay, University of Toronto, Department of Chemical Engineering and Applied Chemistry, Toronto, Ontario M5S 1A4, Canada.



The Reaction is Purely Chemical

Subscribe to these outstanding AMERICAN CHEMICAL SOCIETY publications.
Choose from 23 different titles.



ACS publications are designed for you. They're timely, authoritative, comprehensive. They give you the latest in research, news, and commentary — everything you need to know to keep you on top of every aspect of your professional life.

- Analytical Chemistry
- Chemical & Engineering News
- CHEMTECH
- Environmental Science & Technology
- Accounts of Chemical Research
- Biochemistry
- Chemical Reviews
- Industrial & Engineering Chemistry — Process Design and Development
- Industrial & Engineering Chemistry — Product R&D
- Industrial & Engineering Chemistry — Fundamentals
- Inorganic Chemistry

CALL TOLL FREE 800-424-6747
Cable Address: JIECHEM
Telex: 440159 ACSP UI or
892582 ACSPUBS



AMERICAN CHEMICAL
SOCIETY PUBLICATIONS
1155 Sixteenth Street, N.W.
Washington, D.C. 20036 U.S.A.

- Journal of Agricultural & Food Chemistry
- Journal of the American Chemical Society
- Journal of Chemical & Engineering Data
- Journal of Chemical Information and Computer Sciences
- Macromolecules
- Journal of Medicinal Chemistry
- The Journal of Organic Chemistry
- The Journal of Physical Chemistry
- ACS Single Article Announcement
- Journal of Physical and Chemical Reference Data
- Organometallics
- Langmuir

ES&T CURRENTS

INTERNATIONAL

Transfrontier movements of hazardous wastes are not adequately monitored and controlled, according to the environment ministers of nations in the Organization for Economic Cooperation and Development (OECD). At an OECD hazardous waste conference held in Basel, Switzerland, in March, they called for stronger action to establish internal obligations for monitoring and control of hazardous waste transport and standardization and enforcement of applicable regulations within and among the member nations.

FEDERAL

Half of the 1300 facilities now holding interim permits for land disposal of hazardous wastes could be closed, says Gene Lucero, EPA's head of waste programs enforcement. Under Section 3005(e) of the 1984 amendments to the Resource Conservation and Recovery Act (RCRA), these facilities must certify that they meet RCRA groundwater monitoring requirements or they will be closed on Nov. 8. Lucero estimates that 650 disposal sites do not satisfy the requirements. He says that limited deadline extensions might be granted to facilities that have acted in good faith but have not installed enough wells to comply with the law.

As of July 14, dioxin-containing wastes will be regulated under the Resource Conservation and Recovery Act (RCRA), says EPA administrator Lee Thomas. Regulating such wastes under RCRA provides EPA broader control than is possible under the Toxic Substances Control Act (TSCA). TSCA gives EPA jurisdiction only over tetrachlorodibenzo-*p*-dioxin (TCDD); RCRA furnishes the agency with authority to regulate a number of chlorinated dibenzodioxins, dibenzofurans, and chlorophenols and their phenoxy derivatives, in addition to TCDD, as acutely hazardous wastes. TCDD and similar wastes can be disposed of only in properly certified facilities. Incinera-

tion of dioxin-containing wastes must be done with a removal efficiency of at least 99.9999%.

The Indian Point nuclear power plants (Buchanan, N.Y.) "pose no undue or disproportionate public risk," according to a determination by the Nuclear Regulatory Commission (NRC). At issue are Units 2 and 3, which the Union of Concerned Scientists has tried to have shut down for the past six years. The NRC acknowledges that a radioactivity release could have "more serious consequences than [one] at virtually any other NRC-licensed reactor site" because 15.5 million people live within a 50-mile radius of the reactors. But the commission believes—with one member sharply dissenting—that the chance of a release is no greater than at other plants and may be less. Consolidated Edison operates Unit 2; the New York State Power Authority operates Unit 3.

EPA has begun a priority review of occupational and ambient exposure to methylene chloride since determining that this compound may pose a significant cancer risk to humans. The agency is taking the action under Section 4(f) of the Toxic Substances Control Act (TSCA). EPA must decide whether new data show that the chemical poses a risk of human cancer, gene mutation, or birth defects. After completing the study, the agency will either take regulatory action or publish findings in the *Federal Register* that the risk is not "unreasonable." Among other chemicals that have been given priority review under TSCA are 1,3-butadiene and formaldehyde.

Has ambient air quality improved since 1975? Generally yes, according to EPA, which cites SO₂ reductions of 36% between 1975 and 1983. Lead levels decreased by 67%, carbon monoxide dropped by 33%, and particulate matter fell by 20%. One jarring note is that although ozone levels fell 8% overall between 1975 and 1983, they rose during 1982–83. EPA ascribes the rise to a 3% in-

crease in organic ozone precursors and to meteorological conditions more conducive to ozone formation in 1983 than in previous years.

STATES

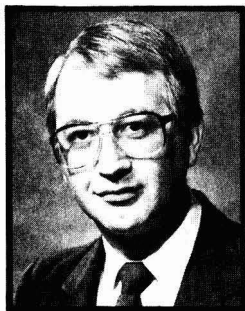
A site in Perth Amboy, N.J., has been chosen for "the most technologically advanced commercial hazardous waste incineration facility in the world," according to Chemcontrol U.S.A. (Columbia, Md.). The firm submitted an application in April to the New Jersey Hazardous Waste Facilities Siting Commission for permission to build the \$90-million plant. The facility will incorporate engineering and operating principles developed by Chemcontrol's parent firm, Danish Chemcontrol, operators since 1974 of Kommunekemi, a hazardous waste plant in Denmark. The proposed plant has the support of many in the New Jersey hazardous waste treatment community but is vehemently opposed by Mayor George Otowski of Perth Amboy.

Officials of the New York State Department of Environmental Conservation (DEC) have expressed reservations about a report that polychlorinated biphenyls (PCBs) in the Hudson River had been degraded by natural bacterial action. Scientists from General Electric (GE) reported at the American Chemical Society's April meeting in Miami, Fla., that degradation had been detected and that PCBs therefore may not be as hazardous as federal and state officials believe them to be. They reported that the bacteria cleave chlorine atoms from PCB molecule rings. DEC Commissioner Henry Williams says GE's findings are insufficient to persuade state officials to slacken efforts to excavate, remove, and destroy PCB-containing sediments in the Hudson River.

Indiana is raising taxes on land disposal of hazardous wastes from \$1.50/t to \$4.50/t, effective Oct. 1. The tax will increase by \$1 a year

through 1989, when it will reach \$8.50/t. If the wastes are suspended or dissolved in liquid, the tax will be levied on the entire suspension or solution. Maximum taxpayer liability for underground injection will be \$25,000 a year, and tax payments are to be made quarterly. Under the law, 75% of the tax proceeds will be earmarked for the state's hazardous substances emergency response fund or for Superfund. The remainder will be paid to counties in which waste disposal facilities are located.

Kansas has challenged EPA's position that diluting hazardous wastes is a valid treatment under the Resource Conservation and Recovery Act (RCRA). Allan Abramson, director of the Kansas Division of Environment, argues that dilution is not acceptable under any circumstances because hazardous components are still present in the same quantity after dilution. His main concern is with wastes that are not listed as hazardous under RCRA but that are still considered hazardous because they are toxic. Abramson objects to a statement by John Skinner, EPA's assistant administrator for solid waste, that dilution performed under conditions set forth in a permit can render a hazardous waste non-hazardous.



Wilms: Priority for coastal waters

Coastal water quality is North Carolina's highest environmental priority, says Paul Wilms, director of the state's Division of Environmental Management. He says that peat mining, septic tank leachate, urban storm water runoff, and fresh-water intrusion resulting from land clearing have damaged coastal waters. Other environmental issues Wilms lists are groundwater protection, toxic materials in air and water, eutrophication of state waters, wastewater treatment plant funding, and acid deposition. Wilms adds that the state enforcement program will be more vigorous and less forgiving than it has been previously.

The state of Wisconsin's groundwater protection law, which took effect Jan. 1, establishes contamination levels for nitrates, pesticides, organics, and other materials above which remedial action must be taken. It also outlines enforcement standards that define when a violation of the law has occurred. The law calls for establishment of a monitoring and sampling system, regulatory programs to control pesticides and fertilizers that could contaminate groundwater, and a fund for financing groundwater-related research activities. Compensation for persons whose wells have become contaminated is to be provided.

AWARDS

The 3M Company (St. Paul, Minn.) was awarded the gold medal of the World Environment Center (WEC) for international corporate environmental achievement at WEC's first annual World Environment Dinner held in Washington, D.C., in May. 3M Chairman Lewis Lehr accepted the award from former EPA Administrator William Ruckelshaus. The company was chosen because of its Pollution Prevention Pays, or 3P program, which it has been managing in the U.S. and in 20 other countries. The program was developed under the leadership of Joseph Ling. WEC also has been conducting a survey to assist rapidly industrializing countries in developing or improving systems for preventing or minimizing the effects of industrial accidents.

SCIENCE

Aquatic organisms exposed to certain organic compounds containing tin may suffer impairments in growth, metabolism, and reproduction, according to a report by National Research Council Canada. A research team led by J.K.J. Thompson of the Institute of Ocean Sciences (Sidney, B.C.) notes that damage results from aquatic concentrations of tributyltin of as little as 200 ng/L. The researchers also warn of the extreme toxicity of butyltin and methyltin. Several organotin compounds are used as agricultural biocides, wood-preserving and antifouling agents, industrial catalysts, and stabilizers for polyvinyl chloride.

The carbon-dioxide-induced warming of the Earth may be accelerated by gases generated by industry, according to scientists from the National Center for Atmospheric Re-

search (Boulder, Colo.). Such gases as chlorofluorocarbons 11 and 12 can exacerbate this warming effect markedly, and methane and nitrous oxide can make significant contributions. A single molecule of certain chlorofluorocarbons absorbs as much heat as 10^4 molecules of carbon dioxide. Chlorofluorocarbons, methane, and nitrous oxide are much rarer in the atmosphere than carbon dioxide, but these gases seem to be accumulating faster than carbon dioxide. One estimate of the combined effect of carbon dioxide and the industrial gases projects an average cumulative global warming of 1.5 K by the year 2030.

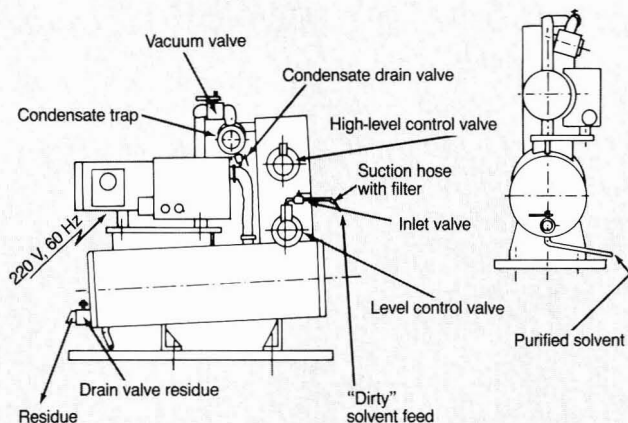
TECHNOLOGY

Activated magnesite clinker may be an efficient remover of phosphorus from water, says S. Kaneko of Hitachi Plant Engineering & Construction (Chiba, Japan). He says that pilot studies conducted since 1982 reveal that after treatment, phosphorus concentrations remain consistently lower than 0.5 mg/L, reported as phosphate. Because the influence of alkalinity is small, the decarbonation step can be omitted. The calcium and phosphate concentrations, as well as pH, are computer controlled. Kaneko estimates that the phosphorus removal process (by crystallization) and the computer control can result in a lowering of costs by 20% compared with costs for conventional chemical treatment processes.

Sewage sludge can be converted to germ-free soil conditioner or fuel rather than being dumped at sea. Foster-Wheeler (Livingston, N.J.) has persuaded Mercer and Ocean Counties, N.J., and Los Angeles-area communities to process their sludge in this manner. The key is a process licensed to Foster-Wheeler by Dehydro-Tech (East Hanover, N.J.), which dries the sludge to <2% water. It costs about 50% less than conventional sludge drying systems, according to Foster-Wheeler. After the anaerobically digested sludge is dehydrated, it is made into a granular product useful as a fertilizer or soil conditioner.

Companies affected by the new Resource Conservation and Recovery Act amendments may be helped by a 15-gal/h solvent recovery unit designed by MENTEC AG (Lucerne, Switzerland). The recovery unit, which is in use in Europe, is being introduced into the U.S. by VACO-SOLV (Cincinnati, Ohio). It

Solvent recovery apparatus



Source: MENTEC AG

is designed to remove reusable solvents from waste materials, thereby lowering the cost of the solvent and of waste disposal. It uses a vacuum pump to vaporize solvents at about room temperature. The vacuum pump doubles as a heat pump to compress solvent vapors into a condenser. According to the company, this approach results in 90% energy savings over conventional atmospheric-pressure or vacuum stills.

The consequences of a meltdown in a nuclear plant may be less severe than widely believed, according to engineers at the Argonne National Laboratory (Argonne, Ill.). Under Electric Power Research Institute sponsorship, Argonne has been simulating meltdowns since 1981. When a molten mass of core material falls into water, less steam and hydrogen are produced than current computer models predict. Argonne engineers now believe that even in the event of a meltdown, pressures will not be high enough to rupture the containment building and release radioactive materials to the environment.

An electron exchange resin can remove selenate and selenite ions from water to produce selenium, says Andrew Murphy, a scientist with the U.S. Bureau of Reclamation (Denver, Colo.). The electron transfer produces quinone groups in addition to selenium. The selenium adheres to a filter below the resin bed and to the resin itself. It is removed from the filter and resin with an organic solvent that can be redistilled for future use. The selenium can then

be sold commercially for such purposes as use in photoelectric cells. The product water has selenium levels below EPA's drinking water standards, according to Murphy.

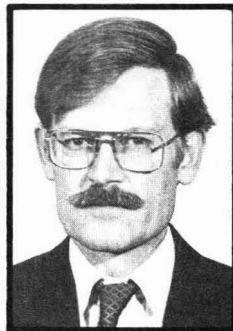
BUSINESS

How should Superfund money be raised? Chemical, oil, and mining industry groups favor a manufacturers' environmental excise tax (MEET), a low-percentage value-added tax levied on all manufacturers. MEET would take some of the Superfund tax burden off the petroleum, petrochemical, and chemical industries. According to the American Petroleum Institute and the Chemical Manufacturers Association, who designed the plan, the tax would have little or no adverse effect on the U.S. economy. It would also allow U.S. exporters to compete overseas because the tax would not be imposed on exports. Industry spokesmen also support an alternative bill (S. 957), introduced by Sens. Lloyd Bentsen (D-Tex.) and Malcolm Wallop (R-Wyo.), which would raise Superfund money by taxing the sale, lease, or import of tangible personal property by a manufacturer or importer.

Westinghouse Electric has agreed to clean up six sites near Bloomington, Ind., where it had disposed of polychlorinated biphenyls (PCBs). Representatives from EPA and the Department of Justice report that Westinghouse will spend between \$75 million and \$100 million to clean the sites; the company esti-

mates that its net costs could be considerably lower. EPA Administrator Lee Thomas says the May agreement represents the largest hazardous waste settlement in the agency's history. Westinghouse plans to recoup some of its costs for building an incinerator and disposing of the wastes by collecting fees for burning municipal wastes in the incinerator and by selling nearby industries steam and power generated from the burning wastes.

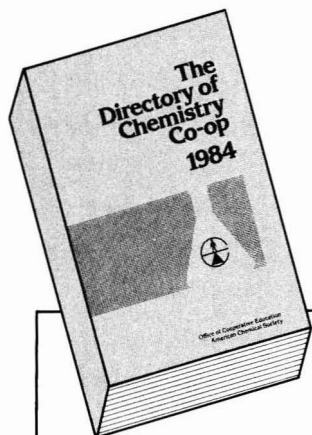
A set of guidelines for labeling pesticides exported to developing countries was evolved by the Agricultural Chemicals Dialogue Group (ACDG) at a meeting held in Washington, D.C., in April. ACDG is a coalition of industry, environmental, and church groups, which is mediated by the Conservation Foundation (Washington, D.C.). The project's goal is to reduce the number of deaths and injuries resulting from misuse of agricultural chemicals. For countries in which illiteracy rates are high, symbols would supplement written label instructions.



Huckabee: Studying forest decline

The Electric Power Research Institute (EPRI, Palo Alto, Calif.) has launched a study of the effects of acid rain and snow on forests. Research will try to document mathematically how atmospheric deposition may affect a forest's nutrient status and soil processes, thereby accelerating the aging and deterioration of its trees and impairing the forest's productivity. John Huckabee, EPRI's ecological studies program manager, says the study seeks the "necessary scientific understanding of the factors and the interactions behind forest decline." It will last four years and cost \$8 million. The prime contractor will be Oak Ridge National Laboratory, which will conduct the study in New York, North Carolina, Tennessee, and Washington State.

RECRUITERS ... EDUCATORS ... CHEMISTS ...



NOW AVAILABLE FROM ACS

THE DIRECTORY OF CHEMISTRY CO-OP

The indispensable guide to cooperative education programs in the U.S. and Canada.

SAVE 25%!

This informative, 280-page paperback volume is available for just \$15.00 a copy (After April 1, 1985, the price will be \$20.00) Order now to take advantage of these special introductory savings.

PHONE TOLL FREE!

Call 1-800-424-6747 (credit card orders only) to order your copy at this special price or mail coupon today!

If you are interested in co-op programs as participant, sponsor, or advisor, take advantage of this unique, authoritative reference! Get practical, accurate information on 265 chemistry, chemical engineering, and chemistry-related cooperative education programs in the U.S. and Canada.

In-depth coverage includes contact names and addresses, program size, typical work schedules, academic requirements, geographical and program indices, and a great deal more.

As a reference, this timely resource is essential for:

- Schools interested in starting co-op
- Employers seeking sources of co-op students
- High school students and advisors wishing to locate co-op schools
- Co-op professionals requiring a convenient source of information

Please send _____ copies of the ACS *Directory of Chemistry Co-op* @ \$15.00 per copy to:

Name _____

Address _____

Check the method of payment: ☐ Check or money order enclosed ☐ Credit card: ☐ Visa ☐ MasterCard ☐ Barclay ☐ Access ☐ American Express

Cardholder Name _____

Card No. _____

Exp. Date _____ Interbank No. _____

(MasterCard and Access only)

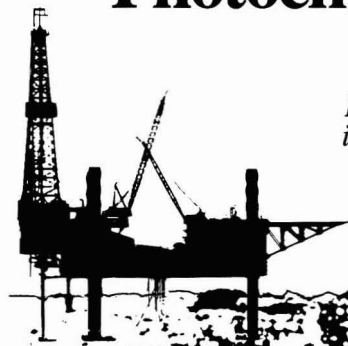
Signature _____

Amount Enclosed \$ _____
Make checks payable to **ACS Co-op Directory**.
Orders must be prepaid. California residents,
add 6% sales tax.

Return to: **Office of Cooperative Education**
American Chemical Society
1155 Sixteenth St., N.W.
Washington, DC 20036

Photochemistry of petroleum in water

*Photooxidation causes changes
in oil and enhances dissolution
of its oxidized products*



James R. Payne
Charles R. Phillips
*Science Applications International
Corporation*
476 Prospect St.
La Jolla, Calif. 92037

When crude oil or refined petroleum products are released into an aquatic environment, immediate changes in their chemical and physical properties occur as a result of several simultaneous weathering processes. These are evaporation, dissolution, dispersion into the water column, photochemical

and microbial oxidation, water-in-oil emulsification (mousse formation), adsorption onto suspended particulate material, agglomeration, and sinking. The individual roles these processes play in the general fate and weathering of petroleum in the marine environment have been reviewed by Jordan and Payne (1).

The importance of photochemical processes in the marine environment was reviewed during a workshop at Woods Hole Oceanographic Institution, sponsored by the NATO Scientific Affairs Program (2). Relevant data from previous petroleum-related laboratory and field studies had been compiled by

the senior author for summation at the NATO workshop. This article presents an updated review based on that earlier work.

Overview of laboratory studies

A summary of several photooxidation studies of crude petroleum is presented in Table 1. Types of petroleum, light sources, identified products, and the presence or absence of sensitizers are listed. Some of the experiments are slightly flawed because of the absence of an aqueous phase or because of the selection of light sources that generate wavelengths below those normally found in ambient sunlight (<295 nm).

TABLE 1

Selected studies of photooxidation of petroleum

Substrate	Products identified	Light source (wavelength)	Sensitizer used
Libyan crude	Aromatic (20%) and aliphatic acids (28%); alcohols (23%) and aliphatic ketones (18%)	> 200-nm Hg lamp, 400 W	—
Ixtoc I crude oil dissolved in heptane, then spread on seawater	nC_9 – nC_{11} fatty-acid methyl ester (FAME) + branched FAME, C_{11} and C_{12} alkylated naphthols, substituted benzoic acids (C_{11} – C_{16}), substituted phenanthroic, benzothiophenoic, and dibenzothiophenoic acids.	Sunlight	No
No. 2 fuel oil layered on water (1:40 oil:water)	Highly alkyl substituted hydroperoxides, phenols, and carboxylic acids (benzoic and naphthanoic). Extensive work with tetralin hydroperoxide. Products separated into "very weak acid fractions"—hydroperoxides (benzylic, tetrahydronaphthol structures). "Weak acids"—alkylated phenols, tetrahydronaphthol backbones. "Strong acids"—alkyl-substituted benzylic acids.	> 280-nm Pyrex filtered Hg vapor lamp or sunlight (for algal studies)	Anthracene, pyrene, etc., present in oil necessary for O_2 generation

Nevertheless, a wide variety of substrates have been considered, and numerous oxidation products have been identified.

Photooxidation products. Berridge et al. (3) and Freearge et al. (4) suggested that acids, carbonyl compounds, alcohols, peroxides, and sulfoxides might result from the photooxidation of petroleum. Qualitative indications of the possible presence of alcohols, aryl and alkyl ethers, carbonyl compounds, and sulfoxides also were noted after infrared (IR) analysis by Kawahara (5). Frankenfeld cited evidence that water-soluble fractions (medium-molecular-weight aromatic alcohols and ethers) are significantly increased for oils in the presence of ultraviolet (UV) light in the aqueous phase beneath a slick composed of a variety of oils, including several Venezuelan crudes and No. 2 fuel oil (6).

Oil-specific differences in weathering behavior were noted when the elemental composition of fresh and weathered oils and aqueous extracts were compared after one day and after two to four months of weathering. Most of the compounds formed were identified as hydroxy compounds, including phenols, naphthols, phenanthrols, and ethers; IR data also suggested the presence of carboxylic acids.

Burwood and Speers simulated oil photooxidation of a paraffinic Middle Eastern crude spread on saline solution and exposed to direct sunlight for 72 h

(7). High levels of a water-soluble residue and a large unresolved complex mixture occurring between Kovats retention values (8) 1500 (corresponding to the normal, or straight-chain alkane nC_{15}) and 2300 (nC_{23}) that increased over a period of one month were apparent from gas chromatographic analyses of water extracts. A variety of thiocyclane-1-oxides (sulfoxides) were identified, and the authors noted the effectiveness of hydrogen peroxide for oxidizing crude oil thioalkanes. The reactivity sequence observed was cycloalkyl > dialkyl > alkyl-benzyl > alkyl-phenyl > diphenyl > thiophene > dibenzothiophene. Partly on the basis of this sequence, Burwood and Speers concluded that thiocyclane oxide formation may have accounted for the fact that about 15% of the less volatile sulfur compounds known to be present in Kuwaiti crude oil were absent from samples collected after the *Torrey Canyon* incident in March 1967. This involved a large spill of crude petroleum from a supertanker that foundered off the coast of Cornwall, England (9).

Viscosity changes. Berridge et al. (3) and Klein and Pilpel (10) were among the first to suggest that photooxidation may alter oil viscosity and water-in-oil emulsification tendencies and that these changes could subsequently affect the spreading properties of various crudes. Several crudes were tested, including a low-boiling Tijuana crude,

a high-boiling Tijuana residual, a Libyan crude, and a Peruvian crude. The researchers used a photosensitizer, 1-naphthol, and a mercury arc with a light filter to remove wavelengths < 305 nm.

Results indicated that viscous oils behave differently from nonviscous oils as photooxidation proceeds and that oils may actually contract rather than spread after initial photooxidation. Changes of about 10% in the diameter of the floating oil lens occurred within two hours of irradiation, when only small amounts of oxidation products had dissolved in the water. Effects of the sensitizer varied with the crude studied, but in general the sensitizer was shown to increase the rate of spreading or contraction of the crude in question. Also, the presence of 1-naphthol affected the total amount of photolyzed oil solubilized during the irradiation.

Weight percents of oils solubilized in the presence of 10^{-3} M 1-naphthol were less than $10^{-3}\%$ /h for Tijuana heavy and about $10^{-2}\%$ /h (over 4 h) for the more reactive Peruvian crude. This rate is equivalent to $10^{-8}\%$ /s in light. Thus, complete photooxidative solubilization of Peruvian crude in an environment illuminated one-third of the time could occur within an extrapolated turnover time of 100 years (11). Decreases in lens diameter following irradiation of the heavier crudes were attributed to the inability of the photo-

Mechanisms proposed	Reaction rates (kinetics) identified	Comments
Yes; light absorption by aromatics — radicals III · H abstraction → radical + O ₂ — peroxy-radical · + ROOH — + ·OH HO· + <i>n</i> -alkanes → R· + ROH	—	19-d constant irradiation. Thick and thin lenses noted with higher MW components in thicker lenses. <i>n</i> C ₈ reduced to <1% of initial value. Photooxidation of oil with <300 nm <i>hν</i> increased by 100×. Aromatic and aliphatic acids quite H ₂ O-soluble; therefore, further CO ₂ loss unlikely. Oxidation products surface active and may enhance water-in-oil emulsions and oil-in-water dispersions (13, 14).
Intermediate aromatic hydroperoxides involved in FAME formation, as opposed to direct ³ O ₂ interaction. Rather propose ³ O ₂ (ox) or free-radical reaction. No attempt made to assess rates or total amount of hydrocarbons removed by this process.	No	Photooxidation products in seawater and oil samples (flakes) collected near wellhead and from rooftop aquarium systems with fresh Ixtoc crude and artificial seawater (4-d exposure, New Orleans, La.). H ₂ O samples from wellhead yielded FAMES and phthalate esters (limited sample size precluded further identifications) (35).
Yes. ¹ O ₂ + 2,3-dimethyl indene (or phenols), H-abstraction ↓ hydroxy radicals; other products ↓ H-abstraction aromatic substances.	Yes. ROOH concentration in H ₂ O over time; reported linear increase over first 108 h. Initially ROOH in oil phase, then partitioned into H ₂ O.	Hydroperoxides not analyzed directly, converted to alcohol by addition of thiocyclopentane. Peroxide content determined iodometrically. Toxicity to yeast and algae: hydroperoxide > carboxylic acids > phenols (37).

oxidation products formed at the oil-air interface to diffuse through the viscous oil layer and to be removed from the oil-water interface.

The accumulation of photooxidized reaction products at the exposed surface of the oil lens also was believed to lead to polymerization, which caused an increase in the oil-air interfacial surface tension and consequent contraction of the lens. This process was then postulated to lead to formation of the intractable tarry residues observed at sea and perhaps to enhance water-in-oil emulsification attributable to the formation of surfactant materials required to prevent water droplet coalescence in the more stable emulsions.

Photooxidation reactions. In a study of the effect of 1-naphthol on the photooxidation of alkyl benzenes, Klein and Pilpel reported that alkyl-substituted benzenes with active hydrogens were susceptible to oxidation (12). In the presence of oxygen, 1-naphthol acts as a photoinitiator responsible for removing active hydrogens, thereby yielding a hydroperoxide, which decomposes to a benzoic free radical and peroxide radical. These compounds decompose further to other oxygenated degradation products, as shown in Figure 1.

The 1-naphthol initially forms a naphthoxy radical, which acts as an initiator for the photooxidation of alkylbenzenes. After the naphthol decomposes, however, free radicals can continue to react via other chain reac-

tions. Reactions of free radicals generated in situ are rate determining and self-sustaining even after the naphthol has been removed. At that point, the reaction ceases because aryl-ethers and and carboxyl products combine with the remaining peroxide to form volatile or inactive products. The importance of a reactive benzylic hydrogen for 1-naphthol sensitization was shown by comparing rates of oxidation of *sec*-butylbenzene and *tert*-butylbenzene in the presence and absence of 1-naphthol.

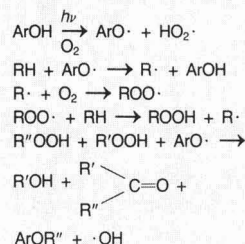
Hansen irradiated a Libyan crude oil with light from a mercury lamp at wavelengths >200 nm (13). Most experiments were completed at wavelengths shorter than those normally encountered in ambient sunlight. Ratios of C—H stretch and C=O stretch in infrared analysis were used to examine percent oxidation. Individual chromatographic ratios of pristane/*n*C₁₇ and phytane/*n*C₁₈ also were reported. Under these conditions, free radicals may have formed that were capable of abstracting hydrogens from tertiary carbon atoms. The ratios of branched isoprenoids to straight-chain alkanes confirmed this prediction.

Hansen observed that when substrates were irradiated with wavelengths <300 nm, the levels of oxidation products in water were one or two orders of magnitude higher than levels obtained when substrates were irradiated with longer wavelengths (>300 nm) (14). When longer wave-

length sunlamps were used, the same oxidation products were isolated but at considerably lower levels and at decreased rates. About 100 carboxylic acid products were identified as their methyl esters by gas chromatography (GC) and gas chromatography-mass spectrometry (GC/MS). In addition, the formation of salicylic and phthalic acids, as well as alcohols and ketones, was reported.

Hansen calculated that a 0.4-mm surface film of hydrocarbons could be de-

FIGURE 1
Photooxidation of alkylbenzenes^a



Where ArOH = 1-naphthol and R' and R'' are radicals with fewer carbons than R

^aInitiated by 1-naphthol
Reprinted with permission from Reference 12.
Copyright 1974, American Chemical Society

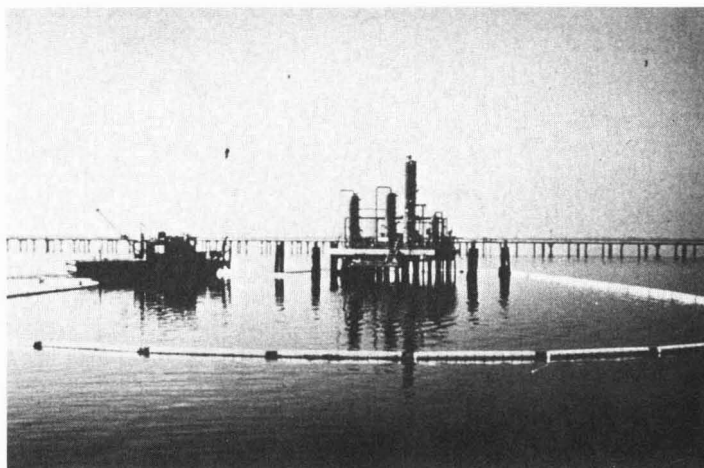
graded photochemically under *natural* conditions at a rate of 0.07%/d. At this rate, periods of more than three years would be required for complete photochemical degradation. However, under natural turbulent conditions, the surfactant molecules generated by this process may enhance dispersion of oil droplets, thereby significantly decreasing their residence time.

Hansen also noted that alkanes were oxidized, but only to their carboxylic acids, which were then removed from the oil film and dissolved in the water—where further photooxidation would be inhibited. Significant levels of benzoic acids were obtained, presumably from the decomposition of alkyl-substituted benzenes, but it was not clear from the experimental evidence whether the formation of salicylic acids or phthalic acids was from oxygen-containing precursors or from the double oxidation of alkyl-substituted benzenes. The formation of salicylic acids is important because of their bacteriostatic activity (14, 15).

Larson et al. spread No. 2 fuel oil (77% aliphatic, 23% aromatic) over a Pyrex pan and irradiated the oil with light from a mercury vapor lamp at wavelengths >280 nm (16). The oil was *not*, however, spread on water. A turbid, resinous precipitate coalesced after approximately 12 h and settled out of the oil after 3 d.

In an early experiment in which Larson et al. initially placed the oil on water, the precipitate evidently was extracted into the aqueous phase (16). Later chloroform extraction of the water yielded material that gave an IR spectrum identical to the oil-insoluble precipitate obtained in the experiment. Concentrations of carbonyls and phenols increased linearly in 7 d, and it was inferred that hydroperoxides form rapidly as initial oxidation products (as determined by sulfoxide formation upon addition of thiocyclohexane). Additional products identified included benzylic carbonyl compounds, lactones, hydroxyaromatic acids, and polyphenols.

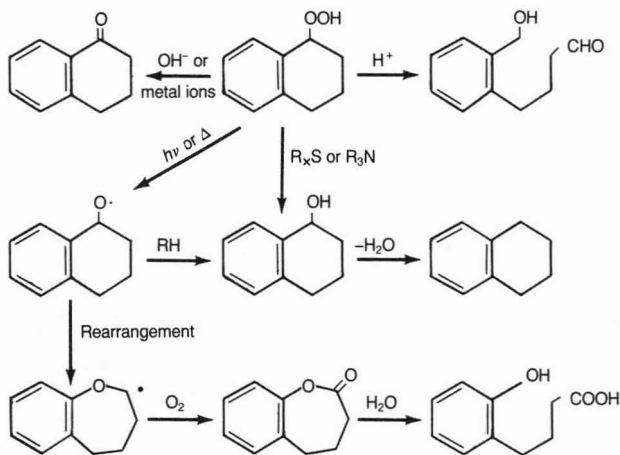
Larson et al. investigated the formation of a number of hydroperoxides from individual petroleum constituents (17). In tests of a variety of individual components, including tetralin, indan, fluorene, acenaphthene, *para*-cymene, ethylbenzene, 1,2,4-trimethylbenzene, and isooctane, only the first four components were susceptible to hydroperoxide formation. Each of these compounds has benzylic hydrogens in a ring system, which appears to be necessary for hydrogen abstraction and peroxide formation. The degradation pathway of organic hydroperoxides, which is exemplified by tetralin, is presented



Oil spill containment could retard the spread of photooxidation products

FIGURE 2

Degradation pathways for organic hydroperoxides^a



^aExemplified by tetralin hydroperoxide

Reprinted with permission from Reference 17. Copyright 1976, American Institute of Biological Sciences

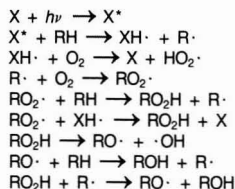
in Figure 2. Larson et al. postulated the formation of a variety of products including phenols, lactones, hydroxy acids, aldehydes, hydroxy aldehydes, and tetralin-substituted alcohols.

Gesser et al. investigated the photooxidation of *n*-hexadecane sensitized by xanthone (18). Hexadecanol was the major product identified, although peroxides were detected at concentrations approximately 1% of that of the alcohol. Less effective sensitizers studied included chloranil, anthraquinone, carbazole, 1-naphthol, triphenylamine, 2'-acetoneaphthone, 1-cyanonaphthalene, and thioxanthone. Gesser et al. suggested a mechanism by which a xanthone triplet abstracts a hydrogen atom

from a hydrocarbon to start a free-radical chain process (Figure 3).

Patel et al. investigated oxygenated products generated from photooxidation of phenanthrene under simulated environmental conditions (19). In these studies, phenanthrene was dissolved in hexane, floated on water, and photolyzed with a 500-W tungsten lamp with a uranium glass filter. Several oxidation products were identified by GC/MS. Patel's experiments were conducted in the presence of the sensitizer methylene blue, which was used to generate singlet oxygen. Patel et al. also photooxidized both an Arabian medium crude oil and oil from the *Amoco Cadiz* spill (the *Amoco Cadiz* was wrecked off the

FIGURE 3

Type 1 photosensitized oxidation of hexadecane

X = xanthone; X* = xanthone triplet;
RH = *n*-hexadecane.

Reprinted with permission from Reference 18.
Copyright 1977, American Chemical Society

coast of Brittany, France, in March 1978) in the presence of molecular oxygen and perylene (a naturally occurring polynuclear aromatic hydrocarbon [PAH] that can act as a photosensitizer) (20). They isolated a variety of dibenzothiophene oxides and alkyl-substituted dibenzothiophene oxides.

Reactions in sunlight. Zepp and Schlotzhauer studied the attenuation of solar radiation in a water body (21). Decreases in direct photolysis rates with increasing depth were more pronounced for those PAHs that absorbed shorter wavelengths than for PAHs that absorbed light at relatively longer wavelengths. Although calculations indicate that photoreactions of many PAHs are relatively rapid throughout the upper (35 m) mixed layer of the ocean, photolysis is greatly slowed in

Photoreactivity of 13 PAHs

Zepp and Schlotzhauer examined the photoreactivity of 13 PAHs, using 313-, 366-, and 436-nm wavelength light (21). Kinetic data for the direct photochemical reactions in water for all aromatics were described by a first-order rate equation. Disappearance quantum yields (ϕ_r) were determined at the wavelength corresponding to that of maximum sunlight absorption for the specific PAH. Most of the ϕ_r values were in the 0.001–0.01 range.

Near-surface half-lives for direct photochemical transformations at 40 °N latitude (midday, summer) were calculated as follows:

naphthalene 71 h
2-methylnaphthalene 54 h
1-methylnaphthalene 22 h
fluoranthene 21 h
phenanthrene 8.4 h
chrysene 4.4 h
anthracene 0.75 h
pyrene 0.68 h
benz[a]anthracene 0.59 h
benzo[a]pyrene 0.54 h
9,10-dimethylantracene 0.35 h
9-methylantracene 0.13 h
naphthacene 0.034 h

Half-lives computed for *photosensitized oxygenation* of most of the aromatics were many orders of magnitude longer, and several reactions proceeded in the absence of molecular oxygen. The authors concluded that singlet oxygen accounts for only a small fraction of photoreaction of dissolved PAHs in water.

turbid water because of light attenuation and partitioning of aromatics onto suspended particulate matter (SPM) and bottom sediments. Photolysis rates in turbid water also are reduced for those higher molecular weight aromatics having the greatest tendency to adsorb onto the SPM.

Mill et al. also carried out photolysis of eight PAHs in water and attempted to predict the rate loss of these compounds in sunlight (22). Using methods of Zepp and Cline (23), Mill et al. calculated rate constants and half-lives of the components undergoing photolysis in sunlight as a function of season at 40 °N latitude. The quantum yield, ϕ , was calculated from the relation:

$$\phi = k_p / 2.3\epsilon I_0 r \quad (1)$$

where ϵ is the molar absorptivity, I_0 is the solar irradiance, and r is a reactor constant.

Rate constants generated in the experiments were after a form of the relation equation developed by Zepp and Cline (23):

$$k_{pE} = 2.3\phi_r \Sigma I_{0\lambda} \epsilon_{\lambda} \quad (2)$$

where k_{pE} is the first-order rate constant (s^{-1}), and $I_{0\lambda}$ is the solar irradiance in surface water (in einstein/L·s) at each wavelength at which absorption is measurable. Estimated quantum yields were generally in the 10^{-2} to 10^{-4} range at extremely low PAH concentrations in water–acetonitrile (10^{-6} to 10^{-8} M). Rate constants were obtained for various seasons, and all data were used to estimate half-lives for component-specific decompositions.

As Zepp and Cline have noted, this approach suffers from several limitations, including the following (23):

TABLE 2

Calculated and measured rate constants for photolysis of aromatics in sunlight at 40 °N latitude^a

PAH	Measured season	Winter	Spring	Summer	Fall	Summer k_{pE} /winter k_{pE}
Benz[a]anthracene	6.0×10^{-5} (spring)	1.4×10^{-4}	2.2×10^{-4}	3.8×10^{-4}	2.2×10^{-4}	2.7
Benzo[a]pyrene	1.8×10^{-4} (winter)	1.8×10^{-4}	2.8×10^{-4}	3.9×10^{-4}	2.3×10^{-4}	2.2
Quinoline	4.0×10^{-7} (summer)	5.0×10^{-8}	2.3×10^{-7}	3.6×10^{-7}	1.3×10^{-7}	7.2
Benzo[f]quinoline	3.7×10^{-4} (summer)	1.5×10^{-4}	2.4×10^{-4}	4.8×10^{-4}	2.0×10^{-4}	3.2
9H-Carbazole	6.6×10^{-5} (winter)	6.5×10^{-5}	1.0×10^{-4}	2.0×10^{-4}	9.0×10^{-5}	3.1
7H-Dibenzo[o,g]carbazole	5.2×10^{-4} (winter)	2.3×10^{-4}	3.9×10^{-4}	5.0×10^{-4}	3.2×10^{-4}	2.2
Benzo[b]thiophene	6.9×10^{-7} (summer)	2.3×10^{-8}	2.7×10^{-7}	5.7×10^{-7}	1.2×10^{-7}	25
Dibenzothiophene	1.0×10^{-6} (spring)	2.9×10^{-7}	1.1×10^{-6}	1.5×10^{-6}	9.1×10^{-7}	5.2

^a k_{pE} in s^{-1}

Source: Reference 22

- Exposure to the sun and whole sky at sea level is assumed. Clouds reduce UV intensity by approximately 50% when the sky is overcast; intensity increases by about 15–20%/km increase in elevation.
- Daily variations in atmospheric ozone can be as high as 30% in midlatitudes. Deviations can affect computed rates, although they do not affect pollutants that absorb sunlight most strongly at wavelengths > 320 nm. Computations further assume that natural organics and humic materials in the water act only as photochemically inert sun screens. The equations do not account for sensitization by humic substances that could further enhance free-radical reactions.
- Effects of light scattering in water bodies also are ignored; they could be important in turbid water.

Miller and Zepp reported that photolysis rates of certain compounds may be altered in turbid waters because of increased light scattering and attenuation (light screening) (24). Zepp and Schlottzauer also measured decreased photoreactivities for several higher molecular weight PAHs adsorbed onto SPM and sediments (21).

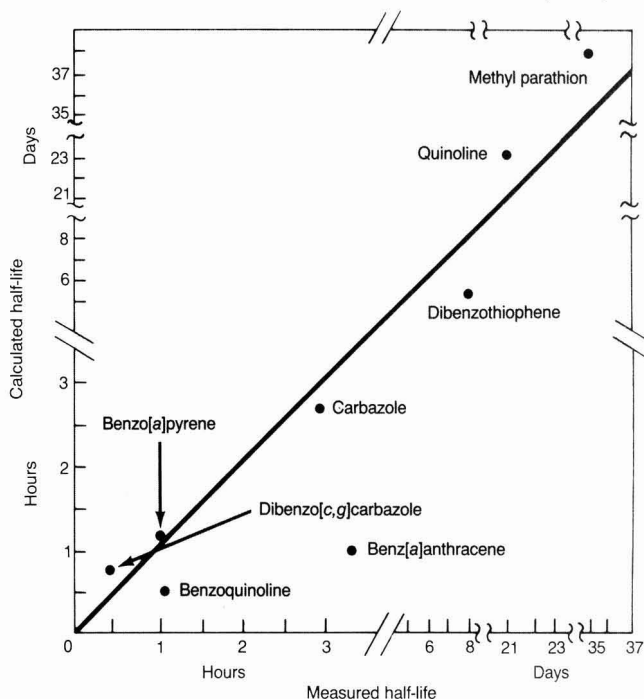
Nevertheless, this technique appears to be a reasonable approach because rates are computed from reproducible, readily obtainable data, such as the estimated quantum yield for the reaction and the electronic absorption spectrum of the pollutant of interest. With this approach, Mill et al. obtained half-lives for benz[a]anthracene and benzo[a]pyrene of from < 1 h to 5 h (22). Longer half-lives were computed for quinoline (25 h), benzoquinone (14 h), and benzothiophene and dibenzothiophene (28–94 h) at initial concentrations in the range of 10^{-6} to 10^{-8} M. Table 2 presents measured seasonal rate constants for various components and estimated rate constants in winter, spring, summer, and fall for eight PAHs. Figure 4 presents a comparison of measured vs. calculated half-lives for direct photolysis of a variety of PAHs.

Compounds affecting photooxidation

Inhibition of photooxidation product formation has been demonstrated for two components: sulfur compounds and β -carotene. High levels of organo-sulfur compounds, particularly thioclanes (thioclanes), are common to many crude oils. Thioclanes are effective inhibitors of radical reactions because of their propensity to form thiocyclane oxides (16). Sulfides are rapidly converted to sulfoxides by hydrogen peroxides and photooxidation. Thus, preliminary evidence that the toxicity of Nigerian crude oil is not

FIGURE 4

Comparison of measured and calculated half-lives for direct photolysis



Reprinted with permission from Reference 22. Copyright 1981, Pergamon Press

PAH photooxidation products

Mill et al. identified a number of photooxidation products (22); however, they obtained complete product balance and identification for benzo[a]pyrene only. A 1:3 ratio of 3,6- and 1,6-benzo[a]pyrene quinones and only a trace of 6,12-quinone were found. Other photolysis mixtures at low conversion of PAHs were analyzed by high-performance liquid chromatography (HPLC) and field ionization mass spectrometry (FIMS) with the following results:

Benzo[a]anthracene. Three products were observed by HPLC, one of which, 7,12-benzo[a]anthracene quinone, accounted for 30% of the substrate photolyzed. The other two products were not identified.

Benzo[f]quinoline. Photolysis in water gave two products that were not identified; different products were found when photolyses were performed in acetonitrile or methanol.

9H-carbazole. Seven major HPLC peaks were observed after photolysis, even at low conversions. FIMS of the mixture gave peaks of 171, 183, 197, 199, 332, 348, and 364 daltons (9H-carbazole has a peak at 197 daltons). These peaks are tentatively taken to correspond to a carbazole monomer and dimer with added hydrogen and oxygen.

7H-dibenzo[c,g]carbazole. Two primary products were separated by HPLC and later subjected to FIMS. The only distinguishing features of the major product spectrum were an apparent molecular ion at 299 daltons and peaks at 270 and 271 daltons. They suggested the presence of at least one phenolic group (25). The spectrum of the major product was compatible with that of a dihydroxylated dibenzocarcbazole; however, no silylated derivative of this product could be obtained.

Dibenzothiophene. Photolysis gave five early eluting, primary products, which were found by HPLC analysis. Attempts to characterize these products by means of GC/MS were unsuccessful. Decomposition of possible sulfoxide products during GC/MS analysis may have been partially responsible, as similar dibenzothiophene sulfoxide instability was reported by Patel et al. (20) following analysis of irradiated Amoco Cadiz oil.

greatly affected by exposure to light could be ascribed to high levels of sulfur in the crude, as compared with refined products (16).

Larson and Hunt examined the role of singlet oxygen and inhibition of photooxidation of refined petroleum by β -carotene (26). Their studies suggest that the presence of singlet oxygen may be required for peroxide formation and for the subsequent breakdown of hydroperoxides via radical and ionic pathways, which lead to the formation of other types of oxidation products. To verify this hypothesis, the researchers added β -carotene to solutions of oil in which singlet oxygen formation might be expected (26). Inhibition of photooxidation for up to 210 h was observed under these conditions. Thus, by quenching singlet oxygen generation at a diffusion-controlled rate, β -carotene appeared to prevent the initiation process for, and almost completely inhibited formation of, photooxidation products. When β -carotene was added to oil that had been photolyzed for 54 h, a slight delay in additional peroxide formation was noted. However, the authors presume that the effect was caused by oxidative destruction of β -carotene, rather than radical quenching activity.

A number of sensitizers have been implicated in photooxidation reactions involving a variety of oils and specific compounds and their oxidation products. Klein and Pipel used 1-naphthol as a photoinitiator for removal of active hydrogens. This yielded a hydroperoxide that decomposed to a benzylic free-radical and peroxide radical (12). Likewise, Gesser et al. used xanthone to show that photoexcitation to a xanthone triplet was implicated in the abstraction of a hydrogen atom from the substrate to initiate the free-radical oxidation of *n*-hexadecane (18).

Natural substances in marine waters also affect photooxidation reaction mechanisms to different degrees. Mill et al. observed that dissolved humic acid and oxygen in the presence of petroleum substrates produced a variety of effects, including both inhibition and acceleration of photooxidation rates (22). In these studies, absorbance by natural waters did not exceed 5% attenuation at the 366-nm wavelength over the 1-cm pathway used for the photolysis experiment. When 8–12 μ g of humic acids was added to 1 mL of seawater, a 30–37% attenuation in the light was observed, and concomitant reductions in photooxidation rates were predicted.

Most of the eight aromatics considered by Mill et al. did exhibit a large reduction in the photooxidation rate, indicating that both light screening and quenching may be occurring. However,

quinoline photolyzed much faster in sunlight on addition of humic acid, which suggests that sensitization may have occurred.

The effects of oxygen on rate constants varied for photolysis of the eight PAHs. For dibenzothiophene and 7H-dibenzo[*o,g*]carbazole, nitrogen purge of the aqueous solutions had no significant effect on the photolysis rate constant. For benz[*a*]anthracene and benzo[*a*]pyrene, purging with nitrogen strongly inhibited photolysis, whereas purging benzo[*b*]quinoline with oxygen significantly accelerated photolysis.

Zepp and Schlotzhauer observed photoreactivities for 9-methylanthracene in water that were identical in the presence and in the absence of dissolved oxygen (21). In their study of the photoreactivities of 11 PAHs, they also concluded that singlet oxygen accounted for a negligible fraction of the photoreaction of individual compounds dissolved in water. Zepp and Schlotzhauer did point out, however, that this situation may not apply to photoreactions in petroleum slicks on the water surface.

Although they were not specifically investigating petroleum hydrocarbon products, Zepp and Cline observed that pure water and river water containing humic substances show reduced photolysis rates of UV-sensitive compounds because UV radiation is absorbed more strongly by these materials than is visible light (23). The presence of humic acids has a less significant effect on photolysis rates of compounds in the visible and longer UV wavelength region.

Zepp et al. reported that humic substances could photosensitize transformations of several organic compounds that did not ordinarily undergo photochemical reactions in distilled water (27). This photosensitization process is significantly different from photolysis, which causes compounds to absorb light directly. In these studies, dimethylfuran (DMF) was involved in a rapid intermediate step in which energy absorbed by humic substances was transferred to molecular oxygen to form singlet oxygen, which then oxidized the substrate. Zepp et al. hypothesized that humic substances are first excited to a singlet state in which intersystem crossing occurs in the triplet, and then the triplicate energy acceptor material reacts with ground-state triplet oxygen to yield singlet oxygen.

A variety of compounds were investigated, including DMF, aniline, and *cis*-1,3-pentadiene. Several commercial humic and fulvic acids were examined, and kinetic data were presented. Solutions of *cis*-1,3-pentadiene, a known acceptor of triplet energy transfer reac-

tions, were used to monitor isomerization to the trans compound to demonstrate further the importance of the humic triplet.

No detectable isomerization occurred when solutions of distilled water and *cis*-pentadiene were exposed to sunlight. However, isomerization to a mixture of 56% *trans*-pentadiene and 44% *cis*-pentadiene was observed in solutions of humic acid in river water. The same mixture formed when *para*-trimethylammoniumbenzophenone chloride, a known triplet energy donor, was used as a photosensitizer.

In another study that used DMF in varying concentrations, Zepp et al. reported that reaction rates were directly proportional to both the average light intensity and the concentration of humic substances (28). In these systems, it was determined that at low pollutant concentrations, photosensitized reactions were first-order with respect to the pollutant (27, 28). First-order rate constants were directly proportional to the sensitizer concentrations, and in systems that weakly absorb light, reactions became independent of the photosensitizer concentrations when all active light was absorbed.

Baxter and Carey also used oxidation of 2,5-dimethylfuran to *cis*-1,2-diacetylene as a specific test for singlet oxygen in the presence of humic substances (29). Additional photochemical reactions mediated by singlet oxygen included oxidation of histidine and inactivation of α -chymotrypsin in humic-acid-containing waters. Mabey et al. examined photolysis of 2,4,6-trinitrotoluene (TNT) in the presence of humic acids and showed that humic materials in solution appear to affect photooxidation (30). Evidence of indirect photolysis showed that humic substances absorb light and then induce further reaction of the chemical substrate.

As noted by Zepp and Cline (23) and Zepp et al. (27, 28), photodecomposition of TNT generally showed first-order kinetics for oxidation. Thus, although mixed results were obtained by Zepp and Schlotzhauer (21) and Mill et al. (22) with a variety of PAHs in water, the potential for humic-acid-sensitized oxidation of water-soluble aromatic hydrocarbons appears viable and warrants further study.

Mechanisms of photooxidation

Numerous pathways have been suggested for the photochemical oxidation of petroleum components. As shown in Figures 1–3, these pathways include free-radical oxidations in the presence of oxygen, the implication of singlet oxygen in hydroperoxide formation, and ground state triplet oxygen combin-

ing with hydrocarbon free radicals to yield peroxides (14, 17, 18, 26, 31). Along with mechanisms already discussed, two additional reaction pathways, shown in Figure 5, illustrate the variety of photosensitized and free-radical pathways believed to be important for the oxidation of aliphatic and aromatic petroleum products.

Data illustrating the importance of alkyl-peroxy radicals and alkyl-hydroxy radicals in aqueous solutions have been provided by Mill et al. (32). In their study, pyridine and isopropylbenzene were photolyzed in dilute aqueous solutions, and products characteristic of reactions with alkyl peroxides and hydroxyl radicals were formed. Proportions of side chain and ring rotation products with the substrates used indicated that both $\text{RO}_2\cdot$ and $\text{HO}\cdot$ were required. In their experiments, Mill et al. used pyridine as a probe for those free-radical components. Pyridine reacts slowly with $\text{RO}_2\cdot$ to give pyridine-N-oxide, whereas the hydroxy radical generates hydroxy pyridine and other polar products but not N-oxide.

In aerated waters illuminated either by a xenon lamp or by sunlight, both pyridine-N-oxide and hydroxy pyridine were formed in small amounts, together with large amounts of polar products. Kinetic equations were derived for the disappearance of cumene by reaction with $\text{RO}_2\cdot$ and $\text{HO}\cdot$, and rate constants were determined for the reaction of pyridine with $\text{RO}_2\cdot$. An average radical concentration in steady-state systems was estimated from integration of these rate constants. Fairly close agreement for $\text{RO}_2\cdot$ radical values was obtained with both the cumene and pyridine probes, indicating that values were reproducible.

Steady-state $\text{RO}_2\cdot$ concentrations of 10^{-9} mol/L and steady-state $\text{HO}\cdot$ concentrations of 10^{-17} mol/L were determined. Half-lives were estimated for other components, as was their reaction with $\text{RO}_2\cdot$ in aqueous systems. In general, only the most reactive chemicals were labile under $\text{RO}_2\cdot$ attack; half-lives of a few days or less were predicted for phenols, aromatic amines, hydroxyl amines, and hydroquinones. Despite the high reactivity of $\text{HO}\cdot$, the very low steady-state concentrations measured suggested that $\text{HO}\cdot$ may not be important in the aquatic oxidation of organic compounds. Given the $\text{HO}\cdot$ concentration measured in this experiment, the half-life of even the most reactive structures was estimated to be at least 80 d.

Quantum yields for the photooxidation of a variety of aromatic compounds have been estimated by Mill et al. (22). Estimated quantum yields in the range of 10^{-2} to 10^{-4} at extremely low con-

centrations (10^{-6} to 10^{-8} M) were obtained for eight PAHs in a variety of water and acetonitrile solvents. Zepp (33) and Zepp and Schlotzhauer (21) also investigated quantum yields for reactions of pollutants, including 13 PAHs, in dilute aqueous solutions; similar values were obtained.

Zepp and co-workers developed the most comprehensive set of kinetic equations for predicting photolysis rates and half-lives, based on the compounds' absorption spectra, quantum yields for reactions, and pollutant concentrations (23). Thus, when the light intensity, extinction coefficient for the pollutant of interest at a given wavelength, and path length for photooxidation are known, quantum yields can be computed from a first-order plot of the logarithm of pollutant concentration vs. the exposure time.

The authors derived the following equation for predicting half-lives of organic compounds in near-surface waters:

$$t_{1/2} = \frac{0.693}{k_a \phi} = \frac{0.693j}{2.023 \phi \Sigma \epsilon_{\lambda} Z_{\lambda}} \quad (3)$$

where Z_{λ} is the underwater solar irradiance at a unit wavelength interval centered on λ , and ϵ_{λ} is the average extinction coefficient at the wavelength interval. The value for j is 6.02×10^{20} photons/mol.

It was assumed that quantum yield is independent of wavelength in the region of sunlight absorption. This assumption is probably valid for most complex molecules in solution because photoreaction from second or higher electronic excitation states usually does not compete with rapid (radiationless) decay of excited molecules to their first excited state. For example, the disappearance quantum efficiency for fluoranthene drops sharply from wavelengths of 313 nm to 366 nm. However, fluoranthene is a nonalternant aromatic hydrocarbon; even at 313 nm, it is considerably less reactive than most other PAHs studied (21).

Photooxidation at spills

Specific photooxidation products have been identified in oil and water samples obtained during investigations of the *Amoco Cadiz* spill and at the Ixtoc I blowout. The latter was the rupture of an oil well in the Bay of Campeche, Gulf of Mexico, in June 1979, which spilled millions of barrels of crude petroleum into the gulf. Patel et al. identified a number of alkyl-substituted dibenzothiophene sulfoxides in oil samples collected from the vicinity of the *Amoco Cadiz* spill (20). Calder et al. also reported the occurrence of several dibenzothiophene sulfoxides in oil

samples collected near the *Amoco Cadiz* wreck (34).

During investigations of the Ixtoc I blowout, Overton et al. identified a wide variety of oxidation products from Ixtoc oil in rooftop aquarium studies (35). After fresh Ixtoc crude in hexadecane was layered on seawater and exposed to ambient sunlight for 4 d, a crust formation was noted on the surface of the oil, which was discolored by an orange-brown flaky material. Similar observations were made near the wellhead (36).

Gas chromatograms of the aliphatic fraction of the exposed and control Ixtoc oil showed that the control oil contained n -alkanes from $n\text{C}_{11}$ through $n\text{C}_{32}$, whereas photooxidized oil contained no alkanes below $n\text{C}_{15}$. Aromatic fractions of the control oil contained more aromatics of intermediate molecular weight, including alkyl-substituted naphthalenes. In general, these materials were absent from the photooxidized oil, although that oil did contain alkylated phenanthrenes and dibenzothiophenes at higher relative concentrations.

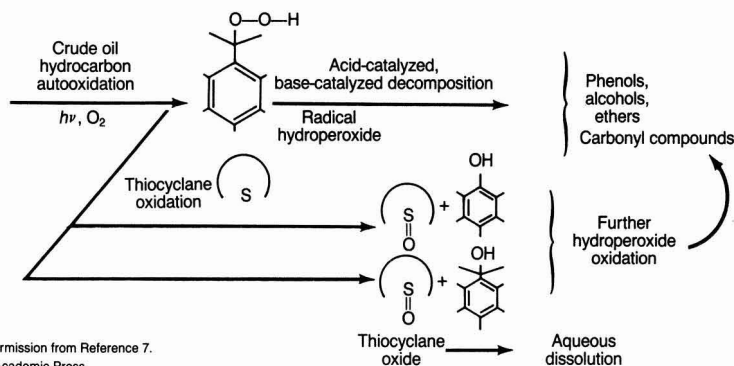
Acidified seawater extracts from the rooftop aquarium systems showed significantly greater complexity after photooxidizing treatment. Numerous C_{9-11} fatty-acid methyl esters (FAMES) were identified, in addition to a wide variety of methyl-substituted aromatic esters and benzylic methyl esters. The authors indicated that singlet oxygen usually is not directly involved in oxidation of saturated hydrocarbons, so other mechanisms were suggested to account for the formation of FAMES. One possible explanation may be the presence of oxidized aromatic intermediates, such as hydroperoxides, which could then interact with saturated hydrocarbons to form fatty acids, as described by Gesser et al. (18).

A number of benzoic acids, substituted naphthanoic acids, and phenanthroic, benzoanthroic, and dibenzothiophenoic acids also were present in the acidified seawater extracts. Side chain oxidation of C_1 - and C_2 -substituted naphthalene compounds also was observed. Each of these photooxidized components had enhanced water solubility and was removed from the slick and diluted in the water of the rooftop aquarium ecosystem used to test effects of these photooxidized materials.

Extracts of water samples obtained near the Ixtoc I blowout site contained a number of phthalate esters and FAMES. However, most of the extracts were obtained from 20-L water samples. This volume was not large enough for the identification of trace level organic compounds that would be generated from the photochemical oxidation of

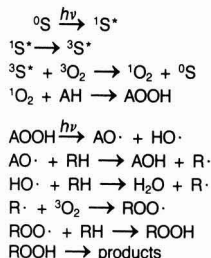
FIGURE 5
Additional mechanisms proposed for photooxidation of petroleum

(a) Suggested route for crude oil hydrocarbon and thiocyclane autooxidative process



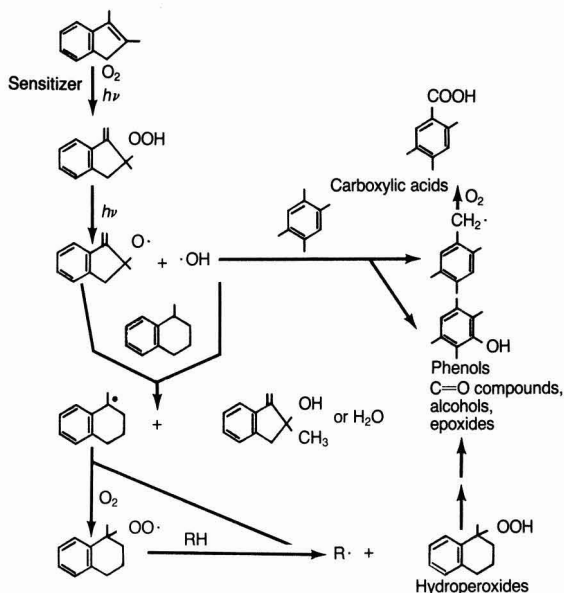
Reprinted with permission from Reference 7.
Copyright 1974, Academic Press

(b) Mechanisms, including singlet oxygen and radical processes, for the photooxidation of petroleum



Reprinted with permission
from Reference 26.
Copyright 1978, Pergamon Press

(c) Proposed mechanism for fuel oil photooxidation



Reprinted with permission from Reference 31. Copyright 1979, American Chemical Society

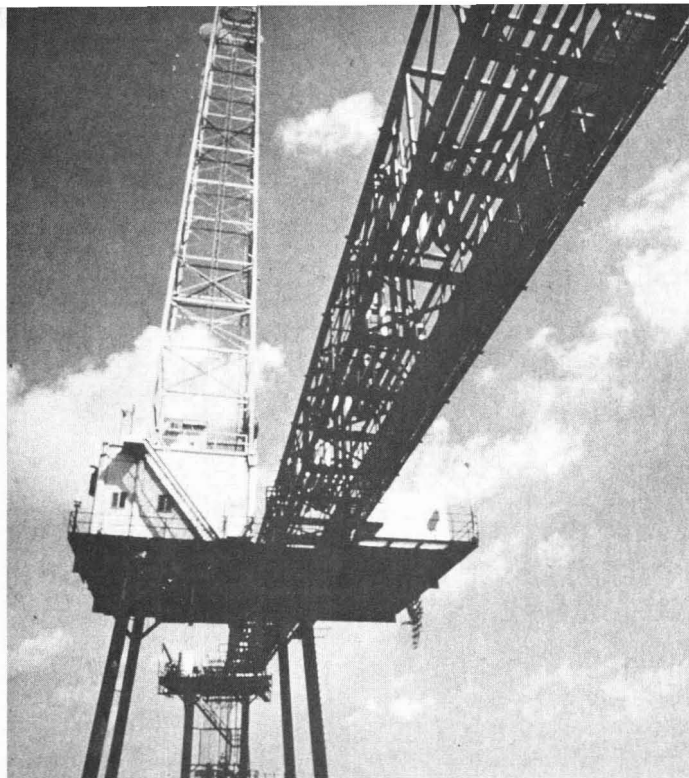
the Ixtoc crude. Overton et al. made no attempt to determine either the amount of petroleum removed by photochemical processes or rates at which these processes may have occurred under natural conditions in the Gulf of Mexico at the time of the incident.

Patton et al. performed a cursory examination of Ixtoc mousse and flakes isolated near the Texas coast and discussed photochemical oxidation of the surface of the emulsified oil (37). Den-

sity estimates indicated that the surface material would sink after sloughing off the main oil pancake. Surface flake material was depleted of *n*-alkanes below *n*C₁₆, but contained slightly higher levels of polar materials relative to components present in the interior of the mousse pancakes.

Thominette and Verdu reported that photooxidation of a light crude oil (Zarzaitine) under laboratory conditions results in phase separation because of

the formation of oil-insoluble, high-molecular-weight aromatic species (38, 39). The insoluble phase is distinguished as a colored, high-viscosity coating on the surface of photooxidized oil. This oxidized surface may be similar in composition and origin to the outer crust material of mousse and oil pancakes observed by Patton et al. in the Gulf of Mexico after the Ixtoc blowout (37). Thominette and Verdu suggested that photooxidation and



Petroleum that leaks from this well could be a source of photooxidation products

phase separation subsequently may alter the behavior of the oil spill under natural open-ocean weathering (38, 39). Similar conclusions were presented by Klein and Pilpel (10) and by Berridge et al. (3).

Photooxidative changes in oil

The results of previous research have demonstrated that photooxidation processes may have considerable importance in the long-term weathering of spilled oil, both by enhancing dissolution of products and by increasing the general toxicity of the water-soluble fraction. The majority of the products of photooxidation are removed from the parent oil by dissolution, which may represent losses of equal or greater magnitude than those associated with microbial degradation.

Photooxidation also is responsible for discernible changes in both the composition and physical properties of the exposed parent oil. Detectable increases in the nonvolatile residual fractions of weathered oil accompany increases in the water-soluble extractable components of the underlying waters. Changes in viscosity, spreading or contraction rates, and water-in-oil emulsification tendencies also may occur as a function of oil photooxidation. Observations from laboratory and field studies have shown that these changes can

occur at rates comparable to evaporation (depending on latitude and cloud cover) and at rates greater than microbial degradation processes.

Several mechanisms for the photooxidation of petroleum have been described, including free-radical oxidation in the presence of oxygen, singlet oxygen initiation of hydroperoxide formation, and ground state triplet oxygen combining with free radicals to form peroxides. Rates of photooxidation are considered to depend on wavelength but also are affected, to some extent, by turbidity levels and SPM concentrations (particularly for higher molecular weight aromatics). Photosensitized reactions are described by first-order kinetics.

The presence of inhibitors, such as sulfur compounds (e.g., thiocyclanes) or β -carotenes, can restrict the formation of radical species or inhibit singlet-oxygen-mediated peroxide formation. Humic substances can reduce the photolysis rates of UV-sensitive compounds, but they also photosensitize transformations of other organic compounds through an immediate transfer of energy to molecular oxygen.

Field studies at spills have detected the presence of several photooxidized products, including alkyl-substituted dibenzothiophene sulfoxides in oil samples and benzoic acids and fatty-acid

methyl esters in seawater extracts. These photooxidized compounds had an enhanced water solubility and consequently were removed from surface slicks and diluted in ambient waters.

Some caution is necessary in applying observations of photooxidative weathering behavior under laboratory conditions to predictions of oil weathering in the open ocean. For example, in several of the studies previously described, crude oils or petroleum products were photooxidized with artificial light from a variety of lamps and selective filters. These generated UV or visible light within narrow wavelength bands or at wavelengths appreciably shorter than that of solar radiation at sea level.

The selection of an appropriate light source for photooxidation studies is important because the fraction of light absorbed by varying hydrocarbon film thicknesses changes as a function of wavelength (4). Furthermore, interactions of oil and seawater often are simulated by layering crude oil or individual petroleum components on top of synthetic seawater mixtures confined within small glass vessels or aquaria.

These laboratory conditions are generally unavoidable and may even be necessary both to differentiate the effects of photooxidation from other weathering processes and to allow identification of photooxidation products. Under field conditions, simultaneous weathering processes can obscure the effects of photooxidation that contribute to progressive changes in the physical or chemical characteristics of the parent oil. In addition, sampling problems can occur because it is necessary to collect noncontaminated seawater in volumes large enough to allow isolation and identification of products that may be dissolved in trace quantities in the water beneath the oil slick.

Estimates of photolysis rates and quantum yields also can be affected by natural variations in cloud cover, atmospheric ozone, conditions affecting the transmittance of light in the water (such as turbidity), and levels of natural humic substances present. These variations, which are not accounted for in bench-scale experiments, may lower or raise predicted photooxidation rates for dissolved or particulate hydrocarbon compounds.

Additional research is needed to characterize the products derived from photooxidation of weathered oil, as well as their fate and chemical transformation. Similarly, additional data on the toxicity of such photochemical products are required to define the environmental effects of long-term weathering. Further study should reveal the possible effects of photooxidation proc-

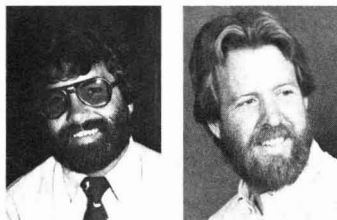
esses on water-in-oil emulsification. Continued work in these areas will improve the ability of future models to predict photochemical effects as they apply to oil weathering.

Acknowledgment

Before publication, this article was reviewed for suitability as an *ES&T* critical review by William R. Cherry, Louisiana State University, Baton Rouge, La. 70803 and Richard Lee, Skidaway Institute of Oceanography, Savannah, Ga. 31406.

References

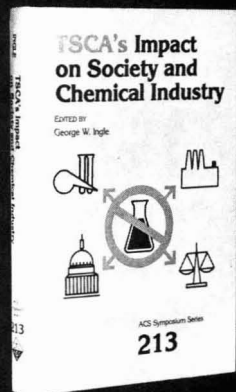
- (1) Jordan, R. E.; Payne, J. R. "Fate and Weathering of Petroleum Spills in the Marine Environment; A Literature Review and Synopsis"; Ann Arbor Science Publishers: Ann Arbor, Mich., 1980.
- (2) Miller, S. S. *Environ. Sci. Technol.* **1983**, *17*, 568-70A.
- (3) Berridge S. A. et al. *J. Inst. Petrol.* **1968**, *54*, 300-309.
- (4) Freegarde, M.; Hatchard, C. G.; Parker, C. A. *Lab. Pract.* **1971**, 20-4, 35-40.
- (5) Kawahara, F. K. *Environ. Sci. Technol.* **1969**, *3*, 150-53.
- (6) Frankendorf, J. W. In "Proceedings of Joint Conference on Prevention and Control of Oil Spills"; American Petroleum Institute: Washington, D.C., 1973; pp. 485-98.
- (7) Burwood, R.; Speers, G. C. *Estuarine Coastal Mar. Sci.* **1974**, *2*, 117-35.
- (8) Kovats, E. *Helv. Chim. Acta* **1958**, *41*, 1915-32.
- (9) Brunnock, J. V.; Duckworth, D. F.; Stephens, G. G. *J. Inst. Petrol.* **1968**, *54*, 325-40.
- (10) Klein, A. E.; Pilpel, N. *Water Res.* **1974**, *8*, 79-83.
- (11) Zafiriou, O. C., presented at the National Academy of Sciences meeting, "Petroleum in the Marine Environment," Washington, D.C., 1981.
- (12) Klein, A. E.; Pilpel, N. *J. Chem. Soc. Faraday Trans.* **1974**, *70*, 1250-56.
- (13) Hansen, H. P. *Rapp. P. V. Reun. Cons. Int. Explor. Mer* **1977**, *171*, 101-6.
- (14) Hansen, H. P. *Mar. Chem.* **1975**, *3*, 183-95.
- (15) Lacaze, J. C.; Villedon de Naide, O. *Mar. Pollut. Bull.* **1976**, *7*, 73-76.
- (16) Larson, R. A.; Hunt, L. L.; Blankenship, D. W. *Environ. Sci. Technol.* **1977**, *11*, 492-96.
- (17) Larson, R. A.; Blankenship, D. W.; Hunt, L. L. In "AIBS Symposium on Sources, Effects and Sinks of Hydrocarbons in the Aquatic Environment"; American Institute of Biological Sciences: Washington, D.C., 1976; pp. 298-308.
- (18) Gesser, H. P.; Wildman, T. A.; Tewori, Y. B. *Environ. Sci. Technol.* **1977**, *11*, 605-8.
- (19) Patel, J. R. et al. In "EPA Symposium on Carcinogenic Polynuclear Aromatic Hydrocarbons in the Marine Environment"; U.S. Environmental Protection Agency: Washington, D.C., 1978; pp. 1-32.
- (20) Patel, J. R.; Overton, E. B.; Laseter, J. L. *Chemosphere* **1979**, *8*, 557-61.
- (21) Zepp, R. G.; Schlotzhauer, P. F. In "Polynuclear Aromatic Hydrocarbons, Third International Symposium on Chemistry and Biology—Carcinogenesis and Mutagenesis"; Jones, P. W.; Labor, P. Eds.; Ann Arbor Science Publishers: Ann Arbor, Mich., 1979; pp. 141-58.
- (22) Mill, T. et al. *Chemosphere* **1981**, *10*, 1281-90.
- (23) Zepp, R. G.; Cline, D. M. *Environ. Sci. Technol.* **1977**, *11*, 359-66.
- (24) Miller, G. C.; Zepp, R. G. *Water Res.* **1979**, *13*, 453-59.
- (25) McLafferty, F. W. "Interpretation of Mass Spectra," 2nd ed.; W. A. Benjamin: New York, N.Y., 1973.
- (26) Larson, R. A.; Hunt, L. L. *Photochem. Photobiol.* **1978**, *28*, 553-55.
- (27) Zepp, R. G.; Baughman, G. L.; Schlotzhauer, P. F. *Chemosphere* **1981**, *10*, 109-17.
- (28) Zepp, R. G.; Baughman, G. L.; Schlotzhauer, P. F. *Chemosphere* **1981**, *10*, 119-26.
- (29) Baxter, R. M.; Carey, J. H. *Freshwater Biol.* **1982**, *12*, 285-92.
- (30) Mabey, W. R. et al. *Chemosphere* **1983**, *12*, 3-16.
- (31) Larson, R. A. et al. *Environ. Sci. Technol.* **1979**, *13*, 965-69.
- (32) Mill, T.; Hendry, D. G.; Richardson, H. *Science* **1980**, *207*, 886-87.
- (33) Zepp, R. G. *Environ. Sci. Technol.* **1978**, *12*, 327-29.
- (34) Calder, J. A.; Lake, J.; Laseter, J. In "The AMOCO CADIZ Oil Spill, a Preliminary Scientific Report"; National Oceanic and Atmospheric Administration-Environmental Protection Agency Environmental Research Laboratory: Boulder, Colo., 1978; p. 21.
- (35) Overton, E. B. et al. In "Proceedings of a Symposium on Preliminary Results from September 1979 Researcher/Pierce IXTOC I Cruise"; Office of Marine Pollution Assessment, National Oceanic and Atmospheric Administration: Key Biscayne, Fla., 1980; pp. 341-86.
- (36) Atwood, D. K.; Benjamin, J. A.; Farrington, J. W. In "Proceedings of a Symposium on Preliminary Results from September 1979 Researcher/Pierce IXTOC I Cruise"; Office of Marine Pollution Assessment, National Oceanic and Atmospheric Administration: Key Biscayne, Fla., 1980; pp. 1-16.
- (37) Patton, J. S. et al. *Nature* **1981**, *290*, 235-38.
- (38) Thominette, F.; Verdu, J. *Mar. Chem.* **1984**, *15*, 91-104.
- (39) Thominette, F.; Verdu, J. *Mar. Chem.* **1984**, *15*, 105-15.



James Payne (l.) is a senior chemist with the Applied Environmental Science Division of Science Applications International Corporation. He received his Ph.D. in chemistry from the University of Wisconsin—Madison in 1974 and completed a postdoctoral scholarship at Woods Hole Oceanographic Institution while investigating polychlorinated biphenyl and petroleum hydrocarbon pollution in the marine environment. He and Charles Phillips are coauthors of "Petroleum Spills in the Marine Environment," which is scheduled for publication by Lewis Publishers of Chelsea, Mich., in July.

Charles Phillips (r.) is a staff scientist with the Applied Environmental Science Division of Science Applications International Corporation. Phillips received an M.A. in marine science from San Francisco State University in 1978. His research includes biochemical cycling of organic material and the fate of organic pollutants in the marine environment.

TSCA's Impact on Society and Chemical Industry



George W. Ingle, Editor
Chemical Manufacturers Association

Identifies and evaluates major effects of Toxic Substances Control Act (TSCA) on the chemical industry and on society as a whole. Covers detection and analysis of these effects from a variety of viewpoints. Helps to delineate beneficial and detrimental consequences of this law.

CONTENTS

Background, Goals, and Resultant Issues • Impact on Market Introduction of New Chemicals • Future for Innovation • Harmonizing the Regulation of New Chemicals in US and EEC • Control of Existing Chemicals • Overview After Five Years • Initiatives of Chemical Industry to Modify TSCA Regulations • Management of TSCA-Mandated Information • Impact on Corporate Structure and Procedures • Confidentiality of Chemical Identities • Impact on Reactive Polymer Industry • Effects of TSCA on Metalworking Fluids Industry: Increased Awareness of Nitrosamine Contamination • Impact on Public Health • Quantitative Analysis as Basis for Decisions Under TSCA • Educating the Environmental Chemical Professional • Overall Costs and Benefits • Summary

Based on a symposium jointly sponsored by the ACS Divisions of Industrial and Engineering Chemistry, Chemical Information, Organic Coatings and Plastics Chemistry, Small Chemical Businesses, and the Board Committee on Corporation Associates

ACS Symposium Series No. 213
244 pages (1983) Clothbound
LC 83-2733 ISBN 0-8412-0766-6
US & Canada \$34.95 Export \$41.95

Order from:
American Chemical Society
Distribution Office Dept. 21
1155 Sixteenth St., N.W.
Washington, DC 20036
or CALL TOLL FREE 800-424-6747
and use your VISA or MasterCard.

Proposed air toxics legislation



Richard M. Dowd

Congressional concern over air toxics continues to shape the future regulation of sources of potential pollutants. Reps. Timothy Wirth (D-Colo.), Henry Waxman (D-Calif.), and James Florio (D-N.J.) are cosponsors of H.R. 2576, the Toxic Release Control Act of 1985 (TRCA), which they would like to see replace Section 112 of the Clean Air Act. H.R. 2576 outlines strategy for controlling specific potentially toxic pollutants, regulating certain sources of pollutant emissions to the air, and providing technical assistance to states for their own regulatory programs.

The legislation incorporates many earlier provisions of Section 112 and adds new ones. It covers 85 specific chemicals and groups of substances; methods for establishing standards; permit and reporting requirements, including citizens' right-to-know rules; regulations for monitoring; and schedules for compliance.

Control procedures

Several chemicals known to be seriously toxic, such as methylisocyanate, hydrogen cyanide, and phosgene, are listed in the 85 substances that TRCA cites as potentially hazardous. Many others that have been under EPA study, such as beryllium, asbestos, benzene, dioxins, and ethylene dibromide, are also included.

The new act would control several classes of emissions, including those from coke ovens, and radionuclides, polycyclic organic matter, and PCBs.

The bill's list of hazardous releases would be reviewed by the EPA administrator and possibly amended once a year, depending on whether additional substances were determined hazardous. The legislation states that the list of hazardous chemicals will include "each substance . . . released into the air and which causes or contributes to air pollution which may reasonably be expected to result in an increase in serious irreversible, or incapacitating reversible, illness." Carcinogenic substances—as defined by the National Toxicology Program, the International Agency for Research on Cancer, EPA's Cancer Assessment Group, or the National Cancer Institute—also would be included.

Other substances of concern, such as those listed by the Occupational Safety and Health Administration, those with established threshold level values, those cited under Superfund legislation, and all pesticides that have been classified for restricted use, would be considered as potentially hazardous substances. Each company producing these chemicals and each source operator would be required to provide EPA with an inventory of hazardous substances released into the air. The agency in turn would make these reports available to the public.

Section 204 of the proposed legislation would provide for the protection of trade secrets. In addition, source monitoring would be required to "quantitatively measure ambient concentrations of each hazardous substance released into the air." The agency would be required to provide "accurate, reliable, and representative data" on ambient concentrations of hazardous air pollutants in urban areas and near so-called hot spots within six months of the law's enactment.

Setting standards

To control ambient levels EPA would be required to regulate releases from

stationary sources. It also would be given the authority to establish requirements for leak prevention, detection, and plant safety and inspection. National standards would be established "at the level which, in the judgment of the administrator, provides an ample margin of safety to protect the health and safety of persons." Rigorous schedules and "fall back" provisions specify that if a standard for a given pollutant is not promulgated on schedule, the standard that then becomes applicable for that substance is one "which prohibits any detectable release."

EPA would have authority to propose interim national standards that would account for the technological ability to reduce emissions while protecting public health and safety. EPA also would be expected to issue permits for new and modified sources and for existing sources, which would be required either to receive a permit from the agency within 18 months of enactment or cease operating. In addition, TRCA seeks to regulate releases of hazardous substances from mobile sources.

The bill eliminates risk assessment from the determination of the hazard-ousness of a substance. It assumes that if a known carcinogen or other toxic substance is emitted into the air, that substance is a hazardous air pollutant subject to regulatory control, regardless of whether it poses a risk to human health or the environment via atmospheric exposure. In essence, the proposed legislation is a stringent national approach to the regulation of ambient hazardous air pollutants, rather than a strategy based on controlling high-risk substances from specific sources.

Richard M. Dowd, Ph.D., is a Washington, D.C., consultant to Environmental Research and Technology, Inc.

Blind technology transfer: The Bhopal example

In October 1981, the International Society for Tropical Ecology convened a special silver jubilee symposium in Bhopal, India. The theme of the meeting was, appropriately, "Ecology and Resource Management in the Tropics." Data from a multitude of environmental studies that had been completed on several continents were presented and discussed.

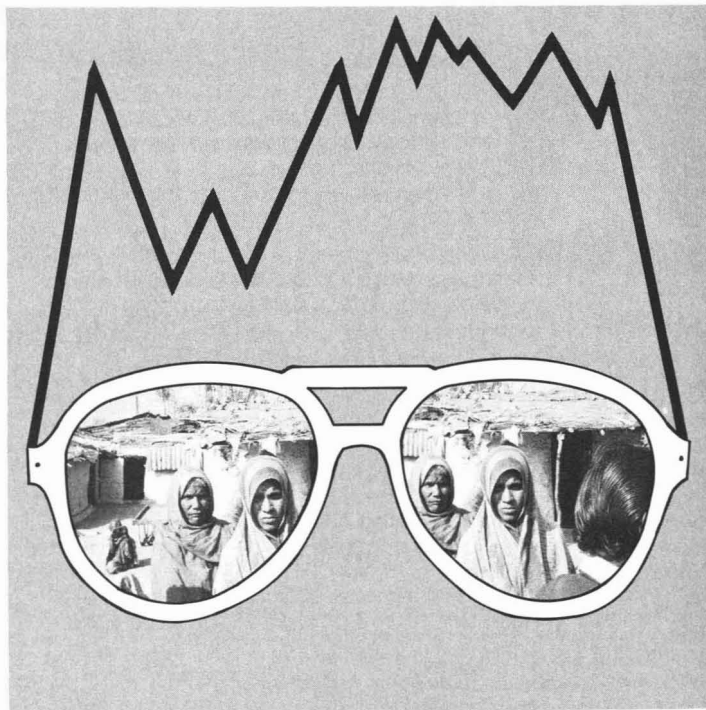
We scientists pondered most of the fundamental environmental questions. For example, what would be the result of the wide-scale use of agricultural chemicals in tropical, developing countries? We did not concern ourselves with producing chemicals, but rather with their potential use, transport, and effects on the environment. Producing chemicals was the domain of the chemical engineer—a technological rather than an ecological concern.

A small group of us was invited by environmental officials in Bhopal to participate in an expert panel discussion of environmental concerns in the central Indian state of Madhya Pradesh. The meeting was held in the elegant guest house facilities maintained at the Union Carbide complex. After the meeting, I was confident that we had identified several areas of environmental concern, even with the severe time constraints involved. Clearly, it had been a useful exercise.

A short three years later I was stunned and dismayed by news of the Bhopal tragedy. Something had gone terribly wrong.

Questions raced through my head as the casualty toll jumped in decimal increments from hundreds to thousands. How could it happen? Was it an example of corporate and government irresponsibility? Was it just another industrial mishap, the result of an equipment malfunction?

I think not. Governments and large corporations generally are not irresponsible with human life. Mishaps often are controlled by quick, informed responses.

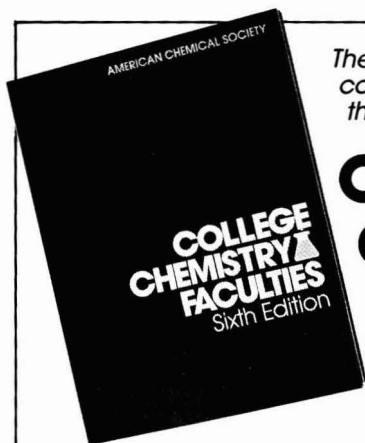


The real cause of the Bhopal tragedy is blind technology transfer. It is the result of establishing a highly complex chemical facility in a region with no extensive history of technological evolution. This kind of facility is often put in place hurriedly. The same sequence of events can be seen with ill-placed dams for water resources or nuclear power plants in other parts of the world.

Poor and unskilled workers flock to the site of the new technology in search of jobs and wages that meet the basic human needs of food and shelter. Often they are assigned to jobs without understanding how to respond to the unusual situation, the mishap. They are the blameless victims of technological blindness.

This pattern is becoming alarmingly common: Technological innovation is rushed into position. The population responds by migrating to the new site in search of better living conditions. And once the new high-density population is in place—because of the technological magnetism and the hopes that accompany it—the risk of density-dependent, negative environmental incidents is greatly increased.

A lake formed by water impounded behind a new dam designed for irrigation schemes and hydroelectric power entices one-time farmers to become fishermen. Waterborne disease transmission blossoms, fertilized by inadequate sewage treatment in high-density villages located on the shores of the new lake. The result is an epidemic.



*The most complete listing of
college chemistry faculties in
the U.S. and Canada*

COLLEGE CHEMISTRY FACULTIES

SIXTH EDITION



multi-purpose reference, COLLEGE CHEMISTRY FACULTIES is an important tool for researchers, recruiters, industrial chemistry labs, students and teachers as well as college and high school counselors and libraries.

For convenient researching, the directory provides:

1. State-by-state listings of institutions showing degrees offered, staff members and their major fields, department address and phone number.
2. Index of faculty members' names.
3. Index of institutions.

Covering 2,400 two-year and four-year colleges and universities in the U.S. and Canada, COLLEGE CHEMISTRY FACULTIES lists the current affiliations and major teaching fields of over 18,000 faculty members.

State-by-state listings make it easy for students and faculty to find chemistry departments in any area they choose, and for marketers to use the state listings for planning sales and service territories.

Just published, the Sixth Edition of COLLEGE CHEMISTRY FACULTIES is available in time for the fall semester. Order now and keep your information up-to-date. Soft cover, 8 1/2" x 11". 204 pages. . \$34.00

CALL TOLL FREE 1-800-424-6747

(for credit card orders),
write, or mail coupon below.

American Chemical Society Distribution Office 1155 Sixteenth Street, NW,
Washington, DC 20036

Please send _____ copies of **COLLEGE CHEMISTRY FACULTIES**
@ \$34.00. On prepaid orders, ACS pays shipping and handling charges.

- ☐ Payment enclosed (payable to American Chemical Society)
☐ Bill me ☐ Bill company

Charge my ☐ MasterCard ☐ VISA ☐ Barclay Card ☐ ACCESS

Card # _____ Interbank # _____
(MasterCard only)

Expiration Date _____ Signature _____

Name _____

Company/Organization _____

Address _____ Telephone Number _____

Billing Address _____

City _____ State _____ ZIP _____

5-170/2904/E710

Anthropologists and others skilled in interpreting social evolution tell us that culture is a system of social learning. If that is true, then we all must rethink our social applications of new technology in developing nations. We can no longer afford merely to place the machinery on site and hope that the comprehension of the highly skilled management personnel will filter down to those who turn the valves and monitor the gauges.

We need to develop attitudes that promote transitional approaches to technological development. Our plans must be suited to the recipient country's specific culture and history of technological development. This suggests the need for an interdisciplinary approach. It is not possible to divide all nations into two broad categories of developed and developing. India is culturally distinct from Thailand, China, and Nigeria. Different approaches to technology transfer should be translated for each country. Suitable scheduling of development should be an inherent part of the planning process.

Cultural change and evolution are mostly a series of gradual processes that are not amenable to all forms of sudden foreign intrusion. Attitudes and technical skills must be part of the transfer process and must filter down to the workers who participate. Only then can the risk of mishap, or catastrophe, be lessened.

Viewing technological evolution as a facet of cultural evolution is not a new idea. Cultures are distinct amalgams of learned and developed skills that can assimilate reasonable change as part of development. But it is essential that we assure appropriate evolution of skills as part of responsible technology transfer.

—Guy R. Lanza

The author is a professor of environmental sciences at the University of Texas at Dallas in Richardson, Tex.

Comet Halley: Once in a Lifetime


Looks at Halley's Comet through the eyes of history, culture, and science. Spans 2200 years of comet fact and fantasy. Includes a complete guide to comet-watching in 1985-86.

Color photos, lavishly illustrated, 190 pages; \$12.95 paperback, \$19.95 hardback.

Call TOLL FREE (800) 424-6747 and charge your book to your credit card. Or order from: American Chemical Society, Distribution Office Dept. 126, 1155 16th Street, N.W., Washington, DC 20036.

If not satisfied, return within 15 days for a full refund or charge credit.

professional consulting services directory




TRADITIONAL SOURCE SAMPLING

- Air Emissions Testing and Compliance Determination for Particulate and Gases
- Control Device Evaluation
- Particle Sizing Studies
- Resistivity Studies
- Specialized Analysis
- Method 1 Alternative
- 3-D Air Flow Studies

D. James Grove, P.E., Director
PO Box 12291, Research Triangle Park, NC 27709 (919) 781-3550 or 1-800-ENTROPY

ENTROPY
ENVIRONMENTALISTS INC.




SPECIALIZED SAMPLING

- (RCRA) Incinerator Testing
- Volatile Organic Compound (VOC) Testing
- Vapor Recovery Unit Compliance/Performance Testing
- Specialized Hydrocarbons Testing
- Testing of High Temperature and Pressure Sources

Walter S. Smith, P.E., Director
PO Box 12291, Research Triangle Park, NC 27709 (919) 781-3550 or 1-800-ENTROPY

ENTROPY
ENVIRONMENTALISTS INC.



CONTINUOUS EMISSIONS MONITORING (CEM)/ENGINEERING

- Performance Specification Tests of Opacity, SO₂, NO_x, O₃, CO₂, CO, and TRS CEMS
- Stratification Tests (All Pollutants)
- CEM Performance Audits (RAA and OGA)
- Real-time Measurements Using Transportable CEM System — Boiler Tuning (NO_x) — FGD Performance Evaluation — Combustion Efficiency Studies
- Performance Tests of Gas Turbines (Method 20)

James W. Peeler, Director
William G. DeVries, Associate Director
PO Box 12291, Research Triangle Park, NC 27709 (919) 781-3550 or 1-800-ENTROPY

ENTROPY
ENVIRONMENTALISTS INC.

Cenref Labs
P.O. BOX 68, BRIGHTON, CO 80601
(303) 659-0497

ENVIRONMENTAL TESTING

GC/MS • PSD • PCB'S
RCRA • NPDES
STACK TESTING



COMPLETE ANALYTICAL SERVICES GC/MS CAPABILITIES

- ☐ Screening & Analysis of Industrial & Hazardous Waste.
- ☐ Superfund & RCRA Requirements.
- ☐ Sampling to EPA Protocols.
- ☐ Toxicity Studies.

(516) 334-7770
75 URBAN AVE, WESTBURY, NY 11590
NYTEST ENVIRONMENTAL INC.

HITTMAN EBASCO

Analytical Laboratories

- EPA Priority Pollutants - GC/MS
 - Water Monitoring
 - Hazardous Waste Characterization
 - Sampling Services
 - NPDES and RCRA Services
- EPA Approved and State Certified—

HITTMAN EBASCO ASSOCIATES INC.
A Subsidiary of EBASCO SERVICES INCORPORATED
9151 Rumsey Road, Columbia, MD 21045
(301) 730-8525



ENVIRODYNE ENGINEERS

a consulting engineering and sciences firm

- environmental engineering
- analytical chemistry
- priority pollutant analyses
- environmental monitoring and assessment
- hazardous waste management
- transportation engineering
- energy engineering
- construction management

12161 Lackland Road
St. Louis, Missouri 63146
(314) 434-6960

Baltimore / Chicago / New York



COMPLETE ANALYTICAL SERVICES

- Gas Chromatography/Mass Spectroscopy
- Trace Metal Analyses - ICAP, AA, GFAA
- Drinking Water Analyses
- Industrial Hygiene Services
- Research and Development
- Environmental Field Sampling
- EPA Priority Pollutant Analyses

Brochure and/or fee schedule available on request

BARRINGER MAGENTA LTD.

304 Carlingview Drive, Rexdale, Ont. Canada (416) 675-3870
US Office Denver CO 80401 (303) 232-8811

THE CONSULTANTS' DIRECTORY

UNIT	Six Issues	Twelve Issues
1" X 1 col.	\$55	\$50
1" X 2 col.	110	100
1" X 3 col.	160	140
2" X 1 col.	110	100
2" X 2 col.	200	180
4" X 1 col.	200	180

Jay Francis

ENVIRONMENTAL
SCIENCE & TECHNOLOGY

25 Sylvan Road South

P.O. Box 231

Westport, CT 06881

Or call him at (203) 226-7131

MAIN 1893

Complete Environmental and Engineering Services

THE C.T. MAIN CORPORATION

OFFICES WORLDWIDE
CORPORATE HEADQUARTERS
PRUDENTIAL CENTER, BOSTON, MA 02199
617-262-3200

GYMNURS LABORATORIES, INC.

- HAZARDOUS WASTE-RCRA ANALYSIS
- PRIORITY POLLUTANT ANALYSIS
- INDUSTRIAL & MUNICIPAL DISCHARGE ANALYSIS INCLUDING AIR, WATER & WASTE
- OCCUPATIONAL SAFETY & HEALTH ANALYSIS
- AGRICULTURAL PESTICIDES & PCB ANALYSIS
- GUARANTEED 5-DAY ROUTINE ANALYSIS

MODERN COMPUTERIZED INSTRUMENTS

1303 COLUMBIA DR., SUITE 221, RICHARDSON, TX 75081 (214) 690-9431

CLASSIFIED SECTION

ATMOSPHERIC ENVIRONMENTAL SCIENTIST

Assist in data processing and analysis, proposal and report preparation, atmospheric measurement and modeling, and project management of air quality and meteorological research programs. Requires M.S., Ph.D., or equivalent accomplishment in atmospheric science or related environmental sciences, plus five years experience in air quality and meteorological research programs. Experience in as many of the following areas as possible is highly desirable: atmospheric measurements, chemical receptor modeling, analysis of pollution samples, computer applications, dispersion modeling, quality assurance, environmental assessment, project management, business development, and report preparation. Starting salary approximately \$26,000, full benefits. Send resume and letter of application, postmarked by Aug. 5, 1985 to Personnel Office, Desert Research Institute, University of Nevada System, P.O. Box 60220, Reno, Nevada 89506. An Affirmative Action/Equal Opportunity Employer.

ENVIRONMENTAL CHEMIST

Woodward-Clyde Consultants is seeking senior and junior environmental chemists/geochemists for the Wayne, NJ office. The preferred candidates will have a degree in chemistry and experience in evaluation of the fate and mobility of chemicals in environmental media. Send resume to: **Esther Fernandez, Woodward-Clyde Consultants, 201 Willowbrook Blvd., Wayne, NJ 07470. An equal opportunity employer.**

CLASSIFIED ADVERTISING RATES

Rate based on number of insertions used within 12 months from date of first insertion and not on the number of inches used. Space in classified advertising cannot be combined for frequency with ROP advertising. Classified advertising accepted in inch multiples only.

Unit	1-T	3-T	6-T	12-T	24-T
1 Inch	\$100	\$95	\$90	\$85	\$80

(Check Classified Advertising Department for rates if advertisement is larger than 10").

SHIPPING INSTRUCTIONS: Send all material to:

Environmental Science & Technology

Classified Advertising Department
25 Sylvan Rd. South
Westport, CT 06881
(203) 226-7131

INDEX TO THE ADVERTISERS IN THIS ISSUE

ADVERTISERS

PAGE NO.

Pierce Chemical Co. IFC

Seastar Instruments Ltd. IFC

Advertising Management for the
American Chemical Society Publications

CENTCOM, LTD.

President

Thomas N. J. Koerwer

Executive Vice President Senior Vice President

James A. Byrne Benjamin W. Jones

Alfred L. Gregory, Vice President

Clay S. Holden, Vice President

Robert L. Voepel, Vice President

Joseph P. Stenza, Production Director

25 Sylvan Road South

P.O. Box 231

Westport, Connecticut 06881

(Area Code 203) 226-7131

Telex No. 643310

ADVERTISING SALES MANAGER

James A. Byrne, VP

ADVERTISING PRODUCTION MANAGER

Jay S. Francis

SALES REPRESENTATIVES

Philadelphia, Pa. ... Patricia O'Donnell, CENTCOM, LTD., GSB Building, Suite 725, 1 Belmont Ave., Bala Cynwyd, Pa 19004 (Area Code 215) 667-9666

New York, N.Y. ... Dean A. Baldwin, CENTCOM, LTD., 60 E. 42nd Street, New York 10165 (Area Code 212) 972-9660

Westport, Ct. ... Edward M. Black, CENTCOM, LTD., 25 Sylvan Road South, P.O. Box 231, Westport, Ct 06881 (Area Code 203) 226-7131

Cleveland, Oh. ... Bruce Poorman, CENTCOM, LTD., 325 Front St., Berea, OH 44017 (Area Code 216) 234-1333

Chicago, Ill. ... Michael J. Pak, CENTCOM, LTD., 540 Frontage Rd., Northfield, Ill 60093 (Area Code 312) 441-6383

Houston, Tx. ... Michael J. Pak, CENTCOM, LTD., (Area Code 312) 441-6383

San Francisco, Ca. ... Paul M. Butts, CENTCOM, LTD., Suite 1070, 2672 Bayshore Frontage Road, Mountainview, CA 94043. (Area Code 415) 969-4604

Los Angeles, Ca. ... Clay S. Holden, CENTCOM, LTD., 3142 Pacific Coast Highway, Suite 200, Torrance, CA 90505 (Area Code 213) 325-1903

Boston, Ma. ... Edward M. Black, CENTCOM, LTD., (Area Code 203) 226-7131

Atlanta, Ga. ... Edward M. Black, CENTCOM, LTD., (Area Code 203) 226-7131

Denver, Co. ... Paul M. Butts, CENTCOM, LTD., (Area Code 415) 969-4604

United Kingdom:

Reading, England—Technomedia, Ltd. ... Wood Cottage, Shurlock Row, Reading RG10 0QE, Berkshire, England 0734-343302

Lancashire, England—Technomedia, Ltd. ... c/o Meconomics Ltd., Meconomics House, 31 Old Street, Ashton Under Lyne, Lancashire, England 061-308-3025

Continental Europe ... Andre Jamar, Rue Mallard 1, 4800 Verviers, Belgium. Telephone (087) 22-53-85. Telex No. 49263

Tokyo, Japan ... Shuji Tanaka, International Media Representatives Ltd., 2-29, Toranomon 1-Chrome, Minatoku, Tokyo 105 Japan. Telephone: 502-0656



All forward thinking environmental scientists depend on ES&T. They get the most authoritative technical and scientific information on environmental issues—and so can you! Have your own

subscription delivered directly to you each month!

☐ **YES!** Enter my own subscription to *ENVIRONMENTAL SCIENCE & TECHNOLOGY* at the rate I've checked below:

One Year	U.S.	Mexico & Canada	Europe	All Other Countries
ACS Members *	<input type="checkbox"/> \$ 26	<input type="checkbox"/> \$ 34	<input type="checkbox"/> \$ 40	<input type="checkbox"/> \$ 49
Nonmembers—Personal *	<input type="checkbox"/> \$ 35	<input type="checkbox"/> \$ 43	<input type="checkbox"/> \$ 49	<input type="checkbox"/> \$ 58
Nonmembers—Institutional	<input type="checkbox"/> \$149	<input type="checkbox"/> \$157	<input type="checkbox"/> \$163	<input type="checkbox"/> \$172

☐ Payment Enclosed (Payable to American Chemical Society)
☐ Bill Me ☐ Bill Company Charge my: ☐ VISA ☐ MasterCard

Card No. _____

Exp. Date _____ Interbank # _____ (Mastercard Only)

Signature _____

Name _____

Title _____ Employer _____

Address _____

City, State, Zip _____

Employer's Business: ☐ Manufacturing, type _____

☐ Academic ☐ Government ☐ Other _____

*Subscriptions at these rates are for personal use only.

All foreign subscriptions are now fulfilled by air delivery. Foreign payment must be made in U.S. currency by international money order, UNESCO coupons, U.S. bank draft, or order through your subscription agency. For nonmember subscription rates in Japan, contact Maruzen Co., Ltd.

Please allow 45 days for your first copy to be mailed. Redeem until December 31, 1985.

MAIL THIS POSTAGE-PAID CARD TODAY!

3144P



All forward thinking environmental scientists depend on ES&T. They get the most authoritative technical and scientific information on environmental issues—and so can you! Have your own

subscription delivered directly to you each month!

☐ **YES!** Enter my own subscription to *ENVIRONMENTAL SCIENCE & TECHNOLOGY* at the rate I've checked below:

One Year	U.S.	Mexico & Canada	Europe	All Other Countries
ACS Members *	<input type="checkbox"/> \$ 26	<input type="checkbox"/> \$ 34	<input type="checkbox"/> \$ 40	<input type="checkbox"/> \$ 49
Nonmembers—Personal *	<input type="checkbox"/> \$ 35	<input type="checkbox"/> \$ 43	<input type="checkbox"/> \$ 49	<input type="checkbox"/> \$ 58
Nonmembers—Institutional	<input type="checkbox"/> \$149	<input type="checkbox"/> \$157	<input type="checkbox"/> \$163	<input type="checkbox"/> \$172

☐ Payment Enclosed (Payable to American Chemical Society)
☐ Bill Me ☐ Bill Company Charge my: ☐ VISA ☐ MasterCard

Card No. _____

Exp. Date _____ Interbank # _____ (Mastercard Only)

Signature _____

Name _____

Title _____ Employer _____

Address _____

City, State, Zip _____

Employer's Business: ☐ Manufacturing, type _____

☐ Academic ☐ Government ☐ Other _____

*Subscriptions at these rates are for personal use only.

All foreign subscriptions are now fulfilled by air delivery. Foreign payment must be made in U.S. currency by international money order, UNESCO coupons, U.S. bank draft, or order through your subscription agency. For nonmember subscription rates in Japan, contact Maruzen Co., Ltd.

Please allow 45 days for your first copy to be mailed. Redeem until December 31, 1985.

MAIL THIS POSTAGE-PAID CARD TODAY!

680

3144P



(800) 424-6747 (U.S. only)



NO POSTAGE
NECESSARY
IF MAILED
IN THE
UNITED STATES

BUSINESS REPLY CARD

FIRST CLASS PERMIT NO. 10094 WASHINGTON D.C.

POSTAGE WILL BE PAID BY ADDRESSEE

American Chemical Society

Periodicals Marketing Dept.

1155 Sixteenth Street, N.W.

Washington, D.C. 20036



(800) 424-6747 (U.S. only)



NO POSTAGE
NECESSARY
IF MAILED
IN THE
UNITED STATES

BUSINESS REPLY CARD

FIRST CLASS PERMIT NO. 10094 WASHINGTON D.C.

POSTAGE WILL BE PAID BY ADDRESSEE

American Chemical Society

Periodicals Marketing Dept.

1155 Sixteenth Street, N.W.

Washington, D.C. 20036

Occurrence of Chlorinated Polynuclear Aromatic Hydrocarbons in Tap Water

Hiroaki Shiraishi,* Norman H. Pilkington,[†] Akira Otsuki, and Keiichi Fuwa

Division of Chemistry and Physics, National Institute for Environmental Studies, Yatabe, Tsukuba, Ibaraki 305, Japan

■ Organic compounds in tap waters were extracted by a modified continuous liquid-liquid extractor and analyzed by computerized gas chromatography/mass spectrometry using a fused silica capillary column. The results indicate the presence of monochlorinated derivatives of naphthalene, dibenzofuran, fluorene, fluorenone, phenanthrene, and fluoranthene and dichlorinated derivatives of naphthalene, phenanthrene, and fluoranthene. The parent polynuclear aromatic hydrocarbons (PAHs) and their oxygenated derivatives such as fluorenone and anthraquinone were also found. It was demonstrated that chlorinated PAHs (Cl-PAHs) were really present in tap waters at 10^{-1} – 10^{-2} ng/L levels.

The use of chlorine for disinfection of public water supplies has been shown to form halogenated organic compounds, such as trihalomethanes, and "nonvolatile" mutagens (1), but the identity and extent of halogenated compounds in drinking water are still unknown. Among the numerous organic compounds identified in tap water samples, the presence of polynuclear aromatic hydrocarbons (PAHs) has been reported (2–7). Laboratory studies using pure standards have shown (8–11) that both oxygenated and chlorinated derivatives can be formed during chlorination of PAHs in dilute aqueous solutions. It was therefore suspected that such compounds might also be present in tap waters.

Because of the low concentration of organic compounds in tap water, preconcentration was required before the analysis of these compounds by gas chromatography/mass spectrometry (GC/MS). An attempt to analyze PAHs in water by a closed loop stripping method (12) failed, because elution of PAHs from the carbon filter was difficult. A continuous liquid-liquid extraction method (13–15), often used in pesticide analysis, can both conveniently handle several hundred liters of water and also provide an extremely low reagent blank, because it requires only 100 or 200 mL of organic solvent. For the present work, such a continuous liquid-liquid extractor was used, with some modifications, to extract nonpolar organic compounds in tap water. The concentrates were analyzed by GC/MS using a fused silica capillary column.

Experimental Section

Materials. The hexane was pesticide grade (Wako Pure Chemicals Ind., Ltd) and required no further purification

before use. Water was purified by distillation, and passage through the Milli-Q system (Millipore Corp.) and XAD-2 resin column before use.

Chlorinated PAHs (Cl-PAHs) for use as reference standards were prepared by chlorination of the parent PAH. PAH (0.1 g) was dissolved in 10 mL of acetic acid, and 1.5 times the stoichiometric amount of 10% sodium hypochlorite solution was added dropwise into this solution while stirring. After the mixture had been stirred for 3 h, water and ether were added. The organic layer was washed with water and then with sodium carbonate solution and dried over sodium sulfate. Ether was removed by distillation, and the residual solid was purified by vacuum distillation (or sublimation) and recrystallization from methanol.

Modification of Extractor. As reported by Stachel et al. (15) the decrease in water level which occurred during extraction made operation of the Ahnoff and Josefsson extractor (19) difficult. In order to overcome this undesirable phenomenon, the continuous liquid-liquid extractor (see Figure 1) was modified to regulate the water level. A commercial automatic water level controller (Nissin Rika Co., Model AL-66r) operating in on-off delay mode was used. The water level is monitored by an infrared sensor on the side arm of the extractor. If the water level sinks down, air is pumped out through a one-way glass valve, thus causing a partial vacuum inside the extractor. The flow rate of water into the extractor then increases. The pumping speed and delay time were adjusted so as to prevent chattering of the water level. In order to make it easy to change the head of the extractor, a transparent glass joint was adopted instead of the stainless steel flange originally used (19).

Apparatus. Mass spectrometry was performed on a DX-300 double-focusing mass spectrometer (JEOL, Japan) fitted with a Hewlett-Packard Model 5700 GC. A flexible capillary column (25 m), methyl silicone (Hewlett-Packard), used with helium as the carrier gas, was directly coupled to the mass spectrometer. The column temperature was set at 40 °C for 4 min followed by an increase to 250 °C at a rate of 4 °C/min and then held at 250 °C. The injector temperature was 250 °C, and the head pressure of the column was 1.0 kg/cm². The mass spectrometric conditions were as follows: accelerating voltage 3 kV; ionizing current 300 µA; ionizing voltage 70 V; scan range *m/z* 10–400; scan interval 2 s. Mass resolution was 500. A JMS-3500 mass data analysis system (JEOL, Japan) was used.

Extraction Procedure. Hexane (0.15 L) was charged to the extractor, and 200 L of tap water (Tsukuba, Japan)

[†]Permanent address: CSIRO Division of Chemical and Wood Technology, Clayton, Victoria 3168, Australia.

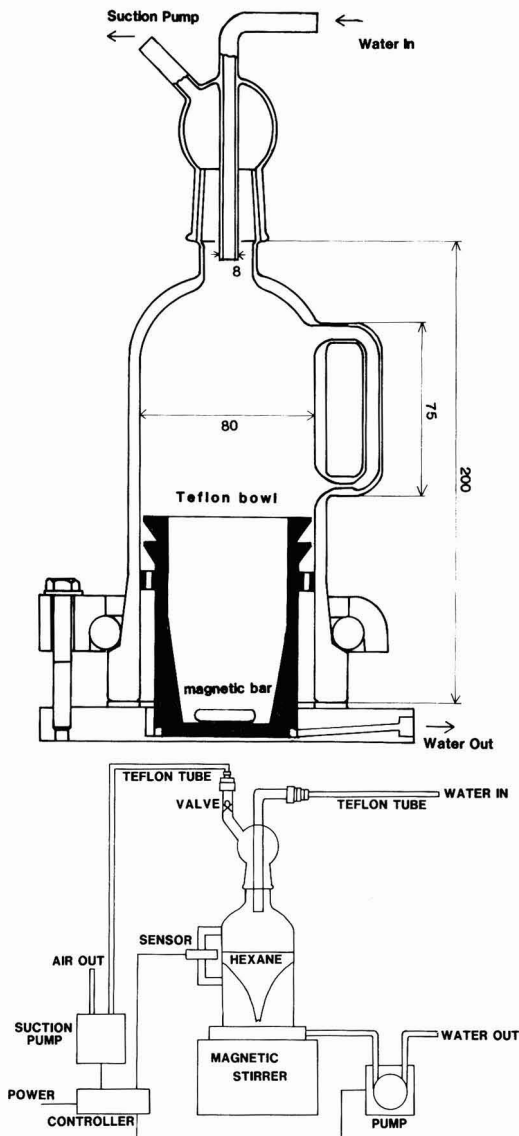


Figure 1. Modified liquid-liquid extractor.

was passed through at a flow rate of 50–60 mL/min. Recovery of hexane was about 0.14 L (more than 94%). The hexane extract was dried by sodium sulfate (5–10 g) and concentrated to a few milliliters on a rotary evaporator and finally to 0.10 mL under a nitrogen stream at room temperature.

Recovery Test. The extractor was fitted with a small reservoir and a Hershberg type dropping funnel. Water (100 mL) was poured into the funnel, and then 5 μ L of a standard methanol solution (0.5 mg/mL) of PAHs and Cl-PAHs was added to the water. This solution was dynamically diluted by adding it dropwise to a glass reservoir through which water was flowing at 55 mL/min. The dilution factor in the cell was 250, so that the net concentration flowing through extractor was 100 ng/L per component. The total volume of water extracted was 25 L, and 150 mL of hexane was used. At first, hexane was concentrated to 1.0 mL and finally to 0.10 mL as described

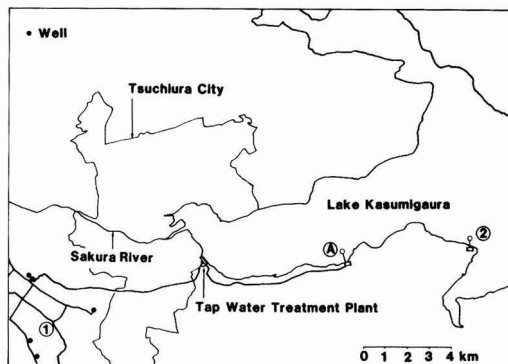


Figure 2. Sampling sites and the tap water supply system in Tsukuba. (1) Institute; (2) Branch of Institute.

above. Recoveries were determined on each evaporation step using 1-chlorodecane and 1-chlorotetradecane as internal standards.

Compound Identification and Quantification. The occurrence of mono- and dichlorinated PAH derivatives was confirmed by comparison of its mass spectrum and GC retention time with those from the authentic standards. In cases when the authentic standard was not available, identifications were done by comparison with reported mass spectrum (16, 4). Cl-PAHs and PAHs were quantified from the peak area of mass chromatograms using an external standard technique. Molecular ion, M^+ , and its isotope ion, $(M + 2)^+$, were selected for Cl-PAHs, and the diagnostic ion for PAH was its molecular ion. Reproducibility for the determination of Cl-PAHs and PAHs by external standard technique was within 12% (calculated from the recovery experiments), so the precision of tap water analyses was dependent upon this final determination step. The detection limits for PAHs and Cl-PAHs were 0.01 ng. Therefore, if recovery is 80% and 200 L of sample water is concentrated to 0.10 mL, Cl-PAHs and PAHs at 0.003 ng/L can be detected by GC/MS using 2 μ L of concentrates, unless coeluting substances interfere with the determination. As low as 0.1 ng of PAHs and Cl-PAH could be detected by RIC (reconstructed ion chromatogram), which was used for monitoring GC elution.

Sampling. Figure 2 shows the sampling sites and the tap water supply system in Tsukuba. Tap water was sampled in our Institute (site 1) from Dec 1982 to Feb 1984. Two tap water sources were chosen. Tap a was in a 10-year-old building and tap b was in a new building (1 year old). The treatment process used to produce the tap water is as follows. Lake water is pumped to the treatment plant, where chlorination, rapid sand filtration, and activated carbon treatment are carried out. The finished water is chlorinated to 0.7 mg/L free chlorine, then pumped to Tsukuba, and stored in a plastic tank, where a further 0.3 mg/L chlorine is added. Sometimes well water is blended in, but its ratio to lake water is below 10%.

Raw lake water was collected at site 2, where a branch of our Institute is located. Rapid sand filtration was performed before extractions after the model of the process at the water treatment plant.

Results and Discussion

Table I shows the result of recovery experiments of some PAHs and Cl-PAHs using the extractor. It seems that recovery increases with increase in molecular weight. It was considered that this may be due to a decrease in their solubility in water, because published values for the solu-

Table I. Recovery (%) of PAHs and Cl-PAHs at 100 ng/L each

	recovery ^a ± SD ^b	
naphthalene	84 ± 1	74 ± 1
acenaphthylene	89 ± 4	79 ± 4
acenaphthene	92 ± 4	81 ± 4
dibenzofuran	89 ± 4	79 ± 4
fluorene	85 ± 5	77 ± 5
fluorenone	85 ± 4	80 ± 5
anthracene	92 ± 4	90 ± 4
phenanthrene	88 ± 2	83 ± 4
fluoranthene	85 ± 5	84 ± 4
chloronaphthalene	88 ± 2	81 ± 2
chlorodibenzofuran	87 ± 1	78 ± 2
chlorofluorene	84 ± 3	76 ± 3
chlorofluorenone	85 ± 3	78 ± 5
chlorophenanthrene	85 ± 3	83 ± 4
dichlorophenanthrene	80 ± 5	80 ± 5
chlorofluoranthene	81 ± 4	81 ± 5
final volume, mL	1.0	0.10

^a Means of three independent experiments. ^b SD = standard deviation.

bility of naphthalene, fluorene, phenanthrene, and fluoranthene are 31.7, 1.98, 1.29, and 0.26 mg/L, respectively (17). But, it was found that the loss of PAHs occurred in the evaporation step. Volatilization of PAHs was negligible

Table II. Identified Compounds in the Tap Water

no.	retention time	name	formula	identification ^a	no.	retention time	name	formula	identification ^a
1	6 min 24 s	ethylbenzene	C ₈ H ₁₀	a	36	33 min 20 s	hexadecane	C ₁₆ H ₃₄	a
2	6 min 44 s	<i>p</i> - and <i>m</i> -xylene	C ₈ H ₁₀	a	37	33 min 30 s	methyl dibenzofuran, isomer	C ₁₃ H ₁₀ O	b
3	6 min 54 s	bromoform	CHBr ₃	a	38	33 min 50 s	dibenzyl ether	C ₁₄ H ₁₄ O	a
4	7 min 24 s	<i>o</i> -xylene	C ₈ H ₁₀	a	39	35 min 40 s	2-chlorodibenzofuran	C ₁₂ H ₇ OCl	a
5	8 min 26 s	isopropylbenzene	C ₉ H ₁₂	a	40	36 min 16 s	heptadecane	C ₁₇ H ₃₆	a
6	8 min 46 s	1-bromohexane	C ₆ H ₁₃ Br	a	41	36 min 26 s	fluorenone	C ₁₃ H ₈ O	a
7	9 min 50 s	propylbenzene	C ₉ H ₁₂	a	42	37 min 28 s	phenanthrene	C ₁₄ H ₁₀	a
8	10 min 28 s	ethyltoluene, isomer	C ₉ H ₁₂	b	43	37 min 58 s	2-chlorofluorene	C ₁₃ H ₉ Cl	a
9	11 min 04 s	ethyltoluene, isomer	C ₉ H ₁₂	b	44	38 min 42 s	chloromethyl dibenzofuran	C ₁₂ H ₉ OCl	c
10	11 min 30 s	<i>p</i> -dichlorobenzene	C ₆ H ₄ Cl ₂	a	45	39 min 00 s	octadecane	C ₁₈ H ₃₈	a
11	12 min 06 s	trimethylbenzene, isomer	C ₉ H ₁₂	b	46	39 min 22 s	phytane	C ₂₀ H ₄₂	a
12	12 min 22 s	<i>o</i> -dichlorobenzene + unknown compound	C ₆ H ₄ Cl ₂	a	47	39 min 48 s	hydroxyanthracene	C ₁₄ H ₁₀ O	c
13	13 min 36 s	chloroxylene, isomer	C ₈ H ₉ Cl	b	48	40 min 30 s	hydroxyanthracene	C ₁₄ H ₁₀ O	c
14	14 min 02 s	hexachloroethane	C ₂ Cl ₆	a	49	41 min 30 s	chlorofluorenone	C ₁₃ H ₇ OCl	a
15	14 min 38 s	chloroxylene, isomer	C ₈ H ₉ Cl	b	50	41 min 38 s	nonadecane	C ₁₉ H ₄₀	a
16	16 min 54 s	bromoxylene, isomer	C ₈ H ₉ Br	b	51	41 min 54 s	methyl palmitate	C ₁₇ H ₃₄ O ₂	a
17	17 min 54 s	hexyl ether, isomer	C ₁₂ H ₂₆ O	c	52	42 min 20 s	dibutyl phthalate	C ₁₆ H ₂₂ O ₄	a
18	18 min 06 s	hexyl ether, isomer	C ₁₂ H ₂₆ O	c	53	42 min 34 s	anthraquinone	C ₁₄ H ₈ O ₂	a
19	18 min 16 s	naphthalene + hexyl ether isomer	C ₁₀ H ₈	a	54	42 min 58 s	9-chlorophenanthrene	C ₁₄ H ₉ Cl	a
20	19 min 58 s	hexyl ether, isomer	C ₁₂ H ₂₆ O	c	55	43 min 40 s	palmitic acid	C ₁₆ H ₃₂ O ₂	a
21	20 min 14 s	hexyl ether, isomer	C ₁₂ H ₂₆ O	c	56	44 min 10 s	eicosane	C ₂₀ H ₄₂	a
22	20 min 54 s	1-bromodecane	C ₁₀ H ₂₁ Br	a	57	44 min 50 s	fluoranthene	C ₁₆ H ₁₀	a
23	22 min 20 s	Di- <i>n</i> -hexyl ether	C ₁₂ H ₂₆ O	a	58	46 min 34 s	heneicosane	C ₂₁ H ₄₄	a
24	25 min 12 s	1-chloronaphthalene	C ₁₀ H ₇ Cl	a	59	46 min 50 s	methyl stearate	C ₁₉ H ₃₈ O ₂	a
25	25 min 18 s	biphenyl	C ₁₂ H ₁₀	a	60	48 min 04 s	dichlorophenanthrene, isomer	C ₁₄ H ₈ Cl ₂	b
26	26 min 58 s	tetradecane	C ₁₄ H ₃₀	a	61	48 min 14 s	stearic acid	C ₁₈ H ₃₆ O ₂	a
27	28 min 22 s	2,6-di- <i>tert</i> -butylquinone	C ₁₄ H ₂₀ O ₂	a	62	48 min 22 s	9,10-dichlorophenanthrene	C ₁₄ H ₈ Cl ₂	a
28	28 min 50 s	methylbiphenyl, isomer	C ₁₃ H ₁₂	b	63	48 min 52 s	docosane	C ₂₂ H ₄₆	a
29	29 min 06 s	methylbiphenyl, isomer, + chloromethyl-naphthalene	C ₁₃ H ₁₂	c	64	49 min 48 s	3-chlorofluoranthene	C ₁₆ H ₉ Cl	a
30	29 min 52 s	dibenzofuran	C ₁₂ H ₈ O	a	65	51 min 04 s	tricosane	C ₂₃ H ₄₈	a
31	30 min 14 s	pentadecane	C ₁₅ H ₃₂	a	66	52 min 38 s	diethyl adipate	C ₂₂ H ₄₂ O ₄	a
32	30 min 58 s	dichloronaphthalene, isomer	C ₁₀ H ₆ Cl ₂	b	67	53 min 56 s	tetracosane	C ₂₄ H ₅₀	a
33	31 min 04 s	dichloronaphthalene, isomer	C ₁₀ H ₆ Cl ₂	b	68	54 min 50 s	dichlorofluoranthene, isomer	C ₁₆ H ₈ Cl ₂	a
34	31 min 48 s	fluorene	C ₁₃ H ₁₀	a	69	55 min 30 s	bis(ethylhexyl) phthalate	C ₂₄ H ₃₈ O ₄	a
35	33 min 04 s	methyl dibenzofuran, isomer	C ₁₃ H ₁₀ O	b	70	51 min 16 s	hexacosane	C ₂₆ H ₅₄	a
					71	59 min 42 s	heptacosane	C ₂₇ H ₅₆	a

^a Identification: (a) = comparison with authentic standard; (b) = comparison with library MS; (c) = tentative, based on interpretation of MS.

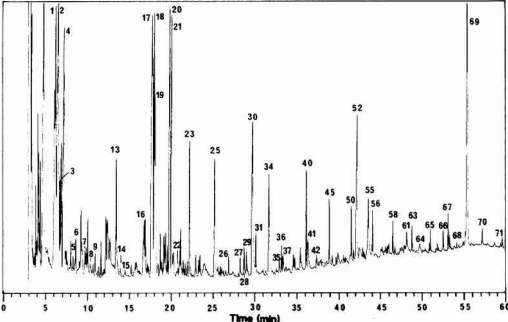


Figure 3. Reconstructed ion chromatogram of the hexane extract (tap a, 83/June, 13-16, 1983). (Peak numbers refer to table II.)

until the volume of hexane became 1.0 mL, but some of the PAHs were evaporated during further concentration. It was very important that more than 3 mL of hexane remained in a flask when the rotary evaporator was used. Otherwise, considerable amounts of the PAHs which are more volatile than fluorene were lost.

Figure 3 shows reconstructed ion chromatogram (RIC) of the Tsukuba tap water extract (tap a; June 13-16, 1983), and Table II lists the compounds identified. Dibutyl and

Table III. Concentration of PAH and Cl-PAH in Tap and Lake Water^a

	ng/L ($\times 10^{-3}$ nmol/L)			
	tap a	tap a	tap b	lake
naphthalene (19)	2.3 (18)	0.31 (2.4)	1.03 (8.0)	0.09 (0.7)
dibenzofuran (30)	56.2 (335)	1.0 (6.0)	39.0 (232)	0.03 (0.2)
fluorene (34)	3.9 (23)	0.25 (1.5)	5.8 (35)	0.04 (0.2)
fluorenone (41)	1.65 (9.2)	0.28 (1.6)	7.3 (41)	ND
phenanthrene (42)	0.86 (4.8)	0.45 (2.5)	1.41 (7.9)	0.34 (1.9)
fluoranthene (57)	0.02 (0.1)	0.04 (0.2)	0.21 (1.0)	NA
chloronaphthalene (24)	0.28 (1.7)	0.03 (0.2)	0.44 (2.7)	ND
chlorodibenzofuran (39)	1.4 (6.9)	0.04 (0.2)	1.24 (6.1)	ND
chlorofluorene (43)	0.13 (0.6)	0.03 (0.1)	0.3 (1.9)	ND
chlorofluorenone (49)	0.11 (0.5)	0.04 (0.2)	1.22 (5.7)	ND
chlorophenanthrene (54)	0.33 (1.6)	0.18 (0.8)	NA	ND
chlorofluoranthene (64)	0.13 (0.5)	0.14 (0.6)	0.17 (0.7)	ND
dichloronaphthalene (32) ^b	0.03 (0.2)	ND	0.15 (0.8)	ND
dichlorophenanthrene (62)	0.08 (0.32)	0.04 (0.16)	0.18 (0.7)	ND
dichlorophenanthrene (60) ^b	0.03 (0.1)	0.02 (0.08)	0.01 (0.04)	ND
dichlorofluoranthene (68) ^b	0.03 (0.1)	0.05 (0.18)	0.10 (0.37)	ND
volume of water, L	200	150	200	150
flow rate, mL/min	57	60	55	60
date	June 13–16, 1983	Feb 14–17, 1984	May 27–30, 1983	Feb 20–23, 1984

^a Compound number refers to Table II and Figures 3 and 4. ND, not detected; NA, not analyzed. ^bBased on relative peak area to the parent PAH (pure standard was not available).

Table IV. Molar Ratio of Chlorinated PAH to the Parent PAH^a

	tap a	tap a	tap b
chloronaphthalene (24)	0.10	0.08	0.34
chlorodibenzofuran (39)	0.021	0.03	0.026
chlorofluorene (43)	0.028	0.1	0.056
chlorofluorenone (49)	0.056	0.12	0.14
chlorophenanthrene (54)	0.32	0.34	NA
chlorofluoranthene (64)	6	3	0.69
dichloronaphthalene (32) ^b	0.008	ND	0.09
dichlorophenanthrene (62)	0.07	0.06	0.09
dichlorophenanthrene (60) ^b	0.03	0.03	0.005
dichlorofluoranthene (68) ^b	1.1	0.9	0.35
date	June 13–16, 1983	Feb 14–17, 1984	May 27–30, 1983

^a Compound number refers to Table II and Figures 3 and 4. ND, not detected; NA, not analyzed. ^bBased on relative peak area to the parent PAH (pure standard was not available).

di(ethylhexyl) phthalates, *n*-alkanes from tetradecane to heptacosane, hexyl ethers, benzyl ether, alkylbenzenes, palmitic and stearic acid, its methyl esters, and PAHs were the major components in every tap water extract. The maximum and minimum concentrations of PAHs, found in four extractions over 1 year at the same location, are the following: naphthalene, 27 and 0.31 ng/L; dibenzofuran 63 and 0.1 ng/L; fluorene, 11.7 and 0.32 ng/L; phenanthrene, 1.3 and 0.44 ng/L; fluoranthene, 0.04 and 0.02 ng/L. Among these, dibenzofuran was the major component in every experiment.

Figure 4 shows the mass chromatogram of the seven PAHs (naphthalene, dibenzofuran, fluorene, methyl-dibenzofuran, fluorenone, phenanthrene, and fluoranthene) and their mono- and dichloro derivatives. Both monochlorinated and dichlorinated derivatives of naphthalene (Figure 4a), phenanthrene (Figure 4d), and fluoranthene (Figure 4e) were found. Only monochlorinated derivatives of dibenzofuran (Figure 4b), fluorene (Figure 4b), methyl-dibenzofuran (Figure 4c), and fluorenone (Figure 4c) were found, although their parent PAHs were present in fairly large amounts. Some other methylated derivatives such as chloromethylnaphthalene and some other oxygenated PAHs such as anthraquinone and hydroxyanthracene (or phenanthrenol) were also found. In general, reaction of chlorine with model PAHs produces oxygenated and chlorinated derivatives (9–11). Fluorenone, anthra-

quinone, and phenanthrenol were reported as oxidation products of fluorene, anthracene, and phenanthrene, respectively. Since Cl-PAHs were not present in the raw water (Table III), they should be produced in the tap water supply system by the reaction of the parent PAHs with residual chlorine. The concentrations of PAHs and Cl-PAHs are shown in Table III. It was found that the concentrations varied in their order of magnitude.

If the reaction of residual chlorine with PAHs remaining in the tap water supply system produces Cl-PAHs, the reactivity and contact time of each individual PAH to chlorine determines the ratio of the parent PAH and chlorinated species. The ratio of the concentrations of the chlorinated derivative to the concentration of the parent PAH is shown in Table IV. The ratio in both tap a and tap b water samples decreased in the following order: fluoranthene, phenanthrene, naphthalene, fluorene, and dibenzofuran. From the comparison of the ratio, it was found that the values are similar in two tap a samples but somewhat different between tap a and tap b samples, especially in the ratio of chlorinated fluoranthenes. If two tap samples have the same contamination sources, the ratio must have similar values. Residence times of tap a and tap b water in the distribution system, which can be considered as reaction times in solution phase, were almost the same, so this implies that two tap waters had different contamination sources.

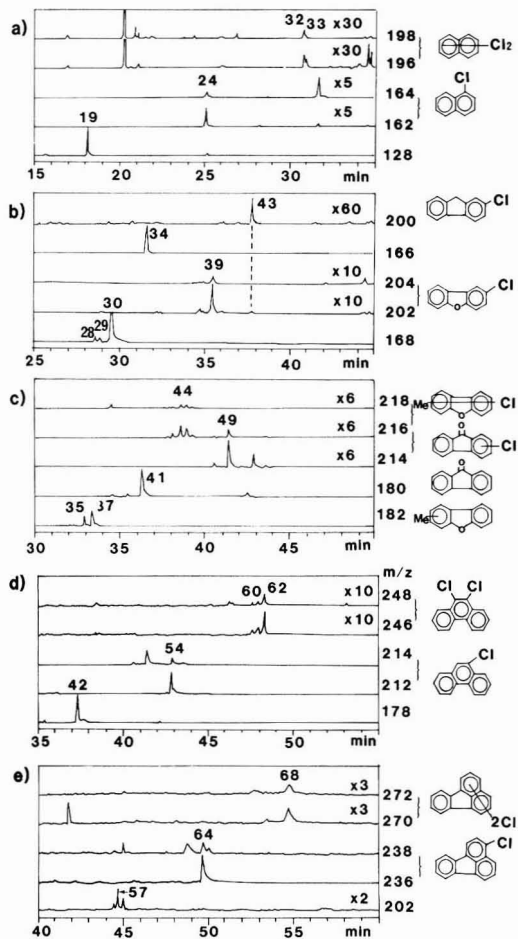


Figure 4. Mass chromatogram of PAHs and chlorinated PAHs in the tap water extract (tap a, 83/June 13–16, 1983). (Peak numbers refer to Table II.) (a) Naphthalene (m/z 128), monochlorinated (m/z 162, 164), dichlorinated (m/z 196, 198). (b) Dibenzofuran (m/z 166), monochlorinated (m/z 200, 202), dichlorinated (m/z 204, 206). (c) Fluorene (m/z 180), monochlorinated (m/z 214, 216), dichlorinated (m/z 218, 220). (d) Phenanthrene (m/z 178), monochlorinated (m/z 212, 214), dichlorinated (m/z 246, 248). (e) Fluoranthene (m/z 202), monochlorinated (m/z 236, 238), dichlorinated (m/z 270, 272).

The fact that dibenzofuran and fluorene were more abundant than the other PAHs in Tsukuba tap water is consistent with that of a chlorination study on coal tar leachate. Alben (18, 19) reported that on the chlorination of coal tar leachate, oxygen-substituted PAHs such as dibenzofuran became more abundant, several new oxygenated PAHs were formed, and of the parent PAHs, fluorene became the most prominent, with a considerably diminished concentration of phenanthrene and fluoranthene. In Japan, the use of coal tar coated pipes in public water supply systems is permitted. In the lines supplying tap a and tap b, half of the pipes are coated with tar epoxy-resin paints which contain about 70% coal tar. The findings that dibenzofuran and fluorene were abundant and that two taps have different Cl-PAH/PAH ratios suggest that the origin of PAHs in Tsukuba tap water is coal tar coated pipes in the water supply system, but further study will be required to differentiate the contamination sources.

Other brominated or chlorinated compounds found in the extracts were dichlorobenzenes, chloro- and bromoxylenes, bromoform, bromohexane, hexachloroethane, and bromodecane. Chloroxylenes and bromoxylenes may be reaction products of xylene which were present in the tap water. Dichlorobenzenes were also found in the lake water, so they seem to be pollutants in the lake water. Although biphenyl was present at almost the same concentration as fluorene, chlorinated biphenyls were not found in the tap water extracts. This may be due to the lower reactivity of biphenyl to chlorine, compared with PAHs, under the conditions of the tap water supply system.

Conclusion

Combination of a modified continuous liquid-liquid extraction and computerized GC/MS using a fused silica capillary column enabled analysis of low concentrations of organic solutes in water. The presence of PAHs and chlorinated PAHs in tap water indicates the reaction of PAHs with chlorine.

Acknowledgments

N.H.P. is grateful to the Australian Department of Science and Technology for the awarding of a grant under the terms of the Australia-Japan Science and Technology Agreement which enabled him to work at the National Institute for Environmental Studies in Tsukuba, Japan.

Registry No. 1, 100-41-4; 3, 75-25-2; 4, 95-47-6; 5, 98-82-8; 6, 111-25-1; 7, 103-65-1; 10, 106-46-7; 11, 25551-13-7; 12, 95-50-1; 14, 67-72-1; 16, 35884-77-6; 19, 91-20-3; 22, 112-29-8; 23, 112-58-3; 24, 90-13-1; 25, 92-52-4; 26, 629-59-4; 27, 719-22-2; 30, 132-64-9; 31, 629-62-9; 34, 84-65-1; 36, 544-76-3; 38, 103-50-4; 39, 51230-49-0; 40, 629-78-7; 41, 486-25-9; 42, 85-01-8; 43, 2523-44-6; 45, 593-45-3; 46, 638-36-8; 49, 85897-29-6; 50, 629-92-5; 51, 112-39-0; 52, 84-74-2; 53, 84-65-1; 54, 947-72-8; 55, 57-10-3; 56, 112-95-8; 57, 206-44-0; 58, 629-94-7; 59, 112-61-8; 60, 59116-88-0; 61, 57-11-4; 62, 17219-94-2; 63, 629-97-0; 64, 25911-51-7; 65, 638-67-5; 66, 103-23-1; 67, 646-31-1; 68, 86329-60-4; 69, 117-81-7; 70, 630-01-3; 71, 593-49-7; acenaphthylene, 208-96-8; acenaphthene, 83-32-9; anthracene, 120-12-7; chloronaphthalene, 25586-43-0; chlorodibenzofuran, 42934-53-2; chlorofluoranthene, 25911-51-7; *p*-xylene, 106-42-3; *m*-xylene, 108-38-3; ethyltoluene, 25550-14-5; chloroxylenes, 25323-41-5; methylbiphenyl, 28652-72-4; methylidibenzofuran, 60826-62-2; dichloronaphthalene, 28699-88-9.

Literature Cited

- (1) Cheh, A. M.; Skochdopole, J.; Koski, P.; Cole, L. *Science (Washington, D.C.)* **1980**, *207*, 90-92.
- (2) Harrison, R. M.; Perry, R.; Wellings, R. A. *Environ. Sci. Technol.* **1976**, *10*, 1151-1156.
- (3) Oyler, A. R.; Bodenner, D. L.; Welch, K. J.; Liukkonen, R. J.; Carlson, R. M.; Kopperman, H. L.; Caple, R. *Anal. Chem.* **1978**, *50*, 837-842.
- (4) Oyler, A. R.; Liukkonen, R. J.; Lukasewycz, M. T.; Cox, D. A.; Peake, D. A.; Carlson, R. M. *Environ. Health Perspect.* **1982**, *46*, 73-86.
- (5) Oyler, A. R.; Liukkonen, R. J.; Lukasewycz, M. T.; Heikkila, K. E.; Cox, D. A.; Carlson, R. M. *Environ. Sci. Technol.* **1983**, *17*, 334-342.
- (6) Harrison, R. M.; Perry, R.; Wellings, R. A. *Water Res.* **1975**, *9*, 331-346.
- (7) Basu, D. K.; Saxena, J. *Environ. Sci. Technol.* **1978**, *12*, 795-798.
- (8) Benoit, F. M.; LeBel, G. L.; Williams, D. T. *Bull. Environ. Contam. Toxicol.* **1979**, *23*, 774-778.
- (9) Benoit, F. M.; LeBel, G. Y.; Williams, D. T. *Int. J. Environ. Anal. Chem.* **1979**, *6*, 277-287.
- (10) Coleman, W. E.; Melton, R. G.; Kopfler, F. C.; Barone, K. A.; Aurand, T. A.; Jellison, M. G. *Environ. Sci. Technol.* **1980**, *14*, 576-588.
- (11) Kveseth, K.; Sortland, B.; Bokn, T. *Chemosphere* **1982**, *11*, 623-639.

- (12) Grob, K. J. *Chromatogr.* 1973, 84, 255-273.
- (13) Ahnoff, M.; Josefsson, B. *Anal. Chem.* 1974, 46, 658-663.
- (14) Ahnoff, M.; Josefsson, B. *Anal. Chem.* 1976, 48, 1268-1270.
- (15) Stachel, B. Baetjer, K.; Cetinkaya, M.; Dueszein, J.; Lahl, U.; Lierse, K.; Thiemann, W.; Gabel, B.; Kozicki, R.; Podbielski, A. *Anal. Chem.* 1981, 53, 1469-1472.
- (16) Heller, S. R.; Milne, G. W. A. "EPA/NIH Mass Spectral Data Base"; U.S. Government Printing Office: Washington, DC, 1978.
- (17) Mackay, D.; Shiu, W. Y. *J. Chem. Eng. Data* 1977, 22, 399-402.
- (18) Alben, K. *Environ. Sci. Technol.* 1980, 14, 468-470.
- (19) Alben, K. *Anal. Chem.* 1980, 52, 1825-1828.

Received for review April 16, 1984. Revised manuscript received October 29, 1984. Accepted January 14, 1985.

Henry's Law Constants for the Polychlorinated Biphenyls

Lawrence P. Burkhard,[†] David E. Armstrong,* and Anders W. Andren

Water Chemistry Program, University of Wisconsin, Madison, Wisconsin 53706

■ Henry's law constants were predicted from the ratio of the liquid (or subcooled liquid) vapor pressure and aqueous solubility for each polychlorinated biphenyl (PCB) congener. The liquid vapor pressures and aqueous solubilities were derived for each PCB congener by using correlations of Gibbs' free energy of vaporization against gas-liquid chromatographic retention indexes and Gibbs' free energy of solubilization of a liquid against molecular surface area. The predicted values were in fair agreement with experimental values, and the error for these constants was estimated to be a factor of 5 in the temperature range 0.0-40.0 °C. For the PCB congeners, Henry's law constants were independent of molecular weight and increased approximately an order of magnitude with a 25.0 °C increase in temperature. The average value for Henry's law constants and air-water partition coefficients for the Aroclor PCB mixtures were approximately 4.0×10^{-4} atm·m³/mol at 25.0 °C.

Introduction

One of the major problems in modeling and predicting the behavior of polychlorinated biphenyls (PCBs) in the environment has been the lack of accurate Henry's law constants. Henry's law constants are used to predict exchange rates of vapors across the air/water interface and fugacity potentials for aqueous systems.

In part, Henry's law constants have not been available due to analytical difficulties in measuring this property. Measurements are often performed with nanomoles or less of the compound. In addition, PCBs were sold commercially as mixtures called Aroclors, and each mixture was composed of numerous, 50-75, PCB congeners (1). Many of these compounds are not readily available in pure form, and thus, much preparatory work is required before any measurements can be performed.

Historically, investigators have circumvented this lack of experimental data by treating each Aroclor mixture as a single entity when estimating Henry's law constants (*H*'s) (2-6). An average *H* was determined by dividing the vapor pressure of the mixture by its aqueous solubility (2). The problem with this approach is that PCB congeners behave in the environment as individual compounds and not as a mixture. Consequently, to model their behavior correctly, *H*'s are needed for each congener.

Recently, Bopp (7), in an attempt to eliminate this problem, grouped PCB congeners by degree of chlorination. The aqueous activity coefficient for each degree of chlorination was assumed to be independent of tempera-

ture, and the logarithm of the subcooled liquid vapor pressure was considered to be linearly related to chlorine number. These assumptions were used in predicting vapor pressures and solubilities for each degree of chlorination. The predicted values were used to calculate *H* for each degree of chlorination.

Four recent investigations (8-11) now permit calculation of *H* for each PCB congener and elimination of the assumptions employed by Bopp. These investigations were performed using the best techniques currently available for measuring aqueous solubilities (9, 12) and vapor pressures (13). The requisite data were derived by measurements of vapor pressures of 4 PCB congeners and aqueous solubilities of 18 PCB congeners. These measurements include vapor pressure and solubility data for decachlorobiphenyl, the highest chlorinated PCB congener.

The object of this investigation is to use the recently acquired data to calculate and evaluate *H* for each PCB congener. Temperature effects and the influence of chemical structure on the *H*'s are also considered.

Determination of Henry's Law Constants

Henry's law expresses the proportionality between the concentration of a gas dissolved in a solvent and its partial pressure (14). In equation form, Henry's law is

$$P = HC \quad (1)$$

where *P* is the partial pressure of the gas, *C* is the concentration of the dissolved gas, and *H* is Henry's law constant. Henry's law represents a limiting behavior for any gas-solvent system as its partial pressure approaches zero. Typically, Henry's law breaks down when partial pressures exceed 5-10 atm and/or when the dissolved concentrations exceed 3 mol % (14). Henry's law constant is a function of temperature only for a particular gas-solvent system. However, each gas-solvent system has a unique *H* value.

Henry's law constants are usually determined by measuring the equilibrium partial pressure and dissolved concentration of the gas and then calculating the ratio of these two quantities. For most environmental contaminants, the aqueous solubilities and vapor pressures of the pure substances are very low. Consequently, Henry's law is valid up to dissolved concentrations equal to the aqueous solubility and to partial pressures equal to the vapor pressure of the pure substance. The validity of Henry's law at these partial pressures and aqueous concentrations makes it possible to derive the *H*'s by calculating the ratio of the vapor pressure of the pure compound to its aqueous solubility.

We used this method to derive *H*'s for each PCB congener. The reasons for employing this approach were

[†]Present address: Center for Lake Superior Environmental Studies, University of Wisconsin, Superior, WI 55880.

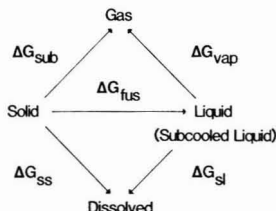


Figure 1. Thermodynamic cycle and Gibbs' free energies.

fourfold. First, excellent aqueous solubility and vapor pressure data exist for many PCB congeners. Second, the temperature dependence of both vapor pressure and aqueous solubility are well understood and are more easily modeled than the temperature dependence of Henry's law constant. Third, methods for predicting solubilities and vapor pressures when experimental data are unavailable have been developed (15-18). Fourth, vapor pressures and solubilities used in this investigation are well below the previously stated limits where Henry's law is not valid. (For biphenyl, the compound with the highest vapor pressure and solubility in this investigation, the vapor pressure and solubility values are 1.0×10^{-5} atm and 8.2×10^{-7} mol/mol at 25 °C.)

To calculate H 's for all congeners, vapor pressures and aqueous solubilities were calculated at the temperature of interest for the PCB congeners with experimental data. Correlations were then constructed from these calculated sets of data. Subsequently, vapor pressures and solubilities were predicted for each PCB congener, and H for each congener was determined from the ratio of these two properties.

The derived H 's were determined by using the liquid (or subcooled liquid) states for both vapor pressure and solubility. The ratio of the solid-state properties was not selected because both predictive methods employed here estimate the properties for the (subcooled) liquid state. Furthermore, this method eliminates the need to account for the change in fugacity between the solid and subcooled liquid states and the errors in making this correction.

Prediction of Vapor Pressures

When recently acquired vapor pressure measurements on four compounds (10) were combined with previously published determinations (19-28), vapor pressure-temperature relationships for 15 PCB congeners were assembled [Table I of supplementary material (see paragraph at end of paper regarding supplementary material)]. For the temperature of interest, vapor pressures were calculated by using these relationships. These values were then used in creating a correlative equation which allowed the prediction of vapor pressures for all congeners.

A comparative study of vapor pressure estimation procedures for PCB congeners has been performed (16), and the most accurate correlative method was used here. This correlative method constructs a relationship between the Gibbs free energy of vaporization, ΔG_{vap} , and the gas-liquid chromatographic retention index for each compound.

The thermodynamic cycle and Gibbs free energies employed by this correlative method are displayed in Figure 1. From basic chemical thermodynamics (29), the Gibbs free energies of sublimation, ΔG_{sub} , and vaporization may be determined by

$$\Delta G_{\text{sub}} = -RT \ln p_s^0 \quad (2)$$

$$\Delta G_{\text{vap}} = -RT \ln p_l^0 \quad (3)$$

where R is the ideal gas constant, T is the temperature of

interest, and p_s^0 and p_l^0 are the vapor pressures of the pure solid and liquid at temperature T .

From equilibrium thermodynamics (14), the Gibbs free energy of fusion, ΔG_{fus} , can be determined by

$$\Delta G_{\text{fus}} = \Delta S_{\text{fus}}(T_{\text{mp}} - T) \quad (4)$$

where ΔS_{fus} is the entropy of fusion of the solid and T_{mp} is the melting point of the solid. ΔS_{fus} was assumed to be a constant for all compounds and was set equal to as the average of 16 individual determinations for PCBs by Miller et al. (8), 13.1 cal/(mol·K). For liquids, ΔG_{fus} is equal to zero. The Gibbs free energy for the transformation between the subcooled liquid and vapor states for a solid is calculated as follows:

$$\Delta G_{\text{vap}} = \Delta G_{\text{sub}} - \Delta G_{\text{fus}} \quad (5)$$

The gas-liquid chromatographic retention indexes (RI) for each PCB congener were derived from the half-retention indexes of Albro et al. (30) for the Apiezon L stationary phase column using the method of Sisson and Welti (31) as described by Albro et al. (30).

The correlative equation was determined by regressing the ΔG_{vap} against the RI for the 15 PCB congeners with experimental values by using an equation of the form

$$\Delta G_{\text{vap}} = m\text{RI} + b \quad (6)$$

where m is the slope and b is the intercept. Using additional constants and/or dependent variables did not improve the fit of the data. Comparison of the predicted and experimental vapor pressures revealed an average factor of error (AFE) of 1.75 at 25.0 °C. (The factor of error is defined as the ratio of the predicted to experimental value. However, if this ratio is less than 1.0, the reciprocal of this ratio is used.) The AFE varied slightly from this value when different temperatures were used in creating the correlations. The AFE for all temperatures between 0 and 40 °C at 5 °C increments was 1.76 with a standard deviation of 0.042. The r^2 for these regression equations had a minimum of 95.0% in this range.

The vapor pressure for each PCB congener was predicted by obtaining the ΔG_{vap} from the correlative equation. The vapor pressure (for the subcooled liquid state) was calculated from the ΔG_{vap} by using eq 3.

Prediction of Aqueous Solubilities

Aqueous solubilities have been measured by using the generator column technique (9, 12) for 18 PCB congeners at 25.0 °C and for biphenyl and 4-chlorobiphenyl at other temperatures (8, 9, 11). Additional solubility data, measured by using different techniques, are available (32); however, the accuracy of the data is unknown, and the precision is poor. Uncertainties in the nongenerator column data arise because of analytical difficulties in measuring submicromolar aqueous solubilities (12). The generator column method is an established technique which circumvents most of these analytical difficulties and has uncertainties which are substantially less than other techniques (12). Consequently, we have chosen to use only the generator column data to minimize overall uncertainties in the predicted H 's. The approach employed here consisted of determining aqueous solubilities for the 18 congeners with experimental values for the temperature of interest. Since aqueous solubilities are limited for temperatures other than 25.0 °C, a relationship defining the dependence of solubility on temperature was developed. By use of the 18 solubility values, a correlative equation was found, and solubilities were determined for each congener. Experimental solubilities, melting points,

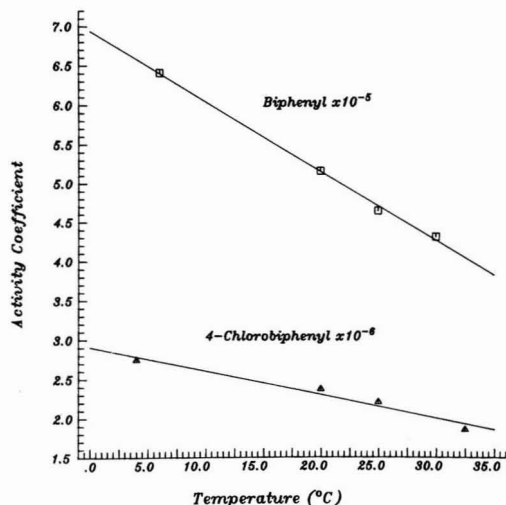


Figure 2. Temperature dependence of biphenyl and 4-chlorobiphenyl activity coefficients.

and entropies of fusion are listed in Table II of the Supplementary Material for the 18 PCB congeners.

From equilibrium thermodynamics (14), the mole fraction solubility of a compound is

$$x = f_s / (f_l \gamma) \quad (7)$$

where x is the mole fraction solubility, γ is the aqueous activity coefficient, and f_s/f_l is the fugacity correction factor for changing from the solid to subcooled liquid states. If the compound is a liquid at the temperature of interest, this correction factor is equal to 1.00. This ratio can be evaluated with little error by using the following formula (14):

$$\ln (f_l / f_s) = \Delta S_{fus} (T_{mp} - T) / (RT) \quad (8)$$

Entropies of fusion and melting points exist for nearly all of the 18 PCB congeners. The only experimental data not available are the entropies of fusion for 4-chlorobiphenyl and 2,5-dichlorobiphenyl. These values were set equal to the average value for the 16 other compounds, 13.1 cal/(K·mol). Consequently, the temperature dependence of the γ or x can be defined, and the temperature dependence of the other variable can be calculated. We have chosen to define the temperature dependence of the γ because this variable is more consistent and uniform in behavior within a family of compounds.

For biphenyl and 4-chlorobiphenyl, activity coefficients were calculated and plotted vs. temperature (Figure 2). This plot reveals that the γ is not a constant in the range 5–30 °C and that its temperature dependence is linear. Regression analysis of the γ against temperature yielded excellent fits of the data. The regression lines for biphenyl and 4-chlorobiphenyl are shown in Figure 2 (r^2 of 99.8 and 96.3%).

Since no experimental solubilities are available at temperatures different from 25.0 °C for higher chlorinated PCBs, we have examined the dependence of the γ -temperature relationship with increasing molecular weight using 11 different polynuclear aromatic hydrocarbons (33). Plots and regression analyses of the calculated γ 's vs. temperature revealed linear behavior between these variables for 10 different compounds with molecular weights ranging from 128.2 (naphthalene) to 228.3 (chrysene). The average r^2 for these regression analyses was 98.5%.

Benzene was the only compound not obeying this relationship. The percentage change in the γ was independent of molecular weight between the temperatures of 5 and 30 °C for the 10 polynuclear aromatic hydrocarbons with linear behavior.

We have also examined the temperature dependencies of the γ 's for the polynuclear aromatic hydrocarbons, biphenyl, and PCBs using UNIFAC (34). UNIFAC yielded very inaccurate γ 's for all of the compounds, and the predictive power of UNIFAC diminished rapidly with increasing molecular weight in the PCB family (e.g., UNIFAC predicted the γ for biphenyl to be greater than that of decachlorobiphenyl). However, the γ -temperature relationship was predicted to be linear for all PCBs and polynuclear aromatic hydrocarbons ($r^2 > 95\%$ for all linear regressions). For the 10 polynuclear aromatic hydrocarbon compounds exhibiting linear behavior, an average decrease of 38.0% in the experimental γ occurred over a temperature range of 5–30 °C, and UNIFAC predicted a decrease of 44.2%. For biphenyl and 4-chlorobiphenyl, experimental decreases in the γ 's were 33.2% (6–30 °C) and 30.6% (4–32 °C). UNIFAC predicted decreases of 39.5% and 53.8%. For the other PCB molecular weight classes, UNIFAC predicted decreases of ca. 68% in the γ with a change in temperature of 5–30 °C.

The analyses done using UNIFAC and the experimental data indicate that the γ is not constant. In addition, the γ data for the polynuclear aromatic hydrocarbons suggest that the γ -temperature relationship is constant in a family of compounds. Consequently, we have assumed that the γ -temperature relationships for biphenyl and 4-chlorobiphenyl are typical of all PCBs. For these compounds, the relationship between temperature and the γ is linear, and γ 's decrease 31.9% and 25.8% with an increase in temperature from 0 to 25 °C. We have adopted the average decrease of 28.8% in the γ with an increase in temperature from 0 to 25 °C as the γ -temperature relationships for all PCB congeners.

The solubilities for the 18 congeners at the temperature of interest were calculated by determining the activity coefficient for each congener at 25.0 °C using the melting point, entropy of fusion, solubility data at 25.0 °C, and eq 7 and 8. By use of γ at 25 °C and the γ -temperature relationship, γ at the temperature of interest was determined. By use of eq 7 and 8, and the γ for the temperature of interest, the solubility was determined. These 18 solubilities were then used in creating a correlative equation for predicting the solubilities for all PCB congeners.

Methods for correlating and predicting aqueous solubilities have been examined extensively (15). We used the method of Hermann (35, 36) as applied by Pearlman (37) and others (32, 38). This method constructs a correlation between the Gibbs free energy of solubilization of the (subcooled) liquid and molecular surface area for the compounds of interest.

The thermodynamic cycle and Gibbs free energies employed by this correlative method are displayed in Figure 1. From basic chemical thermodynamics (29), the Gibbs free energies of solubilization of a solid, ΔG_{ss} , and of a liquid, ΔG_{sl} , can be calculated by

$$\Delta G_{ss} = -RT \ln x_s \quad (9)$$

$$\Delta G_{sl} = -RT \ln x_l \quad (10)$$

where x_s and x_l are the mole fraction solubilities of the solid and liquid. From the thermodynamic cycle, the Gibbs free energy of solubilization of the subcooled liquid can be determined as follows:

$$\Delta G_{sl} = \Delta G_{ss} - \Delta G_{fus} \quad (11)$$

where ΔG_{fus} is calculated as previously discussed.

For the 18 PCB congeners, the ΔG_{sl} was determined by using the above equations and the solubilities at the temperature of interest.

The molecular surface areas for all PCB congeners were calculated by using the numerical method of Pearlman (37), obtained in program form from the Indiana Quantum Exchange Program, Indiana University, Bloomington, IN. Input data to the program consisted of atomic coordinates, a solvent radius of 0.0, and van der Waals' radii. Atomic coordinates were created in-house by using a Fortran program (39). Atomic bond distances and angles for the biphenyl structures were taken from the work of Trotter (40). van der Waals' radii for all atoms and bond lengths for chlorine were obtained from Bondi (41) and Weast (20). On the basis of the gas-phase electron diffraction data of Bastiansen (42), the angle between the two phenyl rings for each PCB congener was set at the smallest angle where no overlap occurs between the adjacent ortho atoms. These angles were 39°, 57°, 57° or 123°, 73°, and 73° for zero, one, two, three, and four ortho chlorines, respectively.

The correlative equation was found by regression of ΔG_{sl} vs. surface area, area using an equation of the form

$$\Delta G_{\text{sl}} = A + B \text{Area} + C \text{Area}^2 \quad (12)$$

where A , B , and C are the regression coefficients. Other forms of the correlation equation were evaluated prior to the selection of this equation form. The addition or removal of constants and/or dependent variable terms to the regression equation did not improve the fit of the data. Comparison of the predicted and experimentally derived solubilities revealed an AFE for the correlative equation of 1.96 for any temperature between 0 and 40 °C. The minimum r^2 for the regression equations was 95.1% in this range.

In predicting the solubilities for each PCB congener, ΔG_{sl} was determined by using the correlative equation. From eq 10, mole fraction solubility, x_1 , for the subcooled liquid (or liquid) state was predicted.

Evaluation of Calculated Henry's Law Constants

Henry's law constants were calculated from the ratio of the predicted subcooled liquid vapor pressures and aqueous solubilities for the temperature of interest for each PCB congener. To assess the accuracy of these predictions, we compared these values to those determined experimentally using the batch technique (43, 44), the purging technique (45, 46), and the ratios of the vapor pressure to aqueous solubility at 25 °C from Tables I and II in the supplementary material. However, before reporting the results of this analysis, a discussion of the possible weaknesses and errors in experimentally determined H 's is presented.

Methods for measuring the H 's are analytically difficult for compounds with low vapor pressures and aqueous solubilities. Difficulties arise because air and water samples containing a few nanograms or less of the compound must be quantified. In addition, for the purging technique, the purge gas leaving the system must be in equilibrium with the liquid solute concentration. Matter-Muller et al. (47) have reviewed the theory for this technique and shown that water depths which are larger than those in use may be necessary for attaining equilibrium. Establishing equilibrium is dependent upon the experimental apparatus and its operating conditions, e.g., gas flow rates and water depths. If equilibrium is not attained, the measured H 's will be too low.

For the data of Mackay et al. (45), the gas leaving the system was at equilibrium (47). However, for the data of

Atlas et al. (46), we were unable to determine whether the exiting purge gas was at equilibrium because of insufficient data. Atlas et al. (46) reported a reproducibility of 10–20% for their determinations.

For the batch technique employed by Murphy et al. (43), an excess amount of an Aroclor mixture or of a single PCB congener was equilibrated with air and water in a closed container. Good agreement was reported between the measured and published values for single congeners. However, differences in measured values were noted when an Aroclor mixture rather than the pure congener was used as the source of the compound. The differences were attributed to analytical error. However, the presence of excess Aroclor mixture in the equilibration vessel may be partly responsible for this difference. These investigators estimated the error in the measured H 's to be a factor of 2–3.

The total uncertainty in the predicted H 's is a combination of the errors in the experimental vapor pressures and aqueous solubilities, the predictive correlations, and the assumed γ -temperature relationship. The error in the experimental vapor pressures is at best 6% but may be much larger, a factor of 2–3. The error in the experimental solubilities is estimated to be 3% by May et al. (12). The error in the predictive correlations was estimated by comparing the ratio of the vapor pressure to aqueous solubilities for the experimental data used in creating the correlations to the predicted ratio. For temperatures of 0, 5, 10, ..., and 40 °C, an overall AFE of 3.33 was obtained. We are unable to derive an error estimate for the γ -temperature relationship, but we believe that an error of a factor of 2–3 would be the upper limit. Combining these errors yields a worst-case total uncertainty, AFE, of ca. 5.0 for the predicted H 's. This AFE, we believe, is very conservative; the error in the predicted H 's is probably lower.

For comparison purposes, we have assumed that the error reported by Murphy et al. (43) is "typical" for all of the experimental determinations, ca. 2.5. For the predicted H 's, the propagation of error analysis suggests the error for these values is ca. 5.0.

H 's were predicted for comparison with experimental values obtained at temperatures of 23.0 (46), 19.0 (43), and 25.0 °C (45, 44; ratio of vapor pressure to aqueous solubility from experimental data). The measured H 's tend to be slightly higher than the predicted values (Figure 3). Also plotted in this figure are the error limits for the predicted H 's (dashed lines). Most of the experimental values, 40 of 51, fall within the error limits for the predicted H 's. When both errors are considered, only a few experimental values, 4 of 51, have error boundaries which do not intersect with the error limits for the predicted H 's.

If all values are included, the AFE between the experimental and predicted H 's is 4.26 for 51 individual measurements ($n = 51$). For the data sets of Murphy et al. (43), Atlas et al. (46), Mackay et al. (45), and Neely et al. (44) and the experimental ratios, AFEs of 4.44 ($n = 30$), 4.88 ($n = 10$), 3.02 ($n = 1$), 1.16 ($n = 1$), and 3.41 ($n = 9$) were obtained, respectively.

Comparison of the experimental and predicted H 's reveals fair agreement between these values. The experimental values tend to be higher than those predicted, and we are unable to explain this trend. Sources of bias in either the predicted or observed H 's are not apparent. Reasons such as nonequilibrium conditions when the measurements were performed, the use of the Aroclor mixtures rather than pure compounds as the source of each congener, and analytical error may bias the experimental values. Also, the predictive models may not be totally

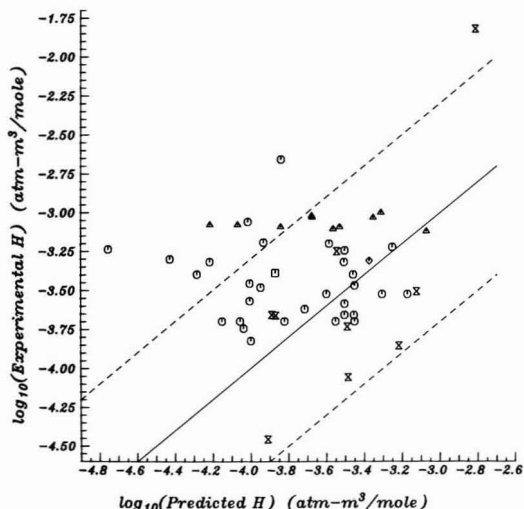


Figure 3. Experimental Henry's law constants of Murphy et al. (43) (O), Atlas et al. (46) (Δ), Mackay, et al. (45) (\square), Neely (44) (\diamond), and the ratios of experimental vapor pressures to aqueous solubilities (hourglass) vs. predicted Henry's law constants. The solid line is where the predicted and experimental H 's are equal. The dashed lines are the upper and lower error limits on the predicted H 's.

correct. Unfortunately, we cannot conclusively demonstrate which of the above sources of error is/are responsible for the observed trend. The poor agreement between the observed and predicted H 's suggests that additional data of highest quality are needed. Additional data would permit a more rigorous evaluation of the predictive methods and eliminate the sources of experimental error presented above.

In view of the analytical difficulties in measuring the H 's and the errors in the predictive method, we believe the accuracy of the predicted values to be reasonable. The error analysis based on available data suggests that the AFE for the predicted H 's in the range 0–40 °C is ca. 5.0. However, the AFE may be much lower.

Examination of Henry's Law Constants

Predicted Henry's law constants for all PCB congeners are plotted in Figure 4 for 25.0 °C and are listed in Table III according to IUPAC number (48) (supplementary material). For temperatures other than 25.0 °C, these values are reported elsewhere (49). The distribution of the H 's displayed in this figure is representative for the temperature range 0.0–40.0 °C. A systematic variation in the H 's with molecular weight of the PCB congeners was not observed (Figure 4). The data of Murphy et al. (43) and Atlas et al. (46) support this observation. However, Bopp (7) using a small data base recently reported that a significant variation of the H 's with molecular weight may exist. Examination of a large data base (Figure 4) indicates that the H 's do not vary systematically with molecule weight when all PCB congeners are considered. However, if the PCB congeners are grouped according to the number of ortho chlorines (Figure 4), a significant variation with molecular weight does occur. In all five groups, zero, one, two, three, and four ortho chlorines, the H 's decrease with increasing molecular weight. Also, the H 's increase in value with increasing number of ortho chlorines for the same molecular weight class. These trends are not apparent in the data of Murphy et al. (43) and Atlas et al. (46), possibly due to the limited number of experimental values for each

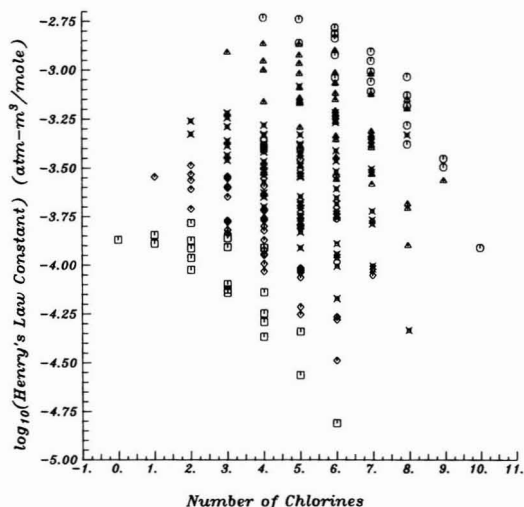


Figure 4. Dependence of predicted Henry's law constants on chlorine content at 25.0 °C. The number of ortho chlorines; zero, one, two, three, or four, are symbolized by (\square), (\diamond), (\times), (Δ), and (O), respectively.

degree of ortho substitution.

This behavior is apparently related to the vapor pressures of the PCB congeners rather than their aqueous solubility. The lowest values of the H 's occur for congeners with no ortho chlorines (Figure 4). These congeners elute from a gas-liquid chromatographic column much later than PCBs with ortho chlorines (30). In general, elution sequence follows the pattern of ortho, meta, and para substitution by chlorines; shorter elution times correspond to higher vapor pressures. This elution order matches the observed pattern for the H 's and supports the hypothesis that differences in the H 's within a molecular weight class are related to vapor pressure.

The predictive model for aqueous solubility in this investigation employs total molecular surface area as the independent variable. This independent variable is quite insensitive to specific structural details of the PCB molecule. Differences in surface areas are small within a molecular weight class but are very large between molecular weight classes. Consequently, the structural detail of the molecule is masked numerically by the molecular weight information included in the total surface area value. When solubilities are predicted, almost identical values are obtained within each molecular weight class for the subcooled liquid solubility because each prediction is based largely on molecular weight information. This general invariance of solubility within a molecular weight class also strongly supports the observation that variation in the H 's is related to the vapor pressure of the PCB congeners.

The temperature dependencies of the H 's are well defined according to chlorine number. The H as a percentage of the value at 25 °C was calculated for the temperature range 0–40 °C for each PCB. These percentages were then averaged for each molecular weight class and for all congeners. These values are reported in Table IV (supplementary material) and are plotted in Figure 5 for biphenyl, the pentachlorobiphenyls, and decachlorobiphenyl. Values for the other molecular weight classes lie between the decachlorobiphenyl and biphenyl curves and follow an ascending order according to molecular weight. The overall average changes in the H 's were very similar to the values for the pentachlorobiphenyls. The largest overall changes

Table I. Air-Water Partition Coefficients for Aroclor PCB Mixtures (atm•m³/mol)

temp, °C	Aroclor						equimolar mixture
	1221	1242	1248	1254	1260	1268	
0.0	0.286 E-4 ^a	0.347 E-4	0.413 E-4	0.226 E-4	0.244 E-4	0.261 E-4	0.344 E-4
5.0	0.452 E-4	0.575 E-4	0.696 E-4	0.394 E-4	0.435 E-4	0.480 E-4	0.592 E-4
10.0	0.697 E-4	0.928 E-4	0.114 E-3	0.670 E-4	0.754 E-4	0.859 E-4	0.995 E-4
15.0	0.106 E-3	0.147 E-3	0.183 E-3	0.111 E-3	0.127 E-3	0.149 E-3	0.163 E-3
20.0	0.157 E-3	0.227 E-3	0.288 E-3	0.180 E-3	0.210 E-3	0.252 E-3	0.262 E-3
25.0	0.228 E-3	0.343 E-3	0.440 E-3	0.283 E-3	0.336 E-3	0.415 E-3	0.409 E-3
30.0	0.326 E-3	0.509 E-3	0.662 E-3	0.437 E-3	0.527 E-3	0.666 E-3	0.627 E-3
35.5	0.483 E-3	0.760 E-3	0.991 E-3	0.665 E-3	0.809 E-3	0.104 E-2	0.949 E-3
40.0	0.668 E-3	0.108 E-2	0.143 E-2	0.981 E-3	0.121 E-2	0.159 E-2	0.139 E-2

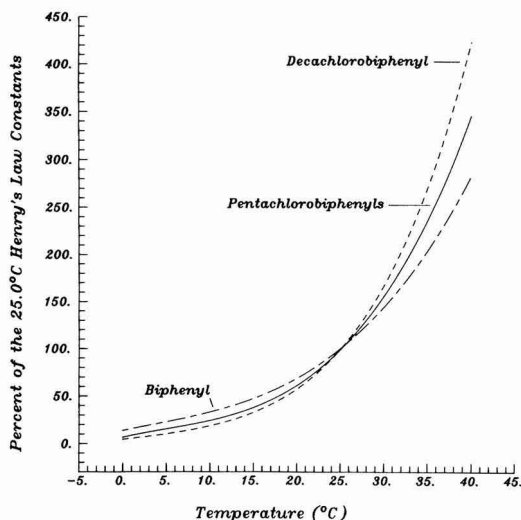
^a E, exponent.

Figure 5. Temperature dependence of predicted Henry's law constants.

in the H 's from 25.0 °C were 8.2 and 346.3% for the temperatures of 0.0 and 40.0 °C, both for decachlorobiphenyl.

Air-water partition coefficients for Aroclor mixtures were calculated from the predicted H 's for temperatures ranging from 0.0 to 40.0 °C (Table I). These partition coefficients are weighted average values based on the percentage of each congener in the PCB mixture. The compositions of the Aroclor mixtures were obtained from Albro et al. (30, 50, 51) for Aroclors 1221, 1242, 1248, 1254, and 1260 and from Mullin et al. (52) for Aroclor 1268. All of these compositions were normalized before calculating the partition coefficients.

The air-water partition coefficients for the PCB mixtures (Table I) are not significantly different for a particular temperature. The general invariance of the partition coefficients was expected since Henry's law constants were independent of molecular weight. (The last two digits of the Aroclor mixture name indicate the percent chlorine in the mixture). However, these partition coefficients change with temperature. Approximately an order of magnitude increase in the partition coefficients occurs when the temperatures change by 25.0 °C. This change was also expected on the basis of the temperature dependencies displayed by the H 's.

Summary

Henry's law constants for all of the PCB congeners have been predicted from vapor pressure and solubility data.

The predicted values are in fair agreement with the experimental Henry's law constants, and additional data are needed to resolve the disparity in these values. The average error for the predicted constants was estimated to be a factor of 5. The approach employed here allows H 's to be predicted at temperatures ranging from 0.0 to 40.0 °C.

The H 's and air-water partition coefficients determined are believed to represent the most accurate values attainable with the data available. Furthermore, this is the most internally consistent data set available for the PCB congeners.

Henry's law constants have been presented graphically for all of the congeners at 25.0 °C and in summarized form as air-water partition coefficients for the Aroclor PCB mixtures. These values demonstrate that the H 's are independent of the molecular weight and that their temperature dependence is approximately an order of magnitude increase with an increase in temperature of 25 °C.

The predicted H 's and the experimental values of Murphy et al. (43) now substantially clarify the values of the H 's for all PCB congeners. The average value for the H at 25.0 °C is ca. 4.0×10^{-4} atm•m³/mol. Previous investigations have suggested H 's (air-water partition coefficients) ranging from 10^{-2} to 10^{-7} (atm•m³/mole) for the PCB congeners (6). The lack of accurate H 's and air-water partition coefficients has caused difficulty and confusion in determining the environmental behavior of PCBs (6). These difficulties should now be reduced, allowing examination of the behavior of the individual PCB congeners.

Acknowledgments

We thank Helen Grogan and Jean Schneider for typing the drafts and manuscript.

Supplementary Material Available

Four tables giving vapor pressure-temperature relationships, aqueous solubilities, and predicted Henry's law constants at 25 °C for PCB congeners and average percentage change in Henry's law constants from their values at 25 °C (9 pages) will appear following these pages in the microfilm edition of this volume of the journal. Photocopies of the supplementary material from this paper or microfiche (105 × 148 mm, 24X reduction, negatives) may be obtained from Microforms Office, American Chemical Society, 1155 16th St., N.W., Washington, DC 20036. Full bibliographic citation (journal, title of article, author, page number) and prepayment, check or money order for \$15.00 for photocopy (\$17.00 foreign) or \$6.00 for microfiche (\$7.00 foreign), are required.

Registry No. Biphenyl, 92-52-4; 2-chlorobiphenyl, 2051-60-7; 3-chlorobiphenyl, 2051-61-8; 4-chlorobiphenyl, 2051-62-9; 2,2'-dichlorobiphenyl, 13029-08-8; 2,5-dichlorobiphenyl, 34883-39-1; 4,4'-dichlorobiphenyl, 2050-68-2; 2,3',4'-trichlorobiphenyl,

38444-86-9; 2,4,6-trichlorobiphenyl, 35693-92-6; 2,2',5,5'-tetrachlorobiphenyl, 35693-99-3; 2,2',4,5,5'-pentachlorobiphenyl, 37680-73-2; 2,2',3,3',5,5',6,6'-octachlorobiphenyl, 2136-99-4; 2,2',3,3',4,4',5,5',6,6'-decachlorobiphenyl, 2051-24-3; 3,3'-dichlorobiphenyl, 2050-67-1; 2,2',4,4',6,6'-hexachlorobiphenyl, 33979-03-2.

Literature Cited

- (1) Hutzinger, O.; Safe, S.; Zitko, V. "The Chemistry of PCB's"; CRC Press: Cleveland, OH, 1974.
- (2) Mackay, D.; Wolkoff, A. W. *Environ. Sci. Technol.* **1973**, *7*, 611-614.
- (3) Mackay, D.; Leinonen, P. J. *Environ. Sci. Technol.* **1975**, *9*, 1178-1180.
- (4) National Academy of Sciences "Polychlorinated Biphenyls"; NRC: Washington, DC, 1979.
- (5) Eisenreich, S. J.; Looney, B. B.; Thornton, J. D. *Environ. Sci. Technol.* **1981**, *15*, 30-38.
- (6) Doskey, P. V.; Andren, A. W. *Environ. Sci. Technol.* **1981**, *15*, 705-711.
- (7) Bopp, R. F. *J. Geophys. Res.* **1983**, *88*, 2521-2529.
- (8) Miller, M. M.; Ghodbane, S.; Wasik, S. P.; Tewari, Y. B.; Martire, D. E. *J. Chem. Eng. Data* **1984**, *29*, 184-190.
- (9) Stolzenburg, T. R.; Andren, A. W. *Anal. Chim. Acta* **1983**, *151*, 271-274.
- (10) Burkhard, L. P.; Armstrong, D. E.; Andren, A. W. *J. Chem. Eng. Data* **1984**, *29*, 248-250.
- (11) Stolzenburg, T. R.; Andren, A. W., University of Wisconsin—Madison, Madison, WI, unpublished data, 1984.
- (12) May, W. E.; Wasik, S. P.; Freeman, D. H. *Anal. Chem.* **1978**, *50*, 175-179.
- (13) Sonnefeld, W. J.; Zoller, W. H.; May, W. E. *Anal. Chem.* **1983**, *55*, 275-280.
- (14) Prausnitz, J. M. "Molecular Thermodynamics of Fluid-Phase Equilibria"; Prentice-Hall: Englewood Cliffs, NJ, 1969.
- (15) Horvath, A. L. "Halogenated Hydrocarbons Solubility-Miscibility with Water"; Marcel Dekker: New York, 1982.
- (16) Burkhard, L. P.; Andren, A. W.; Armstrong, D. E. *Environ. Sci. Technol.*, in press.
- (17) Lyman, W. J.; Reehl, W. F.; Rosenblatt, D. H. "Handbook of Chemical Property Estimation Methods"; McGraw-Hill: New York, 1982.
- (18) Reid, R. C.; Prausnitz, J. M.; Sherwood, T. K. "The Properties of Gases and Liquids"; McGraw-Hill: New York, 1977.
- (19) Westcott, J. W.; Bildeman, T. F. *J. Chromatogr.* **1981**, *210*, 331-336.
- (20) Weast, R. C. "Handbook of Chemistry and Physics"; CRC Press: Cleveland, OH, 1982.
- (21) Augood, D. R.; Hey, D. H.; Williams, G. H. *J. Chem. Soc.* **1953**, 44-50.
- (22) Westcott, J. W.; Simon, C. G.; Bidleman, T. F. *Environ. Sci. Technol.* **1981**, *15*, 1375-1378.
- (23) Aihara, A. *Bull. Chem. Soc. Jpn* **1959**, *32*, 1242-1248.
- (24) Bradley, R. S.; Cleasby, T. G. *J. Chem. Soc.* **1953**, 1690-1692.
- (25) Bright, N. F. H. *J. Chem. Soc.* **1951**, 624-625.
- (26) Seki, S.; Suzuki, K. *Bull. Chem. Soc. Jpn* **1953**, *26*, 209-213.
- (27) Stull, D. R. *Ind. Eng. Chem.* **1947**, *39*, 517-540.
- (28) Smith, N. K.; Corin, G.; Good W. D.; McCullough, J. P. *J. Phys. Chem.* **1964**, *68*, 940-946.
- (29) Lewis, G. N.; Randall, M.; Pitzer, K. S.; Brewer, L. "Thermodynamics"; McGraw-Hill: New York, 1961.
- (30) Albro, P. W.; Haseman, J. K.; Clemmer, T. A.; Corbett, B. *J. J. Chromatogr.* **1977**, *136*, 147-153.
- (31) Sissons, D.; Welti, D. *J. Chromatogr.* **1971**, *60*, 15-32.
- (32) Mackay, D.; Mascarenhas, R.; Shiu, W. Y.; Valvani, S. C.; Yalkowsky, S. H. *Chemosphere* **1980**, *69*, 257-264.
- (33) May, W. E.; Wasik, S. P.; Freeman, D. H. *Anal. Chem.* **1978**, *50*, 997-1000.
- (34) Fredenslund, A.; Gmehling, J.; Rasmussen, P. "Vapor-Liquid Equilibrium using UNIFAC"; Elsevier: Amsterdam, 1977.
- (35) Hermann, R. B. *J. Phys. Chem.* **1971**, *75*, 363-368.
- (36) Hermann, R. B. *J. Phys. Chem.* **1971**, *76*, 2754-2759.
- (37) Pearlman, R. S. In "Physical Chemical Properties of Drugs"; Yalkowski, S. Y.; Sikula, A. A.; Valvani, S. C., Eds; Marcel Dekker: New York, 1980; Med. Res. Ser. 10, pp 321-347.
- (38) Amidon, G. L.; Anik, S. T. *J. Chem. Eng. Data* **1981**, *26*, 28-33.
- (39) Loux, N.; University of Wisconsin—Madison, Madison, WI, unpublished program, 1984.
- (40) Trotter, J. *Acta Crystallogr.* **1961**, *14*, 1135.
- (41) Bondi, A. "Physical Properties of Molecular Crystals, Liquids and Gases"; Wiley: New York, 1968; Chapter 14.
- (42) Bastiansen, O. *Acta Chem. Scand.* **1949**, *3*, 408-414.
- (43) Murphy, T. J.; Pokojowczyk, J. C.; Mullin, M. D. In "Physical Behavior of PCBs in the Great Lakes"; Mackay, D.; Patterson, S.; Eisenreich, S. J.; Simmons, M. S. Eds.; Ann Arbor Science: Ann Arbor, MI, 1983; pp 49-58.
- (44) Neely, W. B. In "Physical Behavior of PCBs in the Great Lakes"; Mackay, D.; Patterson, S.; Eisenreich, S. J.; Simmons, M. S., Eds.; Ann Arbor Science: Ann Arbor, MI, 1983; pp 71-88.
- (45) Mackay, D.; Shiu, W. Y.; Sutherland, R. P. *Environ. Sci. Technol.* **1979**, *13*, 333-337.
- (46) Atlas, E.; Foster, R.; Giam, C. S. *Environ. Sci. Technol.* **1982**, *16*, 283-286.
- (47) Matter-Muller, C.; Gujer, W.; Giger, W. *Water Res* **1981**, *15*, 1271-1279.
- (48) Ballschmiter, K.; Zell, M. *Fresenius' Z. Anal. Chem.* **1980**, *302*, 20-31.
- (49) Burkhard, L. P. Ph.D. Thesis, University of Wisconsin—Madison, Madison, WI, 1984.
- (50) Albro, P. W.; Parker, C. E. *J. Chromatogr.* **1979**, *169*, 161-166.
- (51) Albro, P. W.; Corbett, J. T.; Schroeder, J. L. *J. Chromatogr.* **1981**, *205*, 103-111.
- (52) Mullin, M.; Sawka, G.; Safe, L.; McCrindle, S.; Safe, S. J. *Anal. Toxicol.* **1981**, *5*, 138-142.

Received for review May 9, 1984. Accepted December 26, 1984. This research was funded by the University of Wisconsin Sea Grant College Program under grants from the National Sea Grant College Program, National Oceanic and Atmospheric Administration, U.S., Department of Commerce, and from the State of Wisconsin. Federal Grant NA800-AA-D-00086, Project R/MW-21.

Carbonized Coal Products as a Source of Aromatic Hydrocarbons to Sediments from a Highly Industrialized Estuary

Elizabeth G. Merrill

Department of Oceanography, Old Dominion University, Norfolk, Virginia 23508

Terry L. Wade*

Department of Oceanography, Texas A&M University, College Station, Texas 77843

■ Elizabeth River sediments are contaminated with high levels of hydrocarbons (0.1–2.9 mg/g). Priority pollutant polynuclear aromatic hydrocarbons (PNAs) make up 29% of the hydrocarbons in sediments near a carbonized coal source area. Fingerprinting techniques indicate that point source inputs of carbonized coal products are the major contributors of priority pollutant PNAs to these sediments, while petroleum products from multiple sources are the major contributor of unresolved hydrocarbons. The priority pollutant signature of carbonized coal products is detected in sediments in the source areas and appears to be primarily associated with fine grained particles.

Introduction

Sediments near large urban areas may contain high concentrations of anthropogenic hydrocarbons due to their proximity to source areas (1). Resuspension of contaminated sedimentary material by natural processes (tides, storms, etc.) or by artificial means (dredging, shipping, etc.) can disperse these pollutants to areas much larger than were originally affected. Because of the health hazards associated with anthropogenic hydrocarbons there is considerable interest in determining their sources, fates, and effects in sedimentary environments (2). Polynuclear aromatic hydrocarbons (PNAs) are of particular interest because of their carcinogenic behavior. PNAs generally account for 90% of the chemical constituents of creosote (3). Creosote is a distillate from coal tar made by high-temperature carbonization of bituminous coal (4). Creosote alone or in combination with coal tar or petroleum is the major preservative used in the wood pressure treating industry (5). Blends of creosote with coal tar (50:50) are generally used when treating wood for marine use (4). Creosote has been demonstrated to be a contaminant of shellfish (6–9) and marine sediments (10). Extracts of PNAs from barnacles growing on creosoted pilings have been shown to be carcinogenic in mice (11) and have caused hyperplasia in an estuarine bryozoan growing on creosoted timbers (12). It has also been demonstrated that coal tar coatings of storage tanks leak PNAs into potable water supplies (13).

Three wood-preserving facilities have existed along the Southern Branch of the Elizabeth River, Norfolk, VA, since the early 1900's (Figure 1). Two of these plants ceased operations, one in 1971 and the other in 1981. Although Virginia State Water Control Board (VA SWCB) regulations implemented in 1968 restricted the dumping of industrial process wastewater, each of the three sites is still considered a potential source of pollution due to the leaking of creosote from prior waste dump sites, leaking storage tanks, or spill areas (14). Elevated hydrocarbon concentrations have been found in Elizabeth River sediments from areas adjacent to three wood-preserving plants (15). Since this highly industrialized area may have other hydrocarbon inputs, elevated levels of hydrocarbons can only give circumstantial evidence pointing to the creosote

plants as major contributors of hydrocarbons to the Elizabeth River.

This study compares hydrocarbon distributions in carbonized coal products (creosote, coal tar, roofing tar, and creosoted wood) to that of ship stack and woodstove soot, Kuwait crude oil, no. 2 fuel oil, and a fuel oil spill sample collected from Town Beach, Norfolk, VA. Hydrocarbon distributions characteristic of carbonized coal products were used to estimate the level of creosote contamination in these sediments.

Materials and Methods

Sediment samples were collected by using a grab sampler (which samples approximately the top 10 cm) aboard Old Dominion University's research vessels, ODU-1 and R/V *Linwood Holton*. The sample locations are shown in Figure 1. The samples were stored frozen in clean, solvent-washed jars until analyzed. Creosoted wood samples were collected from areas adjacent to the Elizabeth River (Figure 1). Three samples of refined creosote and one sample of coal tar were also analyzed. Bernuth Lembeck, Inc., a local commercial creosote distributor, supplied samples of no. 1 creosote (creosote A) and coal tar. Creosote B (98.5% refined coal tar creosote, Warner Graham) and creosote C (100% refined creosote oil, Sunnyside Corp.) were purchased locally. Creosote samples from Atlantic Wood Industries, the remaining operative creosoting facility on the Elizabeth River, were not available. The woodstove soot sample was obtained from a domestic woodstove in which predominately hardwoods were burned. The diesel stack soot sample was taken from Old Dominion University's research vessel R/V *Linwood Holton*. The no. 2 fuel oil sample is of the types used locally for home heating. The Kuwait crude oil was kindly supplied by Robert Brown of Mote Marine Lab, Sarasota, FL.

Sediment samples were thawed and mixed to ensure homogeneity. The dry weight and percent water content of the sediment were determined by drying approximately 5 g of the sediment at 105–110 °C for several hours until a constant weight was reached. Grain size distribution was determined by wet sieving and pipet analysis using the techniques of Folk (16).

For hydrocarbon analysis approximately 2 g of wet sediment or other solid sample (such as creosoted wood, soot, etc.) was placed in a 50-mL centrifuge tube. Internal standards, *n*-eicosane (*n*-C₂₀) and 3-methylfluoranthene, were added to the tube along with 5 mL of 0.5 N methanolic potassium hydroxide (MeOH-KOH), 1 mL of toluene, and 1 mL of distilled water which had been preextracted with dichloromethane (CH₂Cl₂). The centrifuge tube was capped tightly and placed in a boiling water bath for 2 h. Every 20 min the samples were removed from the bath and shaken vigorously.

The tubes were cooled to room temperature, 10 mL of preextracted distilled water was added, and the pH was

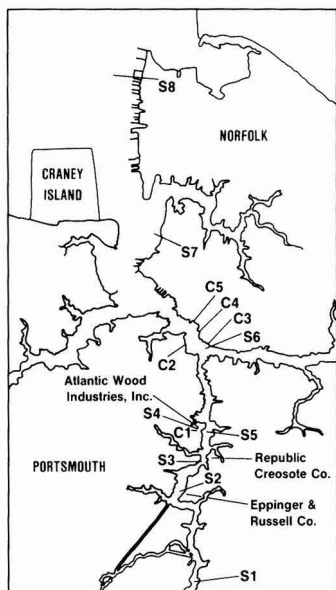


Figure 1. Sampling locations for creosoted wood (C) and sediments (S) and the location of the wood-preserving facilities on the Elizabeth River, Norfolk, VA.

checked to ensure that it was greater than 10. If the pH was less than 10, enough 0.5 N MeOH-KOH was added to bring the pH to greater than 10, and the tube was heated for an additional 20 min.

The sample, still in the centrifuge tube, was extracted 3 times by using 10 mL of petroleum ether each time. If an emulsion formed, it was broken by centrifugation. The petroleum ether phases were combined in a 50-mL pear-shaped flask and reduced to dryness on a rotary flash evaporator under vacuum at a temperature not exceeding 35 °C. Sediment hydrocarbon concentrations determined by using the above test tube extraction technique were within the range of concentrations determined by Soxhlet and reflux/saponification extraction of larger sediment samples (17). The aliphatic (f1) and aromatic (f2) hydrocarbons were separated from other organics by thin-layer chromatography (TLC; 18, 19). Liquid samples (such as creosote, oil, etc.) were analyzed by dissolving the sample in CH_2Cl_2 , and the f1 and f2 hydrocarbons were then separated from other organics by TLC.

The TLC sample fractions were injected on a Hewlett-Packard Model 5830 gas chromatograph equipped with a 25-m SE-54 fused silica capillary column utilizing a flame ionization detector (FID). The signal from the FID was recorded by a Hewlett-Packard Model 18850A reporting integrator. The gas chromatograph was programmed from 70 to 300 °C at 10 °C/min.

Quantitative determinations of hydrocarbon concentrations were made by comparing integrator area counts of the internal standard with integrator area counts of the peaks when an unresolved complex mixture was not present. When the unresolved complex mixture was present, the areas were determined by planimetry. Comparisons of peak areas to the area of the internal standard were used to determine concentrations. Qualitative determination of hydrocarbons in the samples was made by comparison of retention times of known compounds, by coinjection with known compounds, and by gas chromatography combined with mass spectroscopy (GC/MS). A

Table I. Compounds in Creosote That Were Identified by GC (Retention Time and Coinjection) and/or GC/MS

peak	compound	confidence level ^a
A	naphthalene	3
1	biphenyl	2
B	acenaphthylene	3
C	acenaphthene	3
2	dibenzofuran	2
D	fluorene	3
3	methyl dibenzofuran	2
4	xanthene	1
5	methylfluorene	2
6	dibenzothiophene	3
E	phenanthrene	3
F	anthracene	3
8	methylphenanthrene	2
9	methylphenanthrene	2
10	methylphenanthrene	2
11	4H-cyclopenta[def]phenanthrene	2
12	methylphenanthrene	2
13	phenylnaphthalene	2
G	fluoranthene	3
14	unidentified	
H	pyrene	3
15	unidentified	
16	unidentified	
17	benzo[b]fluorene	2
18	benzonaphthothiophene	2
19	benzo[c]phenanthrene	2
J	benzo[a]anthracene	3
K	chrysene	3
20	benzophenanthrene	2
21	methylchrysene or methylbenz[a]anthracene	2
22	unidentified	
L	benzo[k]fluoranthene	3
M	benzo[b]fluoranthene	3
23	benzo[j]fluoranthene	2
24	benzo[e]pyrene	2
N	benzo[a]pyrene	3
25	perylene	2
O	indeno[1,2,3-cd]pyrene	3
P	dibenz[a,h]anthracene	2
Q	benzo[ghi]perylene	2

^aReported in the literature by Borwitzky and Schomburg (22).

Finnagan OWA-Model 20 mass spectrometer coupled to a Sigma 3B gas chromatograph was used for the GC/MS analysis. Procedural blanks and standards were run systematically throughout the analysis period to determine if contamination had occurred and to ensure the proper functioning of the gas chromatograph. Maximum values for the procedural blanks were 2.02 μg for the f1 fraction and 0.60 μg for the f2 fraction. The sample values reported are corrected for the presence of these procedural blanks.

Results and Discussion

Gas chromatograms of hydrocarbon distributions provide a visual comparison of the similarities and differences between carbonized coal products, oil products, and sediment samples. Chromatograms of the aliphatic (f1) and aromatic (f2) fractions of creosote A, the oil spill samples, and sediments from station S6 are shown in Figures 2-4, respectively. The f1 and f2 fractions may contain resolved peaks and an unresolved complex mixture. The f1 fraction contains resolved peaks including *n*-alkanes and pristane and phytane. The resolved f2 peaks were divided into three groupings (Figure 2). The first group consists of the 16 Environmental Protection Agency priority pollutant PNAs (20). The second group consists of 25 other major resolved peaks that were found in most of the creosote samples. These peaks were identified by comparison of peak retention times, coinjection with standards, and/or

Table II. Total Hydrocarbon Concentrations and Weight Percents for f1 and f2 Resolved Peak and Unresolved Peak Designations^a

sample	mg/g ^b	mg/g ^c fines	%						f2 total resolved
			f1 resolved	f1 UCM ^d	f2 PP ^e	f2 MRP ^f	f2 RRP ^g	f2 UCM ^d	
S2	2.9	5.7	40.7	8.3	29.1	14.3	7.6	UD	51.0
S4	0.8	1.6	10.8	43.2	26.2	12.9	6.9	UD	46.0
S5	2.1	2.4	6.3	72.7	5.9	3.1	1.9	10.1	9.9
S3	0.7	3.4	8.4	84.6	3.4	1.9	1.7	UD	7.0
S1	0.1	4.7	19.6	78.4	0.4	0.1	0.3	1.2	0.8
S6	1.1	1.2	7.5	86.5	1.2	0.6	0.3	3.9	2.1
S7	0.4	0.6	7.8	89.2	0.6	0.3	0.2	1.9	1.1
S8	0.4	0.9	8.9	90.1	0.2	0.1	0.2	0.6	0.5
creosoted wood	41-189		5.1	1.5	59.8	21.3	12.3	UD	93.4
creosote	130-550		5.1	0.2	62.5	22.1	10.1	UD	94.7
coal tar	270		12.0	UD	40.5	25.5	22.0	UD	88.0
roof tar	190		2.9	2.1	53.2	20.0	21.8	UD	95.0
woodstove soot	0.4		21.6	3.8	21.0	12.8	14.2	27.0	48.0
diesel stack soot	190		10.6	85.4	0.1	0.2	0.8	2.9	1.1
no. 2 fuel oil	340		30.1	42.3	1.1	1.6	10.3	13.5	13.5
oil spill	180		11.8	40.2	0.4	0.8	10.3	29.5	11.5
Kuwait crude	72		79.0	UD	0.6	0.8	4.2	15.3	5.6

^aThese designations are explained in the text. UD = Undetected. ^bSediment sample calculations were based on dry weights; creosoted wood sample calculations were based on the weight of extractable material. ^cmg/g dry weight basis normalized for the percent fines in the sediments. ^dUCM = unresolved complex mixture (see text). ^ePP = priority pollutant peaks (see text). ^fMRP = major resolved peaks (see text). ^gRRP = remaining resolved peaks (see text).

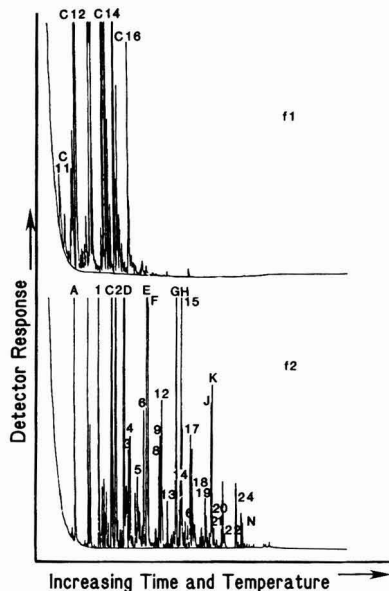


Figure 2. Gas chromatograms of the aliphatic (f1) and aromatic (f2) fractions of creosote A. The f1 fraction contains identified *n*-alkanes in the range *n*-C₁₁ through *n*-C₁₆. Compounds in the f2 fraction are identified in Table I.

confirmation by GC/MS. Specific peak identities and the level of identification (21) are summarized in Table I. The third peak group consisted of all remaining resolved peaks. Concentrations and weight percentages of unresolved complex mixture and resolved peaks in the aliphatic and aromatic fraction of each sample are given in Table II. All carbonized coal products had similar chromatograms typified by Figure 2. Few *n*-alkanes of higher molecular weight than *n*-C₁₆ were detected, and *n*-C₁₅, normally present in unweathered petroleum and biogenic samples (23), was usually not detected. The carbonized coal products contained 2% or less of their hydrocarbons in the form of an unresolved complex mixture, with the majority

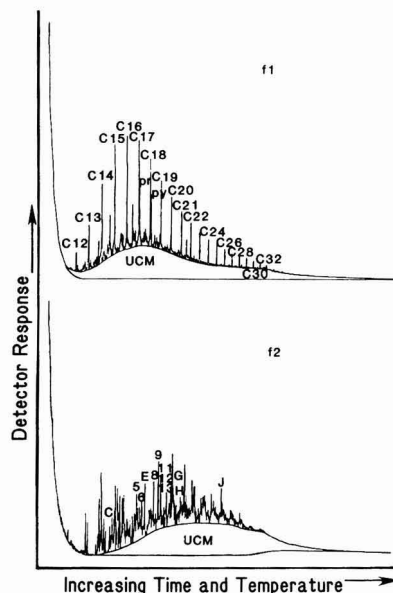


Figure 3. Gas chromatograms of the aliphatic (f1) and aromatic (f2) fractions of the oil spill sample. The f1 fraction contains identified *n*-alkanes in the range *n*-C₁₂ through *n*-C₃₂ and pristane (pr) and phytane (py). UCM, unresolved complex mixture. Compounds in the f2 fraction are identified in Table I.

(41-63%) of the hydrocarbons present as resolved priority pollutants (Table II; Figure 2). Roof tar and coal tar, which are byproducts of the coal tar distillation process (24), had distributions similar to that of creosote, but with a greater relative percent of the higher molecular weight compounds.

In contrast, the f1 fraction of the oil spill sample (Figure 3) has a homologous series of *n*-alkanes from *n*-C₁₂ through *n*-C₃₁ with the dominant peaks in the *n*-C₁₅ through *n*-C₁₈ range. There is also an unresolved complex mixture in both the f1 and f2 fractions. There are resolved peaks in the f2 fraction including some priority pollutants, but they constitute less than 1% of the hydrocarbons on a weight

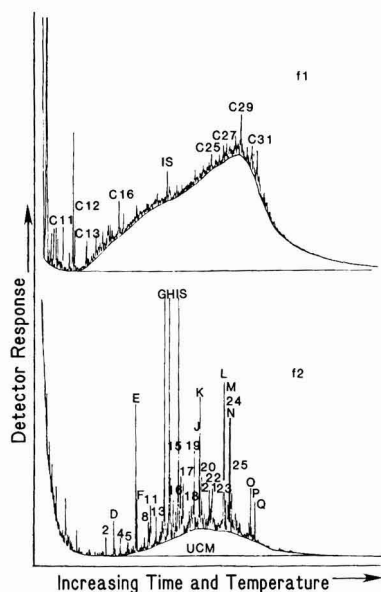


Figure 4. Gas chromatograms of the aliphatic (f1) and aromatic (f2) fractions of the sediment sample from station S6. The f1 fraction contains identified *n*-alkanes in the range *n*-C₁₁ through *n*-C₃₁. UCM, unresolved complex mixture; IS, internal standard. Compounds in the f2 fraction are identified in Table I.

percent basis (Table II). The Kuwait crude oil has no detectable aliphatic unresolved complex mixture which is unusual for petroleum products (25). Woodstove soot, no. 2 fuel oil, diesel stack soot, the oil spill sample, and Kuwait crude oil all contained a substantial percentage of their f2 hydrocarbon in the form of an unresolved complex mixture (Table II). With the exception of woodstove soot, the f2 fractions of these samples contained the highest percentages of remaining resolved peaks and the lowest percentages of priority pollutant peaks. Woodstove soot contained 21% priority pollutants and 14.2% remaining resolved peaks.

The chromatogram of the sediment sample (Figure 4) has a hydrocarbon distribution that could result if weathered petroleum products were mixed with carbonized coal products. There is an unresolved complex mixture present in both the f1 and f2 fractions, similar to the oil spill sample (Figure 3). The resolved f1 fraction contained lower molecular weight (*n*-C₁₆ and below) *n*-alkanes, but *n*-C₁₅ was not detected, similar to the creosote sample (Figure 2). The higher molecular weight resolved *n*-alkane peaks, *n*-C_{25,27,29,31}, are indicative of a biogenic input (26). The resolved peaks in the f2 fraction are also similar to the resolved f2 peaks found in the creosote sample (Figure 2).

Hydrocarbon concentrations for the sediment samples ranged from 0.1 to 2.9 mg/g (Table II). The concentrations are within the range of values previously reported for the Elizabeth River (27, 28). Hydrocarbons have been shown to preferentially associate with fine grained sediments (18, 29). The presence of sand in the sediment acts as a diluent when concentrations are expressed on a dry weight basis. Because fine grained sediments are more easily transported, a more realistic portrayal of hydrocarbon concentrations is given by dividing the hydrocarbon concentration by the sediment's percent silt and clay concentration in order to normalize the hydrocarbon concentrations for the percent fines (30). The hydrocarbon

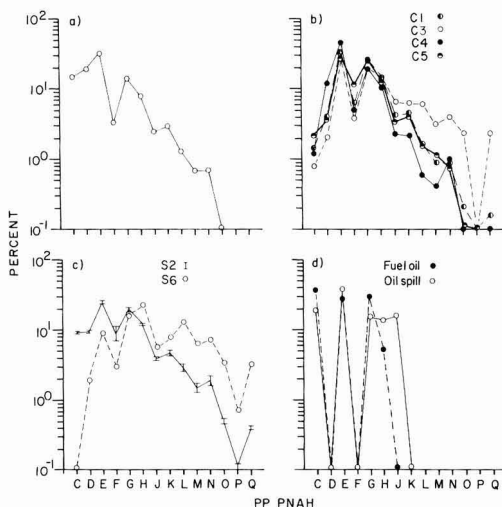


Figure 5. EPA priority pollutant (PP) PNA plots for (a) creosote A, (b) creosoted wood samples, (c) sediment samples, and (d) oil samples. PNAs are identified in Table I.

concentrations for the sediment stations normalized for fines are given in Table II. The high f2 percentages at stations S2, S4, and S5 indicate high inputs of aromatic hydrocarbons at these stations. The f2 normalized fractions have decreasing aromatic hydrocarbon concentrations with increasing distance from the area of the creosoting facility sites, indicating the probability of an aromatic hydrocarbon source in this area. The f1-normalized fraction does not have a similar decreasing concentration pattern but instead has varied concentrations along the length of the Elizabeth River, indicating the presence of multiple sources for the aliphatic hydrocarbons which do not add sufficient quantities of aromatic hydrocarbons to influence the decreasing concentration pattern of the f2 fraction (18).

Aromatic compounds constitute a very high percentage of carbonized coal products (3), and therefore, these compounds may provide a useful fingerprint for carbonized coal products. The weight percent each compound made to the total concentration of the priority pollutants or major resolved peaks group was calculated. The PNAs, in order of increasing GC retention time, were plotted on the x axis, and the log of the percent contribution (in semilog fashion) was plotted on the y axis. These plots describe relative distributions and permit comparison between samples from various sources and with widely varying concentrations. The priority pollutant plots for creosote A and several creosoted wood samples are shown in Figure 5. The error bars in Figure 5c indicate the maximum analytical variability encountered with multiple injections of the same sample. Plots of creosotes B and C were similar to the plot for creosote A with the percentages for most PNAs varying only slightly. The lower molecular weight PNAs (acenaphthene (C) and fluorene (D)) had the greatest variation. The higher molecular weight PNAs (indeno[1,2,3-*cd*]pyrene (O), dibenz[*a,h*]anthracene (P), and benzo[*ghi*]perylene (Q)) were at concentrations close to detection limits. Plots for the creosoted wood samples (Figure 5b) are similar to the plot for creosote A. Weathering processes including evaporation, photochemical oxidation, dissolution, and microbial degradation (2) can preferentially remove the PNAs with molecular weights less than that of fluoranthene (G)

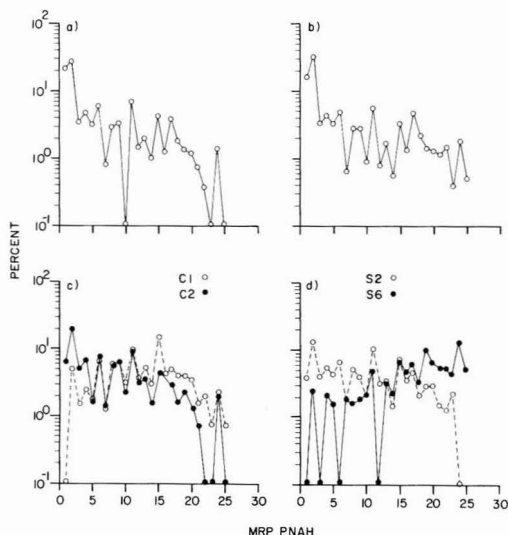


Figure 6. Major resolved peak (MRP) PNA plots for (a) creosote A, (b) 50:50 creosote-coal tar, (c) creosoted wood samples, and (d) sediment samples. MRP PNAs are identified in Table I.

causing the higher molecular weight PNAs (benz[a]-anthracene (J) and above) to have a greater relative percent (31). This removal may explain the different patterns (Figure 5b) seen for the creosoted wood samples which may have undergone less (C4) or more (C3) weathering. Although the priority pollutant PNA plots were similar, the relative percentages of the higher molecular weight PNAs in some creosoted wood samples may be attributable to coal tar formulations and/or to loss of the lower molecular weight PNAs due to weathering. The oil spill sample (Figure 5d), no. 2 fuel oil (Figure 5d), diesel stack soot, and Kuwait crude oil sample PP plots have clearly different patterns from the creosote-related sample plots, containing no detectable quantities of many of the PNAs.

The percent priority pollutant distribution patterns for sediment stations S2 and S6 are given in Figure 5c and are representative of the range of distributions found for all the sediment samples. The sediment priority pollutant group PNA plots are similar to the creosote plots (Figure 5a,b) and did not resemble the PNA distributions of the petroleum-derived samples (Figure 5d).

The plot of the major resolved peaks for creosote A is given in Figure 6a. The creosote B and C plots had a similar pattern. In each, peaks 1–18 followed the same pattern, with peaks 1, 2, 5, 6, 11, 15, and 17 having the highest concentrations. Peaks 7 and 10 had low to undetectable concentrations in all samples. Because creosote-coal tar formulations are commonly used in the wood-preserving industry (4), a more realistic approach when patterning the major resolved peaks, which occur in much smaller concentrations than most of the priority pollutant peaks, is to develop a creosote-coal tar mixture pattern. A pattern for a 50:50 creosote A-coal tar mixture is given in Figure 6b. A 50:50 mixture was chosen because that is the mixture of choice when lumber is treated for marine use (4).

Major resolved peak group PNAs for creosoted wood samples C1 and C2 are plotted in Figure 6c. Wood sample C1 follows closely the rise and fall pattern seen in the creosote-coal tar mixture. The low molecular weight peaks (peaks 1–5) are lower than in the creosote-coal tar mixture and the other peaks correspondingly higher. Wood sample

C2 matches the creosote-coal tar pattern in peak region 1–15. The higher molecular weight peaks have a pattern more similar to those of the creosote samples. These slight peak variations can probably best be explained by the use of different creosotes or creosote-coal tar mixtures than are shown here.

The petroleum-derived samples (diesel stack soot, Kuwait crude oil, oil spill sample, and no. 2 fuel oil) contained no more than 7 of the 25 major resolved peaks at detectable levels, all of which eluted before peak 14. Their plots did not resemble the creosote plots or the sediment plots and therefore were not included. Major resolved peaks from selected sediment stations are plotted in Figure 6d. The plot for station S2 matches the creosote-coal tar major resolved peak plot (Figure 6b) closely, reflecting the same rise and fall pattern and relative percent variations. The major resolved peak plot for station S4 resembled the pattern seen in creosote A (Figure 6a), differing only in the lower relative percentages of the peaks eluting before peak 5 and in the higher relative percentages of the PNAs with higher molecular weights. The plot for station S6 is also given in Figure 6d and displays a similar pattern in the higher molecular weight peaks (peaks 14 and greater) as the other sediment stations (S5, S3, S7, S8, and S1) and the creosote-coal tar. The peaks in the lower molecular weight range appeared to have been preferentially removed at these stations.

The characteristic PNA distribution in creosote is probably altered by environmental processes. PNAs introduced into the marine environment may experience biological uptake, microbial degradation, volatilization, dissolution and dilution, photooxidation, and sedimentation (18, 31, 32). Lee et al. (33) showed, in enclosed ecosystems, that microbial degradation in the water column and evaporation may be the primary removal processes for the lower molecular weight aromatics such as naphthalenes, anthracenes, and phenanthrenes. For the higher molecular weight aromatics such as chrysenes, benzanthracenes, and benzopyrenes, the removal process was dominated by sedimentation and photooxidation. From mesocosm experiments, Lee and Ryan (31) reported that, once reaching the sediments, the PNAs including benz[a]anthracene, chrysene, fluorene, and anthracene were readily degraded at the sediment/water interface, whereas the higher molecular weight PNAs including benzo[a]pyrene and dibenz[a,h]anthracene showed only slight degradation at the sediment/water interface. When PNAs are added to a natural aqueous environment, the removal processes may be dominated by processes such as dissolution and dilution with ultimate sedimentation (32). Degradation and removal are less important once the PNAs reach the subsurface sediment where they can remain unaltered for years (31, 34). Preferential removal processes for the lower molecular weight PNAs in creosote, before reaching the subsurface sediments, could lead to the PNA distributions seen in the sediments from stations S5, S6, S1, S8, and S7. The fact that high concentrations of PNAs remain in these sediments may also be due to large inputs, or to other materials contained in creosote (such as phenols) and not in petroleum that lower microbial activity in the sediments. Differences in the physical states of creosote and oils may also affect the PNA distributions seen. When creosote was mixed with seawater in the laboratory, three phases were formed: one more dense than seawater, one dissolved in seawater, and one less dense than seawater. Analysis of the phase more dense than seawater produced a gas chromatogram indistinguishable from that of intact creosote. At a spill site, the

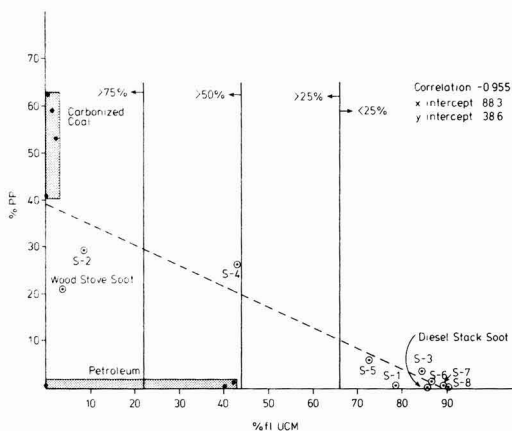


Figure 7. Graph showing the linear relationship between % PP and % f1 UCM of the sediment samples. Source sample areas are identified. Solid lines indicate the percentage contribution of carbonized coal products in the mixing relationship.

phase with a density greater than seawater may be rapidly removed to the sediments with only slight alteration. The water-soluble compounds may then be slowly leached into the water column and act as a chronic PNA source. Petroleum, conversely, is less dense than seawater, and would be subjected to more weathering and dispersal processes than creosote before reaching the sediments.

Since the sediment samples appeared to contain a mixture of carbonized coal products and weathered petroleum products, a plot of the percent priority pollutants (main component of carbonized coal products) was plotted vs. the percent f1 unresolved complex mixture (main component of weathered petroleum products). This plot (Figure 7) shows a linear relationship (correlation of -0.955) which would be expected if the changes in the percent composition were due to simple mixing of these two end members. Sediments that are contaminated predominantly by weathered petroleum (35) are reported to contain 89% on a weight basis of their hydrocarbons as an unresolved complex mixture and less than 0.4% as priority pollutants (18). These percentages are in good agreement with our x intercept of 88% unresolved complex mixtures. The y intercept, 39%, should reflect the carbonized coal end member which ranges from 41 to 63% priority pollutants. The reason this number is low could be due to preferential weathering (such as dissolution) of the priority pollutant compounds in the sediments.

Conclusions

The fingerprinting techniques used in this study show Elizabeth River sediments are contaminated with hydrocarbons from both carbonized coal and petroleum products. Carbonized coal products appear to have point sources associated with creosoting facility sites and are the main source of carcinogenic PNAs in the sediments. Petroleum products appear to have many sources, are highly weathered before reaching the sediments, and are the main source of the unresolved complex mixture. Carbonized coal products may contain compounds in addition to hydrocarbons (such as phenols) that may increase their environmental impact.

Acknowledgments

We thank M. C. Kennicutt II, G. T. F. Wong, and F. E. Scully, Jr., for reviewing the manuscript. We also thank

J. Hall for performing the GC/MS analysis, T. L. Switzer from the VA SWCB for information concerning the creosoting facilities along the Elizabeth River, and Bernuth Lembcke, Inc., for supplying samples of creosote and coal tar.

Registry No. C₁₁, 1120-21-4; C₁₂, 112-40-3; C₁₃, 629-50-5; C₁₆, 544-76-3; C₂₅, 629-99-2; C₂₇, 593-49-7; C₂₉, 630-03-5; C₃₁, 630-04-6; acenaphthene, 83-32-9; dibenzofuran, 132-64-9; xanthene, 92-83-1; methylfluorene, 26914-17-0; phenanthrene, 85-01-8; anthracene, 120-12-7; methylphenanthrene, 31711-53-2; 4H-cyclopenta[def]phenanthrene, 203-64-5; phenylanthracene, 35465-71-5; fluoranthene, 206-44-0; pyrene, 129-00-0; benzo[b]fluorene, 30777-19-6; benzonaphthothiophene, 61523-34-0; benzo[c]phenanthrene, 195-19-7; benzo[a]anthracene, 56-55-3; chrysene, 218-01-9; benzo[ghi]perylene, 65777-08-4; methylchrysene, 41637-90-5; methylbenzo[a]anthracene, 43178-22-9; benzo[k]fluoranthene, 207-08-9; benzo[b]fluoranthene, 205-99-2; benzo[j]fluoranthene, 205-82-3; benzo[e]pyrene, 192-97-2; benzo[a]pyrene, 50-32-8; perylene, 198-55-0; indeno[1,2,3-cd]pyrene, 193-39-5; dibenz[a,h]anthracene, 53-70-3; benzo[ghi]perylene, 191-24-2.

Literature Cited

- (1) Wakeham, S. G.; Farrington, J. W. In "Contaminants and Sediments"; Baker, R. A., Ed.; Ann Arbor Science Publishers: Ann Arbor, MI, 1980; Vol. 1, pp 3-32.
- (2) National Academy of Sciences "Petroleum in the Marine Environment". NAS, Washington, DC, May 21-25, 1973.
- (3) McNeil, D. *Rec. Annu. Conv. Br. Wood Preserv. Assoc.* **1959**, 136-150.
- (4) American Wood-Preservers' Association "The AWP Book of Standards"; AWP: Washington, DC, 1971.
- (5) Webb, D. A. Monroeville, PA, 1980, report from Industrial Products Division, Koppers, Co.
- (6) Zitko, V. *Environ. Contam. Toxicol.* **1975**, 14, 621.
- (7) Dunn, B. P.; Stich, H. F. *Proc. Soc. Exp. Bio. Med.* **1975**, 150, 49.
- (8) Dunn, B. P.; Stich, H. F. *J. Fish. Res. Board Can.* **1976**, 33, 2040.
- (9) Dunn, B. P.; Fee, J. J. *J. Fish. Res. Board Can.* **1979**, 36, 1469.
- (10) Lake, J. L.; Norwood, C.; Dimock, C.; Bowen, R. *Geochim. Cosmochim. Acta* **1979**, 43, 1847.
- (11) Shimkin, M. V.; Kow, B. K.; Zechmeister, L. *Science (Washington, D.C.)* **1951**, 113, 650.
- (12) Powell, N. A.; Sayce, C. S.; Tufts, D. F. *J. Fish. Res. Board Can.* **1970**, 27, 2095.
- (13) Alben, K. *Environ. Sci. Technol.* **1980**, 14, 468.
- (14) Switzer, T. L. Virginia State Water Control Board, personal communication, 1983.
- (15) Alden, R. W., III; Young, R. J., Jr. *Arch. Environ. Contam. Toxicol.* **1982**, 11, 567.
- (16) Folk, R. L. "Petrology of Sedimentary Rocks"; Hemphill: Hemphill, TX, 1980.
- (17) Merrill, E. G. M.S. Thesis, Old Dominion University, Norfolk, VA, 1984.
- (18) Wade, T. L.; Quinn, J. G. *Org. Geochem.* **1979**, 1, 157.
- (19) Moore, W. E.; Effland, M. J.; Roth, H. G. *J. Chromatogr.* **1968**, 38, 522.
- (20) *Fed. Regist.* **1979**, 44, 69494.
- (21) *Environ. Sci. Technol.* **1984**, 18, 203A.
- (22) Borwitzky, H.; Schomburg, G. *Chromatography* **1979**, 11, 418.
- (23) Blumer, M.; Guillard, R. R. L.; Chase, T. *Mar. Biol.* **1971**, 8, 183.
- (24) Berkowitz, N. "An Introduction to Coal Technology"; Academic Press: New York, 1979.
- (25) Farrington, J. W.; Meyers, P. A. In "Environmental Chemistry"; Eglinton, G., Ed.; The Chemical Society: London, 1975; Vol. 1, Chapter 5.
- (26) Ehrhardt, G.; Blumer, M. *Environ. Pollut.* **1972**, 3, 179.
- (27) Bieri, R. H.; Hein, C.; Huggett, R. J.; Shou, P.; Slone, H.; Smith, C.; Su, C. "Toxic Organic Compounds in Surface Sediments from the Elizabeth and Patapsco Rivers and Estuaries"; VA Institute of Marine Science: Gloucester Pt., VA, 1982.

- (28) Virginia State Water Pollution Control Board "The Elizabeth River: An Environmental Perspective". 1983, VA SWCB Basic Data Bulletin 61.
- (29) Meyers, P. A.; Quinn, J. G. *Nature (London)* 1973, 244, 23.
- (30) Brown, R. B.; Wade, T. L. *Water Res.* 1984, 18, 621.
- (31) Lee, R. F.; Ryan, C. *Can. J. Fish. Aquat. Sci.* 1983, 40, 86.
- (32) Farrington, J. W.; Quinn, J. G. *Estuarine Coastal Mar. Sci.* 1973, 1, 71.
- (33) Lee, R. F.; Gardner, W. S.; Anderson, J. W.; Blaylock, J. W.; Barwell-Clarke, J. *Environ. Sci. Technol.* 1978, 12, 832.
- (34) Gschwend, P. M.; Hites, R. A. *Geochim. Cosmochim. Acta* 1981, 45, 2359.
- (35) Zafiriou, O. C. *Estuarine Coastal Mar. Sci.* 1973, 1, 81.

Received for review June 7, 1984. Revised manuscript received November 26, 1984. Accepted February 11, 1985. This research was funded in part by an Old Dominion University Summer Faculty Research Fellowship.

High Molecular Weight Hydrocarbons Including Polycyclic Aromatic Hydrocarbons in Natural Gas from Consumer Distribution Pipelines and in Pipeline Residue

G. A. Eiceman,* B. Davani, M. E. Wilcox, J. L. Gardea, and J. A. Dodson

Department of Chemistry, New Mexico State University, Las Cruces, New Mexico 88003

■ Eight samples of natural gas were collected from consumer distribution lines in five urban centers in the U.S. Southwest. Gas samples were preconcentrated for gas chromatography (GC) and gas chromatography/mass spectroscopy (GC/MS) determination of concentrations of large (C_9 - C_{20}) molecular weight organic compounds in natural gas. Major components in samples included alkylated benzenes, alkylated naphthalenes, and alkanes at total concentrations between 0.3 and 3 mg/m³. Complex mixtures of 30-60 components were detected in these condensates, and complex mixtures of polycyclic aromatic hydrocarbons were found in the natural gas at concentrations of 2-240 µg/m³ for individual PAH. Residues on inner walls of natural gas pipelines were also analyzed by using high-resolution GC and GC/MS. Samples were quantified for PAH, and results were compared to composition of natural gas and to discharge water from hydrostatic testing of gas pipelines. Over 25 PAH were detected in pipeline residue at total concentrations of 1-2400 µg/m² of inner surface area.

Introduction

Natural gas is believed to have an origin common with oil as produced through decomposition of organic matter by microorganisms (1). Often natural gas has been found in the same regions where oil fields are located, and natural gas may be in contact with oil and water at pressures as high as 200 psig or greater. While natural gas is comprised of several major components such as methane, ethane, propane, CO₂, N₂, H₂S, and others, a complex mixture of organic compounds with molecular weights larger than these compounds has also been detected in natural gas samples from the U.S. and several other countries (2-6). These compounds were found at concentrations near 100 mg/m³ and with molecular weights up to 400 amu for as many as 50 components in concentrated gas condensate (3). The presence of these same compounds in aqueous wastes from natural gas transportation (7, 8) was evidence that such compounds also may be widely distributed in consumer distribution pipelines.

The presence and movement of toxic and other organic compounds in the gas phase during natural gas production and distribution is reduced at well heads where certain gases (including methane) are separated from liquids or condensate through a rapid drop in pressure. While this process is reasonably efficient, later formation of additional condensate in pipelines has been a reoccurring problem in distribution of natural gas (9). For example, at Chal-

mers Station near Detroit, as many as 1534 gal of condensate were formed in one day during a period of cold weather (2), and similar problems were also reported in Europe (10). Even though a major research program (11) was used to address this problem, little detailed information was available on composition of condensate, presence of condensate in other consumer distribution lines, and potential for deleterious environmental effects from uncontrolled discharge of pipeline contents, particularly trace organic compounds.

The objective of this research was to measure the complexity, abundance, and composition of natural gas for larger molecular weight compounds (C_9 +) in consumer distribution pipelines. The extent as well as general behavior of retrograde condensation (2) which results in condensation or deposition of toxic and other large organic compounds in pipelines is presently unknown. However, the presence of over 1 000 000 km of pipeline mains with an unknown length of branches in the U.S. (12) was sufficient magnitude for concern, particularly since cleaning of old pipelines is accomplished to remove deposits from inside pipelines. A secondary object of this research was development of background information toward evaluation of composition of wastes generated from cleaning of old natural gas pipelines. Certain wastes from natural gas production including both produced water and discharge water from hydrostatic testing of older natural gas pipelines may be sources for groundwater pollution.

Experimental Section

Instrumentation. A Hewlett-Packard Model 5880A gas chromatograph was equipped with a flame ionization detector (FID), automated splitless injector, and 10 m long × 0.225 mm i.d. fused silica DB-5 capillary column. Conditions for analysis of all samples were the following: initial temperature 30 °C; initial time 1 min; oven temperature program rate 6 °C/min; final temperature 200 °C; final time 5 min; injector port temperature 250 °C; FID temperature 270 °C; carrier gas nitrogen at 30 cm/s average linear velocity; time for splitless injection 1.5 min; chart speed 0.5 cm; area reject 10; threshold 4. A Hewlett-Packard Model 5995A gas chromatograph/mass spectrometer (GC/MS) was equipped with jet separator, Model 5885M disk drive, Model 7225B X-Y plotter, automated splitless injection port, and 10 m fused silica OV-1 capillary column. Chromatographic conditions were identical for scanning GC/MS and GC-FID analyses. Mass spectrometer conditions for scanning analyses were the following: lower mass 45 amu; upper mass 600 amu; scan speed 690

Table I. Masses of Ions for Compounds Determined Using GC/MS Selected Ion Monitoring

compound	mass (amu)	compound	mass (amu)
naphthalene	128.1	anthracene	178.1
C ₁ -naphthalenes	142.1	C ₁ -anthracenes	192.1
C ₂ -naphthalenes	156.1	C ₂ -anthracenes	206.1
C ₃ -naphthalenes	170.1	C ₃ -anthracenes	220.1
C ₄ -naphthalenes	184.1	C ₄ -anthracenes	234.1
biphenyl	154.1	pyrene	202.1
C ₁ -biphenyls	168.1	C ₁ -pyrenes	216.1
C ₂ -biphenyls	182.1	C ₂ -pyrenes	230.1
C ₃ -biphenyls	196.1	C ₃ -pyrenes	244.1
C ₄ -biphenyls	210.1	C ₄ -pyrenes	258.1
fluorene	166.1		
C ₁ -fluorenes	180.1		
C ₂ -fluorenes	194.1		
C ₃ -fluorenes	208.1		
C ₄ -fluorenes	222.1		

amu/s; delay between scans 0.1 s; electron multiplier voltage 1400 V; MS detection threshold 10 linear counts. Mass spectrometer conditions for SIM analysis were the following: electron multiplier voltage 1400 V; SIM window size 0.2 amu; integrate sensitivity 0.05; area threshold 10; smoothing factor 1. Selected polycyclic and alkylated polycyclic aromatic hydrocarbons (PAH) with ions chosen for SIM analyses are presented in Table I. Sample volumes in GC and GC/MS analyses were 1–2 μ L delivered by using a Model 7001 10- μ L syringe (Hamilton Co., Las Vegas, NV). Conditions other than these will be noted as necessary.

Procedures. Adsorbent traps containing 100–120 mg of 100–120 mesh Tenax-GC (Applied Science, Bellefonte, PA) were prepared by using 10 cm long \times 0.6 cm i.d. borosilicate tubes. Packing was retained by using glass wool plugs. Prior to every experiment, each trap was washed with 50 mL of distilled-in glass grade acetone (Burdick & Jackson Laboratories, Muskegon, MI) and dried at 150 °C for 1–2 h. Sampling was accomplished by attached traps to a gas jet in a flume hood, gas was adjusted to 100–150 mL/min, and samples were collected continuously for 24–48 h. The location and detailed specification of the natural gas samples are given in Figure 1 and Table II, respectively. After the sampling step, traps were separated, and organic compounds were extracted with 50 mL of acetone which was delivered to the trap by using a Milton Roy minipump (Ft. Lauderdale, FL). Extracts were condensed to 1 mL by using a rotary evaporator (Buchii Brinkmann Co., New York) and further reduced in volume to 0.1 mL by using nitrogen gas. Each extract was analyzed separately by GC and GC/MS. A procedure blank was used to ensure no contamination from solvents or glassware. In addition, gas was passed through a glass condenser trap cooled to dry ice/acetone temperature and extracted for GC analysis in order to measure possible contamination or reactions from either the Tenax-GC adsorbent material or the tubing used to connect the traps. No contamination from any interferences was detected in chromatograms.

Sections of pipelines were collected from locations in Las Cruces, NM, and were part of the consumer distribution system for this city. Lengths of pipeline from 1 to 2 m and from 5 to 10 cm in diameter were capped at each end with aluminum foil and were stored at room temperature. Deposits on the inside of the pipeline were collected for analysis by washing the inner walls with 150 mL of CH₂Cl₂ with careful spreading of the solvent over the entire inner surface. The washing was condensed to 1 mL as described above.



Figure 1. Location of sites for sampling natural gas from consumer distribution lines. Major pipelines connect each center with two large gas deposits in SE and NW New Mexico. However, interconnection of lines is widespread, and movement of gas is directed into different lines based upon demand.

Table II. Details and Locations of Samples

Gas Samples					
date	times, h	volume, m ³	flow, mL/min	location	
6-19-84	25.5	0.17	110	Las Cruces 2, Chemistry, Bldg, Rm 35, NMSU	
6-25-84	24	0.19	130	Las Cruces 1, Civil Engineering Bldg, Rm 210, NMSU	
6-23-84	40.1	0.29	119	Roswell 1, Science Bldg, NM Military Academy	
6-23-84	40	0.26	109	Roswell 2, Science Bldg, NM Military Academy	
6-20-84	22.5	0.12	91	El Paso 1, Science Bldg, Rm, UTEP	
6-6-84	45.6	0.30	109	Socorro 1, NM Tech	
6-6-84	45.6	0.30	109	Socorro 2, NM Tech	
6-1-84	29.5	0.21	120	Temple 1, Chemistry Bldg, Rm 21, ASU	
Pipeline Samples Location ^a					
			length, m	diameter, cm	age, years
(1) University and Haggerty			1.7	11.2	16
(2) Howell and 5th St.			1.4	5.1	8
(3) Ethyl and 5th St.			0.96	5.1	8
(4) Palmer and 5th St.			2.5T ^b	5.1	16

^aLocation refers to Figure 5. ^bSymbol T refers to a branched line. All other pipes were straight.

Later, pipeline samples were prefractionated for isolation of PAH using solvent-extraction procedures (8). As part of the quantification scheme, deuterated PAH standards were added to the samples before prefractionation. Molecular ions for deuterated standards were used in quantification of PAH with correction for extraction efficiency as well as confirmation of identity using retention indexes.

Reagents and Standard Solutions. Dichloromethane (HPLC grade; Fisher Scientific Co., NJ), cyclohexane

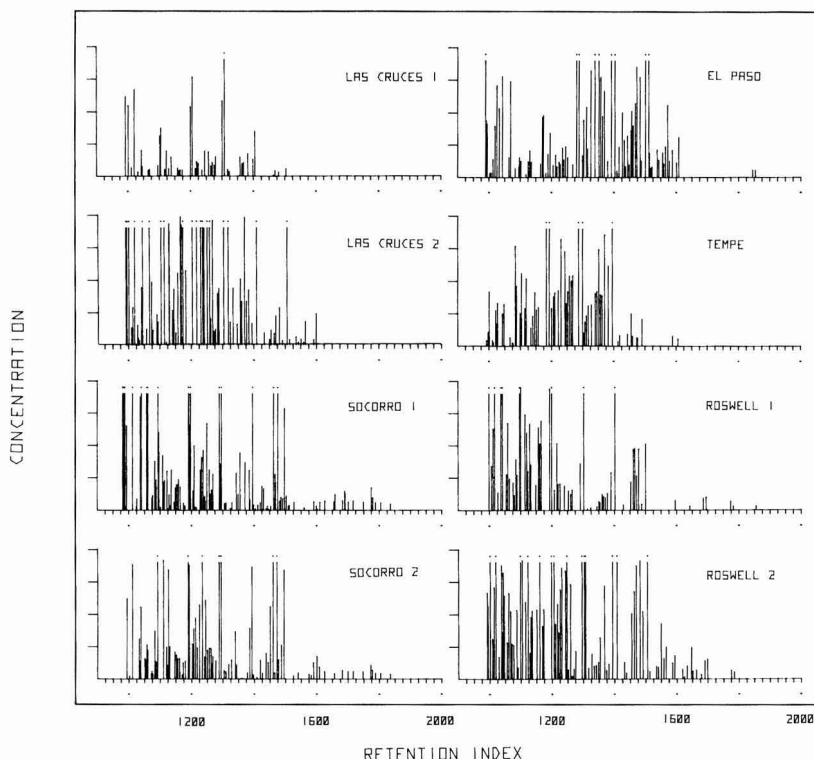


Figure 2. Bar plots of concentration (mg/L; full scale value = 50) vs. retention index from GC analyses of condensate from natural gas sampled using Tenax traps. Locations and details of sampling are given in Table II and Figure 1.

(pesticide grade; Fisher Scientific Co., NJ), methanol (Burdick & Jackson Laboratories Inc., Muskegon, MI), and nitromethane (spectrograde; Eastman Kodak Co., Rochester, NY) were used as purchased. A mixture of deuterated PAH standards containing acenaphthene- d_{10} , naphthalene- d_8 , benz[a]anthracene- d_{12} , chrysene- d_{12} , anthracene- d_{10} , fluorene- d_{10} , and pyrene- d_{10} in CD_2Cl_2 and C_6D_6 with concentration of 1 mg/mL for each component was obtained from MSD Isotopes (Merck Chemical Division, St. Louis, MO).

Results and Discussion

Natural Gas Composition. In prior studies (3), natural gas samples drawn from a limited number of consumer distribution lines were analyzed by using GC and GC/MS techniques for organic compounds with molecular weights above 128 amu or C_{9+} . In these analyses, more than 50 organic compounds between C_{11} and C_{23} hydrocarbons were identified at total concentrations of near 100 mg/m³. In Figure 2, results are shown from GC analyses of eight gas samples drawn in identical manner from five urban centers in a wide geographical range as shown in Figure 1. Results are displayed in Figure 2 as bar plots of concentration ($\mu\text{g}/\text{m}^3$) vs. retention index with a nonpolar (DB-5) capillary column. Since the concentrations have been normalized for sample volume and have been quantified by using an average FID response factor of 14.7 area counts/ng, direct comparisons between samples can be made through bar plots. As shown in Figure 2, GC patterns typical of complex mixtures were found with all samples which were all reasonably similar in comparison qualitatively. Samples were similar with a range of hydrocarbons from C_9 to C_{20} . However, some samples differed quantitatively in relative composition of components

to those in other samples. For example, in the El Paso sample, the majority of major components were between C_{13} and C_{15} with few major components below C_{12} . In contrast, for samples from Las Cruces 2 and Roswell, most major components were between C_9 and C_{14} . No clear explanation for these results are known or proposed here.

Large differences existed between samples with regard to absolute concentrations of organic compounds. Total concentrations (mg/m³) of organic compounds estimated for each sample from integrated GC data and using FID average response factor were following: Las Cruces 1, 0.33; Las Cruces 2, 2.7; Socorro 1, 1.9; Socorro 2, 3.0; El Paso, 2.5; Tempe, 0.98; Roswell 1, 1.2; Roswell 2, 0.23. These differences are not particularly surprising since samples were drawn with gas supplied from different gas fields or from different locations along a pipeline from the same gas field. Moreover, certain volatile (C_5 – C_8) organic compounds including benzene and alkylated benzenes which were found in trap extracts may have been lost largely through breakthrough phenomenon (3) or by volatilization during condensation of extract using rotary evaporation. For example, breakthrough volumes for the following compounds on Tenax-GC traps in methane carrier were estimated from earlier data (3) as the following: $C_{12}H_{26}$, 45 L/g; $C_{16}H_{34}$, 135 L/g; $C_{18}H_{38}$, 450 L/g; $C_{19}H_{40}$, 1080 L/g. Since the volume/mass values for these samples ranged from 180 to 380 L/g, breakthrough should not effect exact quantification for compounds above C_{17} – C_{18} . However, results from GC determination of compounds with molecular weights below values of C_{15} may be considered semiquantitative only, and breakthrough may account for some quantitative errors in these results. Therefore, these should be considered minimum concentrations, and actual concentration should be much larger especially when

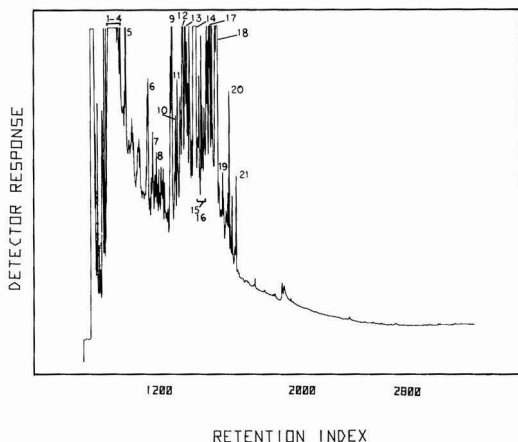


Figure 3. Chromatogram from GC-FID analysis of gas condensate from El Paso, TX. Major components are numbered and listed in Table III.

masses from benzenes and lighter alkanes are included.

Results from scanning GC/MS analyses for the El Paso sample are summarized in Table III for major constituents in these samples although all samples contained the same components but at different concentrations. Since very similar chromatographic conditions were used in GC and

GC/MS analyses, favorable comparisons of GC and GC/MS chromatographic patterns, along with mass spectral data and standards, aided assignment of identity to particular GC peaks. The chromatogram in Figure 3 for the El Paso sample was representative of large complexity of all natural gas samples, and resolution of components was considered good especially in comparison to samples of hydrostatic test discharge water (7) which were also complex due to an excess abundance of normal and branched alkanes and alkenes. In these samples, adequate mass spectra were obtained for many of the major components including aromatic hydrocarbons. Apart from a few references (1, 2, 5, 8), larger molecules including aromatic, alkylated aromatic, polycyclic aromatic (PAH), and alkylated polycyclic aromatic hydrocarbons have not been widely considered as components in natural gas. However, results of this study show relatively large abundances of these compounds in samples from throughout the U.S. Southwest. Analytical data that support these results may be found in reports from USSR (10), Germany (4, 5), U.S. Gulf Coast (14), and U.S. Midwest and East Coast regions (2). However, in other reports on natural gas analyses, such compounds have been ignored or unreported (15).

More detailed information on the gas samples was collected by using selected ion monitoring (SIM) for PAH and alkylated PAH. An 11 ion SIM plot is shown in Figure 4 (left panel) for the El Paso, TX, gas condensate sample. Furthermore, selected quantitative results from SIM analyses of all samples are summarized in Table IV.

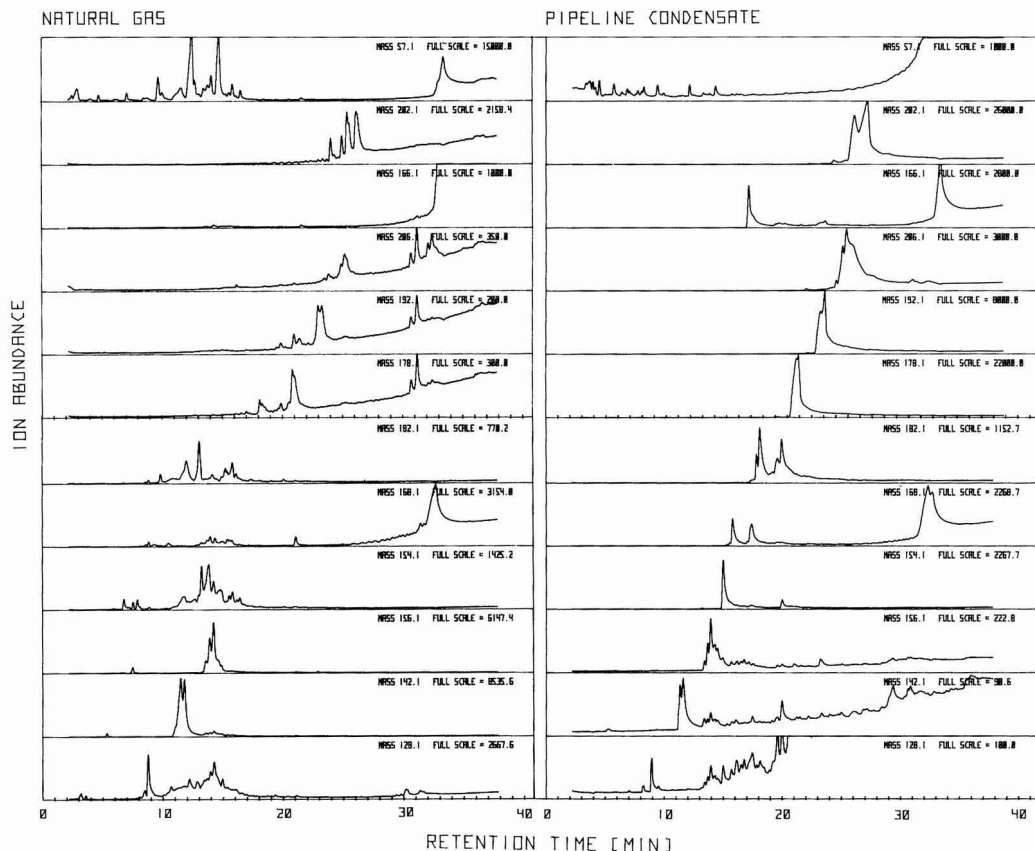


Figure 4. SIM plots from GC/MS analysis of (left panel) natural gas condensate and (right panel) residue washed from natural gas pipelines. An additional ion monitored was m/z 202.1 amu for pyrene and 57.1 amu for saturated hydrocarbons.

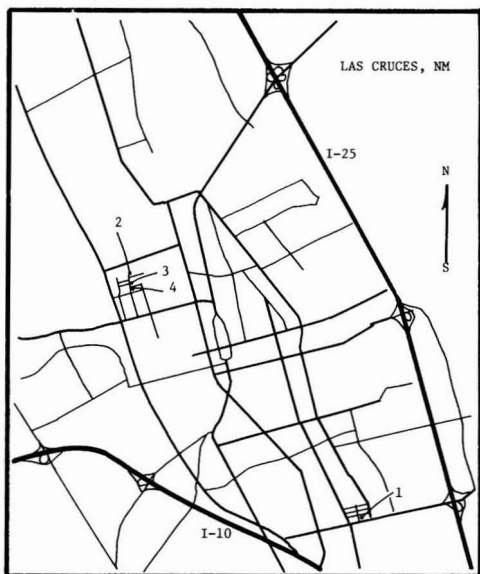


Figure 5. Locations of pipelines selected for removal and analysis in Las Cruces, NM. Locations and details of pipeline collection are given in Table II.

Table III. Major Components from Natural Gas Preconcentrated Using Tenax Traps

peak no. ^a	retention index ^b	identity (retention time)	methods of ID ^c
1	0882	xylene (2.72)	RI, MS
2	0948	C ₃ -benzene isomer (4.28)	MSI
3	0955	C ₃ -benzene isomer (4.46)	MSI
4	0976	C ₃ -benzene isomer (4.94)	MSI
5	1000	C ₁₀ H ₂₂ (5.52)	RI, MS
6	1100	C ₁₁ H ₂₄ (7.90)	RI, MS
7	1126	C ₅ -benzene (8.56)	MSI
8	1143	naphthalene (9.00)	RI, MS
9	1200	C ₁₂ H ₂₆ (10.44)	RI, MS
10	1229	C ₆ -benzene isomer (11.20)	MSI
11	1235	C ₆ -benzene isomer (11.36)	MSI
12	1248	C ₁ -naphthalene isomer (11.72)	MS
13	1253	C ₁ -naphthalene isomer (11.84)	MS
14	1300	C ₁₃ H ₂₈ (13.08)	RI, MS
15	1313	branched C ₁₃ H ₂₈ (13.38)	MSI
16	1327	alkene (13.70)	MSI
17	1377	branched alkane (14.86)	MSI
18	1400	C ₁₄ H ₃₀ (15.40)	RI, MS
19	1425	C ₁₄ H ₂₈ (15.82)	RI, MS
20	1436	branched alkane (16.00)	MSI
21	1500	C ₁₅ H ₃₂ (17.08)	RI, MS

^aIn Figure 3. ^bOn DB-5 phase. ^cRI = retention index of standard, MS = mass spectrum of standard under same conditions, and MSI = match to mass spectrum in data base.

As shown in Figure 4 (left panel), naphthalene, biphenyl, anthracene, and alkylated members of each PAH were detected in natural gas from all consumer distribution pipelines studied here. As a general trend, the larger the

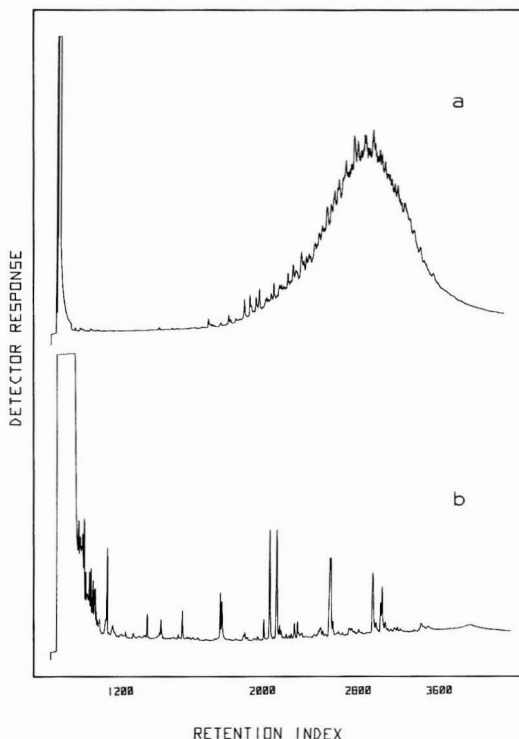


Figure 6. Chromatograms from GC-FID analysis of residue from natural gas pipelines with (a) no prefractionation and (b) prefractionation of residue for PAH. Results for PAH determination are shown in Figure 4 (right panel).

molecular weight, of a component (with a smaller vapor pressure), the lower the gas-phase concentration of that component. While this is consistent with liquid-gas vapor-pressure behavior, absence of details on the liquid residue inside pipelines made precise conclusions on behavior uncertain. Nevertheless, the general pattern held among all samples and concentrations of individual PAH ranged from 2 to 240 $\mu\text{g}/\text{m}^3$ which seemed surprisingly large until residues in pipelines were analyzed.

Pipeline Samples. A partial map of the Las Cruces with designation of origin of pipelines is given in Figure 5. Results from GC analyses of condensed washes are shown in Figure 6a. In GC analyses for pipeline washes, the chromatographic patterns were typical of hydrostatic test discharge water samples with a large amount of unresolved material between RI units of 2000 and 3000 as shown in Figure 6a. Extensive prefractionation procedures (13) were necessary to isolate the compounds of interest (PAH) despite use of a high-resolution GC column due to extreme complexity of samples. Results from prefractionation may be seen in Figure 6b in which a majority of unresolved organic mass was removed and only a few well-resolved components (PAH) remained as detected

Table IV. Concentrations ($\mu\text{g}/\text{m}^3$) of Selected PAH in Natural Gas

compound	Las Cruces 2	Las Cruces 1	Roswell 1	Roswell 2	Socorro 1	Socorro 2	Tempe, AZ	El Paso, TX
naphthalene	26	68	40	21	55	45	21	46
C ₁ -naphthalenes	29	154	232	28	48	41	27	240
C ₂ -naphthalenes	24	50	156	28	32	32	23	132
biphenyl	4	33	15	7	4	4	3	42
C ₁ -biphenyls	5	28	16	4	7	5	2	39
C ₂ -biphenyls	6	26	16	5	7	6	6	44

Table V. Concentrations ($\mu\text{g}/\text{m}^2$) of Selected PAH Inside Natural Gas Pipelines^a

compound	location ^b			
	1	2	3	4
naphthalene	4	6	11	13
C ₁ -naphthalenes	9	2	3	1
C ₂ -naphthalenes	18	2	5	4
biphenyl	75	16	22	1
C ₁ -biphenyls	66	8	16	4
C ₂ -biphenyls	71	2	22	3
anthracene	1200	84	130	18
C ₁ -anthracenes	460	22	37	13
C ₂ -anthracenes	280	14	45	10
pyrene	2400	160	110	26
C ₁ -pyrenes	1030	45	37	4
C ₂ -pyrenes	290	20	25	2

^a Concentrations are expressed in micrograms of PAH per meter squared of surface area of inner wall of pipelines. ^b Locations are in reference to Table II and Figure 5 and are (1) University and Haggerty, (2) Howell and 5th St., (3) Ethel and 5th St., and (4) Palmer and 5th St.

with GC-FID. The isolated fractions were analyzed by GC/MS using SIM, and the results are shown in Table V and Figure 4 (right panel). Polycyclic aromatic hydrocarbons were found in every ion used in SIM analyses, and interesting trends were found as related to the gas-phase composition. Lower molecular weight compounds such as naphthalenes were present at relatively low amounts of 4–13 $\mu\text{g}/\text{m}^2$ of inner surface area. However, the larger molecular weight compounds were found at concentrations of up to 2400 $\mu\text{g}/\text{m}^2$ which were larger by mass or concentration than in any other type of samples seen in this research program. While these results may be interpreted on the basis of phase equilibria as below, substantive parallels exist between composition of this pipeline washing and the composition of discharge water from hydrostatic testing of natural gas pipelines.

Environmental Assessment and Conclusion. Production of natural gas has been evaluated from a point source perspective for atmospheric pollution of light hydrocarbons and inorganic gases (16) and from the point of view of inorganic compounds (17). However, the results of this study in combination with analyses of discharge water are the first results to propose the movement of toxic and carcinogenic compounds widely throughout natural gas systems including distribution lines. The presence of larger molecular weight compounds in natural gas is reasonable on the basis of vapor pressures and abundance of same compounds in pipeline residues as shown in Figure 4. Expected gas-phase concentrations of naphthalene were calculated on the basis of known pipeline composition using saturated conditions at 20 °C and found to be in the range 1–25 mg/m^3 . Since these values were generated by using ideal gas equations, simple geometric arguments, and assumption of equilibrium, major errors were expected, and values are roughly 10^2 too large. This is consistent with conditions of nonequilibrium inside pipelines.

The presence of toxic organic compounds in the pipelines may be explained by using retrograde condensation of compounds through a pressure gradient. The condensate may be carried through the system by flow of gas.

Since these compounds are present in pipeline condensate and in the natural gas, the same compounds may be reasonably expected in aqueous wastes from pipeline maintenance including hydrostatic testing. Moreover, the same compounds should be expected in produced water which is a byproduct of natural gas production. Our preliminary results show the presence of PAH, benzenes, and alkylated derivatives in such waters in patterns typically found in spent test waters and in the pipeline samples studied here.

Acknowledgments

Aid in collection of samples is gratefully acknowledged to the following: M. Parsons, Arizona State University; A. Chang, University of Texas, El Paso; C. Poppe, NM Tech; F. Cadena-C, New Mexico State University; L. Pino, City of Las Cruces.

Registry No. C₁₀H₂₂, 124-18-5; C₁₁H₂₄, 1120-21-4; C₁₂H₂₆, 112-40-3; C₁₃H₂₈, 629-50-5; C₁₄H₂₀, 629-59-4; C₁₄H₂₈, 26952-13-6; C₁₅H₃₂, 629-62-9; xylene, 1330-20-7; naphthalene, 91-20-3; methyl naphthalene, 1321-94-4; biphenyl, 92-52-4; methylbiphenyl, 28652-72-4; methylanthracene, 613-12-7; pyrene, 129-00-0; methylpyrene, 27577-90-8.

Literature Cited

- (1) Katz, D. L.; Cornell, D.; Kobayashi, R.; Poettmann, F. H.; Vary, J. H.; Elenbaas, J. R.; Weinang, C. F. "Handbook of Natural Gas Engineering"; McGraw-Hill: New York, 1959; pp 1–5.
- (2) Katz, D. L.; Bergman, D. F. *Proc. Annu. Conv.—Gas Process. Assoc.* **1976**, 55th, 18–26.
- (3) Eiceman, G. A.; Davani, B.; Gardea-Torresdey, J. J. *Chem. Educ.*, in press.
- (4) van Rossum, G. J.; Wolkote, B. J. *GWF, Gas Wasserfach: Gas/Erdgas* **1980**, 121, H.2, 27–54.
- (5) Herlan, A.; Mayer, J. *GWF, Gas Wasserfach: Gas/Erdgas*, **1978**, 119, H.8, 364–370.
- (6) Huber, L. J. *Chromatogr. Sci.* **1983**, 21, 519–520.
- (7) Eiceman, G. A.; Leasure, C. S.; Baker, B. D. *Int. J. Environ. Anal. Chem.* **1983**, 16, 149–160.
- (8) Eiceman, G. A.; Davani, B.; Dodson, J. A. *Int. J. Environ. Anal. Chem.* **1984**, 19, 27–39.
- (9) Oranje, L. *Int. J. Gas J.* **1973**, 71, 39–42.
- (10) Neft. *Gazov. Promst.* **1976**, 4, 26–29.
- (11) Bergman, D. F.; Tek, M. R.; Katz, D. L. "Retrograde Condensation in Natural Gas Pipelines". American Gas Association, Project No. PR 26-69, 1975, final report to Pipeline Research Committee.
- (12) Cory, P. J. *Relat. Inf. Nondestr. Test. Pipe Syst.*, [Proc. Symp.] **1976**, 142.
- (13) Bartle, K. D.; Lee, M. L.; Wise, S. A. *Chem. Soc. Rev.* **1981**, 10, 112.
- (14) Jonker, R. J.; Poppe, H.; Huber, J. F. K. *J. Chromatogr.* **1979**, 186, 285–289.
- (15) Middleditch, B. S. *J. Chromatogr.* **1982**, 239, 159–171.
- (16) Wade, W. A., "Multimedia Assessment of the Natural Gas Processing Industry", 1979, EPA Report 600/2-79-077.
- (17) Baker, F. G.; Brendecke, C. M. *Ground Water* **1983**, 21, 317–324.

Received for review July 30, 1984. Revised manuscript received January 22, 1985. Accepted February 4, 1985. This research has been supported by New Mexico Water Resources Research Institute and has been developed during a program of investigating discharge of toxic organic compounds into water from activities of natural gas industry.

X-ray Photoelectron Spectroscopy Studies of Coal Fly Ashes with Emphasis on Depth Profiling of Submicrometer Particle Size Fractions

Nurit Kaufherr, Mohsen Shenasa, and David Lichtman*

Department of Physics and Laboratory for Surface Studies, University of Wisconsin—Milwaukee, Milwaukee, Wisconsin 53201

■ The composition of the outer layers of submicrometer fly ash particles originating from the Mojave Power Generating Station was studied by means of XPS in conjunction with Ar ion bombardment. Qualitative as well as semiquantitative compositional changes of the main constituents, i.e., Si, Al, O, Fe, Ca, S, and Na, are given. S and Na were surface enriched. The amount of S vs. Ca exceeds that corresponding to CaSO_4 , suggesting adsorbed sulfur oxide. Also, Si in the Si-Al-O skeleton was somewhat surface enriched relative to Al. The concentration of Ca was little changed while the concentration of Fe increased with depth profiling. Results are critically evaluated in view of effects induced by ion bombardment. Results of the Mojave Station collection are also compared to data from other power plant collections and NBS standard material.

Introduction

Particulate emission from coal-fired power plants is currently controlled in the United States mainly by means of electrostatic precipitators (ESP) (1). Though of high efficiency, their fractional efficiency curve has a minimum in the size range 0.1–1.0 μm . These fine particles are in the respirable size range and are supposed to be surface enriched in toxic trace elements which makes them of high potential health risk (2). The importance of studying submicrometer particles in contact with the respiratory tissue, and especially their surface chemistry, is obvious.

Most of the studies on the chemical composition of fly ash particles so far have focused on particles in the micrometer range, some describing x-ray photoelectron spectroscopy (XPS) data in conjunction with limited depth profiling analysis (3–6).

In the present program, the composition of the outer layers of primarily submicrometer particles up to about 1000 Å was studied by means of XPS employing systematic depth profiling by means of Ar ion bombardment. Semiquantitative data and compositional changes were calculated for the main constituents of fly ash and critically evaluated in view of ion-induced damage and other effects induced by ion bombardment as observed in related systems (7–11). The limitations imposed on XPS studies of elements like Mg, P, N, etc. in low concentration are discussed. Data are compared with results of the effects of sputtering on NBS 1633a fly ash as well as with data from as-received fly ash samples from various power plants.

Experimental Section

This study concentrated mainly on XPS studies in conjunction with Ar ion sputtering of particles collected at the Mojave Generating Station of the Southern California Edison Co. located at Laughlin, NV, on the Colorado River. The plant burns pulverized Black Mesa (AZ) coal. Sampling, using an eight-stage Anderson impactor, was performed at the outlet of the electrostatic precipitator, just before entering the stack. Details on the power station

Table I. Fly Ash Studied

reference code ^a	source	particle diameter, μm	sup-port ^c	studies ^d
MJ-6	Mojave Power	0.7 ^b	C	as-rec, sputt
MJ-7	Station	0.4 ^b	C	as-rec, sputt
NBS-C	SRM 1633a	variable	C	as-rec, sputt
NBS-In	coal fly ash		In	as-rec, sputt
KD	Kincaid Power Plant, IL	5–30	In	as-rec
TENN-2	Bull Run, TVA	4.8 ^b	In	as-rec
TENN-5		1.4 ^b	In	as-rec

*Numbers in coding indicate number of collection stage of the impactor. ^bAverage values: most of the particles were very close to this value. ^cSee also Experimental Section. C, carbon; In, indium. ^das rec, as-received; sputt, sputtering.

operation conditions and collection methods are given elsewhere (12). For comparison, NBS coal ash 1633a was included in the study. Also studied, in the as-received form, were particles from the Kincaid, IL, Power Plant and the Bull Run, TN, Power Plant. Details concerning these collections are given in ref 13 and 14, respectively. Table I summarizes the type of coal ash particles studied and their reference code throughout this work. Also included are particle size and type of support used to mount the samples and studies carried out.

The XPS data were taken on a Perkin-Elmer Physical Electronics Industries 548 AES/ESCA spectrometer with a double pass CMA. Mg $K\alpha_{1,2}$ X-rays (1253.6 eV) were used as exciting radiation. Normal pressure during experiments was about 2×10^{-9} torr. Most of the data was taken at 100 eV pass energy. However, detailed spectra of as-received samples were taken at 25 or 50 eV whenever possible. Estimated uncertainty in BE values due to equipment was ± 0.1 eV (see also Qualitative Results and Discussion). Ion bombardment of samples was carried out with argon ions of 3 keV and an ion current density of $\sim 16 \mu\text{A}/\text{cm}^2$ for different periods up to 36 min of total sputtering time. Detailed spectra were taken after each period. Sputtering rates were estimated to be similar to those found for a standardized layer of SiO_2 on Si which was about 30 Å/min.

The Si 2p peak with a value of 102.6 eV was chosen as reference in both as-received and sputtered samples, which seems a reasonably good choice (6) (see Discussion). Quantitative calculations were carried out by using a quantity proportional to the area of the main photoelectron peak, and concentrations are expressed throughout this work in atomic weight percent unless otherwise indicated (10). The sensitivity factors were taken from ref 15.

For analysis, samples were transferred from the stainless steel support of the impactor collector by means of a carbon tip to a carbon stub on which a flat drop of colloidal graphite in 2-propanol (Ted Pella, Inc., Tustin, CA) was dried. The particles were pressed onto the spot by means of a flat piece of glass. This allowed the analysis of the very small (< 1 mg) sample available (see Discussion and ref 16). For comparison, some samples were pressed into

Table II. Binding Energy Value (BE) of Main Photoelectron Peaks of Fly Ash Sample Studied^a

sample	sputtering time, min	binding energy, eV					
		Al 2p	O 1s	S 2p	Ca 2p _{3/2}	Fe 2p _{3/2}	Na 1s
MJ-6	0 ^b	74.7	531.7	169.4	347.9	ND ^e	1071.3
	1	74.8	531.6	169.3	347.7	710.7	1071.2
	6	74.7	531.6	169.1	347.7	711.1	1071.9
	21	74.5	531.1	168.9 ^c	347.7	709.7	1071.7
MJ-7	0	74.4	531.8	169.2	347.6	708.9	1070.6
	1	74.5	531.7	169.2	348.0	711.1	1071.6
	6	74.5	531.6	168.8	347.7	ND	1071.2
	21	74.5	531.4	168.9 ^d	348.0	710.7	1071.4
NBS-C	36	74.6	531.5	168.3	348.0	710.3	1071.6
	0	74.4	531.3	168.5	347.2	710.6	
	1	74.7	531.6	168.6	347.2	710.5	<i>h</i>
	6	74.6	531.4	169.6 ^e	347.3	709.8	
NBS-In	0	74.2	531.2	169.0	(348.8) ^f	ND	<i>h</i>
KD	0	74.3	531.9	168.8	347.8	709.8	1070.3
TENN-2	0	74.1	531.9	168.5	347.0	710.3	(1068.0) ^f
TENN-5	0	74.2	531.2	169.1	347.7	711.2	<i>h</i>

^aThe basic uncertainty of the instrument is ± 0.1 eV. Si 2p with BE = 102.6 eV was used as the reference. ^bSi 2s, 153.5 eV; Ca 2s, 438.8 eV; Al 2s, 119.0 eV; S 2s, 233 eV. ^cAlso a small feature at 162.3 eV. ^dAlso a small peak at 161.8 eV. ^eAlso peaks at 167.3, 163.8, and 160.7 eV. ^fHigh uncertainty not included in average calculations of Table III. ^gND, not determined. ^hnot detected.

indium foils. The mode of mounting for each sample is indicated in Table I.

Results

Qualitative Results

General Assignment of Peaks. The BE values of the main core level photoelectron peaks of the Mojave and NBS fly ashes studied in as-received form and after sputtering are given in Table II together with the values of as-received fly ash samples from other sources studied for comparison of BE values and the effect of mounting substrate. Also given in Table II are narrow scan BE values of further core level photoelectron peaks of MJ-6. Relevant BE values from the literature are given in Table III together with calculated average values of present data. Si, O, Al, Ca, Fe, S, and Na were identified by their main photoelectron peaks and Auger transitions in all samples studied. For MJ-6, MJ-7, and NBS-C, the main photoelectron peaks of the above elements were studied in detail for the effect of sputtering on BE values and peak shape and are discussed later on. The corresponding values of peak widths at half-maximum are given in Table IV.

The Si 2p with a value of 102.6 eV was taken for referencing throughout this work. Referencing of Si 2p to the spurious C 1s peak with a value of 284.6 eV for samples pressed on indium gave a similar value.

Further elements like P, N, Cl, and Mg were identified, though often with difficulty. Some ambiguity was encountered in the range of BE < 100 eV. In most cases it was hard to assign with reasonable certainty the weak broad peaks in the region between 45 and 55 eV to Fe 3p and Mg 2p. This does not interfere with the identification of Fe, but the identification of Mg is rendered impossible in low concentration due to the overlap of the Mg 2s peak and the Mg K α X-ray satellite of Si 2p. Fe 3p was identified throughout the study of NBS at about 55 eV. Cl 2p was identified in KD at about 199–198 eV but not in MJ-6, MJ-7, NBS-C, TENN-5, and TENN-2. P 2p and P 2s, when identified, were ill-defined broad peaks of very low intensity. Their values correspond to those of phosphates, i.e., about 133 and 191 eV, respectively. P was identified in MJ-7 and was not removed on sputtering. It was also identified in MJ-6 after 6 min of sputtering and in as-received TENN-2 and TENN-5, but not in KD and NBS-C. N 1s was identified in TENN-2, TENN-5, and KD as-re-

ceived samples and in MJ-6 after 36 min of sputtering. Na was identified in MJ-6, MJ-7, TENN-2, and KD. In TENN-5 no Na was detectable. In addition to the Na 1s, which was studied in detail (data given later), the Na 2s at about 64 eV and the auger KLL transition at about 264 eV were observed.

As-Received Samples vs. Effect of Sputtering on Main Photoelectron Peaks of MJ-6, MJ-7, and NBS-C. (1) **Si 2p, Al 2p, and O 1s.** The three main photoelectron signals of the aluminosilicate skeleton have all well-defined Gaussian-shaped peaks. The BE values of Al and O in both as-received and after sputtering samples fall within a narrow range. The BE values of Al 2p and O 1s are 74.6 ± 0.1 and 531.5 ± 0.2 eV, respectively. Most of the data falls within this range. Si 2p with BE 102.6 eV was taken as reference. Sputtering has only a small effect on the width of the peaks which is in the range 3.2–4.0 eV for MJ-6 and NBS-C (Table IV). Somewhat higher values are found for MJ-7, where a small deviation from Gaussian shape is observed toward lower BE values which is easily recognized after 36 min of sputtering. This deviation from Gaussian shape is more of an emerging new feature in Si 2p and Al 2p, while in O 1s it seems like a change in shape. In MJ-6 and MJ-7 as-received samples a small peak to the lower BE side of the main O 1s peak is observed with Δ BE of about 3.3 eV for MJ-7 and 4.2 eV for MJ-6. This peak disappears completely on brief sputtering (1 min).

(2) **S 2p.** The S 2p signal in all as-received samples is a well-shaped peak. Its BE value is essentially in the range 169.0 ± 0.4 eV. This is also the dominant peak in sputtered samples. Sputtering induces changes in the shape of the peak. As the amount of sulfur decreases, the peak is often ill-defined and new peaks are observed. However, those new peaks do not seem to be of a very consistent nature. Thus, we observe, on sputtering MJ-6 for 21 min, a peak at 162.3 eV in addition to the main S 2p at 168.9 eV. In MJ-7 we observe a small additional peak at 161.8 eV after 21 min. However, after a longer sputtering period this peak is no longer observed. In NBS-C, a series of peaks is observed at 169.6, 167.3, 163.8, and 160.7 eV after sputtering for 6 min. Width at half-maximum of S 2p at 169.0 eV was in the range 3.2–3.9 eV, while the values for the sputtered MJ-7 reached 4.5 eV.

(3) **Ca 2p.** Ca 2p_{3/2} was observed with a BE value that falls mainly within the range 347.7 ± 0.3 eV. Reasonably good resolution was obtained only in as-received MJ-7 and

Table III. Core Level Binding Energies (eV)^a

material studied	Si 2p	Al 2p	O 1s	Ca 2p _{3/2}	S 2p	Fe 2p _{3/2}	Na 1s	remarks
Si ⁰	99.15 (15)							
SiO ₂	103.4 (15), 103.05 (17) (a)		532.31 (17) (a)					(a) α -cristobalite
kaolinite	102.25 (18), 102.78 (17)	74.1 (18), 74.48 (17)	531.3 (18), 531.97 (17)				1071.75 (18)	Al ₂ Si ₂ O ₅ (OH) ₄
bentonite	102.5 (17)	74.60 (18)	531.8 (18)				1073.15 (18)	(Al,Mg) ₂ Si ₄ O ₁₀ (OH) ₂
soda glass	102.75 (17), 102.8 (19)		532.36 (17), 532.1 (19)	347.4 (19)			1071.37 (17), 1072.3 (19)	ionic network
albite	102.43 (18)	74.14 (17)	531.68 (17)				1072.03 (17)	NaAlSi ₃ O ₈ , ionic network
silicates	102.6 (15, 6)							
Al ⁰		72.65 (15)						
Al ₂ O ₃		74.7 (15), 73.52 (17) (a)	531.6 (15), 530.85 (17) (a)					(a) γ -Al ₂ O ₃
Al ₂ O ₃		73.9 (17) (a)	530.7 (17) (a)				1071.4 (15)	(a) sapphire
Na ₂ HPO ₄					164.05 (15), 161.2 (15), 162.6 (20)			
S ⁰					160.7 (20)			
FeS					162.0 (22)			
CaS					168.5 (7)			
Na ₂ S					168.9 (22)			
CaSO ₄				347.5 (7)	168.2 (22 [†])			
Na ₂ SO ₄			531.5 (7)		169.8 (22)			
FeSO ₄			532.3 (22)					
SO ₂ /CaO			531.8 (22)					
SO ₂ /MgO			531.7 (22 [†])					
CaCO ₃			532.8 (22)	346.6 (21), 346.8 (15)				
			531.2 (21)	346.3 (15)				
CaO						706.75 (15)		
Fe ⁰						710.7 (15), 711.2 (9)		
Fe ₂ O ₃						709.7 (9)		
Fe ^{II} (Fe ₂ O)								
present data ^b								
A	74.5 ± 0.2	74.5 ± 0.2	531.5 ± 0.2	347.6 ± 0.3	169.0 ± 0.4	710.4 ± 0.7	1071.4 ± 0.4	
B	74.6 ± 0.1	74.6 ± 0.1	531.5 ± 0.2	347.7 ± 0.3	169.0 ± 0.4	710.3 ± 0.7		

^a Reference numbers are given in parentheses. Mode of referencing: (7) C 1s, 284.3 eV; (22[†]) Ca 2p_{3/2}, 345.6 eV; (9) Au 4f_{7/2}, 83.95 eV; (18) C 1s, 284.4 eV; (17) (19) (20) C 1s, 284.6 eV. ^b Calculated from data of Table II. A, average over all data. B, average over data of Mj-6, Mj-7, and NBS-C.

Table IV. Width of Main Photoelectron Peak at Half-Maximum Height of As-Received and Sputtered MJ-6, MJ-7, and NBS-C

sample	sputtering time, min	width of photoelectron peak, eV						
		Si 2p	Al 2p	O 1s	S 2p	Ca 2p _{3/2}	Na 1s	Fe 2p _{3/2}
MJ-6	0	3.6	3.5	3.4	3.6	3.7	ND ^c	ND
	1	3.5	3.3	3.4	3.6	3.2	3.9	5.5
	6	3.4	3.6	3.6	3.9	3.8	3.0	7.1
	21	3.4	3.4	3.7	3.8	3.8	3.5	6.1
MJ-7	0	3.6	3.6	4.5	3.5	3.6	3.9	4.3
	1	3.7	3.7	4.2	4.4	4.2	3.9	6.3
	6	3.7	4.1	4.2	4.2	5.7	3.4	ND
	21	4.5	3.9	4.3	3.5	4.5	4.3	10.4
	36	4.0	4.3	4.5	4.5	5.6	3.4/4.9 ^a	7.1
NBS-C	0	3.4	3.9	3.2	3.4	4.0	<i>d</i>	5.7
	1	3.6	3.7	4.0	3.2	3.5	<i>d</i>	6.3
	6	3.7	3.8	3.9	2.0 ^b	5.5	<i>d</i>	7.8

^a Different values due to different base-line choice. See under Qualitative Results. ^b (2) Value for S 2p at 169.6 eV. See also Qualitative Results. ^c ND, not determined. ^d Not detected.

Table V. Concentration of Main Components of MJ-6, MJ-7, and NBS-C Fly Ash in Percent Atomic Weight before and after Sputtering

sample	sputtering time, min	concentration of element, % atomic wt							Si:Al:O:S:Ca atomic ratio
		Si	Al	O	S	Ca	Na	Fe	
MJ-6 ^a	0	16.7	8.8	61.2	10.0	3.1	ND ^d	ND	1.9:1.7:0.1:1.13:0.35
	1	17.3	8.7	59.7	9.2	3.0	1.7	0.4	2.0:1.6:9.1:0.05:0.34
	6	16.0	10.5	60.6	7.1	4.1	1.1	0.5	1.5:1.5:8.0:0.67:0.39
	21	18.3	14.3	58.3	2.7	4.7	1.2	0.6	1.3:1.4:1.0:0.19:0.32
MJ-7 ^b	0	14.5	7.6	66.9	6.2	2.8	1.6	0.3	1.9:1.8:8.0:0.82:0.36
	1	17.2	11.0	59.5	4.8	4.5	2.4	0.6	1.6:1.5:4.0:0.44:0.4
	6	16.4	14.8	59.2	2.7	5.4	1.5	ND	1.1:1.4:0.0:0.18:0.36
	21	15.8	16.1	59.8	1.7	4.6	1.5	0.5	1.0:1.3:7.0:0.11:0.29
NBS-C	36	16.4	15.7	59.2	1.2	6.1	0.8	0.9	1.0:1.3:8.0:0.08:0.39
	0	25.8	12.3	56.9	3.1	1.3	<i>e</i>	0.8	2.1:1.4:6.0:0.25:0.1
	1	19.0	14.9	61.9	2.0	1.0	<i>e</i>	1.2	1.3:1.4:2.0:0.13:0.07
	6	19.8	15.1	60.7	(0.9) ^c	1.5	<i>e</i>	1.4	1.3:1.4:0.0:0.06:0.1

^a Calculated particle size 0.7. ^b Calculated particle size 0.4. ^c Approximate value; see Table II. ^d ND, not determined. ^e Not detected.

throughout the studies of MJ-6. In the latter case, ΔBE 2p_{3/2}–2p_{1/2} varied between 3.3 and 4.0 eV. The resolution was also reflected in the width at half-maximum. Thus, in MJ-6 the value was in the range 3.2–3.8 eV as well as in as-received MJ-7, while a wide fluctuation was observed for NBS-C and sputtered MJ-7.

(4) **Fe 2p.** The Fe 2p_{3/2} peak could always be assigned, though not always with high accuracy, and its BE value was found to be 710.4 ± 0.7 eV. The 2p_{1/2} peak, however, is rather ill-defined in most cases. Sputtering seems to have a beneficial effect on the Fe 2p peaks. ΔBE 2p_{3/2}–2p_{1/2} was 12.4–13.4 eV in those cases where a reasonably accurate estimate could be done. The width of the 2p_{3/2} peak is the broadest of all the elements, and it was clearly broadened by sputtering, though in somewhat irregular pattern. While the as-received width was about 5 eV after sputtering, values of 8 eV and more were recorded (Table IV).

(5) **Na 1s.** The Na 1s peak has an average value of 1071.3 ± 0.4 eV. Its intensity is low relative to background counts in that region. Sputtering of MJ-7 for more than 5 min reveals a further feature which is not very pronounced. Under certain circumstances it can even be neglected and considered background noise. No pronounced effect of sputtering was observed besides the decrease in intensity as discussed under Discussion. The width at half-maximum was of the order 3.0–4.9 eV.

Semiquantitative Results

Semiquantitative data were worked out for MJ-6, MJ-7, and NBS-C in as-received form and after sputtering for

different periods based on an approach described elsewhere (10), and the data are given in Table V. Also included in Table V are the atomic ratios Si:Al:O:Ca:S. The data do not include the contribution of carbon as carbon stubs were used for support. However, data from as-received NBS(In), TENN-2, TENN-5, and KD samples supported on In were estimated to be in the range 8–18% C.

No evaluation of the concentration of elements is given for those elements of low concentration which are difficult to assign such as Mg and P.

Si, Al, and O. The concentration of Si and O changes very little in MJ-6, MJ-7, and NBS-C on sputtering after the removal of an outer layer of about 30 Å. The Al concentration increases steadily to about 15–16%. The atomic ratio of the three components of the aluminosilicate skeleton varies on sputtering, with an enrichment of Al relative to both Si and O. The amount of oxygen indicates a deficiency with respect to Si, Al, Ca, and S when these elements are assumed to be in their highest oxidation state (Table V).

S. The amount of sulfur is reduced on sputtering over a relatively long period. Thus, in MJ-6, about 60% of the initial amount of S is still found ~180 Å deep into the particle. No complete removal of S was achieved in all three samples. The decrease of S in MJ-7 is more rapid than in the two other samples.

Fe. The concentration of iron increases on sputtering, which is especially obvious in NBS-C.

Ca. The Ca concentration seems to remain essentially constant with some fluctuations after removal of a layer of about 30 Å.

Na. Na was detected in both MJ-6 and MJ-7, and its amount is reduced on sputtering, though it is not eliminated.

Discussion

Qualitative studies of the various fly ash (Table I) in their as-received mode show that the main components of the fly ash are in their highest oxidation state, and their binding energies correspond to those found for Si^{4+} , Al^{3+} , O^{2-} (in glass and aluminosilicate structures), Ca^{2+} , and SO_4^{2-} in CaSO_4 and soda glass, and Fe^{3+} in oxygen compounds (compare Tables II and III). Though some small spread in BE values between the different fly ash samples was observed, they seem to fall within the differences very often reported by different groups for the same material.

A systematic study of the outer layers of the MJ-6, MJ-7, and NBS-C by means of successive Ar^+ sputtering of up to $\sim 1000 \text{ \AA}$ had little effect on the BE values. For the sake of evaluation, BE values from the different measurements taken of the above three samples were averaged (Table III). The standard deviations found for the photoelectron peaks studied did not exceed $\pm 0.4 \text{ eV}$ except for $\text{Fe } 2p_{3/2}$ where the value was as high as $\pm 0.7 \text{ eV}$. The uncertainty in BE values will be discussed in detail later. Essentially little broadening of the Si, Al, and O peaks was observed on sputtering. The broadening observed for the $\text{Fe } 2p$ peak and the small feature toward lower BE observed for the Al-O-Si components in MJ-7 after sputtering are believed to be due to amorphization, though not to the extent of a complete phase separation. The small oxygen peak observed at lower BE values in as-received MJ-6 and MJ-7 is due to oxygen adsorbed on the carbon stub which is evident due to its incomplete coverage by fly ash. It is removed completely after brief sputtering for a minute. Segregation of iron oxide out of a glassy matrix was observed for reference material K-411, and amorphization was reported for carbonates (21) and other materials (11). It seems that no reduction of the iron to lower oxidation states, as often reported, occurred. The large standard deviation in the BE value of the $2p_{3/2}$ peaks is believed to reflect the inability to determine BE values with high accuracy in this case and is essentially in the range of the different values reported in the literature for Fe^{III} (Table III). However, the presence of Fe^{II} cannot be completely ruled out, as well as a reduction followed by rapid reoxidation.

The $\text{Ca } 2p_{3/2}$ BE value of 347.7 eV found in this work corresponds to those of Ca in CaSO_4 and soda glass (Table III). The peak is somewhat broadened on sputtering, which is reflected in the rather sharp fluctuation in the width of the peak due to loss of resolution of the $2p_{3/2}$ and $2p_{1/2}$ peaks. The sulfur, as already stated, is in the sulfate form with an average BE value of $169.0 \pm 0.4 \text{ eV}$, and sputtering has little effect other than to decrease its concentration. However, a small peak at 162.3 eV was observed on sputtering the MJ-6 sample, and less defined peaks were observed on sputtering the NBS-C in the region down to 161 eV . All these values correspond to different stages of reduction of the sulfur (20, 22). Somewhat contradictory results were reported in the literature as to the stability of the SO_4^{2-} when in the form of CaSO_4 . Thus, no reduction was observed by Christie et al. (7) while Coyle et al. observed some reduction (8). Both groups consider CaSO_4 to be a rather stable form, and this is in agreement with the presence of CaSO_4 on the surface. The effect due to the presence of cations like iron, the sulfate of which is less stable, might lead to either a reduction to S^{2-} species in MJ-6 and a range of reduced species in the case of NBS-C or a redeposition of a free sulfur phase of higher

conductivity, especially for MJ-6. However, on the basis of semiquantitative data, part of the sulfur has to be adsorbed as an oxide. BE values of S in SO_2 adsorbed on alkaline earth oxides correspond to those of sulfate (Table III).

The semiquantitative calculated data for MJ-6, MJ-7, and NBS-C indicate that in the aluminosilicate skeleton (Si-Al-O) there is an enrichment of Si relative to Al (Si:Al atomic ratio of about 2) at the outer layers of about 60 \AA . A separation of silica phase is often observed in aluminosilicate glasses of similar composition (with respect to Si-Al-O) (23), and this might also be responsible for the rough morphology of the submicron particles (12). After sputtering and reaching a depth of about 180 \AA , the ratio approaches 1.3, 1.3, and 1.0 for MJ-6, NBS-C and MJ-7, respectively (Table V). The value obtained for MJ-6 is complementary to bulk data from EDX analysis with a value of 1.4. In all sputtered samples, a deficiency of 15–30% in oxygen atomic concentration was observed relative to the calculated oxygen based on the total cations present in their highest oxidation state. This might reflect the semiquantitative approach and the complexity of the multicomponent system; preferential sputtering of oxygen might contribute to the observed deficiency.

Sulfur is surface enriched, but 50% or more of its initial concentration is present after 180 \AA . The Ca concentration as given in Table V is an upper limit mainly because sputtering causes loss of resolution of the two peaks, and thus, values seem to be overestimated. Also, the tendency of Ca ions to migrate toward the surface on sputtering could not be excluded. Ca, however, seems to be part of the glass matrix and extends deep into the core of the particles. Its correlation to sulfur as CaSO_4 is not clear. In as-received samples, the amount of sulfur is much too high on the basis of CaSO_4 , and sulfur is also influenced by sputtering independently of Ca. Thus, our suggestion of adsorbed sulfur oxide seems reasonable. Other potential sulfate species include sulfuric acid, alkali iron, and ammonium sulfates.

The iron concentration increases as more inner layers are exposed by sputtering. In view of the segregation tendency of iron oxide, this may be induced by sputtering, but as in the case of Ca, this would indicate that iron extended deep into the particles, as observed also by Canbiss and Linton (6).

Sodium was detected in as-received MJ-6 and MJ-7, and it is not easily removed by sputtering. This might be due to a redistribution and/or diffusion process (see ref 11 and references cited within).

Phosphorus, nitrogen, and chlorine were identified from time to time as indicated under Qualitative Results. However, due to their ill-defined peaks it was impossible to assign BE values with high confidence. The concentration of these elements, whenever identified, was in the range of 0.5% and below, a value which we consider as the detection limit under the present operating conditions. This value limits also the capability of detection of trace elements.

Throughout this work the BE value of 102.6 eV for Si $2p$ in aluminosilicates was used for reference, as was done by Linton et al. (6) which is a reasonable approach, especially when sputtering is involved, in view of the general complexity of referencing of nonconducting materials (24, 25). Also, for the sake of comparison, different fly ash samples mounted on In were referenced to C $1s$ with a BE value of 284.6 eV . The BE value of Si $2p$ was $102.6 \pm 0.3 \text{ eV}$, well within accuracy limits. The uncertainty in BE value determination in this work is estimated to be ± 0.4

eV for all the elements studied except for Fe and Na which were discussed separately, and only a few BE values are marginal. The average calculated BE values obtained either by averaging over all the samples studied or by averaging the data from MJ-6, MJ-7, and NBS-C are consistent and in good agreement with values from the literature. We consider the spread of ± 0.4 eV reasonable, and similar values are reported in the literature for sputtering studies (19). Contributing to the uncertainty is the problem of referencing in general and oxide type materials in particular, reflected also in the data from the literature (Table III) (24, 25).

A carbon support was technically very useful for the quantitative transfer of the small amounts of fly ash available. As the carbon stub was not completely covered up and its C 1s was evident in the spectra, no quantitative evaluation of carbon could be taken. However, we estimate the amounts of carbon in NBS mounted on In to be about 18% and, for TENN-2, TENN-5, and KD, in the range 8–17%. We consider secondary adsorption of spurious hydrocarbons a major contribution to these high values. Bulk values of ~ 2 wt % corresponding to about 3–4% found for TENN particles in the micrometer range (14) would otherwise indicate an enormous surface enrichment of carbon.

Conclusions

(A) MJ-6, MJ-7, NBS-C: Major Components. (1) We were able to study submicron particles, which are considered major contributors to the hazards of fly ash, using a novel approach of mounting the particles on carbon stubs. The study of the major components of submicron particles indicates that their concentration is in the range observed in studies of non-size-segregated fly ash particles of different origin.

(2) BE values indicate that Si, Al, O, S, Ca, Fe, and Na are in their highest oxidation states corresponding to their values in related oxygen-containing compounds. Little change in BE values due to sputtering was observed. The increase in peak width of iron is believed to indicate amorphization.

(3) Semiquantitative data show a surface enrichment of S and Na, while the Ca concentration remains almost constant and that of Fe increase with depth. Also, Si was surface enriched relative to Al. For Na, Ca, and Fe, data are believed to reflect also diffusion, segregation, and other ion bombardment induced processes. The Si enrichment might originate from SiO_2 phase separation unrelated to sputtering effects.

(4) Major components of similar nature were found for as-received samples of fly ash from different power plants burning different types of coal.

(B) Minor Components. Elements like N, P, Cl, and Mg could be identified, but their concentration and oxidation state could not be asserted. These elements vary in their distribution in different fly ash. Generally, the limit of detection was considered 0.5%.

Acknowledgments

We gratefully acknowledge the contributions of Joasia Kasperkiewicz and John Kovachik in obtaining much of the Kincaid, IL, and Bull Run, TN, data.

Registry No. S, 7704-34-9; Na, 7440-23-5; Si, 7440-21-3; Al, 7429-90-5; O₂, 7782-44-7; Ca, 7440-70-2; Fe, 7439-89-6.

Literature Cited

- (1) Rubin, E. S. *Environ. Sci. Technol.* **1983**, *17*, 366A.
- (2) "Planning Studies for Measurements of Chemical Emissions in Stack Gases of Coal-Fired Power Plants". Report prepared for EPRI, Palo Alto, CA, by Southern Research Institute, Birmingham, AL, Battelle Columbus Laboratory, Columbus, OH, and Roth Associates, Inc., Rockville, MD 1983, EA-2892, Research Project 1776-1.
- (3) Campbell, J. A.; Smith, R. D.; Davis, L. E. *Appl. Spectrosc.* **1978**, *32*, 316.
- (4) Rothenberg, S. J.; Denese, P.; Holloway, P. *Appl. Spectrosc.* **1980**, *34*, 549.
- (5) Jach, T.; Powell, C. J. *Environ. Sci. Technol.* **1984**, *18*, 58.
- (6) Cabaniss, G. E.; Linton, R. W. *Environ. Sci. Technol.* **1984**, *18*, 271.
- (7) Christie, A. B.; Lee, J.; Sutherland, I.; Walls, J. M. *Appl. Surf. Sci.* **1983**, *15*, 224.
- (8) Coyle, G. J.; Tsang, T.; Adler, I.; Ben-Zvi, N.; Yin, L. J. *Electron Spectrosc. Relat. Phenom.* **1981**, *24*, 221.
- (9) Brundle, C. R.; Chuang, T. J.; Wandelt, K. *Surf. Sci.* **1977**, *68*, 459.
- (10) Kaufherr, N.; Lichtman, D. *Surf. Sci.* **1984**, *139*, 347.
- (11) Kelly, R. *Nucl. Instrum. Methods* **1981**, *182/183*, 351, and references cited within.
- (12) Lichtman, D.; Mroczkowski, S. *Environ. Sci. Technol.* **1985**, *19*, 274–277.
- (13) Hock, J. L.; Lichtman, D. *Environ. Sci. Technol.* **1982**, *16*, 423.
- (14) Kaufherr, N.; Lichtman, D. *Environ. Sci. Technol.* **1984**, *18*, 544.
- (15) "Handbook of X-ray Photoelectron Spectroscopy"; Physical Electronics Division, Perkin-Elmer Corp.: Palo Alto, CA, 1979.
- (16) Kaufherr, N.; Lichtman, D., unpublished results.
- (17) Wagner, C. D.; et al. *J. Vac. Sci. Technol.* **1982**, *21*, 933.
- (18) Barr, T. L. *Appl. Surf. Sci.* **1983**, *15*, 1.
- (19) Kohiki, S. *J. Electron Spectrosc. Relat. Phenom.* **1983**, *28*, 229.
- (20) Lichtman, D.; Craig, J. H.; Sailer, V.; Drinkwine, M. *Appl. Surf. Sci.* **1981**, *7*, 325.
- (21) Christie, A. B.; Sutherland, I.; Walls, J. M. *Vacuum* **1981**, *31*, 513.
- (22) Stinespring, C. D.; Cook, J. M. *J. Electron Spectrosc. Relat. Phenom.* **1983**, *32*, 113, and references cited within.
- (23) Beall, G. H. In "High Temperature Oxides"; Alper, A. M., Ed.; Academic Press: New York, 1971; Vol. 5-IV.
- (24) Madey, T.; Wagner, C. D.; Joshi, A. *J. Electron Spectrosc. Relat. Phenom.* **1977**, *10*, 359.
- (25) Kohiki, S.; Oki, K. *J. Electron Spectrosc. Relat. Phenom.* **1984**, *33*, 375.

Received for review September 10, 1984. Revised manuscript received December 31, 1984. Accepted January 24, 1985. This work was supported by the Electric Power Research Institute under Contract RP 1625-1.

Variability of Elemental Concentrations in Power Plant Ash

Larry J. Holcombe*

Radian Corporation, Austin, Texas 78766

Barry P. Eynon

Stanford Research Institute, Int., Menlo Park, California 94025

Paul Switzer

Department of Statistics, Stanford University, Stanford, California 94305

■ Sampling was conducted at a U.S. coal-fired power plant to determine the time variability of coal ash composition. Variance components analysis was used to estimate the relative contributions of time, sampling, and chemical analysis to the total variability in measured concentrations. All of these components were found to contribute to the variability in different degrees depending on the element and method of analysis. The data were statistically treated to evaluate sampling designs for collecting and analyzing ash. As an example, to achieve at least 50% precision in a 30-day average ash composition for all elements, the optimal sampling plan required seven samples, each analyzed twice, for a total of 14 analyses over a 30-day period. Extrapolation of these designs might be made to other coal-fired plants, provided extreme differences do not exist between the plant operations.

Introduction

This paper summarizes a series of projects conducted between 1980 and 1983 to evaluate the variability in elemental concentrations of power plant ash. The projects are part of a program conducted by the Electric Power Research Institute (EPRI) to develop methods for predicting disposal properties of coal ash. The relevant disposal properties include mobilization and migration of chemical elements from ash. This particular aspect of the EPRI program examined the variability of ash composition as input to sampling designs.

A predictive model of contaminant migration from ash disposal must be based on the chemical and physical properties of a descriptive sample of the ash. Therefore, it is extremely important to obtain a sample representative of the coal ash produced and to be able to define the limits within which the sample or sample set represents the coal ash characteristics.

In this paper we will discuss precipitator ash with respect to several major and trace element constituent concentrations. Additional results for coal and bottom ash, as well as several other chemical elements, can be found in a series of EPRI reports (1-4) upon which this paper is based.

The program objectives included quantifying the variance components that contribute to coal ash variability. Particular emphasis was placed on determining the time variability of an ash stream. On the basis of this variability analysis, efficient sampling programs can be designed. And, provided there are sufficient data, the precision of the sampling designs in estimating a time-averaged ash composition can be calculated.

Data Collection

Site Description. The coal-fired power plant used in the study is located on the east bank of a lake in South-eastern United States. The plant has one unit with a maximum generating capacity of 950 MW and was placed

in commercial operation in 1967.

Figure 1 presents a simplified schematic of the material that flows through the plant and identifies locations used for collecting samples of the feed coal and precipitator ash. Coal is transported by train, and the plant uses about 8200 tons of coal/day. From the coal pile, the coal is conveyed by belt to the powerhouse where it is crushed and loaded into bins that hold a 1-2-day supply. The crushed coal passes through the pulverizer where it is reduced to a fine powder. From the pulverizer, it is mixed with hot air and blown through burners into the boiler furnace where the mixture ignites. The heavy ash drops to the bottom of the boiler and is disposed of. Fly ash is carried through the boiler by the flue gas where it is removed by electrostatic precipitators (ESP). The precipitator ash is collected in hoppers beneath the ESP and drawn by vacuum into a Hydrovac where it is slurried with water. The slurried ash travels through fiberglass pipe out to the ash ponds.

Sampling Procedures. Sampling was conducted during the period from Jan 9, 1982, to Oct 19, 1982, with some down time for scheduled plant maintenance during Feb, March, April, and May of 1982.

Precipitator ash was collected from the ash sluice line at a point about $\frac{1}{4}$ mile from the ESP. The sluice line at this point was under a positive head pressure of approximately 20 psig; therefore, pumping was not required to obtain a sample of the slurry.

A probe was permanently fixed to the sluice line by cutting a 4-in. diameter hole through the fiberglass pipe, inserting the probe, and epoxying the probe to the pipe. Figure 2 illustrates the probe assembly. All parts were constructed of high-pressure polyvinyl chloride (PVC) to avoid metal contamination. To sample, a Nalgene line was attached to the faucet and the faucet turned on for 1 min to purge the probe and line. The end of the line was then inserted in an 8-L linear polyethylene (LPE) bottle and a sample taken. This size sample was necessary in order to obtain between 200 and 400 g of dry precipitator ash. The LPE bottle was taken back to the lab where it was allowed to settle for 1 h. The liquid was filtered off (Whatman No. 41 filter paper) by vacuum, and the solids were dried overnight in a 35 °C (95 °F) convection oven. The dried sample was sealed in an LPE bottle and labeled for analysis.

Sampling Design. Figure 3 depicts the schedule for sampling at the plant. Each character in the figure, either an X or an O, represents one calendar day. On days marked by X's samples were taken, and on days marked with O's samples were not taken. This sampling scheme allows for calculations of time variability over lag times between samples as short as 24 h and up to approximately 3 months. Other components of sample variability besides time—sampling, sample preparation, and sample analysis—were also calculated from this design as follows. The sampling episodes are grouped in 3-day periods.

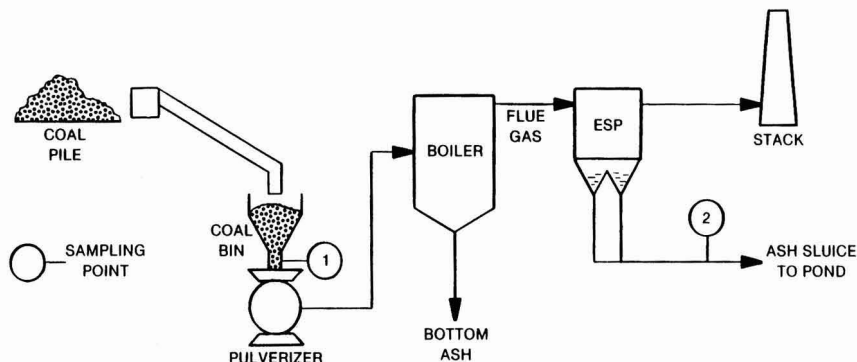


Figure 1. Locations of coal and precipitator ash sampling points.

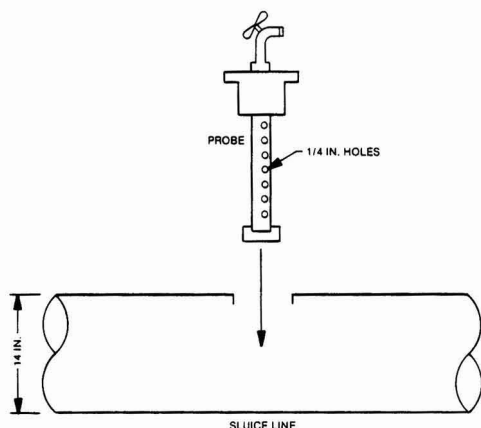


Figure 2. Precipitator ash sampling probe.

Within a 3-day period when samples were taken, a specified number of composite and replicate samples also were prepared. The composite sample consisted of equal portions of the day 1, 2, and 3 samples mixed thoroughly by riffing. This composite was then split for duplicate analysis. On day 2 of each 3-day period a replicate sample was collected to determine time zero variability, or the variability associated with the sampling procedure. This replicate was collected in a separate bottle immediately after the primary sample was taken on day 2.

Analytical Procedures. The variability over time of the coal and ash compositions was calculated on the basis of total chemical concentrations and on concentrations measured in EP extracts (5). The analytical procedures are described below.

(1) **Ash Dissolution.** Prior to instrumental analysis the solid samples were dissolved using nitric-hydrofluoric-perchloric acid digestion (PAD). The PAD technique employed (6) was similar to a recently published

Days From Start of Sampling	START 1-9-82							
1-23	<u>XXX</u>	OO	<u>XXX</u>	OO	(XXX)	OO	<u>XXX</u>	OO
24-156	Scheduled Plant Down-Time							
157-179	<u>XXX</u>	OO	<u>XXX</u>	OO	(XXX)	OO	<u>XXX</u>	OO
180-185	RE-START 10 days after plant start-up (6-9-82)							
186-206	<u>XXX</u>	OO	<u>XXX</u>	OO	(XXX)	OO	<u>XXX</u>	OO
207-212								
213-233	<u>XXX</u>	OO	<u>XXX</u>	OO	(XXX)	OO	<u>XXX</u>	OO
234-239								
240-262	<u>XXX</u>	OO	<u>XXX</u>	OO	(XXX)	OO	<u>XXX</u>	OO
263-268								
269-289	<u>XXX</u>	OO	<u>XXX</u>	OO	(XXX)	OO	<u>XXX</u>	OO

All X's denote ash sampling days.

All O's denote days off.

Underlined X's denote coal sampling and ash sampling days.

Parenthetic X's denote days for which both ash extractions and ash total analyses are done.

Note that the beginning and end of the study period have a higher sampling rate.

Figure 3. Time distribution of model sampling plan.

Table I. Percentage of Variance from Each Source: Daily Samples^a

element	mean concn	units	total variance ^b	time, %	sampling, %	analysis/ prepn, %
aluminum	15.27	% wt	0.0007	13.0	71.8	15.0
arsenic	100.7	µg/g	0.0043	32.1	41.9	25.8
barium	566.3	µg/g	0.0115	85.6	13.8	0.5
beryllium	22.74	µg/g	0.3403	97.5	0.5	1.9
calcium	4124	µg/g	0.0060	79.3	4.5	16.0
chromium	167.7	µg/g	0.0009	0.0	75.9	24.0
cobalt	83.32	µg/g	0.0052	65.6	33.2	1.0
copper	186.9	µg/g	0.0032	56.2	36.3	7.4
iron	2.305	% wt	0.0035	47.6	50.3	2.0
lead	154.6	µg/g	0.0005	0.0	83.1	16.8
magnesium	4553	µg/g	0.0038	76.2	20.8	2.9
manganese	74.61	µg/g	0.0196	63.9	1.7	34.2
mercury	0.2423	µg/g	0.1341	1.5	91.1	7.2
molybdenum	32.33	µg/g	0.0075	54.2	0.0	45.7
nickel	145.1	µg/g	0.0038	45.2	41.5	13.1
potassium	2.059	% wt	0.0036	86.6	11.3	2.0
selenium	14.33	µg/g	0.1118	92.9	5.9	1.1
silicon	21.96	% wt	0.0035	0.0	94.9	5.0
sodium	2167	µg/g	0.0235	0.0	0.0	0.0
sulfur	412.9	µg/g	0.0223	8.5	0.0	91.4
titanium	1.12	% wt	0.0021	64.0	30.4	5.5
vanadium	262	µg/g	0.0020	35.3	55.3	9.2
yttrium	80.59	µg/g	0.0049	45.3	51.1	3.5
zinc	255.8	µg/g	0.0040	23.2	67.1	9.5
gross α	39.68	pCi/g	0.0654	0.0	0.0	0.0
gross β	68.18	pCi/g	0.0149	0.2	0.0	99.7
radium-226	3.57	pCi/g	0.1486	0.0	51.7	48.2

^a Preparation = digestion. ^b Sum of all variance components divided by the square of the mean.

procedure but differed primarily in the amount of acid used.

(2) **Mercury Digestion.** Mercury is an extremely volatile element and incurs significant losses in open-to-the-air digestion procedures. Therefore, total mercury digestions were done on a Paar bomb calorimeter in which the coal or ash is combusted with oxygen in a closed bomb and the mercury is absorbed by a H₂SO₄-KMnO₄ solution. Atomic absorption (AA) cold vapor technique is used to measure mercury content of the solution.

(3) **Extraction Procedure.** The procedure for the EP toxicity test is outlined in an EPA publication (5).

(4) **Chemical Analysis.** The elements analyzed in the ash digests and EP extracts were the eight trace elements regulated under RCRA (arsenic, barium, cadmium, chromium, lead, mercury, selenium, and silver) and additional elements which are minor and major mineral constituents of the ash. Analytical techniques used in this project included inductively coupled argon plasma emission spectrometry (ICAP), atomic absorption (AA) spectrometry, and ion chromatography (IC). Detection limits by ICAP for four elements (lead, arsenic, selenium, and mercury) were too high to provide quantitative results. Therefore, these elements/samples were measured by AA.

Variance Component Analysis

The replication design for the sampling plan in this study allowed estimation of three components of variability for the noncomposite samples: (1) σ^2_T , time variation in the mean concentration of samples taken on different sampling days; (2) σ^2_S , sampling variation between ash samples taken at the same sampling point at the same time; (3) σ^2_A , the combined variation between sample results due to preparation (extraction/digestion) and elemental analysis of each sample.

These three parameters plus the overall data mean, m , were estimated by maximum likelihood methods (4). Situations with a large number of detection limit values (greater than 50% of the data) were not analyzed for

variance components. In other cases the detection limit observation was included in the analysis with a value that was the median probability point of the data below the detection limit, according to the fitted normal probability density function.

The results of this analysis are given in Tables I and II, which list, for each element, the number of cases used in the analysis, the mean concentration and measurement units, and the three components of variability, expressed as a proportion of the total variance

$$100(\sigma^2/\sigma^2_{\text{tot}}) \quad (1)$$

where σ^2 is the variance for each individual component, and $\sigma^2_{\text{tot}} = \sigma^2_T + \sigma^2_S + \sigma^2_A$.

In order to further quantify the effect of time on the correlation between trace element compositions in samples, a variogram analysis was performed on the data. This analysis investigates the persistence of element concentrations over time. In a previous study conducted at a different power plant (3) the variability in ash composition was found to be time dependent, and a variogram analysis was required to provide a rigorous fit of the data. In this study, the majority of elements exhibited constant variability with time. And, although the variance components were fitted by a variogram function in this study, it would be reasonable to describe the variability by a constant function. For the few elements where variability appears to be time dependent, an approach will be described in the following section for estimating sampling precision.

Implications for Sampling Designs

The construction of a representative sampling plan involves a trade-off between precision and cost. The objective is to estimate the average composition of a waste stream for a given time from sample data. The average composition should be within a specified precision at least cost.

The formulas presented here go somewhat beyond those discussed in other sources (5).

Table II. Percentage of Variance from Each Source: Daily Samples^a

element	mean concn, µg/mL	total variance ^b	time, %	sampling, %	analysis/ prepn, %
aluminum	0.3945	0.2421	51.1	40.0	8.7
arsenic	0.0488	0.4595	58.4	30.2	11.3
barium	0.4021	0.1742	70.7	21.8	7.4
calcium	5.144	0.1754	71.1	26.7	2.1
copper	0.0091	1.5445	1.5	85.5	12.8
lithium	0.0063	1.4100	0.0	18.2	81.7
magnesium	0.9537	0.1164	77.6	14.9	7.4
manganese	0.0163	0.2948	33.2	62.9	3.7
molybdenum	0.0856	0.3832	49.8	36.3	13.7
nickel	0.0039	0.4849	8.5	23.0	68.4
potassium	0.4296	1.7302	0.0	91.5	8.4
selenium	0.2193	0.1609	82.8	12.6	4.4
silicon	0.863	0.2008	71.3	26.4	2.2
sodium	0.6217	0.0779	0.0	43.9	56.0
sulfur	2.565	0.1072	57.4	23.5	19.0
vanadium	0.0666	0.3237	60.7	20.0	19.2
zinc	0.0079	0.5451	47.6	43.5	8.8
sulfate	7.22	0.1086	77.4	9.3	13.2

^aPreparation = extraction. ^bSum of all variance components divided by the square of the mean.

Preliminary Notation. Let C_D = cost of daily sampling (per day). C_A = cost of sample splitting, preparation, and analysis per split, (costs of compositing of sample material being assumed relatively negligible), and 100% = specified statistical precision requirement expressed as a percentage of the estimated concentration.

Also, let the waste stream variability characteristics (for each chemical) be σ_A^2 = variance between determinations from splits of a single homogenized sample or composite, $\sigma_S^2 + \sigma_A^2$ = variance between determinations from simultaneous samples of unit volume V_0 , $\sigma_D^2 + \sigma_S^2 + \sigma_A^2$ = variances between determinations on different sampling days from samples of unit volume V_0 , where σ_D^2 is the time variance in sample concentrations from the variogram analysis, and m = concentration mean value.

Sampling Designs. Then (for constant variability with time), the optimal sampling design is parameterized by T = specified length of the time interval for which average concentrations need to be estimated, N_D = number of sampling days, spread evenly over the time interval of length T , i.e., N_D subintervals each of length T/N_D with a sampling point at the center of each subinterval, N_A = total number of sampling splits analyzed, and V = total "sample" volume per analysis (to be made as large as is practical). The analysis and sampling variance components can be combined to yield $\sigma_{AS}^2 = \sigma_A^2 + \sigma_S^2/(V/V_0)$, where V_0 is the sample volume used in this study (1 gal).

Since the cost structure here is relatively insensitive to sample volume, the total cost may be written approximately as

$$C = N_D D_D + N_A C_A \quad (2)$$

The relative precision of estimation may be expressed as

$$\Delta = (1.645/m)[\sigma_D^2/N_D + \sigma_{AS}^2/N_A]^{1/2} \quad (3)$$

where m is the mean concentration. (An upper 95% confidence limit for the mean is approximately $m(1 + \Delta)$.)

For specified precision, the total cost is minimized mathematically when

$$N_D = \sigma_D^2 \left[\left(\frac{C_A}{C_D} \right)^{1/2} \left(\frac{\sigma_{AS}}{\sigma_D} \right) + 1 \right] / \left(\frac{m\Delta}{1.645} \right)^2 \quad (4)$$

$$N_A = \sigma_{AS}^2 \left[\left(\frac{C_D}{C_A} \right)^{1/2} \left(\frac{\sigma_D}{\sigma_{AS}} \right) + 1 \right] / \left(\frac{m\Delta}{1.645} \right)^2 \quad (5)$$

If $N_A \geq N_D$, then on each sampling day one draws N_A/N_D samples each of maximum volume V . If $N_A < N_D$, then on each sampling day one draws a single sample of volume $V(N_A/N_D)$ and composites samples from N_D/N_A consecutive sampling days. From each sample or composite a single split is taken for analysis.

The minimized cost will then be

$$C^* = [\sigma_{AS}(C_A)^{1/2} + \sigma_D(C_D)^{1/2}]^2 / (m\Delta)^2 \quad (6)$$

The mathematical calculation will need to be rounded up since both N_A and N_D need to be integers. As well, either N_A/N_D or N_D/N_A needs to be integers. This will result in precision slightly better than Δ and total cost slightly higher than C^* . Since the variability parameters for different chemical species are likely to be different, it may be necessary to choose a sampling plan that meets estimation precision requirements for the most variable chemical species of interest.

Note that the precision Δ does not depend on the length T of the sampled time interval. This is an approximation that is reasonable provided the time variability of the chemical species in question is constant over such a time range. If T is either very short or very long, then this approximation could break down. For many of the chemicals in this study a fairly constant variability was observed over a range from a few weeks to a few months. The exceptions were variograms that appeared linear over such ranges. The corresponding formula in the case of a linear variogram with slope b is

$$\Delta = \frac{1.645}{m} \left[\frac{1}{6} \frac{(bT)^2}{N_D^2} + \frac{a}{N_D} + \frac{\sigma_{AS}^2}{N_A} \right]^{1/2} \quad (7)$$

Explicit optimization of the sampling plan for fixed precision, Δ , is mathematically difficult in the linear variogram case. As an approximation, one may try using a roughly fitted flat variogram approach with $\sigma_D^2 = \alpha + (bT)^2/3$. This approximation may tend to overstate sampling requirements.

Examples of Sampling Designs. To demonstrate the application of these formulas, we consider several scenarios for the construction of sampling plans. Assume that the object of interest is measurement of the average extract element concentrations over a 30-day period, for the set of elements found in the ash extracts. The sampling cost

Table III. Optimal Sampling Designs: $\Delta = 0.30^a$

element	mean concn, $\mu\text{g}/\text{mL}$	no. of samples	no. of analyses	total sampling cost, \$	achieved precision indiv plan	achieved precision overall plan
aluminum	0.3945	12	3	1440	0.28	0.19
arsenic	0.0488	8	4	1440	0.30	0.15
barium	0.4021	6	1	600	0.30	0.11
calcium	5.144	6	1	600	0.29	0.13
copper	0.0091	3	15	3780	0.30	0.19
lithium	0.0063	6	36	9000	0.30	0.30
magnesium	0.9537	2	1	360	0.27	0.08
manganese	0.0163	1	2	540	0.27	0.06
molybdenum	0.0856	10	5	1800	0.30	0.19
nickel	0.0039	7	14	3780	0.30	0.19
potassium	0.4296	3	18	4500	0.28	0.20
selenium	0.2193	3	1	420	0.27	0.10
silicon	0.863	8	2	960	0.29	0.20
sodium	0.6217	1	2	540	0.27	0.06
sulfur	2.565	8	2	960	0.29	0.17
vanadium	0.0666	8	4	1440	0.29	0.16
zinc	0.0079	24	6	2880	0.30	0.27
sulfate	7.22	8	2	960	0.28	0.20
overall sampling plan		12	36	9360		

^a Preparation = extraction.Table IV. Optimal Sampling Designs: $\Delta = 0.50^a$

element	mean concn, $\mu\text{g}/\text{mL}$	no. of samples	no. of analyses	total sampling cost, \$	achieved precision indiv plan	achieved precision overall plan
aluminum	0.3945	4	1	480	0.49	0.26
arsenic	0.0488	2	2	600	0.47	0.21
barium	0.4021	1	1	300	0.44	0.15
calcium	5.144	1	1	300	0.49	0.17
copper	0.0091	1	6	1500	0.47	0.31
lithium	0.0063	2	14	3480	0.48	0.48
magnesium	0.9537	1	1	300	0.32	0.11
manganese	0.0163	1	1	300	0.37	0.10
molybdenum	0.0856	4	2	720	0.47	0.26
nickel	0.0039	5	5	1500	0.47	0.30
potassium	0.4296	1	6	1500	0.49	0.32
selenium	0.2193	1	1	300	0.38	0.13
silicon	0.863	3	1	420	0.45	0.26
sodium	0.6217	1	1	300	0.37	0.10
sulfur	2.565	2	1	360	0.50	0.23
vanadium	0.0666	2	2	600	0.47	0.22
zinc	0.0079	10	2	1080	0.50	0.37
sulfate	7.22	3	1	420	0.44	0.26
overall sampling plan		7	14	3780		

^a Preparation = extraction.

is estimated to be about \$60 per visit, and the analysis cost per sampling for the whole battery of elements is estimated to be about \$240, i.e., $C_A/C_D = 4$. A modest increase in the sample volume was assumed from that used in this study, from 1 to 3 gal. Two levels of desired precision were considered, for $\Delta = 0.30$ and 0.50 .

In this study, the variance parameters for the cost equations were obtained from a variogram analysis of the data. However, most of the elemental concentrations exhibited little or no time dependence. Therefore, a similar sampling design can be constructed by using the variance parameters in Tables I and II applied to the same cost equations.

For each element separately, the cost equations above were used to find the minimum cost sampling plan meeting the desired precision. The minimum was obtained over all plans with an integral number of samples and analyses and an integral ratio of either N_D/N_A or N_A/N_D . Tables III and IV give the optimal values of N_D and N_A for the plan for each individual element, the cost of that plan, and

the achieved precision of the plan.

The analysis was then extended to consider all elements simultaneously, to produce an overall sampling plan. The sampling plan that achieves the desired precision for all elements is listed at the bottom of each page of Tables III and IV, along with the cost. The achieved precision of this plan for each element is also tabulated. Note that most elements actually achieve a precision somewhat better than the target. If lithium were dropped from the list of elements, these plans would become cheaper by about a factor of 2.

If even less precision is needed, i.e., if the observed concentrations are well below the regulatory limit, then even less sampling would be necessary.

Conclusions

This research has presented methods for obtaining time-averaged samples of coal ash. The statistical methods used for estimating the time-averaged composition and the precision of the estimate consider several components that

affect the overall variability in ash composition. Extrapolations concerning sampling designs might be made to other coal-fired plants, provided extreme differences do not exist in the plant operations. For example, a highly variable coal source might result in time variabilities in ash composition greater than those measured in these studies. The basic approach and equations can be used in sampling designs for other waste discharges from point sources, provided the time variability can be described by a normal distribution.

Acknowledgments

We thank Ishwar P. Murarka, senior project manager at EPRI, for his assistance in preparing this account.

Registry No. Aluminum, 7429-90-5; arsenic, 7440-38-2; barium, 7440-39-3; beryllium, 7440-41-7; calcium, 7440-70-2; chromium, 7440-47-3; cobalt, 7440-48-4; copper, 7440-50-8; iron, 7439-89-6; lead, 7439-92-1; magnesium, 7439-95-4; manganese, 7439-96-5; mercury, 7439-97-6; molybdenum, 7439-98-7; nickel, 7440-02-0; potassium, 7440-09-7; selenium, 7782-49-2; silicon, 7440-21-3; sodium, 7440-23-5; sulfur, 7704-34-9; titanium, 7440-32-6; vanadium, 7440-62-2; yttrium, 7440-65-5; zinc, 7440-66-6; α particle,

12587-46-1; β particle, 12587-47-2; radium-226, 13982-63-3; lithium, 7439-93-2.

Literature Cited

- (1) "Extraction Procedure and Utility Solid Waste"; Electric Power Research Institute: Palo Alto, CA, 1981; EA-1667.
- (2) Eynon, B. P.; Switzer, P. "A Statistical Comparison of Two Studies on Trace Element Composition of Coal Ash Leachates"; Electric Power Research Institute: Palo Alto, CA, 1983.
- (3) Switzer, P.; Eynon, B. P.; Holcombe, L. J. "Pilot Study of Time Variability of Elemental Concentrations in Power Plant Ash"; Electric Power Research Institute: Palo Alto, CA, 1983; EA-2959.
- (4) Eynon, B. P.; Switzer, P.; Holcombe, L. J. "Time Variability of Elemental Concentrations in Power Plant Ash"; Electric Power Research Institute: Palo Alto, CA, 1984; EA-3610.
- (5) U.S. Environmental Protection Agency "Test Methods for Evaluating Solid Waste", 2nd ed.; Office of Solid Waste and Emergency Response: Washington, DC, 1982.
- (6) McQuaker, N. R.; Kluckner, P. D.; Chang, G. N. *Anal. Chem.* 1979, 51, 1082-1084.

Received for review August 16, 1984. Accepted January 16, 1985. This work was funded by the Electric Power Research Institute (EPRI) under Research Project 1620.

The Mutagenic Activity of the Products of Propylene Photooxidation

Tadeusz E. Kleindienst,* Paul B. Shepson, and Edward O. Edney

Northrop Services, Inc.—Environmental Sciences, Research Triangle Park, North Carolina 27709

Larry T. Cupitt

Atmospheric Sciences Research Laboratory, United States Environmental Protection Agency, Research Triangle Park, North Carolina 27711

Larry D. Claxton

Health Effects Research Laboratory, United States Environmental Protection Agency, Research Triangle Park, North Carolina 27711

■ The reactants and products in irradiated propylene/ NO_x mixtures were brought to a steady-state distribution in a Teflon smog chamber operated in a dynamic mode. The effluent from the chamber was then tested for total mutagenic activity by exposing *Salmonella typhimurium* strain TA100 to it. The data show an increased mutagenic activity for the products when compared with the reactants and controls. In addition, the mutagenic activity at long reaction times is substantially greater than at short reaction times. To examine a subset of the propylene/ NO_x photooxidation products, an exposure of strain TA100 to the products of the propylene/ N_2O_5 dark reaction was conducted. Although a small mutagenic activity was observed for this mixture, a number of mutagenic organic nitrates were identified. The results for the irradiated propylene/ NO_x mixture were analyzed in terms of the mutagenic activities of the individual products. The major products (carbon monoxide, ozone, formaldehyde, acetaldehyde, nitric acid, and peroxyacetyl nitrate) account for no more than 20% of the observed mutagenic response, assuming additivity.

Introduction

There has been a long-standing interest in possible adverse health effects from chemicals emitted into the atmosphere. Over the past decade, toxicologists have developed many short-term biological assays to screen com-

pounds rapidly for possible adverse health effects (1). The testing of compounds emitted or formed in the atmosphere has now begun by using these techniques (2) in both laboratory and field studies.

We have recently undertaken a program to examine the total mutagenic activity of products from irradiated hydrocarbon/ NO_x mixtures using a photochemical reaction chamber operated in a dynamic mode. This reactor has the advantage of maintaining the reactant and product distribution once a steady state is reached. This situation is required in controlled mutagen assays since the sampling time is long compared to the change in product distribution that would occur in a static reaction system.

Recently we reported the results of a study in which irradiated mixtures of toluene/ NO_x were tested for mutagenic activity using the *Salmonella*/mammalian microsome reversion assay (3). In this study, the bacterial strains TA100 and TA98, both with and without S9 metabolic activation, were used. The results showed an increased mutagenic activity for the product mixture when compared to the reactant mixture in both strains. A higher response was also observed for product distributions at longer reaction times. However, the observed response could not be accounted for by summing the responses for the observed products. Although there has been renewed interest in the mechanism of this system (4-6), major uncertainties exist, and a large fraction of the reacted HC remains unaccounted for.

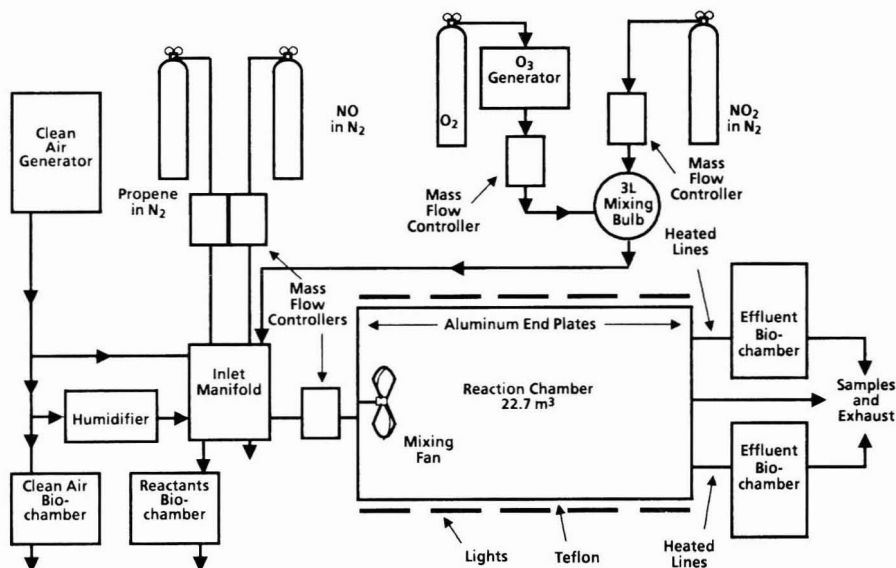


Figure 1. Schematic diagram of the reaction chamber apparatus.

The present study has been undertaken to investigate a system in which the mechanism has been more fully elucidated. The propylene (C_3H_6)/ NO_x system has been studied by several laboratories (7, 8). All of the major products and a number of the minor products have been quantified, and the time dependence of the major products has been established. There has recently been increased interest in reactions of the NO_3 radical with C_3H_6 (9), in part due to the toxicity of one of the reaction products, propylene glycol dinitrate (PGDN) (10, 11). Since nitrated products become increasingly significant as the reaction proceeds, it is possible that some of the mutagens present at long reaction times in irradiated HC/ NO_x systems may be organic nitrates. To focus on this group of products formed in the irradiated C_3H_6 / NO_x system, we also examined a C_3H_6 / N_2O_5 dark reaction mixture.

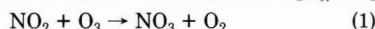
In this paper, we present the results of two irradiated C_3H_6 / NO_x exposures at two different extents of reaction and the results of a C_3H_6 / N_2O_5 exposure. The data are analyzed in terms of individual responses of the component products.

Experimental Section

Most of the experimental apparatus and analytical techniques have been described previously (3), and only an abbreviated description is presented here. The reaction chamber is a 22.7-m³ cylindrical vessel constructed of 0.13-mm Teflon that is sealed to aluminum end plates coated with fluorocarbon paint. The chamber is surrounded longitudinally with a combination of sunlamps and UV blacklights. The reactants, C_3H_6 , NO, and NO_2 (and O_3 for the C_3H_6 / N_2O_5 exposure), are metered through mass flow controllers and mixed with clean air and added humidity (except in the C_3H_6 / N_2O_5 exposure) in an inlet manifold. The manifold is connected directly to the reaction chamber with 13-mm Teflon tubing. The input flow is measured by using a 150-Lpm (liters per minute) mass flowmeter. This configuration is required to sustain a constant, well-mixed reactant flow.

For the C_3H_6 / N_2O_5 exposure, the N_2O_5 was produced by mixing O_3 and NO_2 (at ~1% concentration in N_2) in a 3-L Pyrex mixing bulb. The O_3 was produced at ~1%

with a Welsbach Model T-408 O_3 generator supplied with zero-grade O_2 . The O_3 reacts with NO_2 in the mixing bulb to produce NO_3 , which is in equilibrium with N_2O_5 , as shown in reactions 1 and 2. The resultant N_2O_5 / NO_2



mixture was then diluted with clean dry air in the inlet manifold at 140 L/min. When either the NO_2 or the O_3 was allowed to flow separately into the inlet manifold, the concentrations were ~1.8 and ~1.5 ppm, respectively. However, because of the possibility of NO_3 reacting with itself at the relatively high mixing bulb concentrations, and because it is unknown how the NO_x monitors respond to N_2O_5 , the actual inlet manifold N_2O_5 concentration was uncertain. The inlet manifold O_3 concentration was determined to be zero throughout the exposure, and the inlet C_3H_6 concentration was ~1.2 ppm.

The product effluent was sampled at the end plate opposite the input flow. Chemical analyses generally required 3–13 Lpm, whereas the biological assay consistently required 28 Lpm. The walls of the rectangular biological exposure chambers (which are 190 L volume) are coated with fluorocarbon paint. A schematic of the experimental apparatus is shown in Figure 1.

The sampling and analytical techniques for the measurement of NO, NO_x , O_3 , peroxyacetyl nitrate (PAN), the aldehydes, the relative humidity, and the physical parameters were conducted as previously described (3). Propylene was measured on a Hewlett-Packard Model 5840A gas chromatograph (GC) employing a 6.4 mm × 2 m stainless steel column packed with 80/100 Porapak QS operated isothermally at 130 °C. Injection was accomplished by using a Seizcor six-port gas sampling valve with a 5-mL sample loop. Propylene standards were prepared by diluting a 100-μL sample of pure C_3H_6 with 100 L of pure air in a Teflon bag. Organic nitrates were measured on a Varian 1200 GC employing a 6.4 mm × 2 m glass column packed with 10% SP-1000 on 80/100 Supelcoport operated isothermally at 155 °C. Detection was achieved on a Valco Model 140B electron capture detector. Samples were injected with a 5-mL glass and Teflon syringe.

Products were identified under the same conditions using a Hewlett-Packard Model 5985 GC/MS. Details of the product identification and the calibration procedure are in a separate publication (12).

Nitric acid (HNO_3) was collected on 47-mm nylon filters by using a Teflon filter holder. The filters were extracted in 10^{-5} M perchloric acid, and HNO_3 was measured as nitrate ion by ion chromatography (IC) using a $\text{CO}_3^{2-}/\text{HCO}_3^-$ eluent. Weak acids (e.g., HCOOH) that might be formed in this system were collected by bubbling the effluent through a 1 mM NaOH solution. Ion chromatography employing a 2.5 mM $\text{B}_4\text{O}_9^{2-}$ eluent was used for separation and detection of the weak acid anions. Calibrations were made with solutions prepared from the alkali salts.

The biological assay used in this work employs the bacteria *Salmonella typhimurium*, strain TA100. The plates were prepared by adding 0.1 mL of the *S. typhimurium* culture to 3 mL of an agar overlay at 45 °C (with or without 0.5 mL of S9 mix). This mixture was then poured onto ~40 mL of plate agar in a glass Petri plate. The *S. typhimurium* tester strain TA100 was provided by Dr. Bruce Ames (University of California, Berkeley, CA). Colony counting was done with an Artec 880 automatic colony counter using previously published guidelines (13). The test procedures used were those of Ames et al. (14), except for the following modifications: (1) glass Petri dishes were used, (2) 45 mL of base agar per plate was used, (3) minimal histidine at the same final total concentration was placed in the bottom agar rather than the top agar, and (4) 3 mL of overlay agar with $\sim 1 \times 10^8$ bacteria was used. The rat-liver homogenate (S9) fraction was prepared from male Charles River CD-1 rats (Wilmington, MO) induced with Aroclor 1254 (14). Surrogate plates representing the biological assay were also placed in the exposure chambers. One set of surrogates contained water buffered to the same level as the assay (i.e., pH 7.4); another set contained deionized water only. These were analyzed for formaldehyde (HCHO) by chromatographic acid and nitrate, nitrite, formate, and acetate by using IC. Mutagenic activities for pure compounds were performed by using the standard plate incorporation test (14). The synthesis and quantitation for compounds first observed experimentally in this system are presented elsewhere (12). In each case, the compounds were diluted in a suitable solvent (sterile water, dimethyl sulfoxide (Me_2SO), and methanol) at the nanomole to micromole level, and the response was measured at six concentrations. For some compounds that are unstable or exist in the vapor phase, a second technique, the single-component, gas-phase exposure, was performed. This technique was used to determine the mutagenic activity of PAN (15).

The procedures employed for performing the photo-oxidation experiments are similar to those previously described (3). To establish the desired extent of reaction for the dynamic experiments, a static $\text{C}_3\text{H}_6/\text{NO}_x$ experiment was performed. For this experiment the reactor was operated as a conventional smog chamber. The reactants were added through the mixing manifold to the desired initial concentrations at a relative humidity of approximately 50%. In the dynamic mode, the reactor provided a continuous stream of products with a constant distribution. The extent of reaction giving rise to the distribution was established from the average residence time, τ , of the gases in the reactor (τ = volume of reactor/flow rate). For the $\text{C}_3\text{H}_6/\text{NO}_x$ irradiations, the reaction chamber was operated at flows of 50 and 140 Lpm, yielding average residence times of 7.5 and 2.7 h, respectively. In

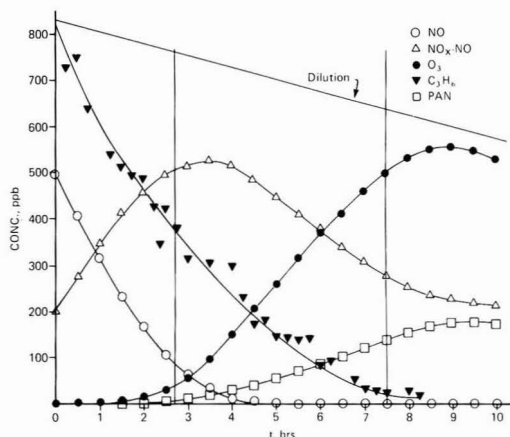


Figure 2. Time profiles for the major products in the $\text{C}_3\text{H}_6/\text{NO}_x$ irradiation (static mode). The concentrations intersecting the vertical lines at 2.7 and 7.5 h represent the nominal product distributions for the two residence times.

the $\text{C}_3\text{H}_6/\text{N}_2\text{O}_5$ exposure, the average residence time was 2.7 h.

For the $\text{C}_3\text{H}_6/\text{NO}_x$ irradiations, the effluent from the reactor flowed through two exposure chambers in parallel. One chamber contained plates with TA100 and the other with TA100 plus S9. Surrogate plates for chemical analyses were placed in both chambers. The flow through the exposure chambers was 14 Lpm, yielding an exposure chamber residence time of 13.5 min. The exposures were conducted at 25 °C for 20 h, and the total gas volume through each chamber was 17 m³. Two additional exposure chambers were employed. Clean air was passed through one chamber and the reactant mixture through the second. Each chamber contained TA100, with and without metabolic activation, and two sets of surrogate plates.

For the $\text{C}_3\text{H}_6/\text{N}_2\text{O}_5$ exposure, the two effluent exposure chambers contained 25 plates each of TA100 with and without S9 mix. To one of these exposure chambers we added 0.7 ppm of NO (continuously) to test for the presence of mutagenic peroxyxynitrates (which are removed due to the presence of NO). For the $\text{C}_3\text{H}_6/\text{N}_2\text{O}_5$ exposure, a reactants exposure chamber was not employed since N_2O_5 would react with the water evaporated from the plates to produce gas-phase HNO_3 , which is toxic to the bacteria.

Each of the exposures was conducted by adjusting the reactant concentrations to the desired levels in the inlet manifold and allowing the product distribution to reach a steady state in the chamber. Once it was determined that this was the case, the exposure chambers were loaded with the covered test plates. The exposure chambers were then resealed, and the product concentrations in the exposure chambers were brought back to their steady-state levels. At this point, the plates were uncovered, effectively starting the exposures.

Results

$\text{C}_3\text{H}_6/\text{NO}_x$ Irradiations. Figure 2 shows the time profiles of O_3 , NO, NO_x/NO , C_3H_6 , and PAN measured in the $\text{C}_3\text{H}_6/\text{NO}_x$ static run, which had the same initial conditions as employed in the dynamic experiments. The NO_2 photolysis rate constant under these conditions was $\sim 0.3 \text{ min}^{-1}$, and the dilution rate was 0.037 h^{-1} . The relative humidity was maintained at $\sim 50\%$. In Figure 2, the vertical lines at 2.7 and 7.5 h indicate the product distributions predicted for dynamic experiments with

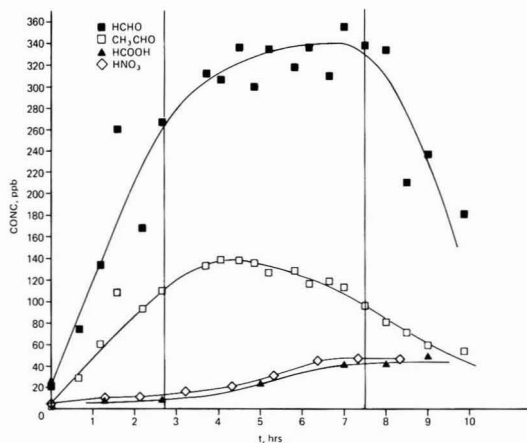


Figure 3. Time profiles for the aldehydes and nitric and formic acids in the C_3H_6/NO_x irradiation.

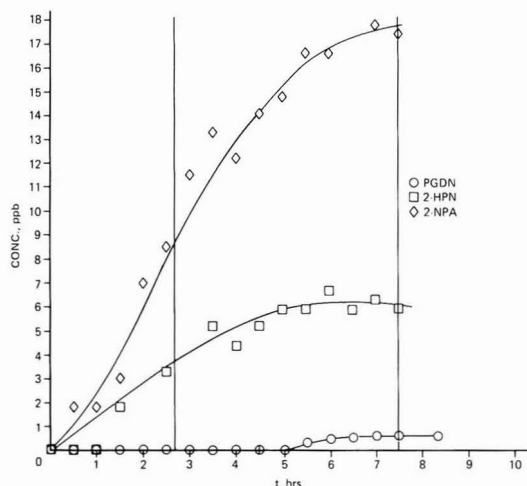


Figure 4. Time profiles for nitrates in the C_3H_6/NO_x irradiation.

residence times of 2.7 and 7.5 h, respectively, and performed under the same initial conditions as the static experiment. At 2.7 h, the reaction is still at a relatively early stage since there is approximately 20% (100 ppb) of the initial NO remaining. At 7.5 h, the reaction is near the O_3 and PAN maxima.

The time profiles of HCHO, acetaldehyde (CH_3CHO), NO_3^- , and formate are given in Figure 3. The aldehydic concentration difference between the two residence times is minimal. Nitrate extracted from nylon filters is generally identified with HNO_3 . In this experiment, the measured formate is associated with formic acid ($HCOOH$). For conditions under which the sampling was performed, the detection limit for $HCOOH$ is 15 ppb. Figure 4 shows the formation of the following nitrates produced during the photooxidation: PGDN, 2-hydroxypropyl nitrate (2-HPN), and 2-nitratopropyl alcohol (2-NPA). The reaction of OH with C_3H_6 in the presence of O_2 and NO forms 2-HPN and 2-NPA as stable products.

Dynamic experiments conducted at the two residence times had the same initial concentrations as the static experiment within experimental uncertainty. The inlet concentrations, total flow, and irradiation intensity remained constant throughout the dynamic experiments and

Table I. Average Reactant and Product Concentrations (ppb) for C_3H_6/NO_x Irradiation (Dynamic Mode)

compd	input concn	effluent concn ($\tau = 2.7$ h)	effluent concn ($\tau = 7.5$ h)
C_3H_6	826 \pm 33	548 \pm 24	100 \pm 13
NO	505 \pm 24	155 \pm 29	BDL ^b
NO_x -NO	200 \pm 39	521 \pm 38	347 \pm 21
O_3		18 \pm 7	451 \pm 29
HCHO		219 \pm 32	247 \pm 71
CH_3CHO		118 \pm 8	90 \pm 4
PAN		6 \pm 3	181 \pm 12
HNO_3		40 \pm 10	73 \pm 17
CH_3ONO_2		1.2 \pm 0.2	1.4 \pm 0.2
PGDN		BDL	0.8 \pm 0.2
2-HPN		1.8 \pm 0.4	3.0 \pm 1.0
2-NPA		5.6 \pm 1.1	10.4 \pm 2.6
CO	81	163	
RH ^a (%)		52	65
HCOOH		BDL	40

^a RH, relative humidity in units of percent. ^b BDL, below detection limit.

Table II. C_3H_6/NO_x Irradiations: Concentrations of Species Detected from Exposure Chamber Decrease (eq I) and/or Appearance in the Surrogate Plates (Concentration given as Micromoles per Plate)

compd	$\tau = 2.7$ h		$\tau = 7.5$ h	
	chamber decrease	surrogate plates	chamber decrease	surrogate plates
HCHO	1.62	1.15	2.28	1.65
PAN	0.048	—	0.89	1.48 ^b
HNO_3	— ^a	0.085	0.78	0.83
CH_3ONO_2	0.001	—	0.004	—
PGDN	0	—	0.0024	—
2-HPN	0.017	—	0.034	—
2-NPA	0.047	—	0.10	—
$HCOO^-$	—	0.21	—	1.29

^a Not measured. ^b From nitrite measurement.

yielded steady-state product distributions. The average values for the observed product concentrations in the reaction chamber for each of the two dynamic experiments are given in Table I. These concentrations can be compared with those of the static experiment by examining Figures 2-4 at the appropriate extent of reaction. A nominal correspondence between the two can be seen.

Chemical sampling of gas-phase products was also performed from the exposure chambers before and during the exposure of the biological assay. These values are used as one means of estimating the amount of material deposited into each plate. The net deposition of material into the plates during the exposure is tabulated in Table II under the heading "chamber decrease". These values are calculated from the relationship given in eq I where

$$X_i \left(\frac{\mu\text{mol}}{\text{plate}} \right) = \left(\frac{P_i(R) - P_i(E)}{RT} \right) \left(\frac{V_E}{N_P} \right) \quad (I)$$

X_i is the plate concentration of species i , $P_i(R)$ and $P_i(E)$ are the partial pressures (μatm) of species i in the reaction and exposure chambers, respectively, V_E is the volume of effluent passing through the exposure chamber, and N_P is the total number of plates. The amounts of material presented in Table II represent upper limits since some of the material may be lost to the exposure chamber walls.

A second method for determining the amount of material deposited into the biological assay is from the analysis of the surrogate plates. The results for each measured compound are given in Table II. A comparison of the

Table III. Measured Mutagenic Activity for Exposure of TA100 to the Experimental Gas Streams in Revertants per Plate for the C₃H₆/NO_x Irradiations

exposure condition	clean air irradiation		$\tau = 2.7$ h		$\tau = 7.5$ h	
	w/o S9	w/S9	w/o S9	w/S9	w/o S9	w/S9
spontaneous	164 ± 12	178 ± 11	142 ± 10	131 ± 8	184 ± 29	131 ± 18
15.4 nmol of sodium azide	909 ± 73		919		1388	
2.6 nmol of 2-aminoanthracene		1525		421		536
clean air chamber ^a	361 ± 60	379 ± 70	194 ± 15	225 ± 32	278 ± 92	290 ± 58
reactant chamber ^a	356 ± 48	363 ± 67	261 ± 41	293 ± 54	294 ± 58	268 ± 44
effluent chamber ^b	374 ± 59	404 ± 69	356 ± 69	373 ± 48	903 ± 69	968 ± 101

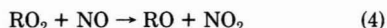
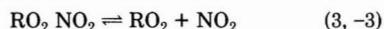
^aNumbers are averages for ~25 plates. ^bNumbers are averages for ~50 plates.

results for the two methods can be made for HCHO, PAN, and HNO₃. In each case, the agreement is within 50%. This enhances the confidence for a species that can be measured by using only one of the techniques.

The mutagenic activities observed for the C₃H₆/NO_x photooxidation mixture are presented in Table III. Three sets of experiments are presented, each with its own set of laboratory controls and background measurements. The first three rows in Table III represent laboratory measurements of the characteristics of the particular assay used in the experiment. The "spontaneous" plates measure the natural reversion rate observed under sterile conditions in the laboratory. These serve as a check to establish the viability of the bacteria. The strain sensitivity is determined by adding 1.0 and 0.5 µg, respectively, of known mutagens, sodium azide and 2-aminoanthracene, to TA100 and TA100+S9, respectively. A clean air control chamber was employed to measure the background reversion rate in the ambient environment under which the photochemical experiments take place. In addition, a reactants exposure chamber, which samples the reactant gases directly from the inlet manifold, was used to check for mutagenic activity of the reactants. The clean air irradiation (Table III) is a separate experiment that serves as a check to ensure that the observed revertant level is due to the photochemical effluent rather than a chamber artifact. The revertant levels at both residence times show increased values over the clean air control. However, the mutagenic activity for the long residence time is substantially greater than that for the short residence time. It is also observed that the addition of S9 metabolic activation does not statistically increase the mutagenic activity, relative to those plates without S9 mix, indicating that the mutagens present are direct acting.

C₃H₆/N₂O₅ Exposure. To determine the extent to which NO₃ reaction with C₃H₆ may lead to mutagenic products that could account for the large mutagenic activity observed in the irradiated C₃H₆/NO_x system (at $\tau = 7.5$ h), we conducted a C₃H₆/N₂O₅ exposure.

As mentioned previously, to one effluent stream we added NO at ~0.7 ppm. It has been reported (9) that the reaction of C₃H₆ with NO₃ leads to the production of large yields of nitroxypoxypropyl nitrate (NPPN). Since we have shown that PAN (a peroxy nitrate) is a mutagen with TA100 (15), it is possible that NPPN or other peroxy nitrates formed may be mutagenic as well. Since peroxy nitrates such as PAN are in equilibrium with their respective peroxy radical and NO₂ (16), they can be removed via NO addition as shown in reactions 3 and 4 where R



is an organic group. The resultant alkoxy radical would then be removed by reaction with O₂ or NO₂ or by unimolecular decomposition. The presence of mutagenic

Table IV. Average Reactant and Product Steady-State Concentrations for the C₃H₆/N₂O₅ Exposure

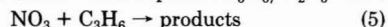
parameter measured ^a	inlet	effluent
inlet reactant flow, L/min	140 ± 0.1	
NO ₂	1.76 ± 0.20	1.94 ± 0.19
C ₃ H ₆	1.26 ± 0.04	1.00 ± 0.04
HCHO		0.017 ± 0.004
CH ₃ CHO		0.023 ± 0.007
α -nitratooacetone		0.032 ± 0.011
PGDN		0.002 ± 0.001
2-HPN		0.008 ± 0.002
2-NPA		0.002 ± 0.001
PAN		0.020

^aConcentrations in parts per million.

peroxy nitrates can therefore be checked by comparison of the results for the two exposure chambers, since these compounds will not be present in the exposure chamber with added NO.

The average inlet and effluent reactant concentrations, chamber parameters, and steady-state concentrations for the products measured in the C₃H₆/N₂O₅ exposure are presented in Table IV. This experiment was conducted without added humidity.

Since the reactants C₃H₆ and N₂O₅ are diluted and mixed in the inlet manifold, they can react there as shown in reactions -2 and 5. In a separate C₃H₆/N₂O₅ static



experiment under similar conditions (12), we observed a value of $\Delta\text{N}_2\text{O}_5/\Delta\text{C}_3\text{H}_6$ of roughly 2/1. Since $\Delta\text{C}_3\text{H}_6$ in this experiment is 0.26 ppm, the assumption can be made that the initial N₂O₅ concentration was ~0.5 ppm. This then leads to an initial NO₂ concentration of ~0.8 ppm, given the total NO_x value of 1.8 ppm listed in Table IV. By use of the values for k_2 and k_{-2} of 4.6×10^{-12} cm³ molecule⁻¹ s⁻¹ and 3.7×10^{-11} s⁻¹, respectively (17), an equilibrium NO₃ concentration of 2.2 ppb is obtained. Using the value $k_5 = 4.2 \times 10^{-15}$ cm³ molecule⁻¹ s⁻¹ (18), and a residence time in the inlet manifold of 1 min, leads to $\leq 1\%$ C₃H₆ reacted in this time. Therefore, the inlet manifold concentrations can be accurately taken as those before the reaction begins.

The mechanisms for formation of the products listed in Table I have been presented elsewhere (9, 12). A mass balance of the product concentrations from Table IV indicates that we cannot account for a large part of the reacted C₃H₆. It may be that much of it is present as NPPN, which we could not detect. The PAN concentration was measured in a separate experiment under equivalent conditions and was found to be present at 0.020 ppm.

The results of the bioassays performed are presented in Table V, along with the laboratory controls. The final plate concentrations for each product of the C₃H₆/N₂O₅ reaction are presented in Table VI, as calculated from eq I.

Table V. Observed Mutagenic Activities in Revertants per Plate for the C₃H₆/N₂O₅ Exposure

exposure condition	TA100	TA100+S9
spontaneous	133 ± 13	122 ± 21
15.4 nmol of sodium azide	668	
2.6 nmol of 2-aminoanthracene		590
clean air chamber ^a	180 ± 31	169 ± 33
effluent chamber ^a	375 ± 122	351 ± 102
effluent (+NO) chamber ^a	323 ± 81	369 ± 112

^aNumbers are averages for ~25 plates.

Table VI. Concentrations of Products (C₃H₆/N₂O₅ Exposure) Detected in Micromoles per Plate As Calculated from Equation I

product	μmol/plate (max, eq I)	product	μmol/plate (max, eq I)
HCHO	0.2	PGDN	0.02
HNO ₃	0.6	CH ₃ ONO ₂	
PAN	0.2	HCOOH	
2-HPN	0.1	CH ₃ C(O)CH ₂ ONO ₂	0.4
2-NPA	0.02		

In trying to account for an observed mutagenic response in a complex mixture, summing the mutagenic activities of the individual species is the most straightforward approach, assuming the individual responses are additive. These responses are clearly a function of concentration (19). (Note, although CH₃CHO is a major product in this photooxidation, it is not listed in Tables II and VI, since it appears that *S. typhimurium* bacteria produce CH₃CHO in the course of their metabolism. This was evidenced by the fact that CH₃CHO was observed in the clean air exposure chamber when the plates were opened.)

The final step in our analysis is the compilation of mutagenic activities for major and minor products formed in the oxidation system. These are used to determine a calculated total response, R_T , from a summation of the response of the individual components according to eq II

$$R_T = \sum_i \beta_i X_i \quad (\text{II})$$

where β_i is the mutagenic activity for species i , and X_i is its concentration per plate. The mutagenic activities are determined from plate incorporation experiments and the single-component, gas-phase exposures. The majority of compounds has been tested by using the plate incorporation procedure. However, O₃, HCHO, H₂O₂, and PAN were measured by gas-phase exposure. Table VII gives mutagenic activities in terms of revertants per micromole per plate. The experimental data found in Tables II, VI, and VII are used in conjunction with eq II to calculate R_T . The values are then compared with the data in Tables III and V.

Discussion

C₃H₆/NO_x Irradiations. For the purposes of this discussion, we will consider the results for TA100 without S9 only, since the response observed is essentially the same in the two cases and since the mutagenic activities for the mutagenic products we have detected are not dependent on the presence of S9 mix.

As can be seen from the data in Table III, the clean air and reactant exposure chambers exhibit revertant levels somewhat higher than those of the laboratory spontaneous plates. We attribute this to a brief exposure of the plates to ultraviolet light during handling in preparation for the exposure. Therefore, the data for the effluent exposure chambers should be compared with that of the clean air

Table VII. Mutagenic Activities for Products of the C₃H₆/NO_x Irradiation

compd	mutagenic activity, revertants/ μmol per plate	
	TA100	TA100 + S9
O ₃	BDL ^{a,b}	BDL ^a
HCHO	12 ^a	12 ^a
CH ₃ CHO	BDL	BDL
PAN	41 ^a	50 ^a
HNO ₃	BDL	BDL
CO	BDL	BDL
2-HPN	3	3
2-NPA	3	3
PGDN	BDL	BDL
CH ₃ ONO ₂	BDL	BDL
CH ₃ C(O)CH ₂ ONO ₂	55	55
HCOOH	BDL	BDL
H ₂ O ₂	10 ^a	10 ^a
(CH ₃) ₃ COOH	100	284
CH ₃ C(O)OOH	BDL	BDL

^aSingle component, gas-phase exposure. BDL, below detection limit, 2 revertants/μmol.

or reactant chamber. The number of clean air chamber revertants per plate can be subtracted from the effluent chamber revertants per plate to obtain the number of excess revertants. The data presented in Table III show that there is essentially no increase in the bioactivity (revertant level for TA100 without S9) of the reactant biochambers above that found in the clean air biochamber; there is a small response (~160 excess revertants/plate) found at a residence time of 2.7 h, and there is a large excess (~625 revertants/plate) in the effluent biochambers at a residence time of 7.5 h.

It is reasonable to attempt to account for the excess revertants found in the effluent biochambers by summing the contributions of the individual reaction products (even though we have no evidence of additivity in such a complex mixture). As shown in eq II, the total response can be taken as the product of the mutagenic activity times the amount of each component deposited in a plate. Therefore, a very mutagenic minor product can be just as or more important than weakly mutagenic major products. Studies have shown that mutagenic activities as large as 100 000 revertants/μmol for TA100 exist (19). Because of this, even though a large number of reaction products have been determined for an irradiated C₃H₆/NO_x mixture, it may be that a chemical whose yield is small is responsible for the increased mutagenic activity. However, as a first step in trying to account for the response, the contributions of the major products should be considered.

The major products formed during the photooxidation are O₃, HCHO, CH₃CHO, CO, CO₂, HNO₃, NO₂, and PAN. The steady-state concentrations at 2.7 and 7.5 h are shown in Table I. In the table, NO₂-NO is approximately equal to the sum of NO₂ and PAN. Carbon dioxide concentrations were not determined since a background level of 320 ppm was present in the diluent air. The amounts of HCHO, PAN, and HNO₃ in the surrogate plates are shown in Table II.

Table VII shows that, of the major products listed, only HCHO and PAN have mutagenic activities above the detection limit. A numerical value for the mutagenic activity of NO₂ has not been given, but the fact that the revertant level in the reactant chamber that was exposed to 200 ppb of NO₂ is similar to that found in clean air demonstrates that NO₂ does not contribute to the revertant levels found at 2.7 and 7.5 h. Calculations using eq

II shows that HCHO accounts for 19 revertants/plate at 2.7 h and 27 revertants/plate at 7.5 h. Similarly, PAN accounts for 2 revertants/plate at 2.7 h and 36 revertants/plate at the longer residence time. Therefore, the major products account for only a small percentage of the measured mutagenicity; at 2.7 h HCHO and PAN contribute 21 revertants/plate total, or 13% of the total revertant level, and at 7.5 h the total contribution of HCHO and PAN is 63 revertants/plate or 10% of the total.

The minor products identified in the system were CH_3ONO_2 , PGDN, 2-HPN, 2-NPA, and HCOOH . On the basis of the amounts of material deposited into the plates and the mutagenic activities, the total contributions of the minor products for both 2.7 and 7.5 h are found to be less than 1 revertant/plate, assuming additivity.

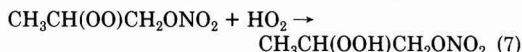
It therefore appears that the bioactivity found in the effluent exposure chambers cannot be accounted for by species identified and quantified during the experiment. However, it is well-known (9) that other minor products are formed during the irradiation. These include H_2O_2 , CH_3OOH , and $\text{CH}_3\text{C(O)OOH}$. Organic peroxides have been found to be strong mutagens in the strain TA102 (20). Plate incorporation tests using TA100 were conducted for H_2O_2 , $\text{CH}_3\text{C(O)OOH}$, and *tert*-butyl hydroperoxide, which served as a model for CH_3OOH . Their mutagenic activities are included in Table VII. A reasonable upper limit for the concentrations of these species at 7.5 h is 50 ppb. Assuming such a contribution and that all the material goes into the plates, 0.60 μmol /plate of each would be deposited during these experiments. The mutagenic contributions for the chemicals would be the following: H_2O_2 , 6 revertants/plate; $(\text{CH}_3)_3\text{COOH}$ (CH_3OOH), 60 revertants/plate. The mutagenic activity of $\text{CH}_3\text{C(O)OOH}$ was below the detectable limit. The calculation is presented only for 7.5 h because at 2.7 h there still remains some NO that prevents the RO_2 - HO_2 reactions necessary to generate the hydroperoxides. If the 66 additional revertants contributed by the peroxides are added to the 7.5 h contributions due to PAN and HCHO, 20% of the measured excess revertants can be accounted for.

$\text{C}_3\text{H}_6/\text{N}_2\text{O}_5$ Exposure. Since it has been shown that NO_3 reaction with C_3H_6 produces products that are toxic (9-11), and because a large response was observed at long residence time where NO_3 would be expected to be present, the $\text{C}_3\text{H}_6/\text{N}_2\text{O}_5$ exposure seemed a reasonable means for attempting to determine to what extent the $\text{C}_3\text{H}_6/\text{NO}_3$ reactions may be the cause of this large response.

As shown in Table V, the two sets of effluent chamber plates exhibit revertant levels of approximately 180 revertants/plate above the clean air values. There seems to be no significant difference between those with and those without metabolic activation, indicating that the mutagens present are direct acting. In addition, there is no significant difference in the results for the two effluent exposure chambers. Although this may indicate that the peroxy nitrates present are not mutagenic, their transfer efficiencies to the exposure chambers may be low, or they may be deposited on the reaction chamber walls during the 2.7-h average residence time. Bandow et al. (9) have observed that NPPN has a significant wall loss rate in their reaction chamber.

Using the data presented in Tables VI and VII, we can estimate to what extent each of the products of the $\text{C}_3\text{H}_6/\text{N}_2\text{O}_5$ reaction that we measured could account for the total observed response. Although nitric acid (HNO_3) is listed in Table VI, since it was undoubtedly present, we were unable to measure its concentration accurately due to an interference caused by the presence of N_2O_5 . As

indicated in Table VII, several of the organic nitrates are mutagenic but would be classified as weak mutagens (21). The compound that contributes the most, although very little relative to the total, is α -nitratooacetone. HCHO, PAN, and α -nitratooacetone could contribute 2, 8, and 22 revertants/plate, respectively. Each of the two hydroxy nitrates (2-HPN and 2-NPA) could account for no more than 1 revertant/plate. It should be noted that organic hydroperoxides such as 2-HPPN may be present and would be produced as shown in reactions 6 and 7. These



organic hydroperoxides may be, like *tert*-butyl hydroperoxide, significantly mutagenic.

It is clear, however, that for the $\text{C}_3\text{H}_6/\text{N}_2\text{O}_5$ exposure we have accounted for only a small fraction of the total observed response ($\sim 19\%$) with known reaction products. Although there are several possible reasons for this, the most likely is that we have not detected all the mutagenic products in this system. As stated previously, although a presumably major product for which we have no biotesting data is NPPN, if this compound were very mutagenic there would likely have been significant differences in the results for the two effluent exposure chambers. It would appear then that there may be other unidentified stable products that are mutagenic such as an organic hydroperoxide. Since we have found several organic nitrates that are mutagens, and we know that organic hydroperoxides (e.g., $(\text{CH}_3)_3\text{COOH}$) are mutagens, a species such as 2-HPPN is likely.

In this experiment, we have shown that chemical mutagens are produced from the reaction of NO_3 with C_3H_6 . However, a computer modeling study that we have conducted of the $\text{C}_3\text{H}_6/\text{NO}_x$ irradiated system indicates that NO_3 reaction with C_3H_6 would have occurred only to the extent of ~ 0.010 ppm at 7.5 h. Since $\Delta\text{C}_3\text{H}_6$ due to NO_3 reaction in the $\text{C}_3\text{H}_6/\text{N}_2\text{O}_5$ exposure was 0.26 ppm, we can estimate that NO_3 reactions would have contributed on the order of only 10 revertants/plate in the irradiated $\text{C}_3\text{H}_6/\text{NO}_x$ system at 7.5 h.

It is therefore clear from the above analysis that the observed mutagenic response in the irradiated $\text{C}_3\text{H}_6/\text{NO}_x$ system cannot be accounted for, although there are a number of possible explanations. It is conceivable that there exist small yields of a very potent mutagen. If the remaining ~ 500 excess revertants found at 7.5 h were due to the presence of a single unknown mutagen present at 10 ppb, it would have a mutagenic activity of ~ 4000 revertants/ μmol . This would certainly be classified as a strong mutagen (19).

It is also possible that the mutagen responsible may be produced from a reaction that occurs in the test medium. However, to test this possibility we conducted a 20-h exposure of an irradiated $\text{C}_2\text{H}_4/\text{NO}_x$ mixture under similar conditions. This system yields, as products, HCHO, O_3 , NO_2 , HNO_3 , H_2O_2 , and HCOOH , which represent (as seen in Table I) a subset of the $\text{C}_3\text{H}_6/\text{NO}_x$ photooxidation products. In this experiment at long residence time, no detectable mutagenic response was observed over the clean air control. This, then, to a limited extent, argues against the possibility of reactions in the medium playing a significant role. In addition, further studies are required to compare the results obtained from the gas-phase exposures and the standard plate incorporation tests. Unless special precautions are taken, the possibility of losses of material when the plate incorporation test is performed for volatile

compounds exists. It is also possible that there are other systematic differences between results obtained with these two tests. Finally, the possibility that mutation processes exist that require the presence of two (or more) chemicals simultaneously has not been eliminated. (Experiments are currently being planned for testing various binary and tertiary mixtures of known mutagens.) However, such investigations should take place in conjunction with reasonable attempts for an explanation by single chemical components.

Conclusion

In this work, we have demonstrated that the photooxidation products of C_3H_6 are mutagenic, as determined with the Ames test. This is a fairly significant result given the fact that C_3H_6 is a simple hydrocarbon that is an important reactive constituent for urban air. Although the total observed response could not be accounted for, HCHO, PAN, and several organic nitrates were found to contribute significantly. It is possible that the organic nitrates that are products of NO_3 /alkene reactions may be an important source of the chemical mutagens present at night in urban air. Much more work is necessary to better determine the photooxidation products of sample atmospheric hydrocarbons that represent a human health hazard.

Acknowledgments

We thank G. R. Namie and J. H. Pittman of Northrop Services, Inc.—Environmental Sciences for their valuable assistance in conducting these experiments. We express our appreciation to E. Perry of Environmental Health Research and Testing, Inc., for conducting the mutagen testing.

Registry No. PAN, 2278-22-0; PGDN, 6423-43-4; 2-HPN, 20266-65-3; 2-NPA, 20266-74-4; C_3H_6 , 115-07-1; NO_x , 11104-93-1; N_2O_5 , 10102-03-1; NO, 10102-43-9; O_3 , 10028-15-6; HNO_3 , 7697-37-2; CO, 630-08-0; CH_3ONO_2 , 598-58-3; H_2O_2 , 7722-84-1; $HCOOH$, 64-18-6; $CH_3C(O)CH_2ONO_2$, 6745-71-7; $CH_3C(O)OOH$, 79-21-0; $(CH_3)_3COOH$, 75-91-2; CH_3CHO , 75-07-0; HCHO, 50-00-0.

Literature Cited

- (1) Hoffman, G. R. *Environ. Sci. Technol.* **1982**, *16*, 560A-574A.
- (2) Schairer, L. A.; Van't Hof, J.; Hayes, C. G.; Burton, R. M.; de Serres, F. J. In "Applications of Short Term Bioassays in the Fractionation of Complex Environmental Mixtures"; Walters, M. D.; Nesnow, S.; Huisingh, J. L.; Sandhu, S. S.;

- Claxton, L., Eds.; Plenum Press: New York, 1979; pp 421-440.
- (3) Shepson, P. B.; Kleindienst, T. E.; Edney, E. O.; Namie, G. R.; Pittman, J. H.; Cupitt, L. T.; Claxton, L. D. *Environ. Sci. Technol.* **1985**, *19*, 249-255.
- (4) Besemer, A. C. *Atmos. Environ.* **1982**, *16*, 1599-1602.
- (5) Killus, J. P.; Whitten, G. Z. *Atmos. Environ.* **1982**, *16*, 1973-1988.
- (6) Shepson, P. B.; Edney, E. O.; Corse, E. W. *J. Phys. Chem.* **1984**, *88*, 4122-4126.
- (7) Carter, W. P. L.; Lloyd, A. C.; Sprung, J. L.; Pitts, J. N., Jr. *Int. J. Chem. Kinet.* **1979**, *11*, 45-101.
- (8) Sakamaki, F.; Okuda, M.; Akimoto, H.; Yamazaki, H. *Environ. Sci. Technol.* **1982**, *16*, 45-52.
- (9) Bandow, H.; Okuda, M.; Akimoto, H. *J. Phys. Chem.* **1980**, *84*, 3604-3608.
- (10) Clark, D. G.; Litchfield, M. H. *Toxicol. Appl. Pharmacol.* **1969**, *15*, 175-184.
- (11) Jones, R. A.; Strickland, J. A.; Siegel, J. *Toxicol. Appl. Pharmacol.* **1972**, *22*, 128-137.
- (12) Shepson, P. B.; Edney, E. O.; Kleindienst, T. E.; Pittman, J. H.; Namie, G. R.; Cupitt, L. T. *Environ. Sci. Technol.*, in press.
- (13) Claxton, L. D.; Toney, S.; Perry, E.; King, L. *Environ. Mutat.* **1984**, *6*, 331-342.
- (14) Ames, B. N.; McCann, J.; Yamasaki, E. *Mutat. Res.* **1975**, *31*, 347-364.
- (15) Kleindienst, T. E.; Shepson, P. B.; Edney, E. O.; Claxton, L. D. *Mutat. Res.*, in press.
- (16) Hendry, D. G.; Kenley, R. A. *J. Am. Chem. Soc.* **1977**, *99*, 3198-3199.
- (17) Hampson, R. F., Jr.; Garvin, D., Eds. *NBS Tech. Note (U.S.)* **1975**, No. 866.
- (18) Japar, S. M.; Niki, H. *J. Phys. Chem.* **1975**, *79*, 1629-1632.
- (19) Haworth, S.; Lawlor, T.; Mortelmans, K.; Speck, W.; Zeiger, E. *Environ. Mutagen. (Suppl.)* **1983**, *1*, 3-142.
- (20) Levin, D. E.; Hollstein, M.; Christman, M. F.; Schwers, E. A.; Ames, B. N. *Proc. Natl. Acad. Sci. U.S.A.* **1982**, *79*, 7445-7449.
- (21) McCann, J.; Choi, E.; Yamasaki, E.; Ames, B. N. *Proc. Natl. Acad. Sci. U.S.A.* **1975**, *72*, 5135-5139.

Received for review August 23, 1984. Revised manuscript received January 25, 1985. Accepted February 5, 1985. Although the research described in this article has been funded wholly or in part by the U.S. Environmental Protection Agency through Contract 68-02-4033 to Northrop Services, Inc.—Environmental Sciences, it has not been subjected to the Agency's required peer and policy review and therefore does not necessarily reflect the views of the Agency, and no official endorsement should be inferred.

Aqueous Solubility and Octan-1-ol to Water Partition Coefficients of Aliphatic Hydrocarbons

Michael Coates, Des W. Connell,* and Diane M. Barron

School of Australian Environmental Studies, Griffith University, Nathan, Qld. 4111 Australia

■ The aqueous solubility (S) and octanol-water partition coefficients (P) of homologous series of n -, 2-methyl-, and 3-methylalkanes, as well as 1-alkenes, have been determined by extrapolation of known results, direct measurement, and high-pressure liquid chromatography (HPLC). Long-term equilibration experiments, used to reduce aggregate formation, indicated that n -dodecane and n -tetradecane have S values in agreement with those obtained by extrapolation of the data on lower members. HPLC data from reverse-phase columns further validated the use of extrapolation. By use of published values for P and S for lower n -alkanes, the relationships between $\log P$, $\log S$, and N_c were obtained. Cochromatography of n -alkanes with members of the other series then allowed these relationships to be determined for the 2- and 3-methylalkanes and the 1-alkenes. The derived S values were in reasonable agreement with values from previous work and those obtained by extrapolation. The $\log P$ values have not been previously determined for these compounds.

Introduction

The hydrocarbons are important petroleum-derived contaminants in the world's oceans (1-3). Little work has been carried out on the hydrocarbons relating their physicochemical properties to their bioaccumulation by aquatic organisms. However, as a general rule, the bioaccumulation of persistent lipophilic compounds by aquatic organisms is positively correlated with their hydrophobicity, particularly as measured by the octan-1-ol to water partition coefficient, P (e.g., see ref 4-6). For a wide range of lipophilic compounds, P is inversely proportional to S , the aqueous solubility (7).

Thus, to develop an understanding of the bioaccumulation of the hydrocarbons, data on their S and P values are required. McAuliffe (8-10) has determined the aqueous solubilities of C_7 - C_{12} n -alkanes and C_5 , C_6 , and C_8 1-alkenes and found linear relationships between $\log S$ and N_c (carbon number) for each group. Later, Price (11) found a linear relationship between $\log S$ and N_c for C_6 - C_8 3-methylalkanes. By extrapolation of McAuliffe's data (8-10), the theoretical values for the S values of the n -alkanes above C_{12} can be obtained. However, S values obtained in this way and those of other workers (12, 13) determined experimentally are in substantial disagreement. McAuliffe (10) has suggested that errors occur due to the incomplete removal of clusters or aggregates of hydrocarbon during the solubility experiments. In addition, solubilities of the longer chain length compounds are very low, making the concentrations difficult to measure. Recently, Hutchinson et al. (14) have reported $\log P$ values for C_6 , C_8 , C_{10} , C_{12} , and C_{14} n -alkanes which exhibit a linear relationship between $\log P$ and N_c .

In recent years high-pressure liquid chromatography (HPLC) using reverse-phase columns has been shown to be a valuable method for estimation of P for lipophilic compounds from their retention times. Our objectives in this present work were to determine the S and P values for various homologous series of aliphatic hydrocarbons, particularly those members with chain lengths greater than

C_{10} , utilizing the HPLC technique and other methods as appropriate. It was expected the HPLC technique would eliminate many of the difficulties due to the presence of aggregates or clusters that occur with more direct measurement techniques. Further, it was expected that the HPLC method would allow the determination of P values for the higher aliphatic hydrocarbons whose insolubility in water ($\log P > 6$) prevents use of the classic shake-flask method. By using homologous series, we expected to be able to make use of any systematic relationships between physical properties and carbon number to confirm or estimate values.

Experimental Section

The hydrocarbons were obtained from Analabs Co., North Haven, CT. Hexane solvent was twice distilled in an all-glass fractional distillation apparatus with an efficiency of about 10 theoretical plates using a reflux ratio of about 10 to 1. Water was deionized by mixed bed resins and glass distilled. Analytical-grade absolute ethanol was used for HPLC after filtration through a 0.45- μ m Millipore filter for organic solvents.

Aqueous Solubility Experiments. Short-term experiments were performed by shaking 150 μ L of n -alkane with 1 L of water for 16 h. The aqueous layer (200 mL) was then filtered through 0.45- μ m Millipore filters with gentle suction (12, 13, 15) and extracted with hexane (3 \times 20 mL). An internal standard consisting of 2 μ g of the n -alkane one carbon longer than the n -alkane under investigation was added to the first extractant. The extract was then concentrated to <50 μ L on a steam bath and 5 μ L of this gas chromatographed.

In long-term experiments, (1) 300 μ L of n -alkane was shaken with 2 L of water, and (2) the pure hydrocarbon was layered carefully with no mixing, onto the water surface. The mixtures were allowed to stand and 200-mL aqueous samples withdrawn periodically over 3 months. The samples were then extracted and analyzed as in the short-term experiments.

All experiments were performed at an ambient atmospheric temperature controlled to 23 ± 2 $^{\circ}$ C.

HPLC Experiments. HPLC was performed on a Varian Model 5000 HPLC with a Varian Micropak CH-10 octadecyl reverse-phase column and a Waters Model 510 HPLC with a Brownlee Labs RP-8 Spheri-10 octyl reverse-phase column. Samples (25 μ L) containing about 2 mg of hydrocarbon/mL were injected. Eluting solvent was 80, 90, 95, or 100% ethanol in water with a flow rate of 1.0 mL/min. The hydrocarbons were detected by collecting 0.5-mL fractions which were analyzed directly by gas chromatography (5- μ L injection).

Performance of the hydrocarbons was characterized by using the capacity factor, k' (16).

$$k' = (t_r - t_0)/t_0$$

t_r = elution time of a compound of interest and t_0 = elution time of an unretained compound (methanol).

Gas Chromatographic Analysis. The gas chromatograph was a Shimadzu Model GC-6A fitted with a flame ionization detector, utilizing 2 m \times 5 mm o.d. packed glass

Table I. Aqueous Solubilities (*S*), log *S*, and log *P* Values for the *n*-Alkanes

carbon no.	aqueous solubility, $\mu\text{g/mL}$		log <i>S</i>	log <i>P</i> (14) ^c
	McAuliffe ^a (8-10)	other workers ^b		
4	61.4		1.79	
5	38.5		1.59	(2.37)
6	9.5		0.98	(2.90)
7	2.93		0.47	(3.44)
8	0.66		-0.18	4.00
9	0.22		-0.66	4.51
10	0.052	0.020 (12)	-1.28	5.01
11	0.0044 (0.014)		-2.36 (-1.84)	(5.58)
12	(3.87×10^{-3})	8.41×10^{-3} (12); 3.7×10^{-3} (13); ($4.1-19.7$) $\times 10^{-3}$ ^d ; 3.5×10^{-3} ^e	(-2.41)	6.10
13	(1.04×10^{-3})	($4.7-21.7$) $\times 10^{-3}$ ^d	(-2.98)	(6.65)
14	(2.82×10^{-4})	6.93×10^{-3} (12); 2.2×10^{-3} (13); 3.3×10^{-4} ^e	(-3.55)	7.20
15	(7.6×10^{-5})		(-4.12)	(7.72)
16	(2.1×10^{-5})	6.28×10^{-3} (12); 0.9×10^{-3} (13)	(-4.69)	(8.25)
17	(5.5×10^{-6})		(-5.26)	(8.79)
18	(1.4×10^{-6})	2.1×10^{-3} (13)	(-5.83)	(9.32)
19	(4.0×10^{-7})		(-6.40)	(9.86)
20	(1.1×10^{-7})	1.9×10^{-3} (13)	(-6.96)	(10.39)
21	(2.9×10^{-8})		(-7.53)	(10.93)
22	(7.9×10^{-9})		(-8.10)	(11.46)
23	(2.1×10^{-9})		(-8.68)	(12.00)
24	(5.8×10^{-10})		(-9.24)	(12.53)
25	(1.6×10^{-10})		(-9.80)	(13.07)

^a Values in parentheses are extrapolated from *n*-C₅ to *n*-C₁₀ values of McAuliffe (8-10). ^b Franks (12); Sutton and Calder (13); unnumbered, this study. ^c Values in parentheses are extrapolated and interpolated from *n*-C_{8,10,12,14} values of Hutchinson et al. (14). ^d Short-term experiments; this work. ^e Long-term experiments; this work.

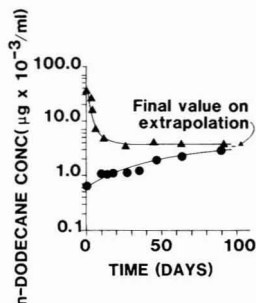


Figure 1. Plots of the change in *n*-dodecane concentration with time in long-term experiments. (▲) Shaken flask; (●) unshaken flask.

columns (2% SP-2100 on Gas-Chrom Q 80/100 mesh) with linear programming from 80 to 280 °C at 6 °C/min and nitrogen as carrier gas. For quantitation, a Hewlett-Packard reporting integrator, 3390A, was employed (17).

Results

In the short-term experiments, the procedures used by Peake and Hodgson (15) and Sutton and Calder (13) to determine *S* values were repeated with *n*-dodecane and *n*-tridecane. Results were highly variable and consistently greater than expected from extrapolation of McAuliffe's measurements (8-10) (Table I).

Figures 1 and 2 show the changes in concentration with time in the long-term equilibration experiments with *n*-dodecane and *n*-tetradecane. With dodecane, the final

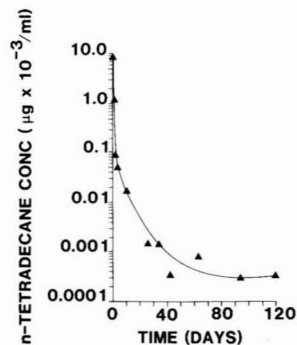


Figure 2. Plot the change in *n*-tetradecane over time in a long-term experiment using a shaken flask.

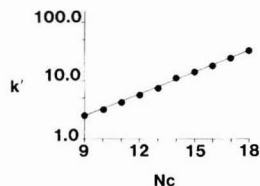


Figure 3. Typical plot of log *k'* vs. *N_c* for the HPLC of the *n*-alkanes.

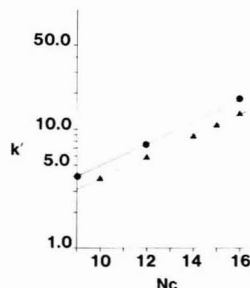


Figure 4. Plot of log *k'* vs. *N_c* for the HPLC of a mixture of *n*-alkanes and 1-alkenes using 80% ethanol in water. (●) *n*-Alkanes; (▲) 1-alkenes.

value, after 90 days, for the shaken flask was 3.8×10^{-3} $\mu\text{g/mL}$ while that for the unshaken flask was 2.8×10^{-3} $\mu\text{g/mL}$, giving a final *S* value on extrapolation of both trend lines of 3.5×10^{-3} $\mu\text{g/mL}$. With *n*-tetradecane, only the shaken-flask experiment was carried out, yielding a final *S* value of 3.3×10^{-4} $\mu\text{g/mL}$.

It was found that differing proportions of ethanol were needed in the mobile phase to obtain the optimum resolution of the various homologous series. Figure 3 shows a plot of log *k'* vs. *N_c* (carbon number) for a typical chromatogram of C₉-C₁₈ *n*-alkanes, while Figure 4 is a similar plot derived from a chromatogram of a mixture of *n*-alkanes and 1-alkenes. With all homologous series, the relationship between log *k'* and *N_c* was found to be linear, with the regression equations and correlation coefficients (*r*) shown in Table II.

The *n*-alkanes are the only series under investigation for which *P* and *S* values are known for some members. *P* and *S* values for the other members of this series were obtained by extrapolation (Table I). The *k'* values for members of other homologous series were then found relative to selected *n*-alkanes using consistent mobile-phase compositions (e.g., see Figure 4). Table II gives the relationships of log *k'* to *N_c* found when *n*-alkanes were cochromatographed with 2- and 3-methylalkanes and with 1-alkenes.

Table II. Regression Analysis of the HPLC Data on Homologous Series of Hydrocarbons

homologous series	carbon no. used	packing	mobile phase (% ethanol)	regression equation ^a	correlation coefficient (r)
<i>n</i> -alkanes	9-18	Varian Micropak (4-10)	90	$\log k' = -0.734 + 0.124N_c$	0.999
<i>n</i> -alkanes	15-25	Varian Micropak (4-10)	100	$\log k' = -0.238 + 0.049N_c$	0.996
2-methylalkanes	13, 15, 17, 19, 21	Varian Micropak (4-10)	95	$\log k' = -0.958 + 0.100N_c$	0.998
3-methylalkanes	12, 14, 16, 18, 20, 22, 24	Varian Micropak (4-10)	95	$\log k' = -0.733 + 0.087N_c$	0.997
1-alkenes	10, 12-16	Varian Micropak (4-10)	80	$\log k' = -0.759 + 0.128N_c$	0.999
mixture 1					
2-methylalkanes	13, 15, 17, 19, 21	Brownlee RP-8		$\log k' = -0.819 + 0.056N_c$	0.999
3-methylalkanes	18, 22	Brownlee RP-8	90	$\log k' = -0.801 + 0.055N_c$	
<i>n</i> -alkanes	12, 16, 20	Brownlee RP-8		$\log k' = -0.805 + 0.056N_c$	0.999
mixture 2					
1-alkenes	10, 12-16	Brownlee RP-8	80	$\log k' = -0.293 + 0.088N_c$	0.999
<i>n</i> -alkanes	9, 12, 16	Brownlee RP-8		$\log k' = -0.186 + 0.088N_c$	0.997

^a N_c = carbon number.

Discussion

Solubility and Aggregate Formation. Table I gives the aqueous solubility of the *n*-alkanes from butane to undecane as determined experimentally by McAuliffe (10, 11). For the C_5 – C_{10} compounds, a plot of $\log S$ vs. N_c is remarkably linear with a correlation coefficient (r) of -0.9995 and a regression line equation of

$$\log S = 4.416 - 0.569N_c \quad (1)$$

Assuming a linear relationship above decane, this equation was used to calculate values of $\log S$ and then S up to $N_c = 25$ (see Table I).

Other workers have reported the solubility of the higher alkanes (above C_{12}) as considerably greater than these extrapolated values, often by orders of magnitude (Table II). In fact the S value derived by Sutton and Calder (13) for *n*-tetradecane, which is an order of magnitude greater than the extrapolated value, has been widely accepted as an accurate measure (14, 18). McAuliffe (10) attributes this accommodation of higher than the expected concentrations of hydrocarbon in water to intermolecular associations leading to the formation of clusters or aggregates of hydrocarbon molecules often described as micelles. Peake and Hodgson (15) as well as Sutton and Calder (13) recognized this problem and attempted to remove hydrocarbon aggregates by filtration through Millipore filters. A reduction in the hydrocarbon concentration did occur with filtering, confirming the presence of aggregates, but the final concentrations still exceeded those obtained by extrapolation (see Table I).

During this present investigation repeated attempts were made to remove aggregates of dodecane and tridecane by filtration through 0.45- μ m Millipore filters. Final concentrations were variable and always exceeded the value obtained by extrapolation (Table II). As a general rule, the more vigorously the initial hydrocarbon water mixture was agitated, the higher the final measured concentration. These results suggest the continued presence of aggregates in the final product.

The problem of hydrocarbon aggregates in water was overcome by the long-term equilibration experiments. This method was also used by Price (11) to determine solubilities of various hydrocarbons up to C_9 . In the shaken flasks, the final values of S for *n*-dodecane and *n*-tetradecane (3.8×10^{-3} and 3.3×10^{-4} μ g/mL, respectively) show reasonable agreement with the extrapolated values of 3.9×10^{-3} and 2.8×10^{-4} μ g/mL, respectively. Presumably, the aggregates coalesced with the pool of hydrocarbon in the flask. In the unshaken flasks, containing dodecane, the concentration began low but also tended toward the theoretical value (Figure 1). Apparently, without agitation, aggregates were not formed, and with

long equilibrium times a true solution resulted through diffusion.

Depending on the conditions of agitation, aggregates can be formed in water in different concentrations and sizes, and the concentration of aggregates changes with time after formation. Thus, the concentration of hydrocarbon present in water, when some of the hydrocarbon is in the form of aggregates, can be expected to be somewhat arbitrary. Our confirmation of the correct solubilities of *n*-dodecane and *n*-tetradecane as the extrapolated values suggests that the other alkanes also have solubilities in agreement with the extrapolated values (Table I).

Extrapolation from Known Data for the Estimation of S and P . Another line of evidence in support of the extrapolated values as the correct solubilities stems from our HPLC results and from the relationship between P and S . The partitioning of these hydrocarbons between the polar mobile phase and the nonpolar, reverse phase during HPLC is an analogous process to the partitioning between octan-1-ol and water. Consistent with this, the relationship between $\log k'$ and $\log P$ has been shown to be linear for a wide variety of lipophilic compounds (16, 19, 20). Our HPLC investigations have shown that, for each of the homologous series investigated, there is a linear relationship between $\log k'$ and N_c (Figures 3 and 4 and Table II) up to the highest N_c examined. This suggests a similar relationship between $\log P$ and N_c . Since these hydrocarbons are completely miscible in octanol, P is therefore an inverse function of S (7, 16). Thus, a constant linear relationship between $\log S$ and N_c is implied over the range of N_c investigated in this work.

These conclusions are consistent with Hutchinson et al. (14), who have reported $\log P$ values for some *n*-alkanes (up to C_{12}) (Table I). These values show a linear relationship with N_c , and the regression equation is

$$\log P = -0.302 + 0.535N_c \quad r = 0.999 \quad (2)$$

When eq 1 and 2 are combined, the relationship $\log S$ and $\log P$ for the *n*-alkanes is obtained:

$$\log P = 3.850 - 0.940 \log S \quad (3)$$

Hansch and co-workers (21, 22) have demonstrated the additive-constitutive nature of partition coefficients which supports the conclusion that the relationship between $\log S$ and N_c is linear for the higher alkanes. Hansch et al. (22) introduced the substituent constant, π , defined as

$$\pi = \log P_X - \log P_H$$

where P_X is the partition coefficient of the derivative and P_H that of the parent molecule. With the alkanes each compound can be considered to be the parent of the next lowest member in the homologous series. Thus, π for CH_2

Table III. Comparison of Aqueous Solubility Values ($\mu\text{g/mL}$) Obtained by the HPLC Method, Direct Measurement, and Extrapolation of Measured Values

	2-methylalkanes with N_c of				
	5	6	7	15	20
HPLC method (eq 8)	51.8	14.0	3.8	1.06×10^{-4}	1.51×10^{-7}
direct measurement	47.8, ^a 48.0 ^b	13.8, ^a 13.0 ^b	2.54 ^b	(2.04×10^{-5}) ^c	(1.29×10^{-8}) ^c
	3-methylalkanes with N_c of				
	6	7	8	15	20
HPLC method (eq 10)	10.5	2.90	0.80	9.80×10^{-5}	1.57×10^{-7}
direct measurement	12.8, ^a 13.1 ^b	2.64 ^b	0.79 ^b	(4.15×10^{-5}) ^c	(3.83×10^{-8}) ^c
	1-alkenes with N_c of				
	5	6	8	15	20
HPLC method (eq 12)	183	49	3.6	3.74×10^{-4}	5.35×10^{-7}
direct measurement	148 ^a	50 ^a	2.7 ^a	(2.17×10^{-4}) ^c	(2.32×10^{-7}) ^c

^aValues determined by Price (11). ^bValues determined by McAuliffe (8-10). ^cValues in parentheses are extrapolated from measured values assuming a linear relationship between $\log S$ and N_c . Values of McAuliffe and Price for the same compounds were averaged.

substituents in the n -alkanes can be derived from eq 2 as 0.535. This is comparable with the value of 0.50 ± 0.04 found by Leo et al. (21) for CH_2 groups attached to benzene rings. The hydrophobic fragmental content, f , introduced by Rekker (23) also predicts a linear relationship between $\log P$ and N_c . The f/CH_2 value for aliphatic compounds given by Rekker (23) is 0.527 ± 0.0006 .

Use of HPLC in Determining S and P . The aliphatic hydrocarbons used in this investigation all have close structural similarities and would be expected to have the same relationship between $\log k'$ and $\log S$ or $\log P$ values. When cochromatographed, different homologous series exhibit the same slope of the regression line for plots of $\log k'$ vs. N_c while the intercepts on the vertical axis differ (Table II).

$\log P$ values for the n -alkanes have been calculated by extrapolation of the data of Hutchinson et al. (14) (see Table I). Thus, it is possible to use the HPLC method, with selected n -alkanes as standards, to determine $\log P$ values for the related hydrocarbons. This is particularly useful where direct measurements are impractical due to low aqueous solubility and aggregate formation. Suitable HPLC data were obtained by cochromatography of the various homologous series with n -alkane reference samples (see Table I and Figure 4). This allowed the establishment of the relationship between $\log S$, $\log P$, and N_c for each homologous series.

The relationships for 2-methylalkanes are obtained from the results on mixture 1 (Table II) as follows:

for n -alkanes in mixture 1

$$\log k' = -0.805 + 0.056N_c \quad (4)$$

Combining eq 1 and 4

$$\log S = -3.763 - 10.161 \log k' \quad (5)$$

Combining eq 2 and 4

$$\log P = 7.389 + 9.554 \log k' \quad (6)$$

Now for 2-methylalkanes (Table II)

$$\log k' = -0.819 + 0.056N_c \quad (7)$$

Equations 4-7 apply only for the HPLC conditions used for mixture 1. By combining eq 5 with 7 and 6 with 7, equations for S and P can be obtained which are independent of the chromatographic conditions:

2-methylalkanes

$$\log S = 4.559 - 0.569N_c \quad (8)$$

$$\log P = -0.436 + 0.535N_c \quad (9)$$

Table IV. P Values for Various Homologous Series of Aliphatic Hydrocarbons Determined Using the HPLC Method

	N_c				
	5	6	7	15	20
2-Methylalkanes (eq 9)					
$\log P$	2.23	2.77	3.30	7.58	10.26
3-Methylalkanes (eq 11)					
$\log P$	2.36	2.88	3.41	7.61	10.23
1-Alkenes (eq 13)					
$\log P$	1.72	2.25	2.79	7.07	9.74

By application of the corresponding sequence of calculations the following equations can be obtained for the other homologous series:

3-methylalkanes

$$\log S = 4.376 - 0.559N_c \quad (10)$$

$$\log P = -0.264 + 0.525N_c \quad (11)$$

1-alkenes [using mixture 2 (Table II)]

$$\log S = 5.108 - 0.569N_c \quad (12)$$

$$\log P = -0.957 + 0.537N_c \quad (13)$$

It is of interest to compare the values for aqueous solubility obtained for the 2- and 3-methylalkanes and 1-alkenes by the HPLC method with those obtained by direct measurement and by extrapolation of the measured values (Table III). The HPLC method gives good agreement with the measured values. Extrapolation to $N_c = 20$ gives a difference of more than an order of magnitude only in the case of the 2-methylalkanes. The $\log P$ values for various hydrocarbons obtained by calculation from the equations derived by HPLC are shown in Table IV.

Conclusions

The P values determined by Hutchinson et al. (14) and the S values determined by McAuliffe (8-10), Price (11), and in this investigation, combined with our HPLC data, show that $\log S$ and $\log P$ have a linear relationship to N_c for the n -alkanes. Further, the S values reported by other workers that are not in agreement with this conclusion (12, 13) are in error, very probably because their methods of measurement of solubility failed to eliminate aggregates

of hydrocarbon molecules in the water. Thus, the *S* and *P* values for the higher *n*-alkanes have been determined by extrapolation of the measured values of McAuliffe (8-10) and Hutchinson et al. (14), respectively.

Direct measurement of *P* and *S* values for longer chain length hydrocarbons ($N_c > 12$; $\log P > 6$) is difficult due to aggregate formation and low solubility in water. However, HPLC represents a viable alternative. Our HPLC results indicate that $\log S$ and $\log P$ are linear with N_c for other homologous series of aliphatic hydrocarbons, in particular, 2- and 3-methylalkanes and 1-alkenes. HPLC, utilizing selected *n*-alkanes as reference standards, has been used to determine the $\log S$ and $\log P$ values for these homologous series including those with $N_c > 12$. The values are in reasonable agreement with those obtained by other methods.

Registry No. Butane, 106-97-8; pentane, 109-66-0; hexane, 110-54-3; heptane, 142-82-5; octane, 111-65-9; nonane, 111-84-2; decane, 124-18-5; hendecane, 1120-21-4; dodecane, 112-40-3; tridecane, 629-50-5; tetradecane, 629-59-4; pentadecane, 629-62-9; hexadecane, 544-76-3; heptadecane, 629-78-7; octadecane, 593-45-3; nonadecane, 629-92-5; eicosane, 112-95-8; heneicosane, 629-94-7; docosane, 629-97-0; tricosane, 638-67-5; tetracosane, 646-31-1; pentacosane, 629-99-2; water, 7732-18-5.

Literature Cited

- (1) Connell, D. W.; Miller, G. J. *CRC Crit. Rev. Environ. Control* 1981, 11, 37.
- (2) Clark, R. C.; MacLeod, W. D. "Effects of Petroleum on Arctic and Subarctic Marine Environments and Organisms, Nature and Fate of Petroleum"; Malins, D. C., Ed.; Academic Press: New York, 1977; Vol. 1, p 91.
- (3) GESAMP, Joint Group of Experts on the Scientific Aspects of Marine Pollution, Impact of Oil on the Marine Environment, Food and Agriculture Organisation, Rome, 1977, Report Study 6.

- (4) Neely, W. B.; Branson, D. R.; Blau, G. E. *Environ. Sci. Technol.* 1974, 8, 1113.
- (5) Veith, G. D.; De Foe, D. L.; Bergstedt, B. V. *J. Fish Res. Board Can.* 1979, 36, 1040.
- (6) Mackay, D. *Environ. Sci. Technol.* 1982, 16, 274.
- (7) Mackay, D.; Bobra, A.; Shin, W. Y.; Yalkowsky, S. M. *Chemosphere* 1980, 9, 701.
- (8) McAuliffe, C. *Nature (London)* 1963, 200, 1092.
- (9) McAuliffe, C. *J. Phys. Chem.* 1966, 70, 1267.
- (10) McAuliffe, C. *Science (Washington, D.C.)* 1969, 163, 478.
- (11) Price, L. C. *AAPG Bull.* 1976, 60, 213.
- (12) Franks, F. *Nature (London)* 1966, 210, 87.
- (13) Sutton, C.; Calder, J. A. *Environ. Sci. Technol.* 1974, 8, 654.
- (14) Hutchinson, T. C.; Hellebust, J. A.; Tam, D.; Mackay, D.; Mascarenhas, R. A.; Shiu, W. Y. "Hydrocarbon and Halogenated Hydrocarbons in the Aqueous Environment"; Afghan, B. K.; Mackay, D., Eds.; Plenum Press: New York, 1980; p 577.
- (15) Peake, E.; Hodgson, G. W. *J. Am. Chem. Soc.* 1966, 44, 215.
- (16) Ellgehausen, H.; D'Hondt, C.; Fuerer, R. *Pestic. Sci.* 1981, 12, 219.
- (17) Coates, M.; Chapman, H. F.; Connell, D. W. *J. Mar. Biol.* 1984, 81, 87.
- (18) Mackay, D.; Shiu, W. Y. "Chemistry and Physics of Aqueous Gas Solutions"; American Society Testing Materials: Philadelphia, 1974; p 104.
- (19) McCall, J. M. J. *Med. Chem.* 1975, 18, 549.
- (20) Mirrlees, M.; Moulton, S. J.; Murphy, C. T.; Taylor, C. T. *J. Med. Chem.* 1976, 19, 615.
- (21) Leo, A.; Hansch, C.; Elkins, D. *Chem. Rev.* 1971, 71, 525.
- (22) Hansch, C.; Leo, A.; Nikaitani, D. *J. Org. Chem.* 1972, 37, 3090.
- (23) Rekker, R. F. "The Hydrophobic Fragmental Constant"; Elsevier Scientific Publishing Co.: Amsterdam, 1977.

Received for review September 10, 1984. Accepted January 22, 1985. This work was supported by an Australian Marine Sciences and Technology research grant.

Influence of Aggregation on the Uptake Kinetics of Phosphate by Goethite

Marc A. Anderson,* M. Isabel Tejedor-Tejedor, and Robert R. Stanforth

Water Chemistry Program, University of Wisconsin—Madison, Madison, Wisconsin 53706

■ A coagulation model is postulated in which phosphate bridges to primary goethite particles and causes increased aggregate order, phosphate burial, and oscillatory uptake kinetics. This hypothesis is supported by electron diffraction patterns of single aggregates, decreases in exchangeable phosphate, phosphate-induced reduction in BET surface area, and long-term kinetic results showing slow release of phosphate.

Introduction

This paper addresses the role of chemical and physical coagulation on the uptake of inorganic phosphate by goethite (α -FeOOH). The overall objective is to emphasize that adsorption measurements carried out in batch suspensions are a function of system dispersivity which may change with adsorbate addition as well as with pH, ionic strength, and solid/liquid ratio. This paper also illustrates that some adsorbates such as phosphate may form oriented intercrystalline bonds between primary crystallites which more permanently alter the physical array of the particles. Such bonding by phosphate anions, in addition to causing physical coagulation between goethite particles, directly influences maximum levels of adsorption, kinetics of adsorption, and the exchangeability of adsorbed phosphate.

Literature Review

Kinetics. Protolyzable anion and hydrolyzable cation adsorption and exchange kinetics in hydrous oxide suspensions have been difficult to analyze and interpret by using traditional kinetic expressions. While initial adsorption is often rapid (within minutes), reaction rates generally decay long before a sizeable fraction of surface sites have been exhausted (1, 2). Initial uptake can be dependent on solid/liquid ratio; typically, more adsorbate is removed from solution at a lower ratio (3). Attempts to describe adsorption processes by first- or second-order kinetics have often failed unless reaction time was divided into stages with each stage having its own rate constants, dependent variables, and reaction orders (4, 1). These arbitrary stages have been explained previously by (A) mono- to bidentate conversion of the adsorbate surface complex (5), (B) unequal energies among surface sites (2), (C) rapid surface adsorption followed by slow diffusion into pores (6), or (D) surface adsorption followed by surface precipitation (7).

Isotopic exchange reactions are generally first order with respect to the radionuclide, regardless of the reaction order, and have been mathematically described by a simple McKay equation which relates the amount of label on the

solid to the time of the reaction (8). However, Atkinson et al. (9) and Kyle et al. (10) have shown phosphate exchange on goethite and gibbsite can only be described by the McKay equation if a number of arbitrary divisions in time are invoked. DeBussetti et al. (11) used a three-phase McKay equation to explain phosphate exchange on both alumina and aluminum phosphate. Vanderdeelen and Baert (6), using short-term isotopic exchange, found that the amount of exchangeable phosphate on gibbsite decreased within 1 h and attributed this to either diffusion into the pore structure or surface precipitation. Cabrera et al. (12) obtained similar results.

Physical/Chemical Coagulation Effects. Morgan and Stumm (13) have shown that adsorption (and desorption) kinetics of manganese uptake by colloidal MnO_2 may depend on the state of primary crystallite aggregation. Kurbatov et al. (14) had earlier found similar results, noting that Co^{2+} uptake by Fe gels decreased with increasing electrolyte. These results may be explained by double-layer compression through increased electrolyte concentration which causes physical coagulation of primary particles and either temporarily or permanently blocks potential adsorbent surface sites. Churms (15) noted that these processes depend not only on electrolyte concentrations but also on solid/liquid ratios, temperature, and degree of agitation.

Since physical coagulation usually results in the formation of a weak hydrogen or van der Waals bond, it would seem that this type of bond would permit the total isotopic exchange of phosphate. In this case, adsorbate adsorption rate and isotopic exchange might be increased simply by increasing system agitation, since this would shear weakly bound agglomerates. Chemical coagulation, on the other hand, would be expected to form much stronger agglomerates via chemical bonding which would more permanently remove free surface sites from surface reactivity as well as reduce exchange.

It is therefore not surprising that Taylor and Kuniski (3) found phosphate uptake kinetics to depend upon solid/liquid ratios in a fashion that could not be normalized in terms of reactivity per unit mass. The dispersivity of their system probably was a function of many variables including solid/liquid ratios as well as the amount of phosphate added. Thus, interpretation of the kinetics of adsorption requires an understanding of the interdependence of adsorption and the physical characteristics of the system.

Experimental Section

Preparation of Goethite. Goethite ($\alpha\text{-FeOOH}$) was prepared by using the method of Atkinson et al. (16). X-ray diffraction powder patterns showed the solid to be pure goethite. Acicular crystals were seen in transmission electron micrographs of this material, and no amorphous iron hydroxide could be identified. BET analysis gave a surface area of $33.0 \pm 0.8 \text{ m}^2/\text{g}$, with no micro- or mesoporosity. A maximum adsorption value was calculated by estimating the number of A-hydroxyls on the 100 face. With respect to phosphate adsorption, A-hydroxyls are considered the reactive surface sites (17). By use of measured values for surface area, single crystal dimensions, and lattice constants, and with the assumption that a monodentate phosphate-goethite complex forms, a maximum adsorption of $140 \text{ } \mu\text{mol/g}$ was calculated.

Adsorption Kinetics. Two approaches to adsorption kinetic studies were followed:

(1) For general adsorption kinetic and isotopic exchange experiments, required quantities of stock goethite suspensions were added to solutions of NaCl, pH buffer,

KH_2PO_4 , and ^{32}P -labeled KH_2PO_4 . Experimental solutions were made up in glass volumetric flasks and then transferred to 250-mL polycarbonate flasks. At appropriate times, a small aliquot was removed and filtered ($0.4\text{-}\mu\text{m}$ Nucleopore filters used in a polycarbonate filtering apparatus).

(2) In studies involving solid/liquid ratio and ionic strength effects, the addition sequence was reversed, with stock goethite suspensions, NaCl solutions, pH buffer solutions, and water being pipetted into a 125-mL polyethylene bottle. After sonification for 10 min, phosphate solutions were added. Immediately after being mixed, the phosphate and goethite samples were placed in a constant temperature shaker at 20°C . All samples for a given kinetic curve were prepared at the same time. At different times during the experiment, two or three bottles were randomly removed from the set and filtered. Duplicate or triplicate phosphate analyses were performed on the solution phase of each bottle.

Phosphate concentrations were determined radiochemically. Blank solutions for standardizing total phosphate and total activity were prepared similarly to the samples.

The sample compositions, unless stated otherwise, were 10^{-3} M NaCl , $10^{-3} \text{ M pH buffer}$, $0.4\text{--}20 \text{ } \mu\text{M phosphate}$, and $0.0034\text{--}0.147 \text{ g/L goethite}$. Experiments were performed at pH 4.5 with an acetate buffer. Acetate does not successfully compete for adsorption sites at these phosphate concentrations (18). All solutions were chosen such that they were undersaturated with respect to amorphous iron phosphate ($pK = 30.5$).

Two-Minute Isotopic Exchange. Flasks were equilibrated and solutions prepared in the same manner as used for adsorption kinetics, except that labeled phosphate was not added. At appropriate times, a 15-mL aliquot was removed and placed in a Teflon beaker. Stock ^{32}P -labeled phosphate (0.4 mL) was added, and solutions were shaken periodically for 1.5 min. Two aliquots (approximately 4 mL each) were taken for rinsing the filtering apparatus and then, at 2 min, a sample was taken for analysis. Standards were determined by filtering 15 mL of the experimental solution and then treating the solution as described above. Generally, each experiment included three or four standards. Adsorption kinetics (from adsorption kinetic experiments above) were measured simultaneously to determine total phosphate adsorbed (Γ) at a given time into the reaction.

X-ray Diffraction and Electron Microscopy. X-ray diffraction of powder samples was performed on a Dicker Nuclear diffractometer with Fe-filtered CoK ($\lambda = 1.790 \text{ \AA}$). Random powder sample analysis served for characterization of synthesized solids. For comparison of particle orientation and aggregation, goethite and phosphate-treated goethite specimens were prepared by sedimentation on glass slides. The same sample weight was used for both phosphate-treated and untreated goethite.

Electron micrographs of goethite and phosphate-treated goethite samples were taken with a JEOL under 80 keV. Specimens for examination were prepared by diluting a sample aliquot with water and then dispersing the solid with an ultrasonic mixer. One drop of the suspension was placed onto a coated grid (coated either with carbon or with formvar fiber) and air-dried at room temperature. (Samples must be dilute enough to provide a clearly visible particle separation.)

Results

Adsorption Kinetics and Rapid Isotopic Exchange. Phosphate adsorption onto $0.1180 \text{ g/L goethite}$ as a function of time at pH 4.5 is illustrated in Figure 1a.

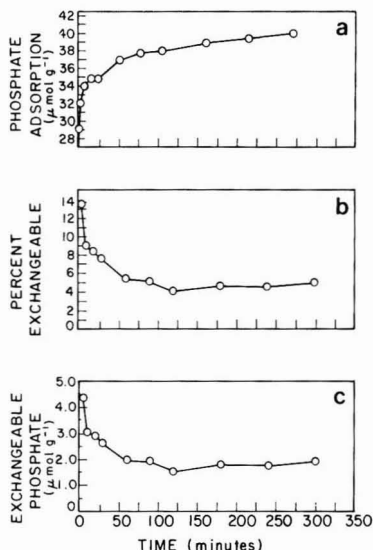


Figure 1. Phosphate adsorption and isotopic exchange vs. adsorption time for conditions of 6 μM initial P concentration, pH 4.5, and 0.118 g/L goethite.

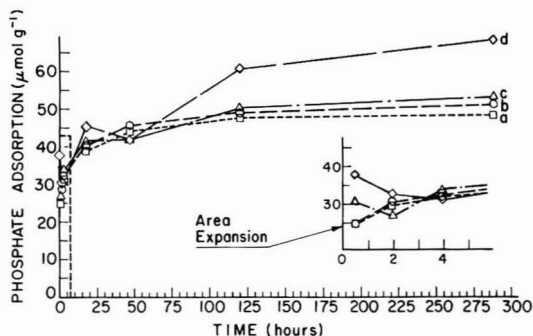


Figure 2. Adsorption kinetics of phosphate on goethite at different solid/liquid ratios. pH 4.5, initial P concentration = 4.0 μM , and $I = 0.001 \text{ M}$. Concentration of goethite: (a) 0.0564 g/L; (b) 0.0338 g/L; (c) 0.0113 g/L; (d) 0.0045 g/L.

Corresponding 2-min isotopically exchangeable phosphate in terms of percentage and absolute amounts is shown in panels b and c of Figure 1, respectively. Although adsorption increases with time, the percentage and absolute amount of exchangeable phosphate both decrease.

In Figure 2 we illustrate *short-term* kinetic dependence on solid/liquid ratios (0.0564, 0.0338, 0.0113, and 0.0045 g/L). These experiments were performed at pH 4.5 and an initial phosphate concentration of 4.0 μM . Initial uptake increases with decreasing solid/liquid ratios, and oscillation (adsorption-desorption) in uptake becomes more apparent with decreasing solid/liquid ratios. (*The reader should note that the symbol size is greater than the error bars representing one standard deviation.*)

The *short-term* kinetic dependence upon ionic strength is shown in Figure 3 for three ionic strengths (0.0001, 0.001, and 0.01 M) adjusted with NaCl. In this set of experiments, pH was again buffered to 4.5, and initial phosphate concentration was 4 μM . (Again, symbols are larger than error bars illustrating one standard deviation.) Initial uptake is greater in the two highest electrolyte concentration systems, and oscillations are apparent in the system

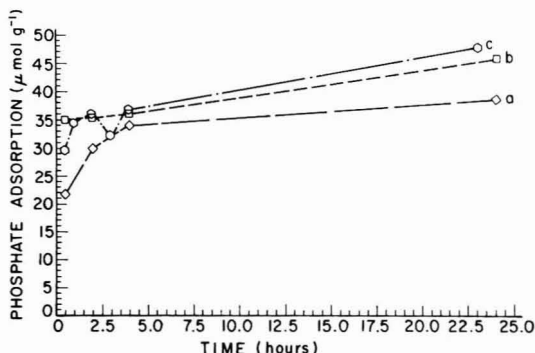


Figure 3. Adsorption kinetics of phosphate on goethite at different ionic strengths. Initial P concentration = 4.0 μM , pH 4.5; concentration of goethite 0.1113 g/L. Ionic strength (M): (a) 0.0001; (b) 0.001; (c) 0.01.

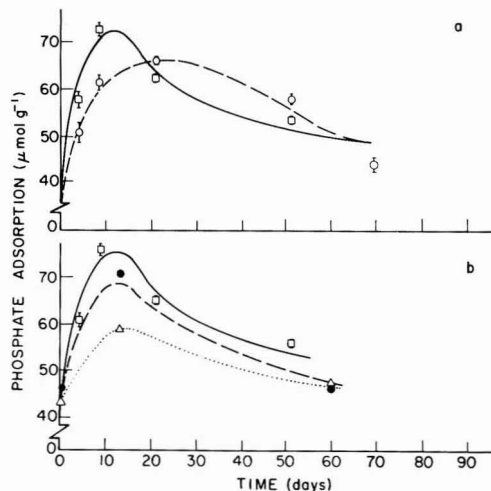


Figure 4. Long-term adsorption kinetics of phosphate on goethite. (a) Concentration of goethite = 0.0035 g/L; (□) initial P concentration = 4 μM ; (○) initial P concentration = 2 μM . (b) Initial P concentration = 4 μM ; (□) 0.0035 g/L goethite; (●) 0.011 g/L goethite; (Δ) 0.023 g/L goethite.

having the highest (0.01 M) electrolyte concentration.

In Figure 4, we illustrate initial concentration and solid/liquid effects on *long-term* phosphate uptake for periods of time up to 70 days. Although a doubling in initial phosphate increases the initial level of phosphate uptake for 0.0035 g/L goethite suspensions, the levels in both systems approach 50 $\mu\text{mol g}^{-1}$ (Figure 4a). A similar uptake level is reached for the three goethite concentrations (0.0035, 0.011, and 0.023 g/L) shown in Figure 4b. As before, the system having the lowest solid/liquid ratio, in the earlier stages, achieves the highest levels of coverage.

Both long-term experiments illustrate significant phosphate desorption. Uptake falls from a maximum approaching 80 to 50 $\mu\text{mol g}^{-1}$ over a period of 2 months. Thus, phosphate is desorbed after initial uptake without changing the suspension composition through dilution, exchange, pH, or other perturbation.

X-ray Diffraction Analysis and Transmission Electron Microscopy. X-ray diffraction patterns of powder-oriented aggregates for both goethite and phosphate-treated goethite consist only of one peak that corresponds to the 110 reflection plane (Figure 5). For the same weight of goethite, intensity of the 110 reflection

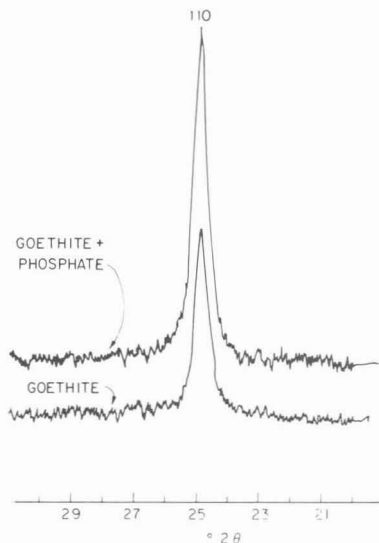


Figure 5. X-ray diffractograms of oriented aggregates of goethite and goethite treated with phosphate for identical sample weights.

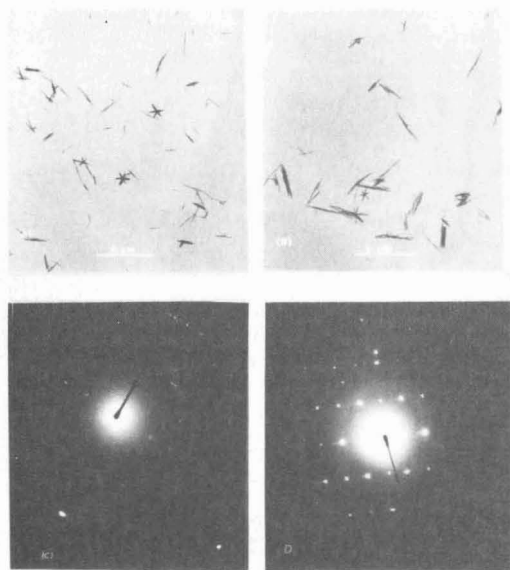


Figure 6. Electron micrographs of goethite and goethite treated with phosphate. (A) Bright-field image of goethite; (B) bright-field image of P-goethite; (C) diffraction pattern of a single particle of goethite; (D) diffraction pattern of a single particle of P-goethite.

plane is higher in the case of phosphate-treated goethite.

Electron micrographs (Figure 6A,B) of goethite and phosphate-treated goethite show that primary goethite particles are generally aggregated and oriented along their longitudinal axis. These combined particles form smaller aggregates for goethite alone than for phosphate-treated goethite. The electron diffraction pattern for phosphate-treated goethite particles can be described as a network of point reflections (Figure 6D) with rectangular symmetry. The analysis of the reflections (in which the observed distances are compared with the theoretical values calculated for the appropriate value of L) indicates

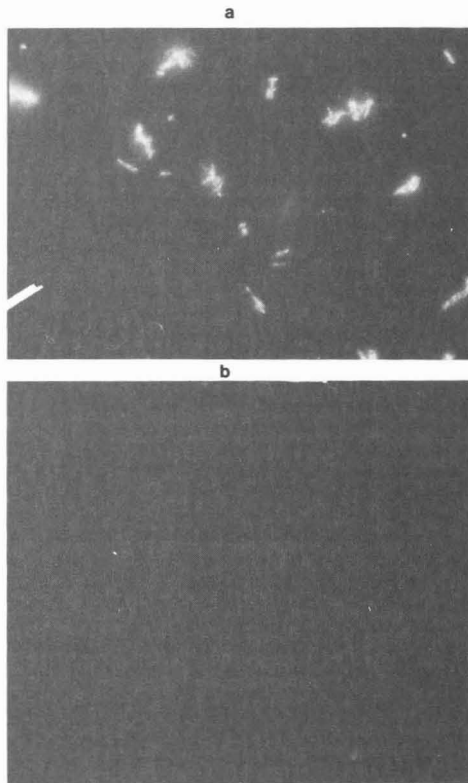


Figure 7. Optical micrographs of goethite suspension obtained after 4 h of equilibration (160 \times). (a) Goethite-phosphate; pH 4.5, concentration of goethite = 0.0045 g/L, ionic strength = 0.001 M, and phosphate concentration = 4 μ M; (b) goethite; pH 4.5, concentration of goethite = 0.0045 g/L and ionic strength = 0.001 M.

that the electron beam is roughly perpendicular to the 100 reflection phase. Since the rectangular network of points is slightly distorted, for most particles we think that the patterns are produced by monocrystal-like particles standing upright on their b edge away from the perpendicular to the beam. By rotation of the acicular particles about the elongated axis c , the rectangular network becomes regular. Electron diffraction patterns from pure goethite particles (Figure 6C) do not show the intense reflections as observed for phosphate-treated goethite (Figure 6D) but show a row of reflections of very weak intensity.

Optical Microscopy and Visual Observations. In Figures 7 and 8, we compare suspensions of goethite and phosphate-treated goethite using optical (160 \times) and visual methods, respectively. (Particles that are moving are the only particles in focus in the optical micrographs.) In both cases, particles show increasing size in the presence of phosphate. Although these visual observations tend to confirm effects of phosphate-induced coagulation, they cannot describe the increased order of the phosphated systems as illustrated in Figure 6D.

BET Analysis of Phosphated Goethite. After phosphate adsorption (0.06 g/L goethite, pH 4.5, initial phosphate 5 mol/L, ionic strength = 10^{-3} M NaCl, and 4 days of equilibration at 20 $^{\circ}$ C), the phosphate-treated goethite showed no micro- or mesoporosity, and its surface area had decreased to 25.9 ± 0.2 m 2 /g. This represents

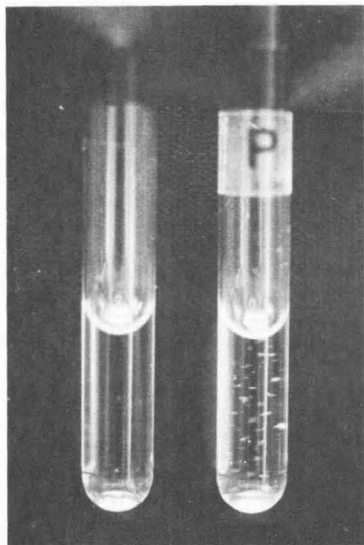


Figure 8. Photographs showing phosphate coagulation effects after 4 days. (Left) Same conditions as in Figure 7b; (right) same conditions as in Figure 7a.

a 22% decrease in surface area after phosphate adsorption.

Discussion

Kinetic Results. Isotopic exchange data illustrated in Figure 1 indicate that phosphate is being "buried" with time and inactivated with respect to exchange. We believe this to be consistent with a coagulation process which "buries" phosphate in intercrystalline space and makes rapid exchange possible only for external, surface-bound phosphate. An increase in system dispersity or a reduction in the coagulation process would be expected to cause an initial increase in the amount of phosphate uptake. This type of behavior is illustrated in Figure 2 where decreases in adsorbent concentration (a decrease in the solid/liquid ratio) cause an increase in initial phosphate uptake.

Figure 2 also shows an oscillatory behavior with respect to phosphate uptake, indicating that phosphate is adsorbed, desorbed, and readsorbed. Although initially considered a possible analytical error, this behavior was demonstrated repeatedly. In fact, the standard deviation of the data illustrated in Figure 2 is smaller than the size of the symbols on the graph. This seems to indicate that phosphate release is real and that oscillations in uptake (adsorption-desorption) shown in Figure 2 are a further indication that a physical-chemical coagulation mechanism is affecting phosphate levels in these polydisperse systems. The oscillations are most noticeable in systems that are low in solid/liquid ratio. Phosphate adsorbed in greater amounts in these more highly dispersed systems, thereby reducing particle ζ potential (18) and causing physical as well as chemical coagulation between the primary particles. Thus, phosphate both seems to reduce ζ potential and acts as a chemical binding agent between crystallites. We hypothesize that as the binding process takes place, not all of the phosphate can be accommodated and some must be expelled, thus causing desorption and subsequent increase in positive ζ potential. (The reader should note that pH is fixed at 4.5 by buffering, and goethite is positive at this pH in the absence of specifically adsorbing anions ($\text{pH}_{\text{iep}} \approx 7.5$).) This positive charge should induce more adsorption, further oscillation, and rearrangement until

equilibrium levels are established.

By lowering the ionic strength, we might expect to reduce the number of effective particle-particle collisions and thereby reduce these types of oscillations. Phosphate, in this instance, would be adsorbed to particle surfaces as if they behaved as single reactants. As is shown in Figure 3, this type of system performance can be invoked by changes in ionic strength. At low ionic strength, uptake kinetics show a smooth pattern as expected for a homogeneous reaction. As ionic strength is increased, particle-particle effective collisions increase as do the oscillations (or abrupt changes in slope). (Again, standard deviation is smaller than symbols illustrated.)

Long-term kinetic studies shown in Figure 4 indicate that uptake gradually increases during the first week, with subsequent desorption for the next several weeks and a gradual approach to an equilibrium condition at 2 months. Adsorption in long-term kinetic studies approaches values ($50 \mu\text{mol g}^{-1}$) representing one phosphate ion adsorbed per every 2-3 of the possible $140 \mu\text{mol g}^{-1}$ of surface sites. (One could alternatively suggest that this may represent somewhere between bidentate and tridentate binding to the surface, but we cannot substantiate this claim directly.)

The long-term kinetic results confirm that the phosphate release illustrated in the short-term uptake studies is occurring. It is therefore not surprising, if one considers that the number of effective collisions between phosphate-treated particles depends upon rearrangement and phosphate release, to see oscillatory behavior as a conditional requirement in the approach to equilibrium.

X-ray and Electron Diffraction Analysis. The kinetic behavior illustrated above is consistent with X-ray and electron diffraction results shown in Figures 5 and 6. Phosphate-treated goethite shows significantly more orientation than untreated goethite.

In X-ray diffraction patterns taken with a diffractometer, only reflections corresponding to crystal planes parallel to the holder surface are observed. When the specimen is prepared, planes parallel to the glass slide will be those parallel to the most developed face of sedimenting particles. Therefore, if goethite particles were single crystals, we should expect only the 100 reflection to appear in the diffractogram; contrary to expectations, they show only the 110 reflections. In order for 110 crystal planes to be parallel to the glass slide, free particles cannot be single crystals, but rather aggregates, in which the primary particles have their 110 planes parallel to each other and parallel to the glass surface, indicating a simultaneous axial and planar orientation, having c as the axis of the aggregate. The fact that the intensity of the 110 reflection increases when the goethite is treated with phosphate for equal sample weights irradiated (Figure 5) indicates larger aggregates and/or higher degree of orientation in phosphate-treated goethite aggregates. Electron micrographs (Figure 6A,B) of goethite and phosphate-treated goethite confirm this argument.

Electron diffraction studies of goethite (Figure 6C) show how the aggregate is formed by a face-to-face association of lath-shaped single crystals with the elongated axis (c) parallel to each other and a limited disorientation about this c axis. This texture in the goethite particle explains why its diffraction patterns (Figure 6C) are similar to those that would be obtained by rotating one of the single crystals a few degrees about the elongated axis, where the reciprocal lattice points would have the symmetry corresponding to rows of spots (19).

Diffraction patterns from these laths of phosphate-treated goethite (Figure 6D) indicate a more monocrys-

talline character of free particles than in those of goethite. This characteristic suggests that phosphate adsorption introduces order in the particle aggregation, so that aggregates increase not only in size but also in orientation. This indicates a specific type of intercrystal bonding.

BET Analysis of Phosphated Goethite. The reduction of the BET surface area from 33.0 to 25.9 m²/g represents a 22% reduction in external surface area. This implies that phosphate bridging between particles forms oriented aggregates which do not allow N₂ to penetrate interparticle space. This provides further evidence supporting the phosphate interparticle bridging mechanism.

Conclusion

We conclude that initial phosphate uptake, which is affected by ionic strength and solid/liquid ratio, is followed by coagulation and rearrangement processes. Effects of ionic strength are larger in dilute solid/liquid suspensions where coagulation is not initially predominant.

These physical-chemical coagulation effects are supported by results obtained in (A) isotopic exchange studies showing decreasing exchange with increasing phosphate uptake, (B) electron micrographs showing increased aggregation in phosphate-treated goethite suspensions over that with goethite alone, (C) X-ray diffraction results which show increasing absorption intensity with increasing phosphate adsorption, (D) electron diffractograms which indicate that phosphate not only increases aggregate size but also increases aggregate order, further substantiating the rearrangement mechanism, and (E) BET results which indicate that phosphate adsorption causes a loss in surface area; this implies that the bridging mechanism prohibits N₂ from penetrating interparticle space.

These findings, interpreted as initial adsorption followed by coagulation and rearrangement, offer an alternative but plausible explanation for the anomalous kinetic results, solid/liquid effects, and isotopic exchange results previously reported. These results also may have direct bearing on the determination of equilibrium adsorption constants, proton binding constants, and the total number of surface sites.

Registry No. PO₄³⁻, 14265-44-2; FeO(OH), 20344-49-4; goethite, 1310-14-1.

Literature Cited

- (1) Chen, Y. R.; Butler, J. N.; Stumm, W. *Environ. Sci. Technol.* **1973**, *7*, 327.
- (2) Benjamin, M.; Leckie, J. O. *J. Colloid Interface Sci.* **1981**, *79*, 209.
- (3) Taylor, A. W.; Kuniski, H. M. *J. Agric. Food Chem.* **1971**, *19*, 827.
- (4) Kuo, S.; Lotse, E. G. *Soil Sci.* **1973**, *116*, 400.
- (5) Kafkafi, U.; Posner, A. M.; Quirk, J. P. *Soil Sci. Soc. Am. Proc.* **1967**, *31*, 348.
- (6) Vanderdeelen, J.; Baert, L. *Pedologie* **1971**, *21*, 360.
- (7) Malotky, D. T. Ph.D. Thesis, University of Wisconsin—Madison, 1978.
- (8) Duffield, R. B.; Calvin, M. *J. Am. Chem. Soc.* **1946**, *68*, 557.
- (9) Atkinson, R. J.; Posner, A. M.; Quirk, J. P. *Proc. R. Soc. London, Ser. A* **1971**, *324*, 247.
- (10) Kyle, J. H.; Posner, A. M.; Quirk, J. P. *J. Soil Sci.* **1975**, *26*, 32.
- (11) DeBussetti, S. G.; Ferreiro, E. A.; Helmy, A. K. *J. Soil Sci.* **1977**, *28*, 610.
- (12) Cabrera, F.; De Arambarri, P.; Madrid, L.; Toca, C. G. *Geoderma* **1981**, *26*, 203.
- (13) Morgan, J. J.; Stumm, W. *J. Colloid Interface Sci.* **1964**, *19*, 347.
- (14) Kurbatov, M. H.; Wood, G. B.; Kurbatov, J. D. *J. Phys. Chem.* **1952**, *56*, 1170.
- (15) Churms, S. C. *J. S. Afr. Chem. Inst.* **1966**, *19*, 108.
- (16) Atkinson, R. J.; Posner, A. M.; Quirk, J. P. *J. Inorg. Nucl. Chem.* **1968**, *30*, 2371.
- (17) Parfitt, R. L.; Russell, J. P.; Farmer, V. C. *J. Chem. Soc., Faraday Trans. 1* **1976**, *72*, 1082.
- (18) Stanforth, R. Ph.D. Thesis, University of Wisconsin—Madison, 1982.
- (19) Zuyagin, B. B. "Electron-Diffraction Analysis of Clay Mineral Structures"; Plenum Press: New York, 1967; pp 1-117.

Received for review September 17, 1984. Accepted January 31, 1985. This work was supported by a contract (DE-AC02-80EV 10467) from the Ecological Research Division Office of Health and Environmental Research, U.S. Department of Energy.

Determination of Equilibrium and Rate Constants for Binding of a Polychlorinated Biphenyl Congener by Dissolved Humic Substances

John P. Hassett* and Edwina Millicic†

Chemistry Department, College of Environmental Science and Forestry, State University of New York, Syracuse, New York 13210

■ Gas purging is a useful approach to distinguish between free and dissolved organic matter bound hydrophobic organic solutes in water. Four mathematical interpretations to extract equilibrium and kinetic binding constants from experimental results under different conditions are described. The dimensionless equilibrium binding constant, K_{DOC} , for binding of 2,2',5,5'-tetrachlorobiphenyl by dissolved humic acid is calculated to be 7.1×10^4 by one interpretation and 7.4×10^4 by another. The rate constant for the release of bound TCB by humic acid is $3.5 \times 10^{-3} \text{ min}^{-1}$, and the rate constant for binding of dissolved TCB by humic acid is $1.7 \times 10^{-4} \text{ L (mg of DOC)}^{-1} \text{ min}^{-1}$.

Introduction

Several laboratory studies have provided evidence for binding of hydrophobic organic compounds by dissolved or colloidal macromolecules in water. Experimental approaches have included solubility enhancement (1-4), gel permeation chromatography (5), dialysis (6, 7), ultrafiltration (8), sorption inhibition (9), and decrease in volatilization (10). Potential environmental consequences of binding of hydrophobic compounds include effects on aqueous solubility (1-4), adsorption (9), volatility (10), photolysis (11), hydrolysis (12), and bioaccumulation (13).

In order to determine the actual environmental significance of binding by dissolved humic substances, it is necessary to quantitatively measure the extent of binding. Several experimental techniques have been or could be used to measure binding. These include dialysis and ultrafiltration, which physically separate bound and free compounds, photolysis and hydrolysis, which measure a change in a chemical reaction when a compound is bound, and volatilization, which measures the decrease in volatilization of a compound from water in the presence of a binding agent. Each approach has its advantages and disadvantages. Dialysis is conceptually simple and requires little equipment, but is slow and is limited to binding agents that do not permeate the membranes and to hydrophobic compounds that do. Some compounds of interest such as bis(ethylhexyl) phthalate (14) and mirex (15), permeate these membranes slowly if at all. Ultrafiltration has similar disadvantages and requires more elaborate equipment than dialysis. Attempts to use ultrafiltration as a method to study binding of 2,2',5,5'-tetrachlorobiphenyl (TCB) at the outset of this study (16) were abandoned because of very high adsorption of TCB to the apparatus. Photolysis and hydrolysis techniques both measure important environmental reactions and as dynamic processes offer possible approaches to study of rate as well as equilibrium properties of binding. However, these methods are limited to compounds that hydrolyze or photolyze at appreciable rates in water, which excludes many environmental contaminants. Volatilization has been suggested by Mackay et al. (10) as a method of studying binding by particles and dissolved organic matter.

Since many hydrophobic pollutants are measurably volatile in water solution (17, 18), this approach should be widely applicable. The experimental system is dynamic and therefore might yield rate as well as equilibrium information. We have used volatilization measurements to obtain equilibrium and rate data on binding of TCB by dissolved humic acid.

Formulation

Cater and Suffet (6) have found that binding of a hydrophobic compound at equilibrium can be described over a wide concentration range by a constant

$$K_b = C_b/C_{aq} \quad (1)$$

where C_b is the concentration of bound compound in water and C_{aq} is the concentration of free compound. A kinetic description of the interaction which is consistent with the equilibrium expression is opposing first-order reactions



where k_{12} and k_{21} are first-order rate constants. A gas-purging experiment is performed by bubbling gas through a solution containing the test compound. In water containing no binding agent, the loss of the compound from solution due to volatilization can be described as an irreversible first-order reaction



where k_{23} is a first-order rate constant and C_g is the concentration of dissolved test compound lost to the gas phase. Mackay et al. (10) have presented theoretical interpretations of k_{23} for experimental systems where the dissolved test compound does and does not equilibrate with the gas phase in a bubble before the bubble leaves the test solution. The value of k_{23} is dependent on temperature, gas flow rate, Henry's law constant, liquid volume, and, if the gas phase does not equilibrate with the liquid phase, the gas-water interfacial area and the overall liquid-phase mass-transfer coefficient. For the purposes of this study, these parameters are held constant, and the value of k_{23} is determined by experiment in pH-buffered distilled water.

The system represented by reactions 1 and 2 can be described mathematically. At equilibrium, reaction 2 is described by eq 1, which may also be expressed as

$$K_b = k_{21}/k_{12} \quad (4)$$

The total concentration of the test compound in solution (C_T) at any time is

$$C_T = C_b + C_{aq} \quad (5)$$

The rate expressions for C_b , C_{aq} , C_T , and C_g are

$$dC_b/dt = k_{21}C_{aq} - k_{12}C_b \quad (6)$$

$$dC_{aq}/dt = k_{12}C_b - (k_{21} + k_{23})C_{aq} \quad (7)$$

*Present address: Galson Technical Services, East Syracuse, NY 13057.

$$dC_T/dt = -k_{23}C_{aq} \quad (8)$$

$$dC_g/dt = k_{23}C_{aq} \quad (9)$$

Implicit in this treatment are the following assumptions: (i) The binding reaction is a set of opposing first-order reactions, and reaction 2 is therefore correct. (ii) The bound test compound is not volatile. (iii) Dissolved organic matter does not affect the magnitude of k_{23} . This assumption is necessary only if the dissolved test compound does not equilibrate with the gas phase. Given these assumptions, the system can be solved for three special cases as well as the general case.

"Equilibrium Binding" Solution

If the rate of gas purging is sufficiently slow so that equilibrium is maintained between C_b and C_{aq} , then eq 1 is applicable at any point in a purging experiment. Combining eq 1 with eq 5 and 8 yields an equation which in integrated form is

$$\ln C_T = -k_{23}t/(1 + K_b) + \ln C_T^0 \quad (10)$$

where t is time and C_T^0 is the initial concentration of C_T . Since k_{23} can be determined by experiment using water without binding agent, K_b can be determined from the slope of a plot of $\ln C_T$ vs. t , but no rate information is provided by this approach. Note that a plot of $\ln C_T$ vs. t should remain linear during the entire course of the experiment if the equilibrium binding solution is valid.

"Initial Slope" Solution

If the initial rate of volatilization of the dissolved compound from solution is much greater than the rate of dissociation of the bound compound into true solution, then eq 5 can be written as

$$C_T = C_{aq} + C_b^0 \quad (11)$$

for a period of time after the start of the experiment. If the system is allowed to equilibrate before the start of an experiment, then the following initial ($t = 0$) conditions exist:

$$C_T^0 = C_{aq}^0 + C_b^0 \quad (12)$$

$$K_b = C_b^0/C_{aq}^0 \quad (13)$$

Solving eq 8 and 11-13 simultaneously yields an expression which, upon integration, becomes

$$C_T = \frac{C_T^0}{1 + K_b} e^{-k_{23}t} + \frac{K_b C_T^0}{1 + K_b} \quad (14)$$

Thus, a value for K_b can be obtained from the ratio of the intercept to the slope of a plot of C_T vs. $e^{-k_{23}t}$. Again, however, no kinetic information is obtained. Note that in this case, a plot of C_T vs. $e^{-k_{23}t}$ will be linear only during the initial phase of an experiment. As release of the bound compound becomes significant, the line will begin to curve.

"Steady State" Solution

As an experiment progresses, the rate of release of bound compound may approach the rate of volatilization of dissolved compound. If the rates become equal, C_{aq} reaches a steady state, and

$$dC_{aq}/dt = 0 \quad (15)$$

Solving eq 5, 7, 8, and 15 simultaneously yields, after integration

$$\ln C_T = -\frac{k_{23}k_{12}}{k_{23} + k_{12} + k_{21}}t + \ln C_T^0 \quad (16)$$

The slope of the linear portion of a plot of $\ln C_T$ vs. t is therefore a function of the rate constants k_{12} , k_{21} , and k_{23} . The value for k_{23} can be determined directly by experiment, but k_{12} and k_{21} cannot be independently measured. However, K_b can be determined by the initial slope solution and used in conjunction with eq 4 and 16 to obtain values for k_{12} and k_{21} . Thus, equilibrium and kinetic information can be obtained from one experiment by applying the initial slope and steady-state solutions to the appropriate data segments. Note that the steady-state solution is applied to a linear segment that occurs after initial curvature in a plot of $\ln C_T$ vs. t .

General Solution

The equilibrium binding solution does not provide kinetic information, and the combined initial slope and steady-state solutions require subjective selection of linear regions of C_T vs. $e^{-k_{23}t}$ and $\ln C_T$ vs. t plots. A potentially more satisfactory approach is to derive the exact mathematical solution to the system described by reactions 2 and 3 and use this solution to extract equilibrium and kinetic information from gas purging experiment results. Methods for integration of simultaneous differential equations have been described previously (19). An approach utilizing matrix methods outlined by Lewis and Johnson (20) is particularly useful. We have used their method to solve eq 6, 7, and 9 for C_b and C_{aq} . Substituting these values into eq 5 and using eq 1 to relate initial values of C_b and C_{aq} (C_b^0 and C_{aq}^0) to the initial C_T (C_T^0) give an expression relating C_T to time:

$$C_T = [C_T^0/[(1 + K_b)(B_{22} - B_{23})]][(K_b B_{22} B_{23} - B_{12} B_{13}) \times (e^{-\lambda_2 t} - e^{-\lambda_3 t})] + [K_b(B_{12} B_{23} e^{-\lambda_2 t} - B_{22} B_{13} e^{-\lambda_3 t})] + B_{12} B_{23} e^{-\lambda_3 t} - B_{22} B_{13} e^{-\lambda_2 t} \quad (17)$$

where the B and λ constants are

$$B_{12} = \frac{\lambda_2 - k_{21} + k_{23}}{k_{12} + k_{21} + k_{23} - \lambda_2} \quad (18)$$

$$B_{13} = \frac{\lambda_3 - k_{21} + k_{23}}{k_{12} + k_{21} + k_{23} - \lambda_2} \quad (19)$$

$$B_{22} = \frac{\lambda_2 - k_{12}}{k_{12} + k_{21} - \lambda_2} \quad (20)$$

$$B_{23} = \frac{\lambda_3 - k_{12}}{k_{12} + k_{21} - \lambda_3} \quad (21)$$

$$\lambda_2 = 1/2[(k_{12} + k_{21} + k_{23}) + \sqrt{(k_{12} + k_{21} + k_{23})^2 - 4k_{12}k_{23}}] \quad (22)$$

$$\lambda_3 = 1/2[(k_{12} + k_{21} + k_{23}) - \sqrt{(k_{12} + k_{21} + k_{23})^2 - 4k_{12}k_{23}}] \quad (23)$$

Thus, eq 17 can be expressed in terms of C_T , t , k_{23} , k_{12} , and k_{21} . Of these terms, C_T , t , and k_{23} are measured directly. Values of k_{12} and k_{21} can therefore be obtained by using computer-assisted nonlinear curve-fitting methods to apply eq 17 to gas purging experiment data. The binding constant, K_b , can then be calculated via eq 4.

It should be noted that K_b and k_{21} are both functions of the concentration of binding agent. If this concentration is expressed in terms of the DOC (dissolved organic carbon) concentration, then a new partition coefficient can be defined:

$$K_{\text{DOC}} = C_{\text{DOC}}/C_{\text{aq}} = K_b/(\text{DOC}) \quad (24)$$

where C_{DOC} is the amount of test compound bound per unit of DOC (e.g., g/g of DOC) and (DOC) is the DOC concentration. If C_{DOC} , C_{aq} , and (DOC) are expressed as weight fractions, then K_{DOC} is unitless. On the basis of a simple partition model, K_{DOC} should be independent of DOC concentration.

The quantity k_{21} should also be a function of the DOC concentration and is actually a pseudo-first-order constant. A new quantity, which has the form of a second-order rate constant, can be defined as

$$k_{21}' = k_{21}/(\text{DOC}) \quad (25)$$

In this study, DOC will be expressed as milligrams per liter for the purpose of calculating k_{21}' , thus giving it units of $\text{L}\cdot\text{mg}^{-1}\cdot\text{min}^{-1}$ and emphasizing its nature as a second-order constant. As with K_{DOC} , k_{21}' should be independent of DOC concentration based on a simple phase partitioning model.

Experimental Section

Humic acid stock solution (530 mg/L DOC) was prepared by adding 2.5 g of sodium humate (Aldrich Chemical Co.) to 1 L of distilled water, stirring for 2 h, and filtering through a glass-fiber filter (Whatman GF/C).

Stock buffer solution was prepared by dissolving 3.4 g of KH_2PO_4 and 3.5 g of K_2HPO_4 in 1 L of distilled water. When 10 mL of this solution was diluted to 500 mL, it provided a pH of 6.4 and an ionic strength of 0.001 M. ^{14}C -Labeled 2,2',5,5'-tetrachlorobiphenyl (0.1 mCi; Pathfinder Laboratories) was dissolved in 250 mL of glass-distilled benzene. This stock solution had an activity of 888 dpm/ μL and a TCB concentration of 19 ng/ μL .

Scintillation cocktail was prepared by dissolving 2 g of 1,4-bis(4-methyl-5-phenyloxazol-2-yl)benzene and 20 g of 2,5-diphenyloxazole in 4 L of scintillation grade toluene.

Gas-purging experiments with TCB in water were carried out in 500-mL gas washing bottles (6 cm i.d.). Nitrogen gas, controlled by a low-pressure regulator and a needle valve, was introduced at a depth of 11 cm below the water surface via a 5-mm (i.d.) glass tube. A glass frit was not used because its large surface area aggravated adsorption problems. All experiments were performed at 25 °C in a temperature-regulated water bath.

Test solutions were prepared by diluting 10 mL of buffer and varied volumes of humic acid stock solution to 500 mL with distilled water. The solutions were spiked with 10 μL of ^{14}C TCB stock solution, stirred for 2 h with a glass-coated magnetic stir bar, and placed in the water bath to equilibrate for 30 min.

Aliquots of test solutions (5 or 10 mL) were withdrawn through the outlet arm of the gas washing bottle by using a 30-mL glass syringe connected to 40 cm of $1/8$ -in. o.d. Teflon tubing. Aliquots were added to 0.5 or 1.0 mL of 10 N NaOH and extracted 3 times with 1 mL of hexane. The syringe and tubing were rinsed with the first portion of hexane. The hexane layers for each aliquot were combined in a scintillation vial containing 9 mL of scintillation cocktail and counted for 40 min in a liquid scintillation counter. The results were corrected for quenching by using the channel ratio technique.

After the initial aliquot was withdrawn, the gas washing bottles were connected to the flow controllers and purged with nitrogen. The flow rate was measured with a rotameter and adjusted to the desired level. For most experiments, samples were taken at 0, 5, 10, 15, 105, 120, 135, and 150 min without interrupting the flow of nitrogen. For one set of experiments, samples were taken every 30 min

from 0 to 300 min. No correction of results was made for loss of volume of sample due to withdrawal of aliquots since the total withdrawn was generally less than 10% of the original volume.

Data from TCB purging experiments were used to solve eq 17 for k_{12} and k_{21} with the aid of the General Purpose Curvefitting Program developed by Dye and Nicely (21). This program provides for weighting data according to the relative variance of the points. For this study, the uncertainty of radioactive decay was considered in determining relative variance, and it was calculated as

$$\text{rel var} = \text{CPM}_s/(\text{CPM}_s - \text{CPM}_{\text{bg}}) \quad (26)$$

where CPM_s is the sample radioactivity and CPM_{bg} is the background. Given experimental data, relative variances and initial estimates of k_{12} and k_{21} , the program finds values of k_{12} and k_{21} that best fit the data, along with estimates of the standard deviations of k_{12} and k_{21} .

Results and Discussion

Values of k_{23} were obtained from the slopes of plots of $\ln C_T$ vs. t (integrated form of eq 8) for purging experiments using humic acid free water. To minimize interference from desorption of TCB from the walls of the apparatus back into solution, only data obtained during the first 15 min of each experiment were used. The results were 0.0512, 0.0804, and 0.0956 min^{-1} at gas flow rates of 2, 4, and 6 L/min, respectively. These values can be used to calculate Henry's law constants if equilibrium between the liquid and gas phase is assumed (10). The results yield calculated Henry's law constants of 0.31, 0.24, and 0.20 $\text{atm}\cdot\text{L}\cdot\text{mol}^{-1}$, which are substantially less than the value of 0.93 $\text{atm}\cdot\text{L}\cdot\text{mol}^{-1}$ reported by Atlas et al. (22) for 2,2',5,5'-TCB. Thus, TCB did not equilibrate with the gas phase in our experiments. This raises concern that if dissolved organic matter affects rates of gas-water exchange, calculated rate and equilibrium constants for binding of TCB would be invalid. For this reason, the effect of dissolved humic and fulvic acid on oxygen gas-water exchange rates were studied. Oxygen was chosen because it presumably does not bind to dissolved humic materials, its gas-water exchange rate is liquid-film controlled according to the two-film diffusion model (23), and it is easily measured in solution. Results (not shown) demonstrate no significant effect of the dissolved humic or fulvic acids on oxygen exchange rates. Jota (24) has confirmed this further by observing that the depth of the bubble inlet in the water column has no effect on the measured binding constant for TCB and Aldrich humic acid. If the humic acid was decreasing k_{23} , the measured binding constant would decrease asymptotically to the true binding constant as the depth of bubble introduction increased because the bubble gas phase would approach equilibrium with dissolved TCB. If humic acid enhanced the gas-transfer rate, the opposite effect on the measured binding constant would be observed. Since neither effect was observed, humic acid had no effect on k_{23} .

First-order rate plots ($\ln C_T$ vs. t) for volatilization of TCB from humic acid were curved concave upward, implying that the "equilibrium binding" calculation approach was inappropriate to interpret the data from this study, but that the other approaches were. Preliminary experiments established the first 15 min as the "initial slope" region and 100–150 min as the "steady-state" region. All data were used to apply the general solution.

Figure 1 shows values of $\log K_{\text{DOC}}$, computed by the initial slope and general solution methods, plotted vs. DOC concentration. The values computed by the initial slope method show little dependence on the DOC concentration

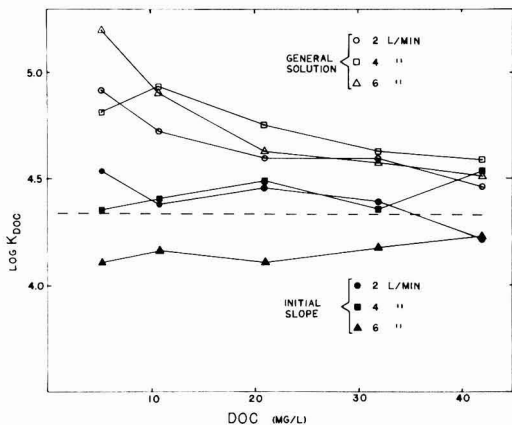


Figure 1. $\log K_{\text{DOC}}$ values obtained by the initial slope and general solution calculation methods for experiments at 2, 4, and 6 L/min purge-gas flow rates and varying DOC concentrations. Dashed line is least-squares linear regression of initial slope values.

(slope = -2.49×10^{-4} , $\sigma = 3.0 \times 10^{-3}$, $R = -0.0232$), and the slope cannot be shown to be different from zero by a t test even at $p = 0.80$. The same holds for a plot of K_{DOC} vs. DOC. This differs from an observation by Carter and Suffet (6) that K_{DOC} for binding of DDT by dissolved humic acid from a lake declines with increasing DOC concentration by a factor of 0.96×10^{-2} to 2.4×10^{-2} log units $\cdot \text{L} \cdot (\text{mg of DOC})^{-1}$. Although there is considerable scatter of the initial slope values in Figure 1, an effect of the magnitude observed by Carter and Suffet should be detectable. Landrum et al. (25) have also reported a dependence of K_{DOC} on DOC concentration for binding of DDT by Aldrich humic acid of approximately the same magnitude as that reported by Carter and Suffet, but as in this study, they found no significant effect of DOC concentration on the binding constant for 2,2',5,5'-TCB. Thus, the influence of DOC concentration on binding constants is uncertain at this point. As Landrum et al. point out, the magnitudes of the observed effects are small and are probably not important from the standpoint of descriptive environmental chemistry. However, all of the studies so far have revealed a negative, but not always statistically significant, correlation between K_{DOC} and DOC concentration, an effect that is not predicted by a simple partitioning model. A satisfactory theoretical description of binding phenomena should account for such an effect.

The values of K_{DOC} calculated by the general solution method (eq 17) decline markedly with increasing DOC concentration and, at the higher DOC concentrations, approach the values calculated by the initial slope method (Figure 1). This effect on the measured binding constant is most likely due to desorption of TCB from the walls of the experimental apparatus as TCB is purged out of solution, buffering the total dissolved TCB and leading to erroneously high calculated K_{DOC} values. As the DOC concentration increases, more TCB is bound and less is therefore available for adsorption (9). Extrapolating the data to infinite DOC concentration, at which point there would be complete binding and no adsorption by the glass, should yield the true value of K_{DOC} . This is done in Figure 2. The values of K_{DOC} , represented by the y intercepts of a linear regression, are 7.9×10^4 ($\sigma = 0.7 \times 10^4$), 7.1×10^4 ($\sigma = 0.7 \times 10^4$), and 7.2×10^4 ($\sigma = 1.5 \times 10^4$) at gas flow rates of 2, 4, and 6 L/min, respectively. These results agree well with the mean value of 7.1×10^4 ($\sigma = 2.4 \times 10^4$) for the 15 values determined by the initial slope approach.

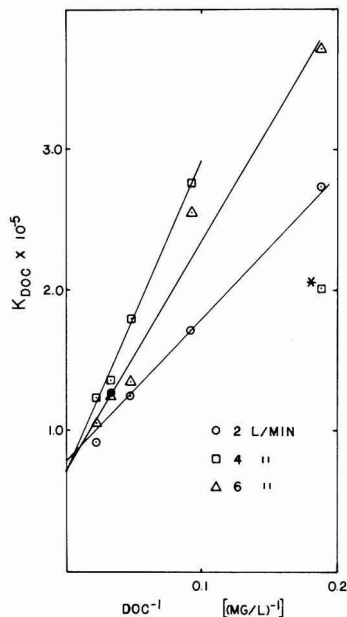


Figure 2. Least-squares linear regression of apparent K_{DOC} values calculated by the general solution method and plotted as an inverse function of DOC. (Asterisk) Not included in linear regression.

Effects of adsorption of TCB by the apparatus are not observed when the initial slope approach is used because, in the short time span of the experiments, desorption of TCB from the glass surfaces is negligible. It should be noted that first-order rate plots of data from experiments with humic-free water showed curvature in the latter parts of the experiments, confirming the role of adsorption of TCB by the glass. For this reason, values of k_{23} were determined by using only data from the initial linear portions of the plots.

The close agreement between K_{DOC} values determined by the two approaches is encouraging and lends confidence to the results obtained since the two methods rely on different underlying assumptions. Landrum et al. (25) have also published K_{DOC} values for binding of TCB by Aldrich humic acid. Those values, obtained by using adsorption and dialysis methods, are lower than ours by factors of 2–2.5. The differences may be due to pH and ionic strength effects (6, 24), methods of pretreatment of the humic acid, or the methods used to measure binding.

Of the two methods discussed here, the initial slope approach would probably be the method of choice to study equilibrium binding constants since it is rapid, has no interference from adsorption by the apparatus, and requires only simple computations. However, it cannot be used to obtain values for rate constants. The general solution does provide values for the forward and reverse rate constants for the binding reaction, and the steady-state approach can be used if K_{DOC} is known, and if the steady-state requirement is fulfilled. Values of k_{21}' obtained by the general solution calculation method are plotted as a function of $(\text{DOC})^{-1}$ in Figure 3. As with values of K_{DOC} obtained by this method, observed values of k_{21}' should approach the true value as the DOC concentration increases. The extrapolated values (and standard deviations) are 2.6×10^{-4} (0.45×10^{-4}), 1.4×10^{-4} (0.21×10^{-4}), and 1.2×10^{-4} (0.76×10^{-4}) $\text{L} \cdot (\text{mg of DOC})^{-1} \cdot \text{min}^{-1}$ at purge gas flow rates of 2, 4, and 6 L/min, respectively, for an average value of 1.7×10^{-4} . Note that

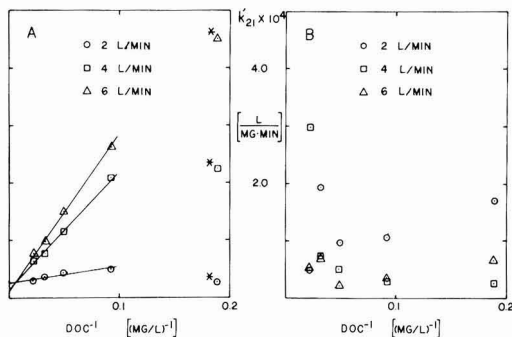


Figure 3. (A) Least-squares linear regression of apparent values of the rate constant k_{21}' calculated by the general solution method and plotted as an inverse function of DOC. (Asterisk) Not included in linear regression. (B) Values of k_{21}' calculated by the steady-state method utilizing K_{DOC} values calculated by the initial slope method for the individual experiments.

the values obtained at 5.3 mg/L DOC do not fall on a line with the values at the other four DOC concentrations and were not used in the linear regressions.

Figure 3 also contains values of k_{21}' obtained by the steady-state calculation method using values of K_{DOC} obtained from initial slope data. The data used to calculate these values of k_{21}' are from the later periods of the purging experiments when the concentrations of TCB remaining in the water are low, and the uncertainties in their measurements are consequently high. For this reason, the calculated values of k_{21}' are scattered and are useful only for order of magnitude estimates of the true value of k_{21}' . However, since they fall in the same range as values obtained by the general solution approach, they lend support to the validity of the value estimated by that approach.

Values of k_{12} computed by the general solution approach are plotted in Figure 4 as a function of $(\text{DOC})^{-1/2}$, which yields a more linear relationship than a plot of k_{12} vs. $(\text{DOC})^{-1}$. Again, the apparent values of k_{12} should approach the true value as the DOC concentration becomes very large. The extrapolated values of k_{12} (and their standard deviations) are 3.1×10^{-3} (0.48×10^{-3}), 2.9×10^{-3} (0.33×10^{-3}), and 4.5×10^{-3} (0.95×10^{-3}) min^{-1} at purge gas flow rates of 2, 4, and 6 L/min, respectively. The average value is $3.5 \times 10^{-3} \text{ min}^{-1}$. The values at 5.3 mg/L DOC have again been eliminated from the linear regression. Values of k_{12} estimated by the steady-state method are also shown in Figure 4, but they are so widely scattered that they are of little assistance in estimating the true value of k_{12} .

If the estimated values of k_{21}' and k_{12} are correct, then their ratio should yield the equilibrium binding constant. By use of the average extrapolated values obtained by the general solution and converting to appropriate units, a K_{DOC} of 4.9×10^4 is calculated. This is in approximate agreement with values of K_{DOC} estimated directly by the initial slope and general solution methods. Figures 3 and 4 indicate that the values obtained by the general solution at a purge gas flow rate of 2 L/min have the least dependence on DOC and should provide the most reliable extrapolations. Using extrapolations of only these data for k_{21} and k_{12} yields a K_{DOC} of 8.4×10^4 , which is an even better agreement with the more directly determined values.

Although the effects of binding and release of TCB by the walls of the apparatus may not have been completely factored out of the estimates of the rate constants, the results presented here are significant in that they establish lower limits for the magnitudes of these constants and

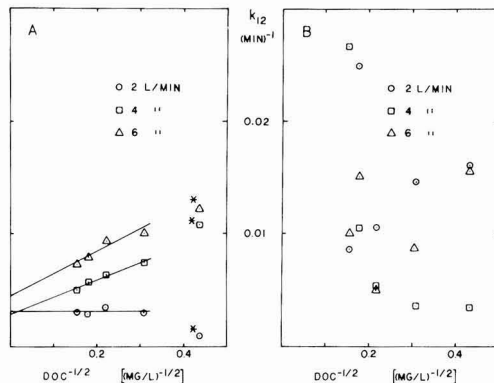


Figure 4. (A) Least-squares linear regression of apparent values of the rate constant k_{12} calculated by the general solution method and plotted as an inverse square root function of DOC. (Asterisk) Not included in linear regression. (B) Values of k_{12} calculated by the steady-state method utilizing K_{DOC} values calculated by the initial slope method for the individual experiments.

indicate that equilibrium of hydrophobic compounds with dissolved organic matter is approached within a matter of hours. Thus, it is probably safe to assume that, in most aquatic systems, hydrophobic solutes are at equilibrium with dissolved organic matter. However, it must be kept in mind that this is the first study of its kind and that TCB and Aldrich humic acid may not be representative of all hydrophobic compounds and dissolved organic matter in water.

Conclusions

Gas purging is a viable method of distinguishing between free and bound hydrophobic organic solutes in water. Its principal advantages are that it requires simple apparatus, it does not require mechanical separation (e.g., filtration) of free and bound solutes, it is rapid, it measures a parameter (volatility) that is directly related to the aqueous chemical activity of the solute, and it can provide both equilibrium and rate information from the same experiment.

Of the three mathematical interpretations discussed that can be used to obtain equilibrium information from gas-purging experiments, the initial slope and general solution approaches were appropriate to apply to the results of this study. The average K_{DOC} determined by using the initial slope interpretation is 7.1×10^4 ($\sigma = 2.4 \times 10^4$) and is independent of DOC concentration. The apparent K_{DOC} determined by using the general solution interpretation is a function of DOC concentration due to interference by adsorption of TCB onto the apparatus. After this interference is factored out, the average K_{DOC} value is 7.4×10^4 . Although these two approaches give comparable results, the initial slope interpretation would be preferable for future equilibrium studies since it is less subject to interference and the calculations are not as complex.

Two of the mathematical interpretations yield kinetic information under appropriate conditions. The apparent values of k_{12} and k_{21}' calculated by using the general solution were dependent on the DOC concentration, probably because of interference from adsorption of TCB by the apparatus. The average corrected value for k_{12} is $3.5 \times 10^{-3} \text{ min}^{-1}$, and the average corrected value for k_{21}' is $1.7 \times 10^{-4} \text{ L} \cdot (\text{mg of C})^{-1} \cdot \text{min}^{-1}$. The magnitudes of these rate constants are such that in most waters TCB would approach equilibrium with dissolved organic matter in less than a day. The rate constants determined by the steady-state

interpretation were too scattered to reliably estimate actual values, but they did tend to fall in or near the range of values calculated by the general solution. The steady-state interpretation did not yield useful results because it was based on data near the detection limit for [^{14}C]TCB in water. This approach might be more useful for systems where bound compounds are released very slowly, as in desorption from sediment particles.

Registry No. TCB, 35693-99-3.

Literature Cited

- (1) Wershaw, R. L.; Burcar, P. J.; Goldberg, M. C. *Environ. Sci. Technol.* **1969**, *3*, 271-273.
- (2) Boehm, P. D.; Quinn, J. G. *Geochim. Cosmochim. Acta* **1973**, *37*, 2459-2477.
- (3) Matsuda, K.; Schnitzer, M. *Bul. Environ. Contam. Toxicol.* **1971**, *6*, 200-204.
- (4) Carter, C. E.; Suffet, I. H. In "Fate of Chemicals in the Environment: Compartmental and Multimedia Models For Predictions"; Swann, R. L.; Eschenroeder, A.; Eds.; American Chemical Society: Washington, DC, 1983; pp 215-229.
- (5) Hassett, J. P.; Anderson, M. A. *Environ. Sci. Technol.* **1979**, *12*, 1526-1529.
- (6) Carter, C. E.; Suffet, I. H. *Environ. Sci. Technol.* **1982**, *16*, 735-740.
- (7) Guy, R. D.; Narine, D. R.; de Silva, S. *Can. J. Chem.* **1980**, *58*, 527-554.
- (8) Means, J. C.; Wijayaratne, R. *Science (Washington, D.C.)* **1982**, *215*, 968-970.
- (9) Hassett, J. P.; Anderson, M. A. *Water Res.* **1982**, *16*, 681-686.
- (10) MacKay, D.; Shiu, W. Y.; Sutherland, R. P. *Environ. Sci. Technol.* **1979**, *13*, 333-337.
- (11) Zepp, R. G.; Baughman, G. L.; Schlotzhauer, P. F. *Chemosphere* **1981**, *10*, 109-117.
- (12) Perdue, E. M.; Wolfe, N. L. *Environ. Sci. Technol.* **1982**, *16*, 847-852.
- (13) Boehm, P. D.; Quinn, J. G. *Estuarine Coastal Mar. Sci.* **1976**, *4*, 93-105.
- (14) Carter, C. E. Ph.D. Thesis, Drexel University, Philadelphia, PA, 1982.
- (15) Hassett, J. P.; Yin, C.-Q. *Prepr. Pap., Natl. Meet.—Am. Chem. Soc., Div. Environ. Chem.* **1983**, *23* (2), 372-374.
- (16) Milicic, E. M.S. Thesis, SUNY College of Environmental Science and Forestry, Syracuse, NY, 1983.
- (17) MacKay, D.; Wolkoff, A. W. *Environ. Sci. Technol.* **1973**, *7*, 611-614.
- (18) MacKay, D.; Leinonen, P. J. *Environ. Sci. Technol.* **1975**, *9*, 1178-1180.
- (19) Frost, A. A.; Pearson, R. G. "Kinetics and Mechanism", 2nd ed.; Wiley: New York, NY, 1961.
- (20) Lewis, E. S.; Johnson, M. D. *J. Am. Chem. Soc.* **1960**, *82*, 5399-5407.
- (21) Dye, J. L.; Nicely, V. A. *J. Chem. Educ.* **1971**, *48*, 433.
- (22) Atlas, E.; Foster, R.; Giam, C. S. *Environ. Sci. Technol.* **1982**, *16*, 283-286.
- (23) Liss, P. S.; Slater, P. G. *Nature (London)* **1974**, *247*, 181-184.
- (24) Jota, M. A. T. M.S. Thesis, SUNY College of Environmental Science and Forestry, Syracuse, NY, 1984.
- (25) Landrum, P. F.; Nihart, S. R.; Eadie, B. J.; Gardner, W. S. *Environ. Sci. Technol.* **1984**, *18*, 187-192.

Received for review July 19, 1984. Accepted February 15, 1985.
This work was funded by NIH Biomedical Research Support Grant 210-E000E and by the Chemistry Department, SUNY College of Environmental Science and Forestry.

NOTES

Toluene-Humic Acid Association Equilibria: Isopiestic Measurements

Charles N. Haas*

Pritzker Department of Environmental Engineering, Illinois Institute of Technology, Chicago, Illinois 60616

Brian M. Kaplan

PRC Engineering, Chicago, Illinois 60601

■ The association between toluene and humic acid was measured by using a closed loop recirculating gas isopiestic apparatus. The association equilibrium could be described by a linear partition coefficient model in which the equilibrium constant was a function of the humic acid concentration; this has been found also to be the case for other trace organic compounds. The magnitude of the equilibrium constant is in accord with prior correlations reported between the humic acid association constant and the octanol-water partition coefficient. The methodology used in this study shows promise for the investigation of a variety of organic compounds.

Introduction

Phase-transfer processes such as adsorption and air

stripping are finding increased application for the removal of trace organic compounds from wastewaters and potable wastes. Design of these removal processes requires a knowledge of both the speciation of the organic compound to be removed and the kinetics and equilibria of the removal processes themselves. It has been shown previously that aquatic humic acids can form associations with a variety of organic compounds, primarily pesticides and other chloro organics. Prior studies are summarized, along with analytical methodology in Table I.

The objective of this study was to determine whether toluene, a common, low molecular weight organic pollutant, could form similar associations with humic acids. In addition, an equilibrium isopiestic method originally described by Sanemasa et al. (14) was employed to make

Table I. Prior Studies on the Association of Trace Organics with Humic Material

method	organic	ref
head space analysis	hexachlorobutadiene chlorinated benzenes	1
volatilization kinetics	PCB's chlorinated benzenes, PAH	2 3
competitive adsorption	DDT, anthracene	4
hydrolysis kinetics	octyl ester of 2,4-D	5
dialysis	DDT	6
fluorescence	perylene	7
liquid chromatography	biphenyl, phthalates atrazine, linuron	8 9
solubility	hexadecane, eicosane, phenanthrene	10
	anthracene, phthalates	4
	phthalates	11
	DDT	12
	DDT	13

measurements with a higher degree of precision than previously reported.

Materials and Methods

The experimental apparatus was similar to that of Sanemasa et al. (14). In this method, a closed gas phase is continuously recirculated by means of a pump through pure solvent (toluene), and reservoirs consisting initially of distilled deionized water and distilled deionized water containing a known concentration of humic acid. At equilibrium, the liquid-phase toluene concentrations in the solution reservoirs are concentrations. Since all solutions are in isopiestic equilibrium, the difference in solution concentrations directly reflects the association of toluene with the humic acid. The entire apparatus was maintained in a temperature-controlled room ($25 \pm 3^\circ\text{C}$), and liquid reservoirs were immersed in a water bath ($25 \pm 0.1^\circ\text{C}$).

Reagent-grade toluene was employed. The humic acid solutions were prepared by filtration of solutions of Aldrich Chemical Co. humic acid (sodium salts) through 0.45- μm glass-fiber filters; it was found that filtration did not alter the dissolved organic carbon concentrations of humic acid solutes (15). Humic acid solutions were prepared in a pH 6.8 buffer at an ionic strength of 0.0838 M (0.25 M each of dibasic potassium phosphate and monobasic sodium phosphate).

Solution-phase toluene concentrations were measured by direct aqueous injection gas chromatography (GC) (Varian 3740, FID) on a 6 ft \times 1/8 inch Chromosorb 80/100 mesh column using direct aqueous injection. The technique was calibrated by comparison with detector response on toluene solutions in CS_2 , and it was found that quantitative measurements of total (bound plus free) toluene with no inhibition of detector response could be made.

Preliminary experiments using contact times up to 16 h indicated that equilibrium was attained after 8 h of gas circulation. This was the case for both the lowest and the highest humic acid concentration employed in this study. Therefore, data were pooled from the 8-, 10-, and 12-h sampling times for the purpose of repeating partitioning equilibrium. At each sampling time, three separate aliquots were taken for analysis, and each aliquot was analyzed 5 times. All data analysis was performed by using a hierarchical two-way analysis of variance (16) for each humic acid concentration, and this analysis consistently indicated no statistically significant effect of sampling time or replication. Variances were those computed for the pooled results of 45 analyses at each humic acid level. All results are reported by using 95% confidence limits.

Dissolved organic carbon concentrations were determined on a Beckman Model 915 carbon analyzer.

Table II. Solubility of Toluene in pH 6.8 Buffer of 0.084 M Ionic Strength*

humic acid concn, mg/L as organic carbon	solubility, mg/L of toluene	K , g/g as C	K (eq 1)
0	476.8 ± 2.8		
0	482.1 ± 2.3		
8.1	488.2 ± 2.1	1.01	1.30
14	502.3 ± 4.3	1.59	1.22
24.5	503.9 ± 2.8	0.98	1.08
24.5	506.4 ± 2.5	1.07	1.08
39	517.3 ± 2.0	0.95	0.876
62.9	511.6 ± 0.13	0.502	0.545
73.1	509.1 ± 7.2	0.398	0.405

* Background TOC of 2.2 mg/L subtracted from HA concentrations. K = excess solubility/HA concentration.

Results and Discussion

The solubility of toluene in distilled deionized water determined in this study was 520.5 ± 0.1 mg/L (5.648 ± 0.029 mol/ m^3). This is in excellent agreement with the results of Sanemasa et al. (14) using the same apparatus, as well as that of previous investigators employing other methods (17, 18). At the buffer ionic strength of 0.084 M, in the absence of humic acid, the solubility of toluene was determined to be 479.5 ± 2.0 mg/L, which agrees with the extrapolated results of Morrison and Billet (17) using a salting-out coefficient of 0.184 M. These results confirm the precision and accuracy of the experimental methods.

The excess solubility of toluene in the presence of humic acid was modeled by using the partition coefficient approach (4, 19). Pooling all data from a regression of excess solubility vs. humic acid concentration, K , was determined to be 0.449 g/g (organic carbon basis for humic acid; correlation = 0.787). Inspection of the data and computation of point estimates of K (Table II) indicated that a linear partitioning model with a constant K of 0.931 g/g (correlation = 0.97) described the data in the range of 0–40 mg/L total organic carbon (TOC), but above 40 mg/L TOC, a monotonic decrease in K could be observed.

In the work of Diachenko (1), correlations between octanol-water partition coefficients and K were developed. On the basis of a toluene log (K_{ow}) of 2.69 (20), Diachenko's estimation equations predict a K of approximately 0.5, at a humic acid concentration of 200–1000 mg/L. This agrees reasonably well with the results obtained in this work at higher humic acid concentrations (Table II).

In prior work, Carter (4) observed a linear decrease of the partition coefficient of DDT on humic acid organic carbon in accordance with the equation

$$K = 0.1578 - (2.69 \times 10^{-3}) \quad (\text{mg/L DOC}) \quad (1)$$

The point estimates of K for toluene from Table II were used to develop an equation analogous to (1). Equation 2 describes the variation of K as a function of DOC (cor-

$$K = 1.41 - 0.0138 \quad (\text{mg/L DOC}) \quad (2)$$

relation = 0.86). Similar decreases in apparent partition coefficients with DOC concentrations were also observed by Landrum et al. (8) for benzo[a]pyrene, DDT, anthracene, biphenyl, and 2,5,2',5'-tetrachlorobiphenyl.

One explanation for the decrease in K with increasing humic concentration may be the formation of micelles at higher humic acid concentrations. Piret et al. (21) determined the critical micelle concentration (cmc) of peat humic acid in 0.26 M NaCl to be approximately 18 g/L, substantially above the values employed in the present study. However, Ekwall et al. (22) noted complex solubility

patterns (with regions of both increasing and decreasing solubility) for decanol in sodium laurate solutions. In the present case, the varying concentration of both humic acid and toluene, it is possible that the toluene alters the cmc of the mixture. Detailed spectroscopic and colligative studies would be required to elucidate the mechanistic basis behind eq 1-2.

Conclusions

By use of the isopiestic apparatus of Sanemasa et al. (14), precise measurements of toluene solubility as altered by humic acid have been obtained. Within the range 0-70 mg/L DOC, solubility increases of up to 8% of the intrinsic, zero organic solubility have been noted. By use of a partition coefficient model, these data show that toluene solubility by humic acid decreases (i.e., the partition coefficient decreases) with increasing humic acid concentration, in a manner similar to that reported for more hydrophobic pollutants.

The results indicate that, while solubilization of toluene by DOC does occur, it may be of limited significance in affecting overall distribution of toluene in natural and engineered aquatic systems. It would be desirable to elucidate the mechanism of solubility and to determine the relative partition coefficients of various volatile pollutants. The present apparatus provides a means for obtaining high precision data for such coefficients, and further studies on these areas are planned.

Acknowledgments

We thank H. E. Allen for his initial suggestion of this problem and P. V. Doskey for continued support and advice concerning analysis.

Registry No. Toluene, 108-88-3; H₂O, 7732-18-5.

Literature Cited

- (1) Diachenko, G. W. Ph.D. Thesis, University of Maryland, College Park, 1981.
- (2) Griffan, R. A.; Chian, E. S. K. "Attenuation of Water Soluble Polychlorinated Biphenyls By Earth Materials" 1980, EPA Report EPA-600/2-80-027.
- (3) Mackay, D.; Shiu, W. Y.; Bobra, A.; Billington, J.; Chau, E.; Yeun, A.; Ng, C.; Szeto, F. "Volatilization of Organic Pollutants From Water" 1982, EPA Report EPA 600/3-82-019.
- (4) Carter, C. W. Ph.D. Thesis, Drexel University, Philadelphia, PA, 1982.
- (5) Perdue, E. M.; Wolfe, N. L. *Environ. Sci. Technol.* **1982**, *16*, 847-852.
- (6) Carter, C. W.; Suffet, I. R. *Environ. Sci. Technol.* **1982**, *16*, 735-740.
- (7) Roemelt, P. M.; Seitz, W. R. *Environ. Sci. Technol.* **1982**, *16*, 613-616.
- (8) Landrum, P. F.; Nihart, S. R.; Eadle, B. J.; Gardner, W. S. *Environ. Sci. Technol.* **1984**, *18*, 187-192.
- (9) Means, J. C.; Wijayarathne, R. *Science (Washington, D.C.)* **1982**, *215*, 968-970.
- (10) Boehm, P. D.; Quinn, J. C. *Geochim. Cosmochim. Acta* **1973**, *37*, 2459-2477.
- (11) Matsuda, K.; Schnitzer, M. *Bull. Environ. Contam. Toxicol.* **1973**, *6*, 200-204.
- (12) Pierce, R. H.; Olney, C. E.; Felbeck, G. T. *Geochim. Cosmochim. Acta* **1974**, *38*, 1061-1073.
- (13) Wershaw, R. L.; Purcar, P. J.; Goldberg, M. C. *Environ. Sci. Technol.* **1969**, *3*, 271-273.
- (14) Sanemasa, I.; Araki, M.; Deguchi, T.; Nagai, H. *Bull. Chem. Soc. Jpn.* **1982**, *53*, 1054-1062.
- (15) Kaplan, B. M. M. S. Thesis, Illinois Institute of Technology, Chicago, 1984.
- (16) Brownlee, K. A. "Statistical Theory and Methodology in Science and Engineering"; Wiley: New York, 1960.
- (17) Morrison, T. J.; Billet, F. J. *Chem. Soc.* **1952**, *52*, 3819-3822.
- (18) Sutton, C.; Calder, J. A. *J. Chem. Eng. Data* **1975**, *20*, 320-322.
- (19) Perdue, E. M. In "Aquatic and Terrestrial Humic Materials"; Christman, R. F.; Gjessing, E. T. Eds.; Ann Arbor Science Publishers: Ann Arbor, MI, **1983**; pp 441-460.
- (20) Chiou, C. T.; Freed, V. H.; Schmedding, D. W.; Kohnert, R. L. *Environ. Sci. Technol.* **1977**, *11*, 475-478.
- (21) Piret, E. L.; White, R. G.; Walthers, H. C.; Mudden, A. J. *Proc. R. Dublin Soc.* **1960**, *1A*, 69-79.
- (22) Ekwall, P.; Mandell, L.; Fontell, K. *Mol. Cryst. Liq. Cryst.* **1969**, *8*, 157-223.

Received for review September 7, 1984. Accepted January 22, 1985.

CORRESPONDENCE

Comment on "Comparison of the Carcinogenic Risks from Fish vs. Groundwater Contamination by Organic Compounds"

SIR: The accumulation of toxic chemicals by fish has long been recognized as a pervasive threat to piscivorous wildlife. Accordingly, the U.S. Fish and Wildlife Service has participated in the National Pesticide Monitoring Program (NPMP; now the National Contaminant Biomonitoring Program) since 1967 by periodically determining chemical residues in avian wildlife and in freshwater fish collected from national networks of stations. More recently, it has been recognized that chemical residues, especially residues of carcinogens, accumulated by food fishes

may also constitute a threat to the public health. The recent note by Connor (1) suggests that such concerns may be justified; however, we have reason to question Connor's conclusions regarding the potential risks associated with contaminants in freshwater fish.

In July, 1982, Connor wrote to our laboratory requesting recent information on contaminant residues in freshwater fish. He was sent copies of two articles that contained such information; both of these articles were correctly referenced under Literature Cited as ref 6 and 7. On pp 140 and 151 of Schmitt et al. (2), and on p 22 of Schmitt et al. (3), it states, in essence, that NPMP data for residues in whole fish are representative of the contaminant levels to which piscivorous wildlife would be exposed but that the values reported are probably higher than concentrations in the edible tissues, to which humans would be exposed.

Whole-fish samples include the viscera, which contains more lipid than does muscle tissue, as well as organs that concentrate organic contaminants. Connor was also advised of this in the cover letter that accompanied the material he requested. Inspection of Connor's Figure 1 suggests that this caveat was ignored in calculating the risks associated with the consumption of freshwater fish; according to the figure legend, the bar labeled "FW" is based upon "average concentrations from 1979 freshwater fish survey for U.S." The only sources cited for freshwater fish residues are our publications (2, 3).

We sincerely hope that we have incorrectly interpreted Connor's article—that he derived estimates of contaminant concentrations in the edible tissues of freshwater fish from FDA market surveys (4) or that our values for whole fish were adjusted before they were used, which cannot be determined on the basis of information in the published article. If we have misinterpreted, we extend our apologies and await clarification of the methods he used; however, if Connor used the 1979 NPMP information without applying some modification to derive his assessment, then freshwater anglers, commercial fishermen, and fishery managers throughout the United States await his revised estimates.

Literature Cited

- (1) Connor, M. S. *Environ. Sci. Technol.* 1984, 18, 628-631.
- (2) Schmitt, C. J.; Ludke, J. L.; Walsh, D. F. *Pestic. Monit. J.* 1981, 14, 136-206.
- (3) Schmitt, C. J.; Ribick, M. A.; Ludke, J. L.; May, T. W. *U.S., Fish Wildl. Serv. Res. Publ.* 1983, 152, 1-62.
- (4) "FY 79 Pesticides and Metals Program"; FDA 7305.007: Washington, DC, 1982.

Christopher J. Schmitt,* J. Larry Ludke

U.S. Department of Interior
Fish and Wildlife Service
Columbia National Fisheries Research Laboratory
Columbia, Missouri 65201

SIR: Schmitt and Ludke (1) were very kind in providing me access to their data. They very clearly indicated that their data were for whole fish. In fact, it was often necessary for me to transform between data for whole fish or fish liver concentrations to concentrations in the edible portion of the fish. The figure legend does cite the lengthier publication where this transformation is explained in more detail ((2) ref 13 in my original publication). In brief, I matched fish by age, lipid content, year, and location where information for both whole fish or edible concentration were available. I used the ratio of edible/whole concentration (for these data, 0.3) to convert the data from Schmitt's laboratory. Naturally, there can be a great deal of variation in this ratio so I used several independent methods to estimate human consumption of contaminants from fish. As I discussed in the explanatory paragraph for the figure, where the lengthier publication is again cited, the different methods are in general agreement.

Literature Cited

- (1) Schmitt, C. J.; Ludke, J. L. *Environ. Sci. Technol.*, preceding paper in this issue.

- (2) Connor, M. S. "Management of Wastes in the Ocean"; Wiley: New York, in press.

Michael Stewart Connor

Region 1
U.S. Environmental Protection Agency
Boston, Massachusetts 02203

Comment on "Red Herrings in Acid Rain Research"

SIR: Regarding the feature article by Havas et al. (1), I agree that it is time for all concerned to work together and not rely on questionable truisms. However, it seems that regulatory zealots with help from the popular media have been the leaders in espousing untested hypotheses as listed below:

- (1) Nitric acid in rain has the same effect as sulfuric acid.
 - (2) Liming of lakes is only useful for research while further controls on NO_x and SO_x should be effected immediately.
 - (3) Effects of alkaline emissions can be ignored.
 - (4) Midwest SO_x - NO_x utility emissions are responsible for the acidity in Adirondack lakes while rain acidity is proportionate to such emissions.
 - (5) Benefits derived from stringent SO_x controls would outweigh their costs.
 - (6) Acid rain causes severe damage to vegetation while benefits are negligible.
- The lack of validity of these hypotheses is discussed in a recent publication (2).

Another unjustified hypothesis is that there are significant human health effects from acid precipitation. Because there is a dearth of evidence on adverse human health effects from acid precipitation, this is usually implied by statements such as used by Havas et al. ("Why must we tolerate decades of emissions, damage to the environment, and often human health before abatement measures are even considered?"). They fail to cite a single reference to support the health effect implication. Pollution control measures for SO_2 , NO_x , particulate, etc. have been considered and effected for decades even though health effects at U.S. ambient levels remain unproven.

Literature Cited

- (1) Havas, M.; Hutchinson, T. C.; Likens, G. E. *Environ. Sci. Technol.* 1984, 18, 176A-186A.
- (2) Innes, W. B. *Chemtech* 1984, 14, 440-447.

W. B. Innes

Purad Inc.
724 Kilbourne Dr.
Upland, California 91786

SIR: Dr. Innes (1) is using the excuse of a rebuttal to our paper to introduce more red herrings into the literature. Little of what he has to say relates directly to our paper. The techniques used by Innes and others are classics. One technique is to alter the wording slightly so that the meaning changes substantially and then claim the

authors said it. For example, we did not say that "nitric acid has the same effect as sulfuric acid". Our statement was that of the inorganic acids, nitric and sulfuric predominate. These two statements are not identical. *Another red herring.*

Another technique, which is even more blatant than the first, is to make a strong statement that has not been "proven" scientifically and associate that statement with the authors. Our paper dealt with the aquatic environment. We do not say that "acid rain causes severe damage to vegetation while benefits are negligible". What is implied by the second half of this statement is that we should test some more untested hypotheses, namely, the beneficial effects of acid rain. *Another red herring.* It is true that S is a plant nutrient but not necessarily if it is delivered as phytotoxic SO₂ and sulfuric acid. Only persistent reports from the Tennessee Valley Authority have made such a claim. If sulfur and nitrogen are so good for plants in the form of air pollution, then why is it that in the most polluted cities very few plants are able to survive and that only a handful of tree species can be planted. Should not sulfur-polluted cities be a veritable jungle of vigorously growing species? Should not trees be bigger and more diverse near smelters? What happened to the trees around Sudbury, Anaconda, and Ducktown? Or do our eyes deceive us?

Points 2, 3, and 5 made by Innes (1) are all concerned with remedial measures. We did not discuss remedial measures in our paper. However, since Innes mentioned this topic we should like to comment. It appears (although we may be wrong) that Innes is opposed to reducing acidic emissions as part of a remedial program. Instead, liming of lakes and alkaline emissions should be considered. Since we know that acid rain is caused by SO₂ and NO_x emissions is it not logical to think that reducing these emissions should help? According to Dr. Innes, it may be much more logical to pollute the atmosphere with alkaline emissions as well as acidic emissions to solve our problem. Is it not wiser to remove the pollutants, perhaps by using neutralizing extracts at the source?

We do not consider liming the *solution* to lake acidification problems. At best, liming may buy us some time, and at worst, it can be harmful to aquatic biota. There are a number of problems associated with liming that tend to be downplayed by liming advocates. The neutralizing effect of liming is temporary, and if we wish to maintain high pHs, liming has to be repeated as frequently as every 4-5 years in some lakes. Not all the effects of liming are beneficial to the biota. The rapid increase in pH and/or associated changes in aluminum speciation killed fish in Sweden (5) and caused zooplankton populations to crash in Canada (8). Liming reduces metal levels in lakes, but in some cases the metal concentrations may not be reduced sufficiently to allow for successful restocking of fish (8). As the lake begins to reacidify, the metals which have precipitated onto surface sediments can redissolve into the water column. Reviews on remedial measures which discuss the advantages and disadvantages of liming conclude that it should be considered only as an *interim* measure and not as the solution to acid rain (6), a conclusion with which we agree. Liming and other measures may be useful in the *short term*, but we believe that reducing acidic emission is the only possible *long-term* solution to the problems associated with acidic deposition. Not only will lakes and streams be protected but so will our forests, our buildings, and our monuments.

The other point made by Innes is that we should consider the cost and benefits of SO₂ control. We agree. To

date there has been little information on what the benefits might be. It was believed that recovery of lakes might be a slow process, if indeed they would recover at all. We have some recent data for the Sudbury region that suggest that not only will lakes recover but also recovery might be quite rapid if acidic emissions are reduced (Hutchinson and Havas, unpublished results). Noticeable improvements in pH, SO₄, and metal concentrations may occur within a decade or less.

Regarding the cost of reducing SO₂ emissions, two recent estimates suggested that the cost of energy would increase by 3% in Europe and by a higher amount in the United States. Since these were based on different reduction schedules, different technology, etc., it is difficult to determine whether they can be directly compared. We know that there will be a substantial overall cost in cleaning up the environment, but it must be remembered there is also a hidden cost if we do not.

One hidden cost that Dr. Innes could not have taken into consideration, since he believes that the proven health effects of air pollution are minimal, is the cost to public health. According to Ostro (4) the annual health costs of air pollution, which includes mortality, morbidity rates, and lost productivity of workers, is calculated to total \$250 per family. This is far greater than the annual inflationary costs of air pollution control which he estimated to be \$31 per family. He concludes that the inflationary costs of air pollution are more than offset by the damages to public health from unabated air pollution.

The fourth point, which deals with the relative contribution of the midwest to problems of acid rain in the Adirondack lakes, has been well documented. According to a report by the New York State Department of Environmental Conservation (3) for 1980, less than 30% of the sulfur deposited in the State of New York came from local sources within the state. Therefore, the remaining 70% must have come from long-distant transport of air pollutants.

The final statement that Innes makes relates to human health effects. It seems incredible to us that Innes suggests that "pollution control measures for SO₂, NO_x, particulates, etc. have been considered and effected for decades even though proven health effects are minimal". Why did the U.K. bring in its Clean Air act to control SO₂ and particulates? One key reason was the *4000 excess deaths* caused by these components during the London smog of Nov 1953.

Or consider the statements made by Lave and Seskin (2): "(1) There is a close, statistically significant association between air pollution (as measured by sulfates and suspended particulates) and mortality rates in the United States; this relationship is evident over time and across metropolitan areas. (2) The close association is relatively robust, as evidenced by analyses of various data bases.... (3) If the estimated relationship is a causal one, the estimated effect of air pollution on health is large, warranting stringent abatement of sulfur oxides and particulates (and perhaps other air pollutants)."

Recently Dr. D. V. Bates found a significant relationship between the number of people admitted into hospitals complaining of respiratory problems and the daily SO₄ levels in Southern Ontario.

Furthermore, there is evidence that groundwater is becoming more acidic and that concentrations of potentially toxic metals are increasing in drinking water from shallow wells in areas exposed to acid rain (7). Several studies have shown that mercury levels are higher in fish from acidic lakes (cited in ref 6 and 7). How much evidence does Dr.

Innes need before he might *consider* the possibility of human health effects?

Literature Cited

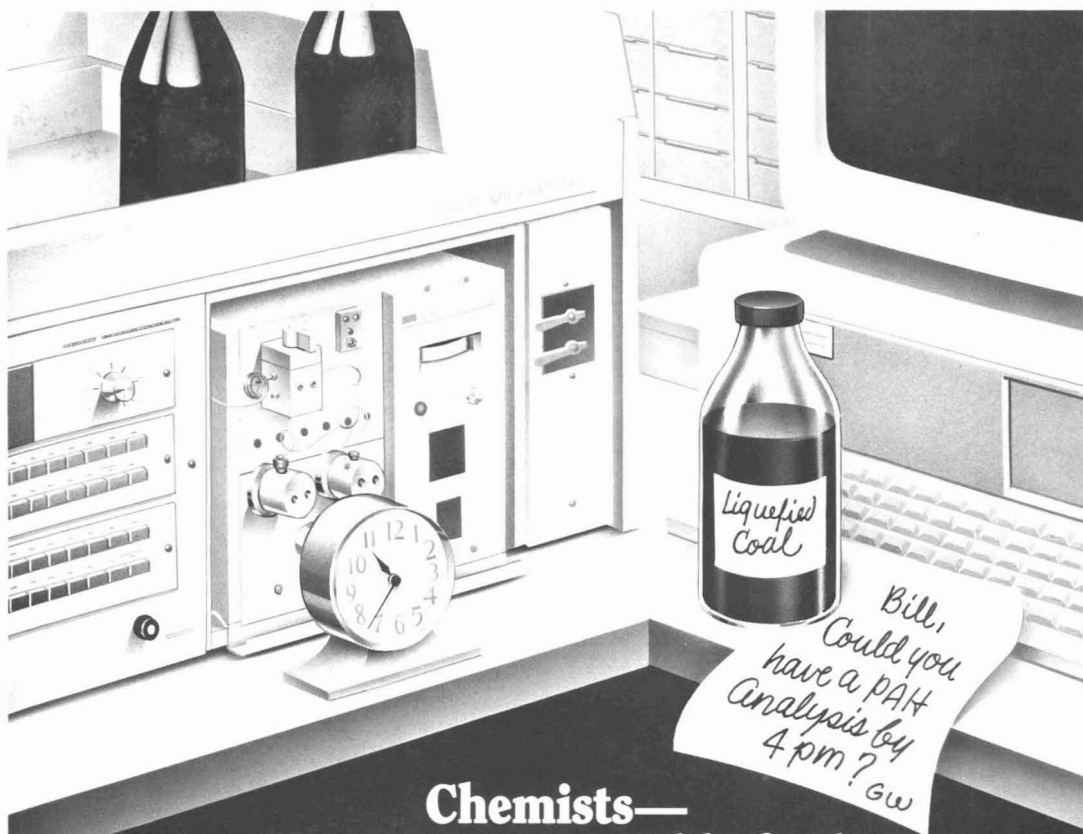
- (1) Innes, W. B. *Environ. Sci. Technol.* 1985, preceding paper in this issue.
- (2) Lave, L. B.; Seskin, E. P. 1980. *Environ. Health Perspect.* 1980, 34, 181-183.
- (3) New York State Department of Environmental Conservation 1984, Policy for New York State to Reduce Sulfur Dioxide Emissions, Executive Summary, pp 1-20.
- (4) Ostro, B. D. *Environ. Health Perspect.* 1980, 34, 185-188.
- (5) Bengtsson, B.; Dickson, W.; Nyberg, P. *Ambio* 1980, 9, 34-36.
- (6) Flick, W. A.; Schofield, C. L.; Webster, D. A. In "Acid Rain/Fisheries"; Johnson, R. E., Ed.; American Fisheries Society: Bethesda, MD, 1982; pp 287-306.
- (7) Swedish Ministry of Agriculture *Stockholm Conf. Acid. Environ.* 1982, 1-232.
- (8) Yan, N. D.; Dillon, P. J. In "Studies of Lakes, Watersheds near Sudbury Ontario: Final Limnological Report"; Ontario Ministry of Environment: Rexdale, Ontario, 1982; SES 009/82, pp 1-60.

Magda Havas,* Thomas C. Hutchinson

Institute for Environmental Studies
University of Toronto
Toronto, Canada M5S 1A4

Gene E. Likens

Institute of Ecosystem Studies
The New York Botanical Garden
Mary Flagler Cary Arboretum
Millbrook, New York 12545



**Chemists—
How can you quickly find
an analytical procedure
to solve this problem?**

Search ACS JOURNALS ONLINE.

ACS JOURNALS ONLINE is a high-efficiency chemical information search system that can save you hours of searching through chemical journals for an analytical procedure.

You can use it right in your laboratory. Just turn on your computer or terminal.

In minutes you'll be reading about the analytical procedure you need.

In this case, it's a high-performance liquid chromatography procedure for determining polycyclic aromatic hydrocarbons in liquid coal.

And with the touch of a key, you can even zero in on specific paragraphs that contain the data you need.

Find out how you can make this high-efficiency chemical information search system work for you. Call an American Chemical Society sales representative today at 800-424-6747. The call is free.

Or write, Sales Office, American Chemical Society, 1155 Sixteenth Street, N.W., Washington, D.C. 20036.

ACS JOURNALS ONLINE contains: Accounts of Chemical Research, Analytical Chemistry, Biochemistry, Chemical Reviews, Environmental Science & Technology, Industrial & Engineering Chemistry—Fundamentals—Process Design & Development—Product Research & Development, Inorganic Chemistry, Journal of Agricultural and Food Chemistry, Journal of Chemical and Engineering Data, Journal of the American Chemical Society, Journal of Chemical Information and Computer Sciences, Journal of Medicinal Chemistry, The Journal of Organic Chemistry, The Journal of Physical Chemistry, Langmuir, Macromolecules, and Organometallics.

The Computer-Powered
Full-Text Search System
From The American
Chemical Society

**ACS JOURNALS
ONLINE**



1155 Sixteenth Street, N.W., Washington, D.C. 20036

STANDARD METHODS—16th EDITION

Proven, Time-Tested Methods for the Analysis of Water and Wastewater

The Industry Standard for 80 Years

Originated in 1905 to establish **uniform and efficient methods** for analyzing water, *Standard Methods* today has earned a reputation as the water and wastewater industries' **most trusted and authoritative source** of water analysis techniques.

Developed and Reviewed by an International Committee of Experts from 16 Different Scientific Disciplines.

The more than **150 analytical methods** described in this valuable reference were developed by specialists from such diverse fields as: organic and analytical chemistry, toxicology, microbiology, civil and sanitary engineering, environmental health, and epidemiology. Its status as an **industry standard** is due in part to the careful review and consensus process by which the 400-member *Standard Methods* Committee determines the book's contents.

Procedures contained in this 1,340-page laboratory guide are **cited by many state and federal regulatory agencies** for permit compliance purposes as acceptable methods for analyzing the chemical, bacteriological and radiological characteristics of water.

Timely Information of Value to Every Water Quality Analyst

Published in February of this year, the 16th Edition continues the tradition of providing practical information in a **well-organized, easy-to-read** format that permits quick referencing of methods, tables, and bibliographies.

The text's general introduction addresses topics of importance to all water quality laboratory professionals and includes discussions on:

- Current laboratory safety and quality assurance practices

- Proper collection and preservation of samples
- Precision, accuracy and correctness of analyses

Subsequent sections on specific chemical analytic techniques describe the chemical reactions taking place during analysis and alert analysts to potential interferences.

The Most Comprehensive, Up-To-Date Source for Instrumental and Non-Instrumental Methods

More than 50 percent of this industry classic has been **revised, updated or rewritten** to reflect new developments in water analysis techniques over the past 5 years. Classical wet chemical methods (e.g. colorimetric method) are still included but new emphasis is given to **contemporary instrumental techniques**.

Changes in the **16th Edition** of importance to chemists include:

METALS

- A new general discussion of emission spectroscopy using an inductively coupled plasma source.

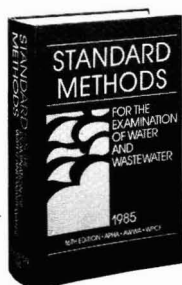
INORGANICS

- Addition of a new instrumental method using an ion chromatograph for measuring most anions.
- A change of indicators used for acidity and alkalinity

ORGANICS

- A new method for total organic halide (TOX)
- Instrumental identification of taste and odor-producing compounds using closed-loop stripping and GC/MS.

Whether you're involved in permit compliance, water supply or wastewater monitoring, *Standard Methods* is your key to confidence in acquiring quality test results.



Standard Methods is published jointly by three leading scientific organizations: American Public Health Association, American Water Works Association, and the Water Pollution Control Federation.

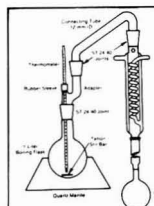


Figure 4131. Direct distillation apparatus for fluoride.

Helpful tables, illustrations and bibliographic references are included throughout this comprehensive text.

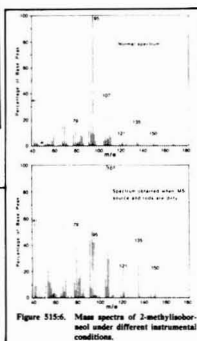


Figure 3156. Mass spectra of 2-methylanthracene under different instrumental conditions.

TABLE B. PREPARATION OF UNIFORM SODIUM HYDROXIDE SOLUTIONS			
Normality of NaOH Solution	Required Weight of NaOH to Prepare 1,000 mL of Solution g	Required Volume of 15% NaOH to Prepare 1,000 mL of Solution mL	
6	240	400	
1	40	67	
0.1	4	6.7	

Make sure there's a copy in your water quality lab!

ORDER FORM

Mail order form to:
Computer Services Department
American Water Works Association
6666 West Quincy Avenue, Denver, CO 80235

YES! Send me the new 16th edition of *Standard Methods*.

Send me _____ copies of **Standard Methods for the Examination of Water and Wastewater—16th Edition** (Members \$72.00; nonmembers, \$90.00; **10035LC**)

☐ Payment enclosed. (Make check payable to AWWA in U.S. or Canadian funds. If Canadian funds, add 15% to total. If this order is to be shipped outside of North America, please add 40% to above prices.)

☐ Personal check ☐ Company check _____ Check no.
☐ Visa ☐ Mastercard ☐ American Express

_____ Exp. date
_____ Card no.

☐ Bill me (AWWA members only).

PLEASE PRINT

NAME _____

ORGANIZATION _____

ADDRESS _____

CITY _____ STATE _____ ZIP _____

PROVINCE _____

PHONE _____ - _____ MEMBER NO. _____